NATIONAL BUREAU OF STANDARDS
MICROCOPY RESOLUTION TEST CHART

LEVEL Ⅱ

Report No. CG-D-41-79

INVESTIGATION OF HAZARDS POSED BY CHEMICAL VAPORS RELEASED IN MARINE OPERATIONS - PHASE I

W. J. ASTLEFORD

T. B. MORROW

R. J. MAGOTT

R. L. BASS

FINAL REPORT
MAY 1979

Prepared for

U.S. DEPARTMENT OF TRANSPORTATION
United States Coast Guard
Office of Research and Development
Washington, D.C. 20590

79 08 20 045

NOTICE

Technical Report Documentation Page

1. Report No.	2. Government Accession No.	3. Recipient's Catalog No.

4. Title and Subtitle	5. Report Date
INVESTIGATION OF HAZARDS POSED BY CHEMICAL VAPORS RELEASED IN MARINE OPERATIONS. - PHASE I.	15 May 1979
	6. Performing Organization Code
	SWRI-02-4986

7. Author(s) W. J. Astleford, T. B. Morrow, R. J. Magott and R. L. Bass	8. Performing Organization Report No.

9. Performing Organization Name and Address	10. Work Unit No. (TRAIS)
Southwest Research Institute P. O. Drawer 28510 6220 Culebra Road San Antonio, Texas	11. Contract or Grant No. DOT-CG-70363-A
	13. Type of Report and Period Covered

12. Sponsoring Agency Name and Address	Final Report. Aug 1977- to May 1979
U. S. Department of Transportation U. S. Coast Guard 400 Seventh Street, S.W. Washington, D. C. 20590	14. Sponsoring Agency Code

15. Supplementary Notes

352 p.

16. Abstract

The flammability and toxicity hazards associated with (1) emission of chemical vapors from tankers and barges during product loading in a marine terminal and (2) man-entry into empty tanks were studied. Initially, five cargo transfer operations were observed for the purpose of documenting the mechanics of the transfer process, shipboard tank gauging and venting systems, and the level of worker activity on the deck and dock with respect to potential sources of vapor exposure. Based on this documentation, analytical models were developed to describe (1) the near field atmospheric dispersion of heavier-than-air vapors during tank loading and (2) the vapor concentrations in an empty tank during ventilation and evaporation of residual chemicals. Sensitivity analyses were performed on the models to identify the important independent variables. These models and their sensitivity analyses guided the planning and execution of laboratory and full scale experiments. Laboratory or small scale experimentation included (1) tests of a 1/150 scale model tanker in a meteorological wind tunnel to visualize plume dispersion and measure vapor concentrations at deck level of heavier-than-air plumes under various atmospheric stability classes, (2) vapor dispersion tests on a 1/4-scale, generalized layout of a chemical tanker deck, and (3) gas freeing tests in a scale model tank to assess the effects of residual cargo evaporation and tank internal structure on the ventilation process. Two full scale tests were conducted. During these tests, a vapor sampling and analysis program was conducted to measure (1) the source concentration-time histories of vapors vented from tanks during loading, (2) deck crew vapor exposures during tank loading as well as during entry into empty tanks, and (3) downwind and lateral plume dispersion. Experimental data are compared with analytical model predictions. The requirements for an expanded model validation test program were also developed.

17. Key Words	18. Distribution Statement
Tankers and barges Vapor dispersion Chemicals Analytical modeling Cargo transfer Tank ventilation Flammability Evaporation Toxicity	This document is available to the U. S. public through the National Technical Information Service, Springfield, Virginia 22161

19. Security Classif. (of this report)	20. Security Classif. (of this page)	21. No. of Pages	22. Price
Unclassified	Unclassified	350	

328 200 DM

ACKNOWLEDGEMENTS

This report presents the results of an 18-month project entitled "Investigation of Hazards Posed by Chemical Vapors Released in Marine Operations." This project studied the flammability and toxicity hazards associated with (1) emission of chemical vapors from tankers and barges during product loading in a marine terminal and (2) man-entry into empty tanks.

The major elements of this Phase I effort included (1) a background study, (2) analytical modeling of marine vapor environments, (3) development of an experimental plan, and (4) model and full scale testing.

Background Study

To evaluate the potential for flammable and toxic hazards during chemical cargo transfer, operational activities were documented in several chemical terminals, on both chemical tankers and barges. Cargo handling operations were defined to include

(1) loading or discharging of chemicals, toxic liquids, or volatile liquids in a marine terminal,

(2) deck and dockside activities in preparation for connecting or disconnecting cargo transfer lines, and

(3) tank cleaning at sea in preparation for either man-entry or change in cargo grade on non-dedicated tanks.

In all, five bulk liquid cargo transfer operations were observed in three marine terminals. In addition, four other chemical terminals were visited and discussions were held with terminal personnel. In the aggregate, seven terminals were visited and cargo transfer operations were documented for large and small organizations, barges and tankers, drugstore and single commodity carriers, and fully automated and manually operated vessels. The purpose of these observations was to become familiar with

(1) the mechanics of liquid cargo transfer including hose connect-disconnect on deck and dock,

(2) shipboard loading techniques, cargo gauging systems, configurations of vapor venting systems, and

(3) the level of worker activity on the deck and on the dock with respect to sources of vapor emission.

The above activities were documented by personal observation with photographic records covering the relevant cargo transfer time period.

The results of the terminal observations show that workers' activities during cargo transfer are random in nature because of the work task flexibility that is required during the loading operation. Typically, three to seven dock and ship workers are involved in tanker loading operations. Normally barge loading requires fewer workers on both the dock and deck, and typically one independent tankerman is responsible for barge loading.

Through observation, a qualitative assessment of potential health hazards was formulated. Sources of cargo liquid and vapor exposure and the corresponding potential health hazard to workers include:

(1) visual and manual gauging of cargo ullage through open hatches and ullage ports during loading of barges and tankers (acute respiratory exposure),

(2) visual observation of product level through open hatches during the lattermost stages of cargo discharge on barges (acute respiratory exposure),

(3) swabbing of tank bottoms on barges using long-handled mops with eventual manual wringing of product into buckets (skin contact and acute respiratory exposure),

(4) exposure to the general background concentration of vapors on the deck of barges and tankers (chronic respiratory exposure),

(5) exposure to multiple chemical cargo vapors (unknown additive, synergistic, etc. effects of multiple respiratory insult),

(6) presence of undiluted, raw product in drip pans on the dock and on the decks of barges and tankers (chronic respiratory exposure). A low flow rate water flush would promote dilution and transport of product to slop tanks or a water treatment plant,

(7) product leaks at the valves on the dock manifold (chronic respiratory exposure),

(8) discharge of large volumes of raw product into the dock drip pans when the flange blind is removed from a valve that does not have a positive seal against product bypass (acute respiratory and skin contact exposure), and

(9) descent into an empty tank, which is presumed to be safe based upon explosimeter readings (acute respiratory exposure).

These observations are made under the assumption that respiratory equipment and protective clothing are not worn. Also, it is re-emphasized that the above conditions may or may not present a health hazard, depending on the degree of exposure (concentration level and time of exposure) which remains to be quantified.

Current and proposed federal regulations relating to the transfer of hazardous chemical cargos are given by the Coast Guard and OSHA. In addition, State and International agencies and groups are formulating regulations dealing with chemical cargo handling. Currently, the USCG regulations are more germane to the regulation of chemical cargo transfer in marine operations than those of OSHA. However, OSHA is contemplating an expansion of their regulations in these areas as are several of the State agencies. Currently, there does not appear to be a conflict of regulations in the areas of vapor flammability and human vapor exposure in the marine environment, although some

jurisdictional conflicts may occur between the Coast Guard and OSHA as a result of an OSHA draft safety and health standard for cargo transfer activities. In addition, there is a significant on-going activity by most of the major oil and chemical companies, as coordinated through the American Petroleum Institute, to generate full scale vapor emissions data to allow an assessment of both environmental pollution and health related problems.

A review of the literature reveals that most of the previous work associated with in-tank vapor hazards has been experimental in nature with emphasis placed on defining operational conditions that can eliminate flammable atmospheres during ship tank washing, preparation for man-entry and hot work. Experimental studies to determine vapor concentration data for the purpose of evaluating potential toxic hazards in a shiptank appear non-existent. In addition, due to the significant number of parameters involved, no comprehensive analytical efforts on in-tank hazardous vapor removal have been undertaken.

Problems associated with hazardous vapors exterior to the shiptank have received little analytical or experimental attention. The activities have been primarily experimental in nature and, as with the in-tank problem, emphasis has been placed on flammability hazards resulting from open venting during loading as opposed to those associated with toxic concentration levels. A few analytical models have been developed for predicting plume trajectory and dispersion as a function of plume vent exit and atmospheric conditions. These models are generally applied to ambient air pollution problems. One source of experimental wind tunnel data has been identified which can be used to establish regions of flammability on a scale model ship deck as a function of ship structure, venting configuration and wind conditions.

Analytical Modeling

Analytical models were developed to describe (1) the dispersion of heavier-than-air cargo vapor plumes that are emitted on-deck during tank loading, and (2) the vapor environment in a tank resulting from cargo evaporation during ventilation. The key features of the modeling analysis are summarized below.

o An analytical model based on the work of Ooms for forced plume dispersion, and the work of teRiele for gaseous dispersion from ground level sources, provides the capability for predicting the spatially dependent concentration field downwind of vents on ships and barges during cargo loading.

o Based upon an evaluation of parameters used in this model, the vapor concentration level at man-height downwind of a vent depends primarily on

- the vapor concentration at the vent,

- the vent height, diameter and geometry,

- the cargo loading rate,

- the wind velocity, direction and turbulence intensity,

- turbulence produced by on-deck structure, and

- atmospheric stability conditions.

o   Based on analytical model predictions, the conditions that cause high levels of vapor concentration at man-height downwind of a vent are

  -   low vent height, typical of a vent on an expansion trunk,

  -   low wind speed and low turbulence intensity as could occur with stable atmospheric stability, and

  -   high vapor concentration at the vent and low vent velocity.

o   An analytical in-tank model allows the prediction of vapor concentration levels during cargo tank ventilation in the presence of vapor regeneration from pure chemical cargo residue. Local evaporation mass flux rates are based on the work of Gray.

o   Based on analytical model predictions, significant periods of time are required to ventilate a tank to safe levels of vapor concentration. For a given cargo, parameters shown to be important for the in-tank ventilation problem include:

  -   blower capacity,

  -   residual cargo thickness,

  -   tank wall temperature, and

  -   all interactive combinations of these parameters.

o   When even small amounts of pure product remain in a shiptank, large ventilation times are required to evaporate the residual liquid and remove the hazardous vapors. The total ventilation time is governed by the time required to evaporate the liquid residue and discharge the resultant vapor. This time may be much larger than the time to ventilate the tank based upon ideal dilution without evaporation.

o   A localized model was developed to predict vapor concentrations in shielded areas of a cargo tank during manual activities such as the mucking of residual cargo. Liquid surface agitation may increase the evaporation rate and produce vapor concentrations that exceed safe levels because convection and diffusion are relatively ineffective in removing vapors from the shielded work area.

Planning and Experimentation

Planning activities centered primarily around the statistical design of a full scale test program. The analytical models indicated the independent variables that are likely to have a significant affect on chemical vapor concentrations on-deck and in-tank. Additional factors that affect on-deck vapor dispersion were identified in a series of scale model wind tunnel tests. Based upon these inputs, a regression algorithm was postulated for vapor concentrations (dependent variable) on-deck and in-tank. Estimates were then made of the number of full scale observations (sample size) that would be

needed to ensure that the test results are statistically significant at a confidence level of 95% and a probability level of 85%. For both the on-deck and in-tank environments, 24 observations or realizations were indicated.

Two full scale tanker tests were then designed and executed. The design included identification of the classes of vapor concentration data that were needed to assess occupational health hazards and to validate the analytical models. Four classes of air sampling were identified (personal monitoring, source sampling, area or grab sampling, and matrix sampling) as were the instrumentation requirements. Vapor concentrations were measured on-deck during tanker loading as well as in-tank following washing and ventilating. The results of these tests are as follows:

o   A comparison of the full scale vapor concentration data to values predicted from the analytical plume model shows reasonably good agreement between analytical model and experiment.

   -   These comparisons confirmed the need for careful selection of vapor sampling locations, sampling methods, and meteorological data gathering methods so that variations in wind speed and direction may be accounted for in the analysis of experimental data.

   -   The best procedure for vapor sampling appears to be simultaneous sampling at a matrix of locations, closely spaced in the crosswind direction and logarithmically spaced in the downwind direction.

o   Continuous cargo loading appears to reduce the vapor concentration at the vent, and it is advantageous to load without interruption from pump startup to tank top-off. The interruption of loading allows diffusion to increase the concentration in the ullage space, giving higher vent concentrations when loading is resumed.

o   For the two full scale tests conducted on this study, the following potential hazards were noted.

   -   A previously ventilated tank that was considered to be safe for man-entry, based on explosimeter readings, had vapor centration levels that exceeded the STEL.

   -   For some tank loading conditions, respirable vapor concentrations (i.e., personal exposures) exceeded the STEL during tank top-off.

   -   Vapor concentrations at the vent and in the neighborhood of the vent were within the explosive range during some loading conditions.

The full scale tests were supplemented by

o   scale model tests of a tanker in a meteorological wind tunnel to visualize plume dispersion and measure deck concentrations

of heavier-than-air plume vapors under various atmospheric stability classes. These scale model wind tunnel tests showed that stable thermal stratification (atmospheric stability) of the wind reduced the dispersion of vapor plumes emitted from shiptank vents. On the other hand, the interference of on-deck structure increased the turbulence of the air stream and increased vapor plume dispersion.

o   vapor dispersion tests on a 1/4 scale, generalized layout of a chemical tanker deck. Using properly scaled vent discharge conditions (Froude scaling), these tests confirmed the full scale sampling strategy, the advantage of b/3 venting as opposed to open venting from an expansion trunk, and the applicability of the plume dispersion analytical model.

o   laboratory experimental studies of gas freeing of a scale model tank including the effects of evaporation of residual cargo and tank internal structure. Laboratory scale in-tank ventilation tests with vapor regeneration confirm that small amounts of cargo residue and tank internal structure significantly increase the length of time needed to gas free a tank to low concentration levels.

This Phase I activity developed the basic building blocks for constructing a hazard predictive method. The remaining Phase II efforts that are required to generate a valid predictive technique have been established and delineated. A logical end product of these remaining activities is a Hazard Assessment Manual that will permit the U. S. Coast Guard to assess hazard potentials resulting from the release of chemical vapors during marine operations.

The observations and limited full scale tests that were conducted on this project indicate that there is a potential for hazard in various facets of marine operations. Whether these results represent isolated cases or are representative of the industry as a whole is an issue that can be resolved by expanded full scale and laboratory scale testing as recommended for the Phase II continuation of this project.

TABLE OF CONTENTS

TABLE OF CONTENTS (CONTD)

LIST OF FIGURES

LIST OF FIGURES (CONTD)

LIST OF FIGURES (CONTD)

LIST OF TABLES

LIST OF TABLES (CONTD)

I. INTRODUCTION

Bulk chemical cargos are transported by water in tankships and barges. This report documents the Phase I results of a research program whose prime objective was to investigate the hazard potential of chemical and petrochemical vapors that are generated in barge and tankship operations. In one case, these heavier-than-air vapors are released to the atmosphere during transfer of chemical cargo between a marine terminal and a vessel. Empty ship cargo tanks also contain residual product vapors which are difficult to remove and maintain at safe levels during man-entry and in-tank work. The extent to which petrochemical vapors constitute (1) an occupational health hazard to ship and dock crews, or (2) a flammability/explosibility hazard, is of concern to the operating companies and those agencies that are responsible for health and safety in this segment of the marine transportation industry.

The explosibility limits for pure chemical vapors are well documented in the literature as are the eight-hour time-weighted-average threshold limit values (TWA-TLV) for chronic human exposure and the short term exposure limit (STEL) for acute exposure. However, there is little published information on (1) the existence and extent of explosive vapor concentrations in marine operations, and (2) the actual concentrations to which workers are exposed. In addition to the lack of personal exposure data, there are the fundamental issues of applying and interpreting chronic exposure limits in terms of the abnormal or unusual work schedules that are characteristic of cargo transfer and marine operations.

Generation and dispersion of chemical vapors in marine operations are complex phenomena which are influenced by a large number of variables such as atmospheric conditions, vessel geometry, venting configuration, chemical and physical properties of the cargo, etc. In-tank vapor removal is an equally complex problem and is affected by such factors as residual cargo characteristics, ventilation flow capacity and gas-freeing time, tank internal structural geometry, the condition of the tank walls, and the placement of ventilation blowers relative to tank internal structure. To achieve an improved understanding of these phenomena and a definition of the relative importance of the variables and their interactions, the scope of the Phase I program was divided into four logical task efforts.

TASK I

A background study to define the problem of release of toxic and/or flammable vapor to the tanker environment based on:

o   pertinent information on flammable and toxic hazards,
o   on-site observation of cargo transfer activities,
o   current or proposed regulations and analogous R&D endeavors.

1

TASK II

An analytical modeling of the problem to include:

- o the capability of predicting temporal and spatial vapor concentrations for both tank interior and exterior chemical vapors, and
- o comparing the predicted vapor concentration with data on hazardous flammable and toxic limits.

TASK III

A development of experimental methods for acquiring vapor concentration data in marine operations for selected chemicals and to include:

- o the necessary information to validate the mathematical models,
- o an experimental design for both model and full scale tests, and
- o a definition of instrumentation and data logging requirements.

TASK IV

An experimental investigation to:

- o include both laboratory and full scale testing,
- o demonstrate the validity of the experimental methods, and
- o compare the experimental data with the predicted results from the analytical models.

This Phase I effort represents a major step in acquiring the necessary concentration data which will subsequently be used to develop a hazard predictive technique (Phase II) for those marine operations described above. Emphasis in this project was placed on developing the basic building blocks on which a valid hazard predictive method could be based. The specific areas which were emphasized and are reported herein include:

- o development of valid analytical models to predict in-tank and on-deck vapor concentrations to which workers will be exposed,

- o establishing the necessary experiments and associated equipment and methodology to provide a data base to validate the analytical models and to gain additional knowledge relative to vapor hazards, and

- o the conduct of the recommended experiments in both model and full scale.

As a result of the work accomplished on this project, the remaining Phase II efforts to provide a hazard predictive technique have been established and delineated.

2

II. BACKGROUND STUDY

II.1 Literature Search

The initial effort on this task was to conduct a computerized and manual search of the open literature. The purpose of the search was to uncover either abstracts or bibliographic citations that relate directly or indirectly to on-going and past research on flammable and toxic hazards of chemical vapors, current laws and regulations governing vapor emissions and exposures, vapor emissions, plume dispersion and tank venting. The search was not restricted to tankship enviroments, but was extended to include other forms of chemical transportation such as barges and tank trucks. Key words or phrases were defined first and then grouped into the topical files shown below.

File	Topical Content
1	General - hydrocarbon chemicals
2	Specific chemical names
3	Explosibility (flammability) and safety
4	Occupational disease and toxicity
5	Tank ventilation, plume dispersion and regulations
6	Mode of transportation.

These files were then combined on the computer using Boolean algebra and applied sequentially to each of the following data banks of the Lockheed Information System, Medlars and DDC. The productivity of these searches is also indicated.

Data Bank	Number of Un-screened Finds	Number of Relevant Finds
Enviroline	185	14
Pollution Abstracts	102	15
Oceanic Abstracts	139	8
Chemical Abstracts (1970-77)	318	26
NTIS	140	11
APTIC	1073	15
SSIC (non-DOD work-in-progress)	65	4
DDC Technical Report File	109	6
DDC Work Unit File (work-in-progress)	53	2
Medline	55	4
Toxline	225	20
Totals	2464	125

In addition to the computer searches, a manual search was made of the Air Pollution Control Association (APCA) Journal for the period covering 1970-77. This source was selected for manual search because of the large number of articles on analytical/experimental plume dispersion studies. While the emission sources covered by this journal were not likely to coincide with the chemical tanker/barge environment, it was felt that the treatment of the problem, assumptions and interpretation of results were potentially applicable to the on-deck vapor release problem. In excess of 100 plume articles were retrieved. Also, the SwRI reference file on tankship atmosphere control, which was developed as a part of a MARAD research project was incorporated into the literature base for this project.

The composite literature base, which was then categorized by topical content, is presented in Appendix A. The majority of the literature citations that are presented in the body of this report refer to the corresponding entry in Appendix A, e.g., Reference A-1 refers to the first reference in Category A.

II.2   Previous Work on Vapor Hazards

II.2.1   In-Tank: Experimental and Analytical

Significant experimental studies have been undertaken in areas associated with the ventilating of hydrocarbon gases from ship tanks. Primarily, the experimental studies have evaluated the operating conditions where flammable atmospheres can occur, and the emphasis has been placed on defining operating conditions that can eliminate flammable atmospheres during ship tank washing and in preparation for man-entry and hot work. For man-entry, emphasis has been placed on determining conditions that are safe from the standpoint of asphyxiation and flammability hazards. No experimental studies or vapor concentration data have been generated to evaluate potential toxic hazards in a ship tank. Both model and full-scale studies have been conducted to determine hydrocarbon and oxygen concentration gradients inside a ship tank. A recent comprehensive review of these studies is given in Reference J-50.[*]

A continuation of the work presented in Reference J-50 has recently been completed (J-52). The objective of this program was to conduct comprehensive laboratory scale model studies to establish the effects of ship tank geometries, ventilation, and vapor regeneration characteristics on hazardous (flammable and asphyxiation) vapor removal requirements. Laboratory information in combination with previous full-scale studies was utilized to provide design and operational guidelines for ship tank atmosphere control systems.

References J-4, J-7, J-13, J-16, J-28, J-29, J-30, J-32, J-35, J-45, J-46, and J-48 contain pertinent technical data on ship tank atmospheres and their control.

---

[*] References given in Appendix A - Categorized Bibliography.

Basic Methods of Gas Exchange

The requirements for tank atmosphere control entail the purging and replacing of hazardous gas conditions in a tank with a safe atmosphere introduced from the tank exterior. A review of the literature shows that two fundamental methods are utilized in the replacing of a tank atmosphere (gas B) with another gas (gas A). These methods are commonly referred to as "dilution" and "displacement." For dilution, the incoming gas mixes with and dilutes the existing tank gas until the required concentration is reached. For displacement, the incoming gas physically displaces the existing tank gas and, ideally, no mixing of the gases occurs except at the interface. The dilution method, therefore, requires a high energy inlet gas stream provide sufficient mixing throughout the tank. On the other hand, the displacement process requires significant density differences between the inlet gas and the tank gas, with velocities low enough to discourage mixing. The displacement process is most effective when the gas B is more dense than gas A and when the gases are extracted from the tank bottom through use of a purge pipe or other methods.

There are a significant number of factors that affect both methods of gas atmosphere control, and these include:

(1) Ship Tank Design

    o Geometry (especially depth)
    o Capacity
    o Internal tank structure
    o Webframe height and open area
    o Swash bulkhead open area
    o Heating coil and cargo piping configurations and locations
    o Pump sumps
    o Location and geometry of tank opening, vents and standpipes.

(2) Tank Atmosphere Conditions

    o Relative density of initial tank atmosphere gas to replacement gas
    o Stratification (density gradients) of gas in tank
    o Sediments and unstripped cargo or other sources of vapor regeneration.

(3) Blower Capacity and Design

    o Type of blower (fixed or portable)
    o Location of blower relative to tank being gas-freed
    o Number of tanks simultaneously gas-freed.

The numerous parameters which affect gas-freeing as related to the above considerations are defined in Table II-1, as taken from Reference J-50.

5

TABLE II-1. SHIP TANK ATMOSPHERE CONTROL PARAMETERS AND NOMENCLATURE

Gas A, (or subscript A)	gas entering tank
Gas B, (or subscript B)	gas originally in tank
B	tank breadth (L, ft)
C	tank concentration (at any position and time) of gas component being monitored.
$\overline{C}$	inlet gas stream concentration of gas being monitored.
C_o	original tank concentration of gas being monitored.
C'	concentration of pertinent chemical vapor being emitted from interior tank surfaces.
d_i	inlet diameter (L, ft)
d_o	outlet diameter (L, ft)
D_{AB}	mutual molecular diffusion coefficient of gas A and B (L^2/T – ft^2/sec)
g	gravitational acceleration (L/T^2 – ft/sec^2)
H	tank height (L, ft)
h	measured depth into tank (L, ft)
ℓ	any length-like dimension, longitudinal depth, etc. (L, ft)
Q_A	gas A flow rate (L^3/T – ft^3/sec)
R_i	flow resistance of piping (–) and tank
t	time after start of gas-exchange process (T, secs)
t_o	time at initiation of gas-exchange process (T, secs)
T	gas temperature (θ, °F)
V	gas velocity (at any position and time) in tank (L/T, ft/sec)
V_i	gas A inlet velocity (L/T, ft/sec)
$\mathcal{V}$	tank volume (L^3, ft^3)
β	coefficient of gas volumetric expansion ($L^3/I^3\,\theta$, ft^3/ft^3 °F)
ρ	gas density (M/L^3, $lb\text{-}sec^2/ft^4$)
μ	gas viscosity (FT/L^2, $lb\text{-}sec/ft^2$)
ν	gas kinematic viscosity (L/T^2, ft/sec^2)

Subscripts:

HC	hydrocarbons
IGS	inert gas system
i	inert gas

F –	Force
L –	Length dimension
M –	Mass
T –	Time
θ –	Temperature

6

Examples of typical full-scale study results for both displacement and dilution gas-freeing are shown in Figures II.1 and II.2. It is noted that the concentration levels measured during these studies relate to the LEL (Lower Explosive Limit), and the lowest concentrations measured are ~ 0.1 LEL which are well above the concentration levels associated with TLV's (time-weighted average Threshold Limit Values) for most hazardous chemicals. No experimental activities associated with measuring in-tank toxic hazards concentration levels have been reported.

No comprehensive analytical efforts have been undertaken to model ship tank atmosphere control. A cursory discussion of tank atmosphere models during loading and discharging of cargo is presented in Reference B-16 in conjunction with plume emission models. However, the in-tank models were not developed to a state that permitted atmosphere concentration predictions. Analytical efforts, indirectly related to ship tank ventilation, have been undertaken on vapor removal problems associated with industrial processes (References J-25 and H-8).

II.2.2   On-Deck: Experimental and Analytical

Chemical vapors are emitted at or above deck level of marine chemical carriers during (1) diurnal breathing of loaded tanks, (2) gas-freeing of dirty tanks before a cargo change or as a prerequisite to work requiring man-entry, and (3) displacing of the ullage atmosphere in an empty tank during loading. The vapor streams are emitted either from stack risers high above the deck (required vent height equal to 1/3 the ship beam dimension)* or close to deck level from P/V (pressure/vacuum) valves, open hatches, or open ullage ports. The composition of the vapor stream depends upon the cargo. For chemical cargos, it consists of the vapor of the chemical mixed with air or inert gas in some concentration ranging from low (near to the end of gas-freeing or at the start of loading into a gas-free tank) to high (approaching the saturated vapor concentration in air at the cargo temperature).

The vapor emission rate is usually high enough for the air or gas/vapor mixture to emerge from the vent as a jet or "forced plume" that entrains fresh air (while lowering the average vapor concentration) and expands as it enters the atmosphere above deck level. The trajectory of the forced plume is determined largely by its momentum and buoyancy, and the strength and direction of the natural wind. Forced plumes of cargo vapor are generally heavier than the surrounding air (negatively buoyant) while typical air pollution plumes of heated or moist air are lighter than the surrounding air (positively buoyant).

On-deck vapor hazards can be estimated by determining the location of forced plumes of chemical vapor emitted during gas-freeing or cargo loading, the vapor concentration in any part of the plume that reaches deck level, and the duration of the exposure.

---

*For certain specified chemicals, this requirement is given in the 46CFR, Part 153, Safety Rules for Self-Propelled Vessels Carrying Hazardous Liquids.
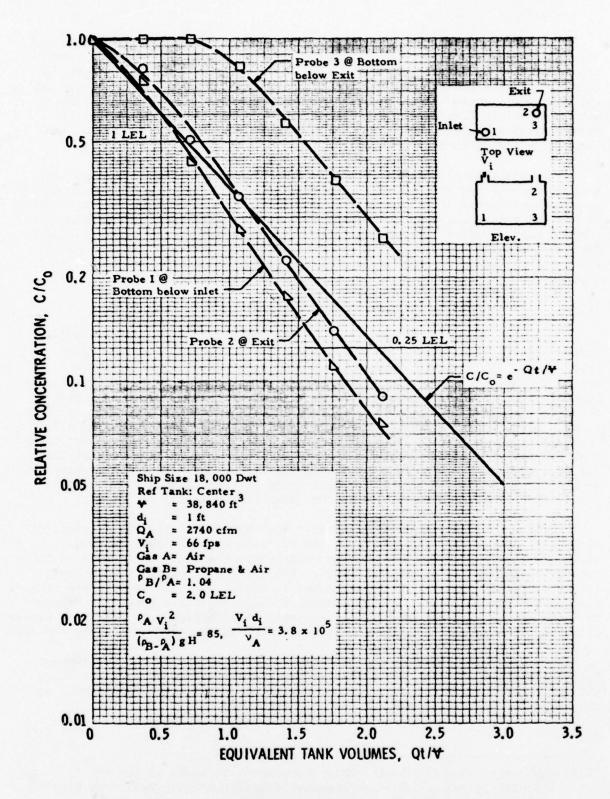
FIGURE II.1. DILUTION GAS FREEING OF CENTER TANK ON AN 18,000 DWT TANKER (REF. J-4)
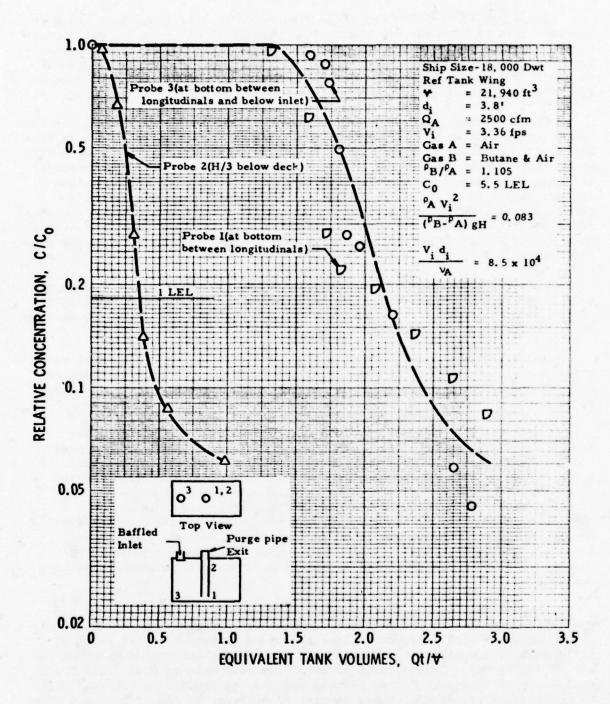
FIGURE II.2. DISPLACEMENT GAS FREEING IN A WING TANK OF AN 18,000 DWT TANKER (WITH MEASUREMENTS ON TANK BOTTOM) (REF. J-4)

Analytical Plume Models

The majority of plume and plume rise references in Appendix A treat the special cases of hot, buoyant plumes from industrial chimneys and wet buoyant plumes from cooling towers under different classes of ambient density stratification. However, a few of the analytical models are sufficiently general to permit modification for predicting the behavior of forced plumes of negatively buoyant chemical cargo vapor.

In the absence of natural wind, negative buoyancy effects can limit the height reached by an upward directed forced plume and cause the plume to fall back onto the deck. Morton (B-120) presents a theoretical analysis of forced plume rise in both uniform and stably stratified environments. He considers the case of a plume with momentum and negative buoyancy and estimates the maximum height in a uniform environment. Morton's theory (see Turner's review article, B-121) considers only the rising motion of the plume and neglects the effect of the outer falling flow in supplying the mass for entrainment by the rising flow. As a result, Morton under-predicts the maximum plume rise height.

Turner (B-122) conducted experiments with salt water jets directed upward in water. His correlation for maximum plume rise height as a function of jet momentum flux and buoyancy flux appears together with other plume rise analytical methods in Appendix C.

Neither Morton nor Turner give useful information on the spatial variation of concentration in the negatively buoyant plume. In particular, the concentration in the radial outward flow after the plume falls to the floor is unknown.

Trent and Welty (B-125) present a method that is capable of numerically computing the full two-dimensional flow field (including concentration distribution) that develops from a turbulent axisymmetric jet with momentum and buoyancy discharged into a quiescent atmosphere with density stratification. In an example, they treat an axisymmetric forced plume directed upward with positive buoyancy and momentum, and make use of a turbulent mixing length distribution, which is known a priori for axisymmetric jets. For this method to be applied to a plume with negative buoyancy, the appropriate spatial distribution of mixing length must be assumed, or a more sophisticated method of estimating turbulent viscosity employed.

The effect of the natural wind is to bend the trajectory of the discharge jet over toward the downwind direction as a function of the ratio of jet momentum to wind momentum. After the plume is bent over, it rises or falls depending upon its buoyancy (whether it is lighter or heavier than the air it displaces). Considerable progress has been made in predicting the trajectory of bent-over forced plumes, and also in predicting the concentration of gas particles (which may consist of pollutants, or a tracer gas mixed with air) from "point" emission sources either above or near the ground.

Kamotani and Greber (B-118) give a correlation of their experimental data for the rise of a turbulent jet in a cross-flow obtained in wind tunnel

tests. They state that for their experiments "the jet motion is inertially dominated with buoyancy playing only a minor role. The result is that the trajectory depends mainly upon the ratio of jet momentum flux to the free-stream momentum flux". Kamotani and Greber's correlation (see Appendix C) is useful for predicting the initial rise of forced plumes, and may be used to generate starting conditions for other plume rise methods.

Briggs (B-10) has published an algebraic equation for plume rise height (see Appendix C) when both momentum and buoyancy are significant in unstratified surroundings. Briggs' equation was developed to describe the rise of lighter-than-air plumes, and may not be as useful in describing the rise and fall of a plume with negative buoyancy.

In addition to algebraic equations that relate plume rise to momentum and buoyancy, there are analytical methods that require the numerical solution of a system of differential equations on a computer to predict the plume trajectory.

Hoult, Fay and Forney (B-48) describe a system of differential equations written for the conservation of mass, momentum, and energy that can be solved simultaneously to predict the plume trajectory. They assume that the actual velocity, density, and/or concentration profiles in the plume are geometrically similar and can be replaced by "top hat" (constant average value across the plume width) profiles. The equations are simplified somewhat (see Appendix C) by the Boussinesq approximation that assigns a constant value to the plume density everywhere except in the calculation of buoyancy.

Ooms (B-76) adopts an approach similar to Hoult, Fay and Forney and derives a set of differential equations for the conservation of mass, momentum and either chemical species or energy. He also assumes that profiles of concentration, velocity defect and density are similar at different distances along the plume axis. However, instead of top hat profiles, he assumes that the profiles have a Gaussian appearance. Ooms' method does not use the Boussinesq approximation, and includes a term in the conservation equations for the effect of wind turbulence on plume entrainment. Ooms' method is described completely in Appendix C.

Note that Hoult, Fay and Forney's method and Ooms' method predict the value of concentration along the plume axis. When Briggs' plume rise equation is used, the concentration field must be predicted independently. Usually, Briggs' equation is used to estimate the plume rise height above the vent for a Gaussian point source diffusion equation (see Appendix C).

Chou and Corlett (B-16) applied a version of the Gaussian point source diffusion equation as developed by Sutton (B-102) to the problem of above-deck emissions from tanker ships. They present 12 example calculations including high and low values of discharge rate and vapor concentration for three classes of atmospheric stability and calculate flammable surface coordinates. They conclude that vent height and (vertical) jet discharge momentum can be chosen for many cases of discharge rate and concentration to insure that the flammable plume surface remains detached from the ship deck.

11

When more than one source of vapor emission is present, the additive effects may be estimated using methods advanced in References B-60 (which uses Sutton's version of the point source diffusion equation), and B-75 (which uses Briggs' plume rise equation together with Gaussian point source diffusion equation).

Experimental Plume Studies

The literature search identified only two references to experimental measurement of above-deck vapor emissions. Brummage (B-12 and B-134) carried out low speed (down to 0.367 ft/sec in model scale, equivalent to 2.5 mph in full scale) wind tunnel experiments using 1/100th scale models of crude oil tanker ships and mixtures of propane and air. The plume location and combustible surface was identified using a portable spark igniter. Brummage advises the release of cargo vapor upward at high efflux velocity to encourage dilution through mixing with the ambient air before the plume reaches the deck and superstructure. He presents guidelines for the minimum height of the vent outlet above the deck that is necessary to prevent flammable gas concentration on the deck, and for the minimum horizontal distances for vent location upwind and downwind from the superstructure beyond which plume dispersion is not influenced by the superstructure.

Brummage's experiments also provide data for validating the results of analytical plume models for heavier-than-air mixtures. This is necessary since the analytical models reviewed here were validated only for positively buoyant plumes.

Brummage investigated the flammable regions for discharge of propane/butane gas in concentrations from 25% to 100% by volume. This would be typical for the final stages of loading crude oil or a boiling cargo. At earlier stages of loading, the vapor concentration is lower, as shown in Reference H-1. Typically, the initial vapor concentration at the discharge vent is the same as the vapor concentration in the empty tank. This may range from low for gas-freed tanks to high (average 7% by volume for gasoline tankers) for dirty tanks. During loading, a vapor blanket forms above the cargo that is typically 6-8 feet in depth. It is the discharge of this vapor blanket that raises the vapor concentration to the values investigated by Brummage.

Reference H-1, a study of tanker gasoline emissions, is a useful source of data for modeling the time history of vapor concentrations at vent exits for gasoline tankers including the effects of loading rates and arrival tank conditions on vapor concentrations. Reference H-1 also provides a description of terminal layouts and equipment associated with tanker loading.

II.3 Definition of Cargo Transfer Activities

II.3.1   Terminals Observed

An objective of the background study was to formulate a definition of the hazards associated with vapor emissions during chemical cargo handling operations on tank ships and barges. Hazards broadly include (1) considerations of vapor flammability and explosibility, and (2) the potential for worker exposure to toxic chemicals and their vapors. Cargo handling operations were defined to include:

12

(1) loading or discharging of chemicals, toxic liquids, or
     volatile liquids in a marine terminal,

(2) deck or dockside activities in preparation for connecting
     or disconnecting cargo transfer lines, and

(3) tank cleaning at sea in preparation for either man-entry
     or change in cargo grade on non-dedicated tanks.

Emphasis was placed upon the vapor hazards that may be posed to the ship or
barge and its crew as well as to dock workers during cargo transfer opera-
tions. Five bulk liquid cargo transfer operations were observed in three
marine terminals. In addition, four other chemical terminals were visited,
and discussions were held with terminal personnel to identify typical oper-
ating procedures and equipment used in cargo transfer and to solicit comments
relative to project objectives. In the aggregate, seven terminals were
visited and cargo transfer operations were documented for small and large
organizations, barges and tankers, drugstore and single commodity carriers,
and fully automated and manually-operated vessels. The purpose of these ob-
servations was to establish:

(1) the mechanics of liquid cargo transfer including hose connect/
     disconnect on deck and dock,

(2) shipboard loading techniques, cargo gauging systems, con-
     figurations of vapor venting systems, etc., and

(3) the level of worker activity on the deck and on the dock
     with respect to sources of vapor emission.

The general substance of these five observations is summarized in Table II-2.
The details of each observation are contained in Appendix B, as are the com-
ments expressed by terminal and ship personnel.

II.3.2   General Description of Observed Loading Operations

Since the terminal observations included loading of both barges and
tank ships, it is logical to present a separate discussion for each type of
operation. These discussions, as presented below, are generally applicable
to the loading of straight chemicals, solvents, gasolines, chemical mix-
tures, and various lube oils. Where specific cargos are cited, it is to
emphasize the presence of potential hazards. Although the loading observa-
tions included a range of terminals and vessels, the following descriptions
are based on these observations only and may not be typical or representative
of other specific terminals. However, it is believed that the composite of the
observed operations provide a definition of the pertinent activities relative
to the objectives of this project.

Loading of Tankships

After the ship docks, the initial 3-4 hours are spent in discharging
the ballast water. During this period, dock activities include connecting
cargo transfer hoses between the dock and ship manifolds. Initially, several
of the hoses are connected before any cargo transfer is undertaken.

Five dock workers are typically involved in the hose connect/disconnect
procedures. Discussions with dock personnel reveal that this operation is
usually performed with four to seven individuals of equal work title. One
of these individuals is designated as the leader for the group.

TABLE II-2. SUMMARY OF MARINE TERMINAL OBSERVATIONS

Terminal	Observation No.	Brief Description
A	1	Discharging acetone and MEK from a 28,125 DWT multi-cargo tanker. Loading of the same tanker with 22 different chemicals, chemical mixtures, and light oils.
A	2	Loading of a 75,649 DWT tanker with gasoline, kerosene, and diesel fuel.
B	3	Loading a 36,600 DWT tanker with 17 different grades of pure chemicals, solvents, gasoline, and other bulk cargos.
B	4	Loading solvents and benzene on three separate barges.
C	5	Loading a 10-barge integrated tow with gasoline.

14

After ship arrival, one individual removes the blinds from the flanges
on the dock manifold for each of the products that are to be loaded. Since
the upstream dock valves normally have pressure on them, a bleed valve lo-
cated between the dock valve and the blind is opened to relieve any pres-
sure created by leakage past the dock valve. It was observed that most of
the lines have pressure between the blind and the dock valve, and when
opening the bleed valve, 1 or 2 gallons of the product is released into a
drip tray beneath the valve.

Dockside hose connection normally requires two men to handle the hoses
while one man operates the hoist which positions the hose to the manifold.
Four bolts are used to hold the hose flange to the manifold flange. Some
hoses are dedicated for specific products where purity is important while
other hoses can be used for a variety of products. Typically, the hoses are
6 inches in inside diameter, although the facility manifolds range from 6
to 12 inches, depending on the products. Usually crude oils are discharged
with the larger diameter while chemicals are transferred with the smaller
hoses.

After several of the product hoses have been connected to the dock
flanges, hose hookup at the shipboard manifolds proceeds (Figure II.3). This
procedure, which can be reversed in some cases, involves typically two to
three men on the ship deck and two men on the dock. One dockside worker
operates the crane while the second dockside worker hooks the lift lines to
the hose on the dock. The hose is then lifted to the deck level of the ship
where the deckhands maneuver the hose to the correct manifold flange on the
ship. Blinds on the deck flanges are removed by the ship's crew prior to
arrival.

After the hose connections have been completed, loading of selected
products is initiated. The dock operator opens the dock valve, and the
ship's crew member opens a bleed valve on the deck manifold to obtain a pro-
duct sample prior to transfer to the tank. After the sample is visually
accepted, the ship crewman opens the globe valve on the ship deck, and the
product is transferred to the appropriate ship tank. Normally, initial flow
is established by gravity feed from the tank farm. To determine if the pro-
duct is indeed going to the correct tank, a visual observation of tank filling
is accomplished by viewing with a flashlight through the ullage port on the
expansion trunk to see if liquid is flowing into the tank. When flow to the
correct tank has been verified, the land-based product pumps are started.
This procedure is repeated in succession for the initial products that are
to be loaded onto the ship. In some cases, such as motor gasoline, the pro-
duct is diverted to several tanks simultaneously with line valves adjusted
to regulate the rates to each of the tanks such that the tanks will not be-
come full at the same time. This staggering of filling reduces the possi-
bility of deck spillage. Subsequent tanks are filled after coordination
between the dock and the ship until approximately all of the connected hoses
are pumping products simultaneously.

As the tanks are filled, hoses are disconnected from the ship manifold
after a final sample is obtained. The remaining product hoses are attached
as the initial hoses are removed from service.

15
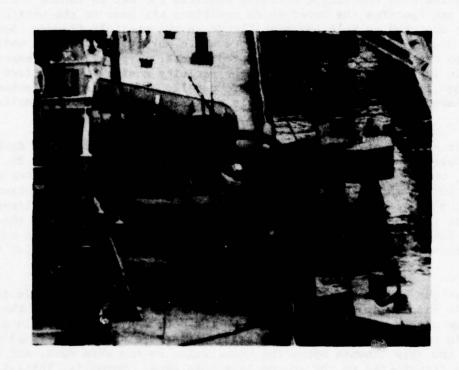
FIGURE II.3   HOSE CONNECTION AT SHIP'S MANIFOLD

As the tanks are nearing full, several ship crew members, including the Chief Mate, take continuous readings of tank ullage in preparation for topping the tank. This operation usually occurs continuously during the last 3 to 4 feet of filling, which lasts roughly 10 to 15 minutes. When the tanks are deemed full, a ship crew member closes the manifold valve on the deck while the dock worker closes the manifold on the dock with a pneumatic actuator or motor-operated valve (MOV). If this sequence occurs before shore pump shutdown, as was the case on one observation, then there is a possibility of rupturing a loading hose because the deck valve was closed first against the flow. With the ship tank isolated from product flow from both the deck and dock, and a final sample having been taken from a deck bleed valve, the bleed valve on the dock is then opened to allow the product trapped in the hose to drain back into the dock drip pan for subsequent distribution to the dock slop handling system. Thus, there is a considerable amount of product surface area available for vaporization.

After a reasonable drain time has passed, the hose is disconnected at the deck flange, lifted with a dock crane to a near vertical position and allowed to completely drain through the dock manifold drain line. In our observations, approximately 200 feet of 6-inch diameter hose was used, and almost 300 gallons of trapped liquid cargo drained back to the dock drip tray. This draining occurred over a period of about 30 to 45 minutes since the draining rate was restricted by the small diameter drain bleed line. During the drain time, additional dock activities are underway to connect, disconnect, or move other hoses. When the hose is drained, a dock worker removes the hose flange from the dock manifold and the hose is placed on the dock. In some cases, the dock valve continues to leak during the hose draining procedure, and after a significantly long period (approximately 1-1/2 hours) it is decided by dock workers that the hose has drained, but that the flow through the dock manifold bleed valve was due to valve leakage. Subsequent tightening of the dock valve reduced this leakage to a drip.

The above hose draining procedures apply to terminals where the ship deck is at an appreciably higher (20 to 40 ft) elevation than the dock. For the case where the ship deck is lower, or about at dock height, the hoses are usually gravity drained into the ship tank prior to and after removal from the dock manifold. This reduces the amount of product returned to the dock drip trays and is, thus, a more desirable operation from a vapor exposure viewpoint.

Dock operating procedures require that respirators be worn when loading or unloading certain chemical products. In some cases the dock workers involved in hose hookup and in hose draining did not wear respirators or any special protective clothing at any time even though required by company regulations. When the dock workers were questioned about this, they indicated that, although it was an official company policy to utilize respirators, wind conditions were faborable during some loadings, and they did not believe it necessary to wear respirators or safety equipment. It was indicated that this was typically the case for handling many chemicals on the list that required respirators and protective clothing.

In summary, the hose hookup operations reveal that the greatest exposure for workers occurs during hose draining from ship to dock where

several products may be drained simultaneously into the drip trays beneath the dock manifold, while workers continue to perform dock operations in the near vicinity. Continuing sources of vapors can occur for periods of from 30 minutes to 1-1/2 hours or longer. Also, short exposures to vapors on the dock occur during initial removal of the flange blinds prior to hose hookup. Periods of from 3 to 5 minutes are spent removing blinds and hooking up hoses as residual products are draining through the manifold lines. Like-wise, short periods (3 to 5 minutes) of exposure can occur to dock workers and the ship's crew during on-deck hose disconnect and product sampling activities.

Loading of Barges

The mechanics of dockside hose hookup and disconnect are basically the same regardless of whether the vessel is a tanker or barge. The essential difference is the duration of these operations. In the case of chemical tankers, up to 25 different cargo hoses must be connected or disconnected throughout the duration of the loading operation which may run 24 to 36 hours. On the other hand, the single barges that were observed loaded, at most, three commodities. Each commodity hose loaded port and starboard tanks through a split drop on the barge deck. Thus, the hookup and disconnect operation was performed on only three hoses. In the case of multiple barge integrated tows, corresponding port and starboard barges are loaded through a single dock hose hookup. Transfer of product to the outer barge is effected by a hose connecting the outflow flange on one barge to the inflow flange on the other barge, (Figure II.4). Installation of the transfer hose is accomplished by the barge crew, whereas the dock hose hookup on the deck is performed by dock personnel.

Barge loading differs from tanker loading in the sense that the former is loaded visually by draft with frequent visual observation of liquid level through hatches or ullage ports. There were no flotation tape gauging systems on barges, and Lufkin tapes were used only after a tank had been topped. Conversely, tanker gauging is somewhat more sophisticated as discussed in the individual observation writeups in Appendix B.

The personnel that are involved in barge loading consist of:

(1) A tankerman who is responsible for deck operations during loading. This may be one individual if the loading duration is not excessive or it is his replacement in the case of an 18-hour, multiple barge, integrated tow.

(2) A dockman supervises the dockside activities, operates the *hose crane and communicates* with the tank farm regarding product pumping.

(3) A cargo inspector boards the barge to collect a sample at the beginning and end of loading. He may also hand-gauge each tank with a Lufkin tape and record product temperature.

(4) Two dockhands perform the deck-side hose hookup on a single barge. The number of dock workers on deck increases roughly in proportion to the number of barge pairs in an integrated tow.

18

FIGURE II.4   LOADING HOSE CONFIGURATION FOR BARGES SHOWING RELATIONSHIP OF BARGE AND DOCK

(5) In the case of an integrated tow, the tankerman is assisted
     by several deck hands. These unlicensed hands perform
     directed duties such as barge winching, visual gauging, etc.

Since the deck level on a barge is generally lower than dock level,
(Figure II.4) the sequence for disconnecting and draining hoses is usually
opposite that of a tanker. For the barge, the dock valves are first closed
against line pressure. A pressure bleed valve, just downstream of the dock
valve, is then opened and the line is gravity drained. The barge loading
valves are then closed, and the deck flange is disconnected. A line is
attached from the boom to the end of the hose, and it is lifted into the
air (~ 20 feet high). Any residual product in the hose drains backwards
through the open pressure bleed valve into the drip pan. When the hose has
finished draining, it is disconnected from the dock loading valves and laid
along the dock.

Although each cargo tank on a barge is fitted with a P/V valve that
is attached to a hatch, vapors are vented through open hatches. None of the
barges that were observed loaded with the hatches closed. Likewise, none of
the barges had a vapor discharge manifold and common mast risers.

II.3.3   Sources of Vapor, Sites of Vapor Accumulation, and Related Safety Hazards

Sources of vapor and sites of vapor accumulation were documented on
each of the terminal observations that were conducted, and they are enum-
erated below. The majority of the items in this list are based on observa-
tions; others are based upon opinions expressed by the workers.

(1) Numerous valve stem and flange blind leaks were observed at
     dock manifolds that were not in service. The liquid collects
     in drip trays for subsequent evaporation or gravity drain to
     a slop disposal system. This situation applies to dock facil-
     ities that utilize loading hoses. At these facilities there was
     no use of a continual water flush to dilute the product liquids
     and promote flushing to the treatment plant. A water flush
     system was observed at one facility that employed automatic
     loading arms.

(2) Large quantities (~ 5 gallons) of liquid can be discharged into
     the drip pan on the dock prior to hose hookup when the main
     product valve does not seal and liquid accumulates in the space
     between the valve and the flange. The discharge into the pan
     can result either from opening of the relief valve or inadver-
     tantly removing a flange blind before the liquid space has been
     drained. In the latter case, the sudden discharge of liquid
     could result in skin as well as vapor contact.

(3) Tankers normally have drip pans beneath the deck manifold, and
     any liquid that leaks past a flange connection drains to the
     ship's slop tank. However, in the case of barges, there is no
     slop tank on board, and material leakage at the deck flange
     accumulates in a catch basin. During one observation, the barge

20

catch basin did not contain dilution water, and a subsequent flange leak nearly filled the basin with raw product; in this case, gasoline. These basins do have a valved drain to which a drain hose can be attached. This situation could represent a site for evolution of both toxic and explosive concentrations of vapor, as well as the potential for a deck spill.

(4) On-deck diesel driven pumps are used to discharge products from barges (Figure II.4). Operation of the diesel engine, while loading operations that vent vapors to the atmosphere are taking place at adjacent berths, could present an explosive hazard. However, based upon experience, marine terminal operators have developed operating and safety procedures for diesel operation in terminals.

(5) During cargo loading, vapors are vented either at or near deck level or at elevation through a common vent riser. When products are vented near the deck, the vapors are discharged through open ullage ports and hatches and, frequently, simultaneously through dedicated P/V valves attached to the expansion trunk, (Figure II.5). The discharged vapor concentration can range from zero to roughly a saturated concentration depending on the stage of loading, the previous cargo in a tank and whether or not the tank was gas-freed at sea before docking. Under adverse wind conditions (negligible wind), heavier-than-air vapors tend to remain at deck level and are not readily disbursed, so it is possible that regions of high concentration that could pose a flammability or toxicity hazard might exist for longer periods of time than if the wind were sufficient to promote rapid dilution. Vapor discharge at elevation through a mast riser (Figure II.7) system may also pose a hazard. Vapors vented at elevations (30 to 40 ft above deck) will be diluted as they either descent toward the deck or are disbursed by the wind. The recently-introduced high speed pressure relief valve in Figure II.6 discharges the vapors near deck level, but the device is designed to project the vapors upward with high velocity, thus promoting more rapid dilution similar to high elevation venting. Deck level concentrations may present no health or flammability hazard if the wind conditions are favorable, a health hazard (hygienically significant concentrations), or both a health and flammability hazard when negatively buoyand plumes descend to deck level during periods of no wind.

There are two schools of thought regarding venting near deck versus venting at high elevation with respect to explosibility. Negatively buoyant vapors discharged near the deck are postulated to descend to deck level where they are free to flow over the side of the ship. Proponents of venting near the deck suggest that these vapors will be transported to areas where ignition sources are not present, i.e., over the water. These same proponents of low elevation venting suggest that, when vapors are discharged at elevation with no wind, there is a possibility that the vapors will descend and cover the entire ship

21
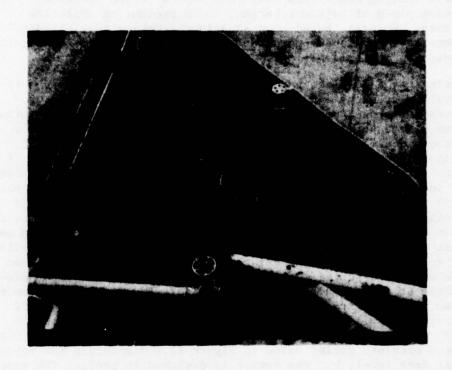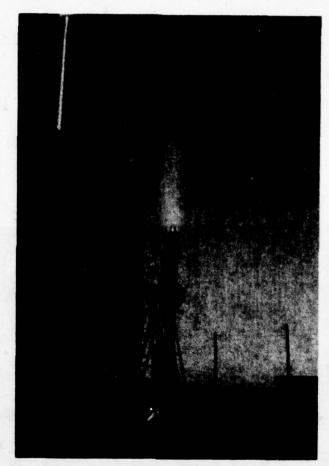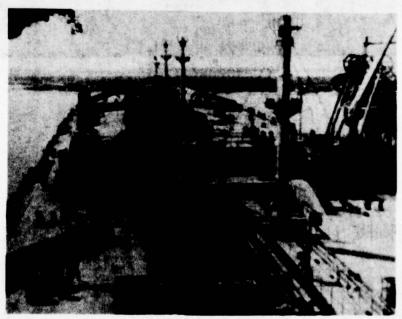
FIGURE II.5 DECK CONFIGURATION SHOWING HATCH, OPEN
ULLAGE PORT, P/V VALVE AND GAUGING
STANDPIPE

A. UNDER TEST

B. TANKER INSTALLATION

FIGURE II.6   HIGH SPEED PRESSURE/VACUUM RELIEF VALVE

23

FIGURE II.7   CLOSEUP OF VAPOR DISCHARGE PORTS
ON A VENT RISER SYSTEM

with an ignitable concentration. This logic, though unverified, does have some merit. On the other hand, proponents of high elevation venting indicate that vapors will have a greater opportunity to become diluted below the LEL regardless of wind conditions. The best method for minimizing the potential for a flammable atmosphere needs to be verified, but either method would appear to offer the possibility of producing hygienically significant vapor concentrations in the work area on deck.

(6) Following loading of a product into a ship tank, elevated above the dock, the deck manifold is disconnected first. The hose is then elevated by a crane, and any residual product is allowed to gravity drain through a drain valve on the dock manifold into a drip pan. The presence of a raw product surface on the dock presents the same potential for a health and flammability hazard as during flange opening, which was cited in Item (2).

(7) Some tanker configurations employ dedicated, steam-driven deep well pumps to discharge product. Under these circumstances, the product goes ashore directly from the tank, and it is not bypassed below deck through a foreward or aft pump room. This is also the case with barges. Dedicated deep-well pumps are usually fitted to cargo tanks that carry a dedicated chemical. Product purity dictates this configuration. However, tanks carrying non-critical product grades may be transported large distances below deck to a pumproom before being discharged. An individual pump in the pumproom may service several non-critical grades - the sequence being controlled by below-deck valves that have on-deck actuators. Any seal leak in the pump mechanism offers the potential for the accumulation of toxic or flammable product vapors in the pumproom. Likewise, vapors may accumulate in the pumproom due to imperfect seals on access ports to the bilge.

II.3.4   Workers' Habits

Some of the activities of the deck and dock crews during loading have been alluded to in previous sections of this report. In those cases, the potential for worker exposure, either through inhalation or skin contact, was also cited. Additional deck activities that have not already been described and which may present excessive exposure to liquids and liquid vapors are discussed below.

Generally, worker location on deck during loading is somewhat unstructured. Normally, one deck officer is in charge of operations during each watch. The watch officer directs the activities of a group of three or four able-bodied and ordinary seamen. None of the members of this group have a rigidly defined work station or work pattern. The loading operation requires periods of intense activity intermixed with periods of inactivity. Elevated exposures may exist while performing an assigned task or, under certain circumstances, during periods of inactivity. The minimum exposure levels correspond to the background concentration on deck.

The major potential vapor exposure related task is manual cargo gauging. This task is frequently performed in addition to checking of flotation tape gauging systems if the tanker is so outfitted. Manual gauging can take two forms:

(1) A deck hand can make a subjective evaluation of the ullage depth by observing the status of the liquid level relative to known internal tank structures (ladder rungs, web frame cutouts, etc.). In so doing, the worker's head is placed close enough to plane of an open ullage port to permit viewing of the liquid surface. During daylight hours, this type of gauging takes a longer period of time than at night because the eye is conditioned to daylight and does not accommodate rapidly when peering into a dark tank. This type of gauging, which is a direct consequence of human nature not to rely on tape gauging systems, may last from a few seconds to a minute. In addition, this type of gauging is routinely performed on barges, (Figure II.8).

(2) On tankers that do not have tape gauging systems, it is necessary to manually gauge with a Lufkin tape. This task can be performed either through open ullage ports or by inserting the tape into a small ID standpipe if the vessel is so outfitted (Figure II.9). In the former case, the potential for vapor exposure is of the same order as in Item (1). The use of a standpipe would appear to greatly reduce the level of exposure to discharged vapors because of the minimal liquid free surface area that is available for evaporation. On tankers and frequently on barges, individual tanks are hand-gauged with a Lufkin tape after the tank has been topped. Hand tape gauging may require 10 to 60 seconds. The length of time is governed somewhat by how rapidly the worker can establish when the tape bob contacts the liquid surface. The frequency of both types of gauging increases during the intermediate to final stages of loading when vapor concentrations are on the ascending portion of the emission curve, i.e., discharge of vapor blanket.

A crucifix may be used for final gauging of barge tanks. Crucifix gauging does not require the worker to put his head in the hatch. He inserts the crucifix into the open hatch or ullage port until the crosspiece contacts the rim of the opening. The crucifix is then withdrawn and the ullage is read in the same way that a crankcase dipstick is read on an automobile. Crucifix gauging, however, would appear to present a possibility for liquid/skin contact if the crucifix was completely withdrawn from the hatch at each reading.

Periods of inactivity pose a special set of problems. Tankermen on barges as well as tanker crews may go without sleep for extended periods of time. This situation can create fatigue, and, during periods of inactivity, these workers may be inclined to fall asleep on deck. Also, during these periods of inactivity, several workers gather around open barge hatches to rest and talk. The gathering point may be just downwind of this hatch.

26

FIGURE II.8   VISUAL GAUGING OF CARGO ULLAGE
THROUGH OPEN HATCH ON A BARGE

FIGURE II.9   MANUAL TAPE GAUGING THROUGH A TANK STANDPIPE

28

For an unloading operation, it was the opinion of the tankermen on barges that this operation should be of interest because, during the latter stages of unloading, the worker has his head in the hatch to ensure that the barge attitude is such that the discharge pump does not lose suction head. Since the product discharge rate is relatively low at this stage, the corresponding inflow rate of fresh air into the tank is minimal, and product vapors diffuse upward into the worker's breathing zone.

Additional comments from both chemical terminal and ship personnel are given in Appendix B.

II.4   Chemical, Physical, and Toxicological Properties Data and Other Health and Safety Related Topics

This section includes discussions of several topics that collectively bear upon health and safety in the marine chemical cargo transfer industry. These topics include:

(1)   Reference documentation of chemical, physical and toxicological properties for a representative group of chemicals that are transported by water.

(2)   Requests for public health record, health statistics and epidemiological data from the U. S. Public Health Service Hospital System.

Chemical, physical, and toxicological properties for a representative group of chemical commodities are presented in Table II-3. These data are utilized as inputs to the analytical models as well as a basis for future evaluation of situations that may be harmful to the worker's health. Data sources for Table II-3 are given in Table II-4.

The U. S. Public Health Service Hospital System administers to the medical needs of seamen. Patient medical records from eight of the system's hospitals are coded for computer storage and retrieval. Coding is based on the International Classification of Diseases-A8, where the suffix indicates that the eighth edition has been adopted for use in the United States. A computer search was conducted by USPHS personnel with a goal of identifying the frequency of morbidity and mortality in seamen due to vapor exposure during fiscal years 1970 through 1977. This search was conducted in each of ICDA-8 diagnostic categories shown in Table II-5. The raw data were reviewed by a toxicologist and an epidemiologist. The conclusion was that the data, as tabulated in the computer, did not permit formulation of statements or judgments as to the existence or absence of excess disease risks in seamen due to vapor exposure. To enable an epidemiologic analysis of the data, the following essential information would be needed:

1.   What is the population covered, i.e., all patients at PHS hospitals or the occupational group of interest?

2.   Definition of "seamen beneficiaries" in terms of eligibility criteria, total number, etc.

3.   What is the meaning of disease incidence: morbidity, mortality or both?

29

4. In light of the probability that some seamen might be seen at more than one PHS hospital, are individuals repeated by hospital, by year or by diagnosis?

5. Are the codes for primary or secondary tumor sites? If metastatic tumors, are these only for persons on whom no primary code exists?

6. What is the basis of diagnosis? Histopathology?

7. What is the age, sex, ethnicity and nationality for all cases?

8. What is the usual occupation and/or previous occupation of each case at the time of diagnosis?

The following information would also be useful in performing an epidemiologic analysis:

1. Who coded the data?

2. What is the employment history of each case in terms of jobs, travel, time on each job, etc.?

3. What is the work pattern: hours, usual shift pattern, etc.?

4. What were the major exposures experienced by each case?

5. What are the personal habits in terms of smoking, use of alcohol, use of drugs, etc.?

6. Usual place of residence.

7. Date and place of birth, marital history, military service.

8. Family history of disease, especially tumors.

9. General health data, illnesses.

10. Dates of admission and discharge.

11. Current status – alive or dead.

12. What is the likelihood that persons eligible for USPHS treatment go elsewhere?

13. What is the total number of "seamen beneficiaries" or of the proposed population to be studied?

TABLE II-3(a). CHEMICAL PROPERTY DATA

COMPOUND	Molecular Weight	Boiling Point @ 1 Atm. °F	Surface Tension Dynes/cm, 68°F	Viscosity Gas, 68°F (cp)	Vapor Specific Gravity	Vapor Pressure (psia, 68°F)	Liq. Specific Gravity (68°F)	Critical Temperature (°F)	Critical Pressure (psia)
Acetic Acid	60.05	244	27.8	.0076	2.07	0.23	1.051	611	839
Acetone	58.08	133	23.7	.0077	2.0	3.7	0.791	455	682
Acrylonitrile	53.06	171	27.3 @ 24°C	---	1.83	1.7	0.8075	505	660
Benzene	78.1	176	28.9	.0074	2.69	1.5	0.879	552	710
n-Butyraldehyde	72.1	167	24.6	.01	2.49	2.9	0.803	484	590
Carbon Tetrachloride	153.8	170	27.0	.0195	5.3	1.8	1.59	541	660
Cresols	108.1	350	37.0	---	3.7	0.012	1.03-1.07	---	---
Cumene	120.2	306	28.2	.0063	4.26	0.28	0.866	676	466
Ethanolamine	61.1	338	51.0	---	2.11	0.006	1.016	646	647
Ethylenediamine	60.1	243	43.0	.0075	2.07	0.20	0.909	608	941
Ethylene Dicl.	99.0	182	32.2	.008	3.41	1.3	1.253	550	735
Ethylene Gly.	62.1	387.7	52.5	.0077	2.14	0.0013	1.115	705	1120
Gasoline	---	58-390	19-23	---	---	---	0.67-0.75	---	---
Iso-Propylamine	75.11	320	17.5	.0076	2.59	0.014	0.961	622	850
Methanol	32.0	148.1	22.6	.0135	1.10	1.9	0.792	469	1142
Styrene	104.0	293.4	32.16	.0064	3.59	0.095	0.906	703	580
Toluene	92.1	231.1	29.0	.0068	3.18	0.42	0.867	605	596
Toluene Di Isocynate	174.2	482.0	25.0 Est.	---	6.0	0.0038 @ 130°F	1.22 @ 77°F	---	---
Vinyl Acetate	86.1	163.2	24.0	.008	2.97	1.8	0.934	486	617

TABLE II-3(b). CHEMICAL PROPERTY DATA

Compound	CHEMICAL AND PHYSICAL PROPERTIES								
	Molecular Weight	Boiling Point @ 1 atm. (°F)	Surface Tension (dynes/cm) (68°F)	Viscosity Gas, 68°F (cp)	Vapor Specific Gravity	Vapor Pressure (psia,68°F)	Liq.Spec. Gravity (68°F)	Critical Temp. (°F)	Critical Press. (psia)
Naphtha VM&P	---	200-300	19-23	---	---	.07 @ 80°F	0.75	---	---
Methy Ethyl Ketone	72.11	175.3	24.4	.069	2.49	1.5	0.8	504	602
n-Heptane	100.21	209.1	19.3	.060	3.45	0.68	0.684	512.6	397
Glycerine (Glycerol)	92.1	554	63.4	.073	3.17	0.2 @ 329°F	1.26	845.6	965
2 - Ethyl Hexanol	130.3	364.5	27.6	---	4.49	0.0036	0.834	711	512
Ethyl Alcohol	46.07	172.9	22.5	.084	1.6	0.82	0.79	469.6	926
Epicloro-hydrin	92.53	239.4	37.0	.083	3.19	0.26	1.18	613.4	721
Fuel Oil #2	---	540-640	25.0	---	---	0.04	0.87-0.90	---	---
Diesel Oil	---	550-640	25.0	---	---	0.04	0.876	---	---
Kerosene	---	392-500	47-49	---	---	0.04	0.8 @ 59°F	---	---

TABLE II-3(c). CHEMICAL PROPERTY DATA

COMPOUND	TOXICOLOGICAL PROPERTIES				FLAMMABILITY PROPERTIES		
	T L V (ppm)	STEL, STIL (ppm/min)	Odor Threshold (ppm)	Excursion Value (Max ppm)	Flash Point °F/Test Type	L.E.L. (% Vol)	U.E.L. (% Vol)
Acetic Acid	$10^{a,b,d}$	$15^a/15$, $40^d/5$	1^d	--	112/O.C. 104/C.C.	5.4	16
Acetone	$1000^{a,b,d}$	$1250^a/15$, $3000^d/30$	100^d	--	4/O.C. 0/C.C.	2.6	12.8
Acrylonitrile	$20^{a,b,d}$(skin)	$30^a/15$, $40^d/30$	--	--	30/C.C. 31/O.C.	3.05	17
Benzene	1^j(skin) $10^{a,d}$(skin)	$75^d/30$	4.68^d	5^j	12/C.C.	1.3	7.9
n-Butyraldehyde	197^1	--	$.0046^d$	--	15/O.C. 20/C.C.	2.5	10.6
Carbon Tetrachloride	$10^{a,b,d}$(skin)	$25^a/15$, $25^d/30$, $200^b/5$ in any 4 Hrs	10^d	25^b	Not Flammable	→	--
Cresols	$5^{a,b,d}$(skin)	--	5^d	--	175-185/O.C.	1.4 Ortho 1.1 Meta,Para	--
Cumene	$50^{a,b,d}$(skin)	$75^a/15$	--	--	111/C.C.	0.9	6.5
Ethanolamine	$3^{a,b,d}$	$6^a/15$	--	--	185/C.C.	--	--
Ethylenediamine	$10^{a,b,d}$	$20^d/5$	--	--	99/O.C.	5.8	11.1
Ethylene Dicl.	$50^{a,b,d}$, 5^{c*}	$75^a/15$, $15^c/15$, $200^b/5$ in any 3 Hrs.	100^d	100^b	60/O.C. 55/C.C.	6.2	15.6
Ethylene Gly.	$100^{a,d}$	$125^a/15$	--	--	240/O.C. 232/C.C.	3.2	--
Gasoline	Composition Dependent	$500^d/30$	0.25^d	--	-50 to 73/C.C.	1.1 - 1.4	7.1 - 7.4
Iso Propylamine	$5^{a,b,d}$	$10^a/15$	10^a	--	165/O.C.	2.2 Calc	12 Est.
Methanol	$200^{a,b,c*,d}$(skin)	$250^a/15$	100^d	--	54/C.C. 61/O.C.	6.0	36.5
Styrene	$100^{a,b,d}$	$125^a/15$, $100^b/30$, $600^b/-$ in any 3 Hrs.	0.148^d	200^b	93/O.C. 88/C.C.	1.1	6.1
Toluene	$100^{a,b,c,d}$(skin)	$150^a/15$, $500^b/10$, $200^c/10$, $600^c/30$	0.17^d	300^b	40/C.C. 55/O.C.	1.27	7.0
Toluene Di-Isocyanate	$0.02^{a,d}$, $.005^c$	$.02^d/5$, $.02^c/20$	$0.4 - 2.14^d$	$0.02^{a,h}$	270/O.C.	0.9	9.5
Vinyl Acetate	$10^{a,d}$	$20^a/15$	0.12^d	--	18/C.C. 23/O.C.	2.6	13.4

TABLE II-3(d). CHEMICAL PROPERTY DATA

Compound	TOXICOLOGICAL PROPERTIES				FLAMMABILITY PROPERTIES		
	TLV (ppm)	STEL, STIL (ppm/min)	Odor Threshold (ppm)	Excursion Value (max.ppm)	Flash Point (°F/Test Type)	LEL (% vol)	UEL (% vol)
Naphtha: VM&P	---	500/30[d]	---	---	20- 55/c.c.	0.9	6.7
Methy Ethyl Ketone	200[a,b,d]	250 or 300/15[a]	10[d]	---	20/c.c. 22/o.c.	1.8	11.5
h-Heptane	500[d,b] 400[a]	500/15[a] 500/30[d]	---	---	250/c.c.	1.0	7.0
Glycerine (Glycerol)	---	---	---	---	350/o.c. 320/c.c.	---	---
2 - Ethyl Hexanol	---	---	---	---	185/o.c. 175/c.c.	---	---
Ethyl Alcohol	1000[a,b,d]	1000/15[d]	10[d]	---	64/o.c. 55/c.c.	3.3	19.0
Epicloro-hydrin	5[d] 5[a,b](skin)	10/30[d] 10/15[a]	10[d]	---	92/o.c. 100/c.c.	3.8	21.0
Fuel Oil #2	---	---	---	---	136/c.c.	---	---
Diesel Oil	---	---	---	---	100 to 125/c.c.	1.3	6.0
Kerosene	200[d]	---	1	---	100 min/c.c.	0.7	5.0

TABLE II-4.   DATA SOURCES FOR TABLES II-3

(a)   A.C.G.I.H., 1977 (American Conference of Governmental
         Industrial Hygienists

(b)   OSHA, 29 CFR and 1910.1000 Table Z-1, Z-2.

(c)   NIOSH Occupational Exposure Publications (8 Hr.W.D., 40 Hr.W.W.)

(c)*   "   "   "   "   (10 Hr.W.D., 40 Hr.W.W.)

(d)   CHRIS Vol. II (Chemical Hazards Response Information System)

(e)   Perry Chemical Engr. Handbook, Table 14.47, Page 14-22.

(f)   Carbide & Carbon Chemical Corporation, 50 East 42nd Street,
         New York, N.Y.

(g)   *Handbook of Chemistry & Physics*, 57th Edition.

(h)   Manufacturing Chemists Association, Inc., Chemical Safety
         Data Sheets.

(i)   Registry of Toxic Effects of Chemical Substances, 1975.

(j)   Federal Register, Vol. 42, No. 85, Thursday, May 3, 1977.

STEL   Short Term Exposure Limit, allows 4 excursions (15 min. each,
         with 60 min. between exposure), (ACGIH)

STIL   Short Term Inhalation Limit, maximum exposure/time interval
         (CHRIS, Vol. II)

TABLE II-5.   DISEASE CATEGORIES FOR USPHS COMPUTER SEARCH

(From 8th Revision, International Classification
of Diseases, Adapted)

Diagnostic Category	Description
140-239 (all)	Neoplasms
283	Acquired hemolytic anemias
284	Aplastic anemia
285	Other and unspecified anemias
289	Other disease of blood
307	Transient situational disturbance
301-315	Mental retardation
348	Motor neurone disease
355	Other neuralgia and neuritis
357-358	Peripheral nervous diseases
378	Other diseases of eye
379	Blindness
425	Cardiomyopathy
490-491	Bronchitis
492,510	Emphysema
515-516	Pneumoconiotic diseases
570	Liver necrosis
571	Cirrhosis of liver
606	Sterility, male
692	Dermatitis
780-781	Symptoms referable to nervous system
783	Symptoms referable to respiratory system
790	Nervousness and debility
791	Headache
980-984,987,989	Toxic effects, various
E860,E864,E865, E867,E869,E876, E877,E909,E924, E942,E945,E980, E982	Accidental poisonings, various

II.5   Current and Proposed Regulations

This section contains a review of the regulations that pertain to the transfer of hazardous chemical cargos in marine operations. Agencies having regulatory input at the Federal level include the Coast Guard, OSHA, and EPA. The states of California and Texas were included in this review because of the extent of chemical marine terminal operations in these states and because of their active approach to health, safety, and environmental subjects. The regulations of these agencies are briefly discussed below and are summarized in Table II-6.

Coast Guard Regulations

The applicable titles in the CFR, which address the Coast Guard's authority to the subject matter, are Titles 33 and 46. In Title 33, Part 126, shore-side transfer or loading of hazardous materials is discussed. Vessel-side regulations are contained in Title 46, Subchapter D, Parts 30 through 40, and Subchapter O, Parts 150 through 154. A very recent revision to some of the above subchapters can be found in the Federal Register, Vol. 42, No. 196, September 26, 1977. The parts that are affected by this revision are Parts 30, 31, 32, 35, 40, and 151. In addition, Part 39 was revoked and Part 153 was added. Further remarks concerning the applicability of the above regulations are shown in Table II-6.

OSHA Regulations

Of particular sections in OSHA Regulations 29 CFR, Parts 1910, 1915, and 1918 are applicable. Excluding ship's personnel, jurisdiction appears to apply to all other workers that are involved in ship repair and cargo handling.

Environmental Protection Agency (EPA) Regulations

The EPA has been primarily concerned with determining the quantity of hydrocarbon emissions from loading and unloading of gasoline and crude oil as indicated by the contents of EPA 450/3-76-038, Volumes A and B, and EPA 450/3-77-024. In the Federal Register for November 6, 1973, ship and barge emission regulations were given for the Houston-Galveston area in the form of requirements for vapor recovery systems. However, this regulation has been suspended indefinitely. There seems to be no national performance standard for ship and barge activites at this time.

Texas Air Control Board (TACB) Regulations

TACB regulations are concerned with the emissions from loading and unloading facilities for tank trucks and railroad tank cars. Marine cargo transfer facilities are excluded.

California Administrative Code (CAC)

A review of the California Administrative Code revealed that, of those sections of the CAC code that pertain to transportation of petroleum, only transportation by pipeline was included and that truck, rail, or ship

transportation was excluded. CAC codes reference OSHA regulations for ship building, repairing, and ship breaking. However, CAC regulations are applicable only up to the dockside end of the gangway.

In addition to reviewing current Federal and selected State regulations on chemical cargo transfer operations, efforts were expanded to include both proposed regulatory standards and international voluntary standards.

Proposed Standards

In the area of proposed Federal regulations, an internal study of chemical cargo transfer operations has been made by OSHA. The results of that study have led to the drafting of a safety and health standard for marine terminal operations. As it pertains to the problem of interest, this standard would

    (1)   require compliance with 33CFR126, and

    (2)   incorporate a modified form of 29CFR 1918.86 to cover hazardous chemical atmospheres in tanks and confined spaces as well as the hazards posed by tank vents and hatch openings.

This standard would require ventilation and monitoring tests to assure a safe tank atmosphere for man-entry. The draft standard addresses the need for warning signs and the conditions under which protective clothing and respirators would be required.

The current OSHA position with regard to jurisdiction in a marine chemical cargo transfer facility is as follows. That portion of the OSH Act which pertains to chemical cargo transfer operations is contained in 29CFR Part 1918. This part, specifically 1918.86, applies to transfer of any hazardous cargo (dry or liquid). It applies to all land-based U. S. citizens engaged in domestic and foreign cargo transfer regardless of whether they are longshoremen or not, but foreign crews are exempt. This part is judged by the OSHA solicitors to also apply to domestic ship crew members; this judgement has not been tested, and, therefore, its legality is still in question. This draft standard is currently under review, and it has not been submitted for rule-making.

International Standards

Information on voluntary international standards was reviewed. Each organization's contribution to the safe handling of hazardous chemical cargos is summarized below.

International Chamber of Shipping (ICS)

The ICS has published a set of voluntary safety standards that are applicable to the shipping of hazardous cargos. These standards are divided into two guides: petroleum and chemical. In Volume 1 of the chemical guide, which is applicable to this project, safe handling procedures for hazardous

chemicals are discussed in depth. Volumes 2, 3, and 4 contain chemical
safety data sheets for a wide range of bulk liquid cargos. The guide dis-
cusses handling of chemical cargos and ballasting, gas freeing, tank clean-
ing, and work in enclosed spaces. In addition, various precautionary steps
are discussed such as fire hazards, ignition sources, and the variation of
vapor concentrations during operations. Also, health hazards from skin
contact are emphasized.

Oil Companies International Marine Forum (OCIMF)

The OCIMF (formerly IOTTSG) published an extensive safety guide
which recommends safe practices for loading and discharging of cargos and
related operations involving crude oil and petroleum products. Its recom-
mendations are compatible with those found in the ICS Guide on Petroleum.
Although not directed specifically to chemical transfer, the guide contains
related material in the form of experimental and analytical treatment of
hydrocarbon gas evolution and dispersal during cargo transfer.

Inter - Governmental Maritime Consultative Organization (IMCO)

The IMCO, through its subcommittee on Carriage of Dangerous Goods, is
currently considering and investigating requirements for the development of
internationally-accepted port regulations. It has been ascertained that many
of the chemicals that have been addressed in this project will be included in
the study. However, it will be some time before any formal document will be
completed.

Organization for Economic Co-Operation and Development (OECD)

The function of the OECD is to promote economic development in its
member countries. Contained in this organization are various groups, one
of which is the Chemical Group. This group has recently prepared a report
on the regulations relating to environmental chemicals. The report is an
overview of legislation from the member countries aimed at control of environ-
mentally hazardous chemicals. The basic content of Parts I and II applies
to existing and proposed legislation that assesses the effect of chemicals,
pesticides, and poisons on humans and the environment prior to their market-
ing. The last part of the report provides a brief description of post market
control of hazardous chemicals. While the bulk of the regulations in Part
III deal with air and water pollution, total disbandment of specific sub-
stances, and protection of the work place, some consideration is given to
the control of transportation of chemicals. However, it is either not
delineated as to what these transportation regulations are, or it is stated
that no action has been taken at the present time.

Additional Regulatory Considerations

The intrusion of chemical substances into the environment and the
possible threats posed to the environment, in general, and human health, in
particular, as a consequence of such intrusions, are receiving increasing
attention. A considerable program of regulation is evolving at the Federal
level.

Typical chemicals of concern to this investigation are listed in Table II-7. Many of these are also included in the program of Criteria Document Development by the National Institute for Occupational Safety and Health; criteria document issuance is preliminary to the issuance of occupational standards by the Occupational Safety and Health Administration. The schedule of criteria document issuance by NIOSH as of October 1977, is also indicated in the table.

Many of these same chemicals are also included in the regulatory plans of the Environmental Protection Agency for the control of spills of chemicals into the aquatic environment. A preliminary list of 306 chemicals was published in the Federal Register on 30 December 1975 (Vol. 40, No. 250) for designation of hazardous substances to be made subject to spill prevention, control and countermeasure regulation. In March of 1978, the list, reduced to 271 chemicals, was officially promulgated; an additional 28 chemicals was also proposed for later designation. This information too is indicated in Table II-7.

Proposed regulatory activity relating to these and other chemicals has resulted in the amassing of a substantial amount of data concerning the physical, chemical, and toxicological properties of the chemicals. However, the chemicals under consideration represent but a tiny fraction of the total number of chemicals known and in use.

TABLE II-6. SUMMARY OF FEDERAL AND STATE REGULATIONS

Agency	Regulation Code No./Title	Applicable Contents	Remarks
USCG	33CFR, Part 126, "Handling of Explosives or Other Dangerous Cargos Within or Contiguous to Waterfront Facilities"	Shoreside regulations for handling cargos listed in 46CFR, Table 30.25-1 and 33CFR Surpart 124.14.	Facility must have proper surveillance, prohibition of smoking, control of hotwork and operation of motor vehicles during cargo transfer, good housekeeping, proper lighting, and fire protection equipment. Prior to transfer of cargo, the person in charge must have warning signs displayed, pans or buckets placed under cargo hose connections, cargo information cards for the specific cargo to be transferred, and a "Declaration of Inspection" from the vessel which is to transfer or receive cargo.
	46CFR, Subchapter D, Parts 30-40, "Tank Vessels"	Requirements for materials, design, construction, inspection, manning and cargo handling for tankships and barges.	Applicable parts of this subchapter are Parts 30, 32, and 35.
	46CFR, Part 30, "General Provisions"	Definition of applicable terms in Subchapter D.	Reid Vapor Pressure (RVP)-Vapor pressure of liquid in pounds per square in.@ 100°F flammable liquid – any liquid whose flash point is less than 80°F (open cup) combustible liquid – any liquid whose flash point is greater than 80°F Grade A Cargo – flammable liquid that has a RVP greater than 14 psi Grade B Cargo – flammable liquid that has a RVP greater than 8.5 psi but less than 14 psi Grade C Cargo – flammable liquid that has a RVP less than 8.5 psi Grade D Cargo – combustible liquid with flash point between 150°F and 80°F Grade E Cargo – combustible liquid whose flash point is greater than 150°F
		Cargos regulated by Subchapter D.	Listed in Table 30.25-1 of Part 30.
	46CFR, Part 32 "Special Equipment, Machinery, and Hull Requirements"	Liquid level gauging for tankships constructed after July 1, 1951.	Gaging of cargo tanks carrying Grade A liquids shall be done without opening ullage hatches, cargo hatches, or Butterworth, such as with a sounding tube.

41

TABLE II-6. SUMMARY OF FEDERAL AND STATE REGULATIONS (CONTD)

Agency	Regulation Code No./Title	Applicable Contents	Remarks
USCG	46CFR, Part 32 "Special Equipment, Machinery, and Hull Requirements"	Pumps, piping and hose for cargo handling on tankships constructed after July 1, 1951.	Fixed piping systems are required for all Grade A through E cargos, and they shall not run through spaces where ignition sources are present.
		Inert gas systems.	Required on all tankships of 100,000 DWT after January 1, 1975, except for liquified gas cargo and Grade E cargo that is transported at a temperature of 9°F below its flash point. Oxygen level of inert gas must be less than 5% by volume.
		Venting requirements for cargo tanks on tankships constructed after July 1, 1951.	All cargo tanks on tankships carrying: Grade A liquid must be fitted with a vent system consisting of branch vent lines connected to vent header terminating at a height of 4 meters above the weather deck and an equal distance away from any living or working space or sources of ignition. The branch vent lines must have either no valves or pressure/vacuum (P/V) valves that allow pressure relief of the cargo tank. A flame arrester or P/V valve must be fitted on the vent header. Grade B and C liquids must be fitted with individual P/V valves and vent lines extending to a reasonable height above the weather deck or a venting system as noted for Grade A liquids. Grade D and E liquids must be fitted with a goose-neck vent and flame screen.
	46CFR, Part 35, "Operations"	Venting requirements for cargo tanks on barges constructed after July 1,1951	All cargo tanks of barges carrying: Grade A,B, and C liquids must be fitted with a vent system as noted for Grade B and C liquids on tankships. Grade D and E liquids must be fitted with a vent system as noted for Grade D and E liquids on the tankships.
		Inspection and testing required for repairs or alterations in and around cargo tanks that have carbulk flammable or combustible liquids.	Inspection will be carried out in accordance with the "Standard for the Control of Gas Hazards on Vessels to be Repaired, NFPA Code No. 306" by a marine chemist or a person authorized by the Officer in Charge. When neither are reasonably available, the senior officer of the vessel will inspect the tank.

42

TABLE II-6. SUMMARY OF FEDERAL AND STATE REGULATIONS (CONTD)

Agency	Regulation Code No./Title	Applicable Contents	Remarks
USCG	46CFR, Part 35, "Operations"	Cargo handling, personnel and procedures	A sufficient number of crew members shall be on duty to perform cargo transfer operations. For an unmanned barge, a person holding a valid license as Master, Mate, Engineer, or Certified Tankerman shall be present. Prior to transfer of cargo, the tank vessel shall be electrically bonded to the shore, sea valve and scupper shall be closed, and pans or buckets shall be placed under cargo hose connections. A "Declaration of Inspection" check list shall be completed to assure readiness for cargo transfer and protection against fire hazards.
	46CFR, Subchapter O, Parts 150-154, "Certain Bulk Dangerous Cargos"	Uniform minimum requirements for unmanned barges and self-propelled vessels as per bulk liquid cargo carried.	Applicable parts of this subchapter are Parts 151, 153, and 154.
	46CFR, Part 151, "Unmanned Barges Carrying Certain Bulk Dangerous Cargos"	Cargo tank venting requirements for unmanned barges are listed in Table 151.05 on a per chemical basis.	Type of cargo venting includes open, pressure/vacuum (P/V), and safety relief (SR) venting. o Open venting of cargo tanks allows no restriction on movement of vapor or liquid to or from the tank through the vent line. The outlet should terminate in a goose-neck bend at a reasonable height above the weather deck. o Pressure/vacuum venting requires that a pressure/vacuum valve be placed in the vent piping to automatically limit the pressure or vacuum in a cargo tank. o Safety relief venting requires that a safety relief valve be placed in the vent line to automatically limit the pressure in the cargo tank.
		Cargo tank gaging requirements for unmanned barges are listed in Table 151.05 on a per chemical basis.	Types of cargo gaging include open, restricted, and closed gaging. o Open gaging allows determination of cargo liquid level through any opening in the tank such as ullage hole or tank hold. This method exposes the gage user to the cargo and its vapors. o Restricted gaging is performed through a gaging device such as a sounding tube that penetrates the tank and

43

TABLE II-6. SUMMARY OF FEDERAL AND STATE REGULATIONS (CONTD)

Agency	Regulation Code No./Title	Applicable Contents	Remarks
USCG	46CFR, Part 151, "Unmanned Barges Carrying Certain Bulk Dangerous Cargos"	Cargo tank gaging requirements for unmanned barges are listed in Table 151.05 on a per chemical basis.	limits the amount of release of cargo vapor. If a sounding tube is used, the vent system shall be designed to prevent pressure buildup in the cargo tank. o Closed gaging is performed through a device that penetrates the cargo tank and prevents any release of cargo liquid or vapor during gaging (e.g., automatic float, and continuous tape).
		Cargo handling, personnel and procedures for unmanned barges.	A certified tankerman must be on duty to perform cargo transfer. Specific duties are similar to those described in 46CFR, Part 35.
	46CFR, Part 153, "Safety Rules for Self-Propelled Vessels Carrying Hazardous Liquids"	Cargo tank venting and vent height requirements for self-propelled vessels are listed in Table I of Part 153 on a per chemical basis.	Open and pressure/vacuum venting are as defined in 46CFR 151. For specific chemicals, discharge height of vents shall be in accordance with the B/3 (1/3 breadth of the ship) or 4m (4 meter) venting systems. For other chemicals there are no specific height restrictions. o B/3 venting system requires that the vent discharge shall be at least 15 meters from any air intake or openings to accommodation or service spaces and shall be at least B/3 of 6 meters above weather deck, whichever is larger. If the discharge is within 6 meters of a walkway, then its height must be 6 meters above the walkway. o 4m venting system requires that the vent discharge shall be at least 10 meters from any air intake or openings to accommodation of service spaces and at least 4 meters above the weather deck or walkway if the discharge is within 4 meters of the walkway. o High velocity vents may be used in place of the B/3 or 4m venting systems as approved by the Commandant.
		Cargo tank gaging requirements for self-propelled vessels are listed in Table I of Part 153 on a per chemical basis.	Types of cargo tank gaging are open, restricted and closed. o Open gaging is as noted in Part 151. o Restricted gaging is as noted in Part 151 and cannot have an orifice diameter of more than 20 cm. If P/V venting is used in conjunction with restricted gaging, the P/V valve will be locked open or the P/V valve will be bypassed.

44

TABLE II-6. SUMMARY OF FEDERAL AND STATE REGULATIONS (CONTD)

Agency	Regulation Code No./Title	Applicable Contents	Remarks
USCG	46CFR, Part 153, "Safety Rules for Self-Propelled Vessels Carrying Hazardous Liquids"	Cargo tank gaging requirements for self-propelled vessels are listed in Table I of Part 153 on a per chemical basis.	o Closed gaging is as noted in Part 151 and must have a vapor return connection and a high level alarm as described in Subpart 153.409.
		Personnel safety requirements for self-propelled vessels are listed in Table I of Part 153 on a per chemical basis.	The Master shall ensure that personnel on the ship wear tight fitting goggles or face mask when sampling, transferring, connecting or disconnecting a hose, tank gaging or opening a cargo hatch, ullage hatch or Butterworth. Additional protection such as coveralls and boots shall be worn for the handling of certain chemical cargos. Man-entry into spaces that have contained certain cargos cannot be performed unless the Master ensures that the space is free of toxic vapors and has sufficient oxygen to support life. The person entering the space must wear a 30-minute self-contained breathing apparatus and be closely supervised by an officer of the ship.
	46CFR, Part 154, "Special Interim Regulations for Issuance of Letters of Compliance"	Interim regulations for foreign vessels carrying certain hazardous bulk cargos.	Plan, review, and examination procedures for foreign shippers that carry dangerous cargos are listed in Table I of Part 154.
OSHA	29CFR, Part 1910 "Occupational Safety and Health Standards"	Definition of flammable liquids.	Flammable liquid - any liquid having a flash point below 100°F by closed cup method. Class IA liquids - flammable liquid with a flash point below 73°F and having a boiling point below 100°F. Class IB liquids - flammable liquid with a flash point below 73°F and having a boiling point above 100°F. Class IC liquids - flammable liquid with a flash point between 73°F and 100°F.

TABLE II-6.   SUMMARY OF FEDERAL AND STATE REGULATIONS   (CONTD)

Agency	Regulation Code No./Title	Applicable Contents	Remarks
OSHA	29CFR, Part 1910 "Occupational Safety and Health Standards"	Definition of combustible liquid.	Combustible liquid - any liquid having a flash point above 100°F by closed cup method. Class II liquids - combustible liquid with a flash point between 100°F and 140°F. Class IIIA liquids - combustible liquid with flash point between 140°F and 200°F. Class IIIB liquids - combustible liquid with a flash point above 200°F
	29CFR, Part 1915, "Safety and Health Regulations for Ship Repairing"	Personnel jurisdiction.	Applies to all persons involved in ship repair other than Master, ship's officers, and crew of vessel.
		Precautions to be taken before entering ship spaces which may contain flammable or toxic vapors.	Atmosphere must not contain a concentration of flammable vapor or gas greater than 10% of the lower explosive limit. Atmosphere must be checked for toxic contaminants. Oxygen content must be at least 16.5% by volume.
	29CFR, Part 1918, "Safety and Health Regulations for Longshoring"	Personnel jurisdiction.	As noted in Part 1915.
		Handling of hazardous material.	Personnel handling hazardous cargo must be informed that the cargo is hazardous and must be provided with necessary personal and fire protection equipment.
EPA	Federal Register, Nov. 6, 1973 Regulation.	Recovery of vapors emitted during loading and unloading of gasoline and other volatile compounds from ships and barges in the Houston-Galveston Area.	Indefinitely suspended, 10/6/76.
TACB	Regulation V, "Control of Air Pollution from Volatile Carbon Compounds"	Maximum emissions concentration at loading and unloading facilities.	Vapor recovery system required unless volatile component partial pressure is less than 1.5 psia, as applied to tank truck trailer and railroad tank car. Facilities for ships and barges are excluded.

46

TABLE II-6. SUMMARY OF FEDERAL AND STATE REGULATIONS (CONTD)

Agency	Regulation Code No./Title	Applicable Contents	Remarks
TACB	Regulation VI, "Control of Air Pollution by Permits for New Construction or Modification"	Control of emission from facilities that emit air contaminants.	No specification of how control is to be achieved. This regulation does not apply to shipboard chemical vapor emissions.
CAC	Chap. 4, "Division of Industrial Safety." Subchapter 15, "Petroleum Safety Order — Refining, Transportation and Handling."	Equipment and operations used in processing, storage and handling of petroleum, natural gas and their products	Transportation regulations are limited to pipeline only. Truck, rail and ship carriers are excluded.
CAC	Subchapter 18, "Ship and Boat Building Safety Orders"	Ship and boat building, repair and breaking operations up to the dock side end of the gangway. All shoreside equipment used in loading or unloading material onto vessel.	Regulations are patterned after OSHA Regulations, Parts 1915, 1916, and 1917.

TABLE II-7. NIOSH AND EPA DISPOSITION ON CHEMICALS OF INTEREST

Chemical	NIOSH Criteria Documents	EPA[h] Hazardous Material Classification
Acetic Acid	---	Yes
Acetone	4/78 [g]	No
Acrylonitrile	8/78 [a]	Yes
Benzene	Issued [b]	Yes
n-Butyraldehide	---	No
Carbon Tetrachloride	Issued [f]	Yes
Cresols	11/77	Yes
Cumene	---	No
Epichlorohydrin	Issued	Yes
Ethanolamine	FY 81	No
Ethylene Diamine	FY 80	Yes
Ethylene Dichloride	Issued	Yes
Ethylene Glycol	FY 81	No
Gasoline	Issued [c]	Yes [d]
Methanol	Issued	No
Metylethyl Ketone	4/78 [g]	No
i-Propylamine	FY 79 [e]	No
Styrene	7/78	Yes
Toluene	Issued	Yes
Toluene Diisocyanate	Issued	No
Vinyl Acetate	4/78	Yes

[a] Suspect carcinogen - proposed ETS 4 ppm

[b] Suspect carcinogen - proposed ETS 1 ppm
 Two criteria documents issued.

[c] Criteria document covers "Alkanes"

[d] Covered under Oil Spill, Prevention, Control and Countermeasures regulations.

[e] Document covers "Aliphatic Primary Amines"

[f] Two criteria documents issued.

[g] Included in Ketone criteria document.

[h] "Proposed Hazardous Chemical Designation," Federal Register 43, No. 49, March 13, 1978.

III. ANALYTICAL MODEL DEVELOPMENT

The development of analytical models was divided into two categories, an on-deck vapor dispersion model and an in-tank gas freeing model with vapor regeneration from cargo residue. The analytical models are presented and discussed in the sections that follow.

III.1 On-Deck Vapor Dispersion

To provide a predictive method to evaluate on-deck hazards associated with chemical vapors vented to the atmosphere during tanker loading, a plume dispersion model was developed. The on-deck plume dispersion model is based on Ooms' method (B-76). This model will be compared with other plume rise and vapor dispersion models in Section III.1.1, with small-scale plume ($\sim 1/100$) dispersion data obtained in wind tunnel tests in Sections III.1.2 and IV.4, with 1/4 scale plume dispersion data obtained in the open air in Section V, and with measured levels of vapor concentration during actual loading operation on full scale ships in Section VI. The model selection effort described in this section compares plume rise predictions given by (1) Kamotani and Greber's correlation, (2) Briggs' equation, (3) Hoult, Fay and Forney's computing method, and (4) Ooms' computing method. Equations for each of these four methods are given in Appendix C.

III.1.1 Comparison of Plume Rise Predictions

Kamotani and Greber's equation (C.3) and Briggs' equation (C.4) are expected to predict similar trajectories for jets with small amounts of buoyancy. Even for buoyant plumes, the trajectory within the first 20 diameters of the vent may be dominated by momentum effects, and the two methods may predict similar trajectories. As a test, trajectories were calculated for two jets having the same value of momentum ratio, $J = \rho_j u_j^2 / \rho_o u_o^2 = 15.3$. The first jet was unheated, $\rho_j/\rho_o = 1$, and the second jet was heated to a value of $T_j - T_o = 178°C$, $\rho_j/\rho_o = 0.625$. Results are shown in Figure III.1. Since Equation (C.3) assumed that jet trajectory depends only on J and x/d, the trajectory is the same for both examples. On the other hand, Briggs' equation (C.4) predicts two different trajectories that differ by about 6% in z/d for the same value of x/d. Since Kamotani and Greber actually performed an experiment for these conditions and found identical trajectories for heated and unheated jets, we will assume that their result is correct. In this case, Figure III.1 shows that the trajectories predicted by Briggs' equation (C.3) are also within 6% of Kamotani and Greber's predictions.

This comparison shows that either equation (C.3) or (C.4) may be used to predict the initial, momentum dominated trajectory of forced plumes. Equation (C.3) is not valid far away from the vent where plume trajectory is dominated by buoyancy. Therefore, Kamotani and Greber's plume rise correlation will be used only to compute the initial development of a plume within 1 to 4 diameters of the vent which is required as input data for Ooms' and Hoult, Fay and Forney's method. Briggs' equation (C.4) will be carried forward for comparison with the other plume computation methods.

49

Unheated Plume

$J = \rho_j u_j^2 / \rho_o u_o^2 = 15.3$

$\rho_j / \rho_o = 1$

○ Equation C.3 Kamotani and Greber

▽ Equation C.4 Briggs

Heated Plume

$J = \rho_j u_j^2 / \rho_o u_o^2 = 15.3$

$\rho_j / \rho_o = 0.625$

○ Equation C.3 Kamotani and Greber

▽ Equation C.4 Briggs
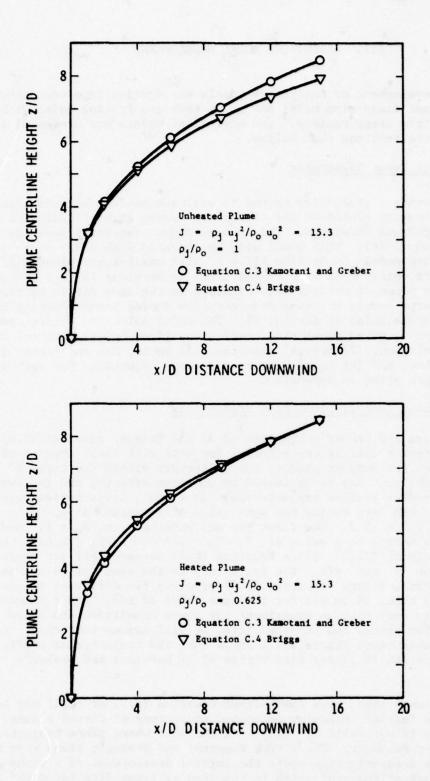
FIGURE III.1.   FORCED PLUME TRAJECTORY

For this comparison, three examples have been taken from Brummage's (B-12 and B-134) wind tunnel experiments. The free stream turbulence level is not cited in the reports of Brummage's work, but the description of the wind tunnel arrangement (models were placed on a raised floor above the tunnel wall boundary layer) implies that the turbulence level was low (1% or less). Therefore, the wind tunnel experiments approximate plume dispersion in a wind with low turbulence, as might be encountered if the air temperature gradient is stably stratified. For these examples, a value of $u' = 0$ (no entrainment by interaction of the plume with atmospheric turbulence) was used in Ooms' method.

Figure III.2 compares forced plume centerline trajectory predictions (height above the deck versus distance downwind along the deck) for a mixture of 50% propane and 50% air emitted vertically upward at a velocity of 20 m/s through a 25 cm diameter vent. The vent is located 6.1m above the ship deck, and the wind speed is 1.1 m/s parallel to the deck. Brummage's combustible plume boundary (see Figure II.3 of Reference B-134) is shown in shading for comparison. Ooms' method and Hoult, Fay and Forney's method predict plume centerline trajectories that are similar. Briggs' equation gives a trajectory that is noticeably higher than the other two, but closer to the combustible plume boundary reported by Brummage.

It can be noted that the plume trajectories predicted by Ooms' and Hoult's methods are different near the vent. Hoult, et al. employ the Boussinesq assumption in their model. This permits the plume density to vary with concentration only in the buoyancy term of the momentum balance. This assumption simplfies the computing equations, but makes the solution less realistic near the vent when the plume density is significantly different from the ambient density. In preparing Figures III.2, III.3, and III.4, the plume density used in Hoult's mass and momentum flux equations (except for the buoyancy force) was set equal to the ambient air density, and the initial plume rise was underpredicted. Another set of computations (not reported here) were made using the actual plume density at the vent in the mass and momentum flux terms. Although the initial plume rise matched Ooms' prediction, the influence of the high initial momemtum continued too far downwind, and the far field trajectory was overpredicted.

Another observation may be made from Figure III.2. While the trajectories predicted by Hoult's and Ooms' methods are falling back towards the deck at a distance of 15m from the vent, the trajectory predicted by Briggs' equation is still rising. Thus, the effect of negative buoyancy has not yet been seen in Briggs' prediction, although it has begun to influence the trajectories predicted by Hoult's and Ooms' methods.

Figure III.3 compares plume trajectory prediction for a 50% propane, 50% air mixture emitted upwards at a velocity of 9.1 m/s through a 25 cm diameter vent into a 1.1 m/s wind. Again, the plume trajectories predicted by Ooms' method and Hoult's method are very similar except near the vent as discussed above. Briggs' equation predicts a plume trajectory that rises above the others in the first 10m downwind of the vent, then falls abruptly toward the deck. Inspection of Briggs' equation (C.4) shows that the contribution of momentum and buoyancy terms to the plume rise height are additive within a cube root radical. Thus, when the negative buoyancy term

51
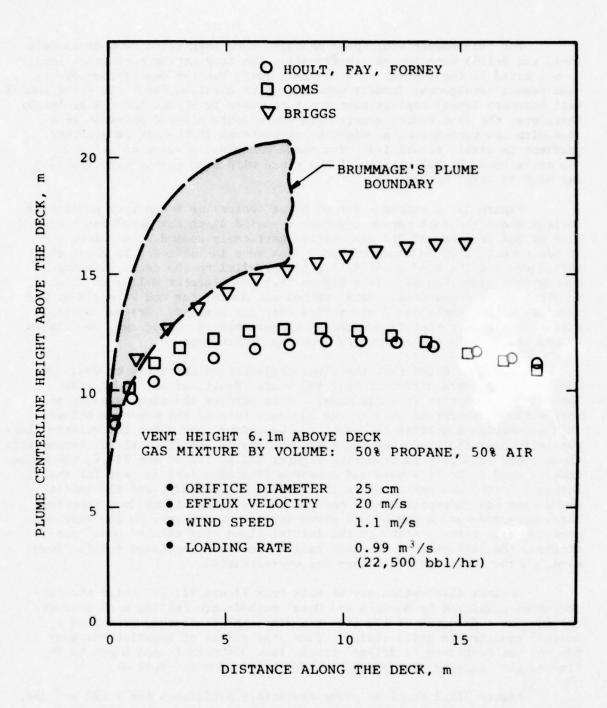
FIGURE III.2. PLUME CENTERLINE TRAJECTORY

VENT HEIGHT 6.1m ABOVE DECK
GAS MIXTURE BY VOLUME: 50% PROPANE, 50% AIR

- ORIFICE DIAMETER   25 cm
- EFFLUX VELOCITY   9.1 m/s
- WIND SPEED   1.1 m/s
- LOADING RATE   0.46 m^3/s
                      (10,446 bbl/hr)

BRUMMAGE'S
PLUME BOUNDARY

○ HOULT, FAY, FORNEY
□ OOMS
▽ BRIGGS

PLUME CENTERLINE HEIGHT ABOVE THE DECK, m

DISTANCE ALONG THE DECK, m
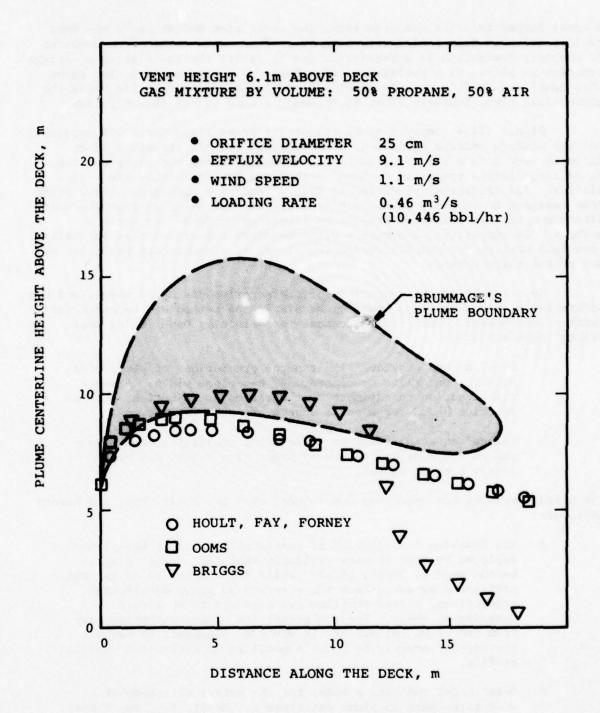
FIGURE III.3.   PLUME CENTERLINE TRAJECTORY

53

becomes larger than the momentum term, the plume rise height above the vent rapidly switches from positive to negative. This rapid switch from momentum to buoyancy domination is unrealistic, and it limits the application of Briggs' equation to plumes with positive or zero buoyancy. Figure III.3 also shows that Ooms' and Hoult's methods predict plume trajectories that lie below the combustible plume boundary found in Brummage's wind tunnel investigation.

Figure III.4 compares plume trajectory predictions for a 50% propane, 50% air mixture emitted upwards at a velocity of 3.0 m/s through a 25-cm diameter vent into a 1.1 m/s wind. Just as in the other two examples, the plume trajectories predicted by Ooms' method and Hoult's method are very similar. The trajectory predicted by Briggs' equation undergoes a transition from momentum to buoyancy domination at a distance of about 2m from the vent. After that, it lies below the trajectory predicted by Ooms' and Hoult's methods. In comparison, Brummage's plume boundary appears to rise initially, then fall back rather quickly toward deck level in a manner not predicted by any of the three methods.

As a result of the comparison of trajectories discussed above, and consideration of other factors, Ooms' plume dispersion method was selected for further development. The primary reasons for selecting Ooms' model over Briggs' equation are:

o   Ooms' method provides simultaneous predictions of plume rise height, centerline concentration, and plume width. A separate equation to estimate concentration distribution, such as equation (C.25) for a point source, is not required.

o   Briggs' equation gives an unrealistic transition from momentum to buoyancy domination of plume rise height for negatively buoyant plumes.

The primary reasons for selecting Ooms' model over the Hoult, Fay, and Forney model are:

o   The Gaussian distribution of concentration within the plume employed by Ooms is more realistic than the top-hat distribution used by Hoult, et al. While the assumption of top-hat profiles does not affect the accuracy of plume development predictions, actual profiles are expected to be closer to Gaussian in shape. For the prediction of concentration away from the plume centerline, it would be necessary to convert the top-hat profile in Hoult's model to an equivalent Gaussian profile.

o   Ooms' model contains a model for the effect of atmospheric wind turbulence on plume entrainment. Hoult, Fay, and Forney assume that the affect of atmospheric turbulence may be ignored for some (unspecified) distance downwind of a vent in comparison to the effect of turbulence generated by the plume. This assumption affects the predictions of both plume rise and vapor concentration decay. Far downstream of the vent, where

54

VENT HEIGHT 6.1m ABOVE DECK
GAS MIXTURE BY VOLUME: 50% PROPANE, 50% AIR

- ORIFICE DIAMETER   25 cm
- EFFLUX VELOCITY   3.0 m/s
- WIND SPEED   1.1 m/s
- LOADING RATE   0.15 m^3/s
    (3482 bbl/hr)

○ HOULT, FAY, FORNEY
□ OOMS
▽ BRIGGS

BRUMMAGE'S PLUME BOUNDARY

PLUME CENTERLINE HEIGHT ABOVE THE DECK, m

DISTANCE ALONG THE DECK, m
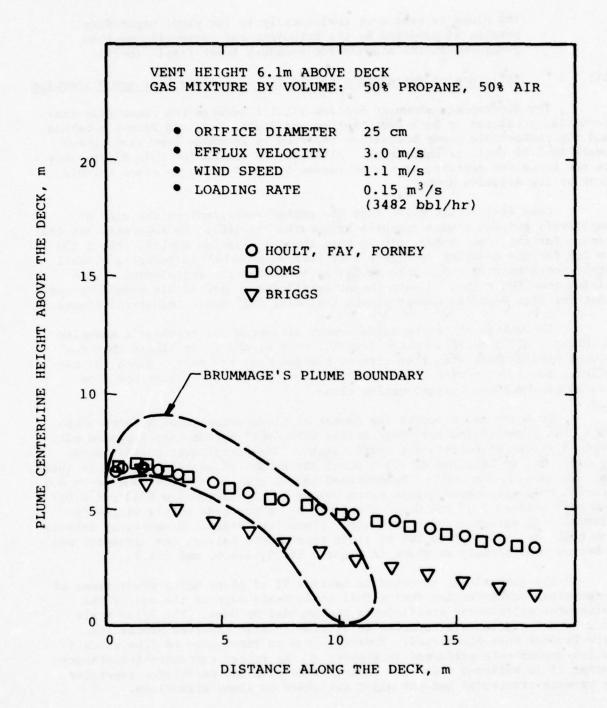
FIGURE III.4. PLUME CENTERLINE TRAJECTORY

the plume is bent over horizontally by the wind, vapor dispersion is promoted by the turbulent and convective motions generated in the atmospheric boundary layer itself (B-79).

III.1.2   Influence of Entrainment Coefficients on Plume Rise and Dispersion

The discrepancy shown in Section III.1.1 between the plume rise trajectories predicted by both Ooms' method and Hoult, Fay, and Forney's method and the combustible plume boundaries reported by Brummage from wind tunnel tests in 1:96 scale is surprising. Although the reason for this discrepancy is not known for certain, it may be caused by a reduction in plume entrainment at low Reynolds number.

Ooms (B-137) has noted that his method underpredicts the rise of negatively buoyant plumes measured by Bodurtha (B-140). He suggests that the reason for the disagreement may be that the jet Reynolds numbers (about 533 to 669 for the examples in Figure 2 of Reference (B-137) in Bodurtha's small scale model experiments may be so low as to reduce the entrainment. Ooms claims that the values of entrainment coefficients used in his model are correct for high Reynolds number plumes including full scale industrial plumes.

The values of jet Reynolds number estimated for Brummage's examples in Figures III.3 to III.4 range from 101 to 658, and it is likely that the plumes were laminar when they were discharged from the vent. Since the turbulence level in the wind tunnel was very low, plume entrainment would be caused by shear and buoyant motion alone.

To learn how reducing the amount of plume entrainment affects plume rise, the plume trajectory computations with Ooms' method were repeated with reduced values of entrainment coefficients. The entrainment coefficients, α_1 and α_2 in Equation (C.16) control the amount of entrainment due to shear, and buoyancy, respectively. Recommended values are $\alpha_1 = 0.057$ and $\alpha_2 = 0.5$. Several computations were made using values of α_1 between 0.0043 and 0.057 and α_2 between 0.05 and 0.5. Changing α_1 alone made only a slight improvement in agreement with Brummage's plume boundaries. However, by decreasing both α_1 and α_2 to 20% of their recommended values, the agreement was improved considerably as shown in Figures III.5, III.6, and III.7.

The comparisons reported in Section VI of plume model predictions of cargo vapor concentration during full scale tests support the use of the values for entrainment coefficients recommended by Ooms. The 1/150 scale wind tunnel experiments reported in Section IV also involved plumes that were laminar when discharged. However, from an inspection of flow visualization experiments performed in support of the tracer concentration measurements, it is believed that wind tunnel turbulence and turbulence generated by on-deck structures had the major influence on plume dispersion.

III.1.3   Description of the Analytical Plume Dispersion Computing Method

The analytical plume model developed for use in this project is based largely upon Ooms' method (B-76), with a transition to teRiele's method (B-139) if the plume axis sinks to deck level. Two sets of numerical computing equations were derived from the equations shown in Appendix C for Ooms' and teRiele's methods. The first set of computing equations is integrated
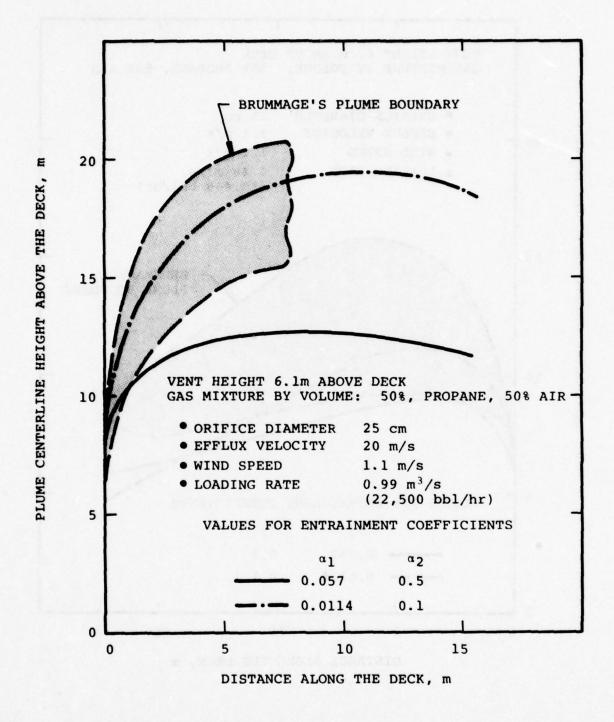
FIGURE III.5. PLUME CENTERLINE TRAJECTORY COMPUTED FOR
TWO SETS OF ENTRAINMENT COEFFICIENT VALUES

VENT HEIGHT 6.1m ABOVE DECK
GAS MIXTURE BY VOLUME: 50% PROPANE, 50% AIR

- ORIFICE DIAMETER   25 cm
- EFFLUX VELOCITY   9.1 m/s
- WIND SPEED   1.1 m/s
- LOADING RATE   0.46 m^3/s
                      (10,446 bbl/hr)

BRUMMAGE'S
PLUME BOUNDARY

PLUME CENTERLINE HEIGHT ABOVE THE DECK, m

VALUES FOR ENTRAINMENT COEFFICIENTS

	α_1	α_2
——	0.057	0.5
—·—·—	0.0114	0.1

DISTANCE ALONG THE DECK, m

FIGURE III.6.   PLUME CENTERLINE TRAJECTORY COMPUTED FOR
TWO SETS OF ENTRAINMENT COEFFICIENT VALUES

58

VENT HEIGHT 6.1m ABOVE DECK
GAS MIXTURE BY VOLUME: 50% PROPANE, 50% AIR

- ORIFICE DIAMETER   25 cm
- EFFLUX VELOCITY   3.0 m/s
- WIND SPEED   1.1 m/s
- LOADING RATE   0.15 m^3/s
                      (3482 bbl/hr)

VALUES FOR ENTRAINMENT COEFFICIENTS

	α_1	α_2
——	0.057	0.5
—·—	0.0114	0.1

BRUMMAGE'S PLUME BOUNDARY

FIGURE III.7. PLUME CENTERLINE TRAJECTORY COMPUTED FOR
TWO SETS OF ENTRAINMENT COEFFICIENT VALUES

numerically along the plume axis until either the downwind limit of integration is reached or the plume axis height becomes negative. In the latter case, integration is continued with the second set of computing equations (for teRiele's method) until the downwind integration limit is reached. A listing of the plume model computer program is given in Appendix D, together with sample input and output.

To start the computation of plume development, a certain amount of initial data must be specified including:

o   the concentration of chemical vapor, (kg/m^3)

o   the plume characteristic width, (m)

o   the difference between the plume velocity and the component of wind velocity along the plume axis, (m/s)

o   the angle between the plume axis and the horizon, (radians)

o   the vertical, starting height of the plume axis above the deck, (m)

o   the horizontal, starting distance of the plume axis from the vent, (m).

Following Ooms' (B-76) the computing method does not begin calculation at the vent, but at a short distance, ζ, above the vent where the velocity and concentration profiles have become fully developed and self-similar. The data of Keefer and Baines (B-136) provides values of the jet profile development length, ζ, for three values of the ratio of jet velocity to wind velocity, $R = u_j/u_a = 4$, 6 and 8. A least squares linear fit was calculated for these three values and used to estimate values of ζ/d for values of R ranging from 0 to 8, as shown in Table III-1.

TABLE III-1

DISTANCE FROM THE JET ORIFICE TO THE ONSET OF AXIAL VELOCITY DECAY

$R = u_j/u_a$	ζ/d from (B-136)	ζ/d from linear curve fit
0	–	0.972
1	–	1.049
2	–	1.227
3	–	1.404
4	1.59	1.580
5	–	1.759
6	1.92	1.937
7	–	2.114
8	2.30	2.292

60

The Kamotani and Greber plume rise equation (C.2) is used to compute the initial plume rise from the vent to a point on the plume axis where profiles become self-similar. A value of $J = \rho_j u_j^2 / \rho_a u_a^2$ must be computed in order to determine the coefficients a_v and b_v in equation (C.2). The value of jet velocity, u_j, may be estimated from the vent discharge rate (equal to the cargo loading rate) and the vent area. The value of emitted gas density, ρ_j, will depend upon the cargo vapor concentration at the vent. Values of ρ_a and u_a, the air density and wind speed, will be estimated from meteorological data.

Next, it is necessary to find the correct values of x/d, the downwind starting length, and z/d, the plume rise height, that give a plume path length matching the proper value of plume development length ζ/d from Table III-1. The search for correct values of x/d and z/d is performed by trial and error. When complete, the value of starting length, x, needed for input data is known directly. The value of the plume rise height, z, from equation (C.2) is added to the vent height to give the value of starting height for input data.

The angle between the plume axis and the horizon is computed simply by differentiating the plume rise equation (C.2) and equating the slope to the tangent of the plume angle.

$$\tan \theta = \frac{d(z/d)}{d(x/d)} = a_v \, b_v \, (x/d)^{b_v - 1}$$

Once the initial value of plume angle, θ, is known, the initial value of the difference between plume velocity and the component of wind velocity along the plume axis may be calculated as

$$u_j - u_a \cos \theta$$

The initial value of plume characteristic width, b, at the starting height, ζ, is taken to be

$$b = 1.15 \, d/(2\sqrt{2})$$

where d is the vent diameter. The 1.15 factor allows for growth of the plume width during the profile development stage.

Additional information required as input data to the computer program includes:

o   integration limits and integration step size

o   the value of molecular weight for the gas emitted from the vent

o   the local air temperature and pressure

o   the time average value of wind velocity at a reference height above the ground

o   the average wind turbulence level

o   the height of the ship deck above the ground

o   the equivalent roughness height of deck structure

o   the height above the deck for which vapor concentration predictions are required

o   specific values of concentration for which contour lines are required (for example, the LEL, TWA-TLV and STEL)

o   profile constants required by teRiele's method for the appropriate class of atmospheric stability.

The input data is discussed further in Appendix D.

The computing method calculates values for six output variables for each integration step along the plume axis. The output variables are

o   concentration on the plume axis (also called plume centerline concentration)

o   characteristic width of the plume

o   velocity difference between the plume centerline velocity and the component of wind velocity along the plume axis

o   the angle of the plume axis above the horizon

o   the vertical height from the vent to the plume axis

o   the horizontal distance from the vent to the plume axis.

In addition, several derived quantities are calculated from the output variables. These are

o   the concentration of vapor directly downwind of the vent at a selected height above the deck. This quantity could be the concentration at breathing level, or could represent the concentration at air sampling level when comparing plume predictions with experimental data.

o   values of crosswind distance from the vertical plume axis plane to the location where the vapor concentration reaches specified values of interest such as the LEL or STEL. These quantities are useful for plotting contours of concentration at a selected height above the deck.

When the plume characteristic width grows so large that the plume radius is as large or larger than the distance from the plume axis to the deck, z, it is reasonable to suppose that ground effect will increase the concentration level at locations close to the deck. To simulate ground effect, the computing method uses a mirror image technique. This supposes that a second plume with the same radius and centerline concentration as the real plume is located at a height, -z, below the deck. Then, the influence of both the real and the image plume are added together to estimate the concentration levels above the deck.

If the plume axis sinks to deck level, the computing method switches to solving teRiele's computing equations. The transition is carried out internally, and no additional data is required. The output variables, become

o   the concentration at deck level downwind of the vent

o   the value of vertical dispersion coefficient

o   the value of horizontal dispersion coefficient.

Initial values for these variables are computed from the last values of centerline concentration and plume characteristic width. Prediction of derived quantities is continued as before.

III.1.4   Examples of Plume Model Sensitivity to Variation of the
           Input Data

Several example calculations have been performed to demonstrate the
sensitivity of the plume model to input data variations. The example pre-
sented here concerns the venting of hexane vapor mixed with air from an open
vent 25-cm in diameter into the air above the ship deck. Base conditions
are

o   venting rate, 0.132 m^3/s (3000 bbl/hr)

o   concentration at the vent, 0.188 kg/m^3 (50,000 ppm)

o   wind velocity at 10m height, 2.24 m/s (5 mph)

o   wind turbulence level, 20%

o   vent height above deck level, 1.07m (3.5 ft).

Variation conditions are

o   venting rate, 0.264 and 0.066 m^3/s (6000 and 1500 bbl/hr)

o   wind velocity, 1.12 and 4.47 m/s (2.5 and 10 mph)

o   turbulence level, 0 and 10%

o   vent height, 2.14 and 3.20m (7 and 10.5 ft)

The output variable of interest is the concentration of hexane at breathing
level, 1.68m (5.5 ft) above the deck, directly downwind of the vent.

Figure III.8 shows the effect of the variation of the vent discharge
rate, with all other parameters held at their base condition. As expected,
the concentration at breathing level increases with increased vent discharge
rate. However, the concentration at breathing level is also affected by the
plume trajectory, which is affected by the vent discharge rate. At a dis-
tance of 25m downwind of the vent, the height of the plume axis above the deck
is 1.49m, 1.67m, and 2.09m for the low, base condition, and high venting rate
plumes, respectively. Note that the plume centerline for the base condition
plume is at breathing level.   However, the plume centerline for the high
venting rate plume lies above breathing level so that the concentration at
breathing level is less than the plume centerline concentration value. It
should also be noted that the concentration predicted at breathing level
exceeds the STEL (short term exposure limit) for hexane at all distances up
to 15 to 25 meters downwind of the vent.

Figure III.9 shows the effect of varying the vent height above the
deck on the concentration at breathing level. Note that when the vent height
is above breathing level, high vapor concentrations close to the vent may be
avoided. The concentration increases (as the plume radius increases) to a
maximum value and then declines. Note that at a vent height of 1.07m (typical
of some tankerships) the concentration of hexane at breathing level exceeds
the STEL for all distances up to 20m downwind of the vent. A vent height of
2.14m gives concentrations at breathing level that exceed the STEL from 3.5m
to 16m downwind of the vent. But a vent height of 3.20m above the deck gives
concentrations at breathing level that do not exceed the STEL at all.
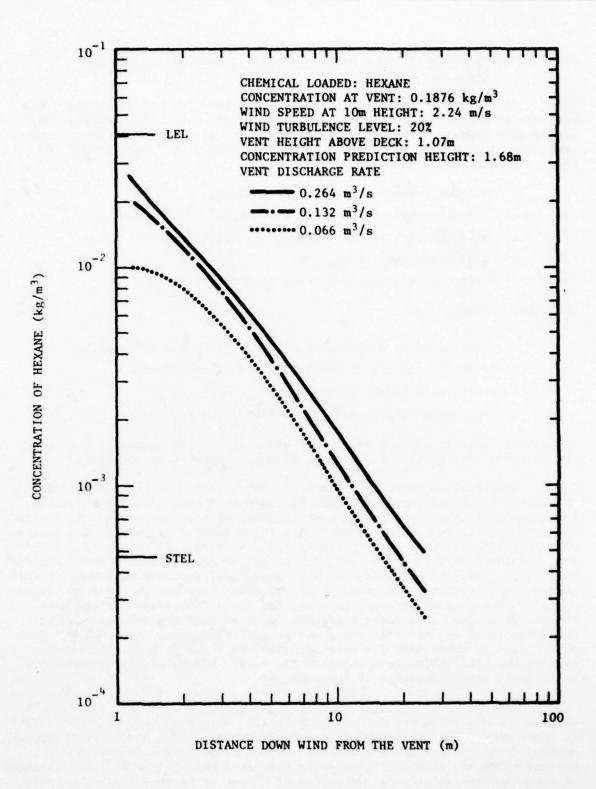
FIGURE III.8. EFFECT OF VENT DISCHARGE RATE ON THE PREDICTED
LEVEL OF HEXANE CONCENTRATION DOWNWIND OF THE VENT
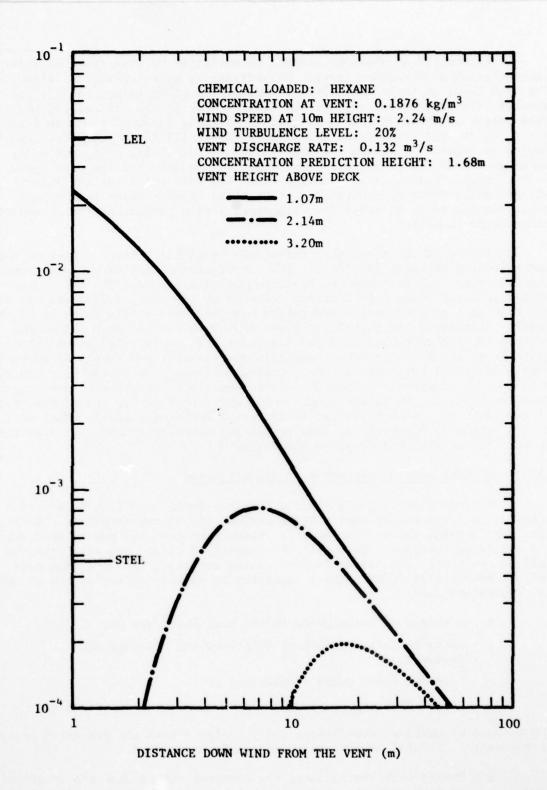
FIGURE III.9. EFFECT OF VENT HEIGHT ABOVE DECK ON PREDICTED
LEVEL OF HEXANE CONCENTRATION DOWNWIND OF THE VENT

Figure III.10 shows the effect of variation of wind speed on vapor concentration at breathing level. This figure is quite similar to Figure III.8. The high level of turbulence, 20%, disperses the plume rather rapidly and greatly affects the tendency to sink down to deck level. Therefore, the rise height of these plumes is determined by their value of momentum ratio, $J = \rho_j u_j^2/\rho_a u_a^2$. The three examples in Figure III.10 and the three examples in Figure III.8 have the same values of $J = 5.83$, 1.46, and 0.36, although the discharge velocity was varied in one case and the wind speed in the other. Hence, we may conclude that low wind speed has the affect of increasing vapor concentration at breathing level similar to a higher vapor venting rate, at least for turbulence levels representative of neutral atmospheric stability.

Figure III.11 shows that turbulence level has a large effect on vapor concentration at breathing level. The computation for 0% turbulence shows that the vapor concentration at breathing level can exceed the LEL (lower explosive limit) from 0 to 2 meters downwind of the vent, and exceed the STEL for much greater distances (computation was concluded at 25m downwind of the vent). Increasing the turbulence level from 0 to 10% and from 10% to 20% reduces the concentration at breathing level noticeably. Values of turbulence level are based on meteorological measurements, and levels of approximately 15 to 20% have been recorded during full-scale tests (see Section VI) with neutral atmospheric stability conditions. Deck structures such as pipe runs, pump houses, expansion trunks, will serve to increase the dissipation of the plume in a manner similar to increased turbulence level. More work in full-scale is necessary to resolve the influence of atmospheric stability on turbulence level and on plume dispersion.

III.2 In-Tank Liquid Evaporation and Gas Freeing

A simplified duty cycle for a chemical tanker consists of a series of alternating laden and ballast voyages between two marine terminals. During the laden voyage, chemical product is transported from the supply terminal to the discharge terminal. Following off-loading of cargo, the ship takes on ballast for the return voyage to the loading terminal. It is during this ballast voyage that certain empty tanks may be washed and ventilated at sea in preparation for:

o   a change of cargo grade on the next laden voyage,

o   entry by ship's personnel to accomplish cleaning and inspection,

o   biennial Coast Guard inspection, or

o   repair work.

The process of washing, ventilating and entering a tank may present a hazard to personnel. Several hazard scenarios can be postulated.

o   During tank ventilating, the chemical vapors that are discharged on deck through a Butterworth opening may be present in explosive and/or toxic concentrations throughout a portion of the venting period. The duration of this hazard would be enhanced by the evaporation of liquid chemical from the tank walls and bottom.

66

CHEMICAL LOADED: HEXANE
CONCENTRATION AT VENT: 0.1876 kg/m^3
VENT DISCHARGE RATE: 0.132 m^3/s
VENT HEIGHT ABOVE DECK: 1.07m
CONCENTRATION PREDICTION HEIGHT: 1.68m
WIND TURBULENCE LEVEL: 20%
WIND SPEED AT 10m HEIGHT
——— 1.12 m/s
—·—·— 2.24 m/s
··········· 4.47 m/s

DISTANCE DOWN WIND FROM THE VENT (m)
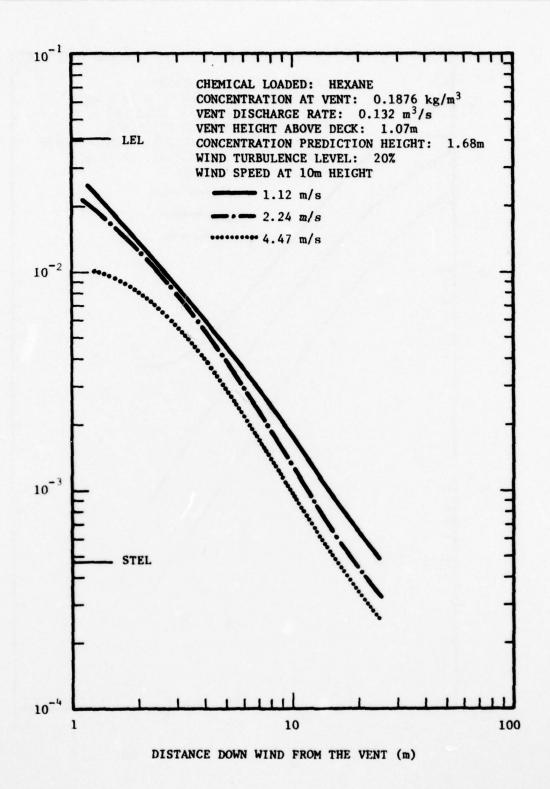
FIGURE III.10. EFFECT OF WIND SPEED ON THE PREDICTED LEVEL OF HEXANE CONCENTRATION DOWNWIND OF THE VENT

67
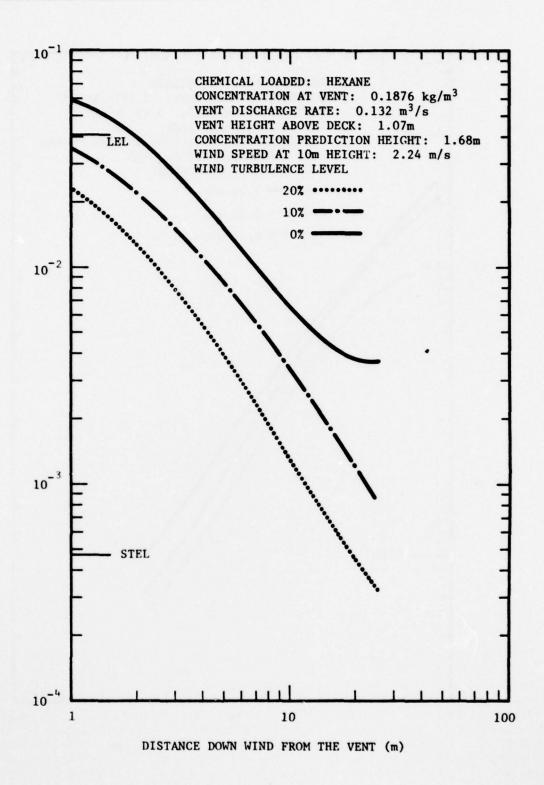
FIGURE III.11. EFFECT OF WIND TURBULENCE LEVEL ON THE PREDICTED
LEVEL OF HEXANE CONCENTRATION DOWNWIND OF THE VENT

68

o   Following forced ventilation, the criterion for man-entry into
    the tank is usually based upon concentration measurements that
    are obtained using an on-deck explosimeter and a long sample
    line that is inserted into the tank through the hatch or a
    Butterworth opening. Men entering the tank may be exposed to
    toxic and/or explosive vapor levels because

    a)   the explosimeter is not designed to provide an accurate in-
         dication of vapor concentration at the levels of a Threshold
         Limit Value or a Short Term Exposure Limit.

    b)   tank internal structure does not permit all portions of the
         tank to be gas freed equally or at the same rate. There are
         likely to be stagnation regions or dead spots in the tank,
         particularly behind bulkheads and in corners, where the
         vapor cannot be effectively removed by forced convection.
         In these regions, gas freeing is controlled by the much slow-
         er process of diffusion. Thus, the vapor concentrations in
         these diffusion-controlled regions may still be present in
         hazardous levels despite the fact that the majority of the
         tank has been gas freed. It should be noted that all of
         these potential stagnation regions cannot be sampled through
         the limited number of on-deck openings regardless of instru-
         mentation sensitivity.

    c)   the process of mucking or manual cleaning of residual cargo
         disturbs and increases the liquid surface area, thus en-
         hancing the generation of vapor through local evaporation.
         Local vapor concentrations may increase to hygienically
         significant levels.

o   On the ballast voyage, a tank may be sealed after explosimeter
    tests indicate that vapor concentrations are nearly zero. In
    this sealed tank, vapor concentration levels will increase with
    time due to diffusion mixing and continued evaporation of liquid
    that has been trapped in the crevices of rough tank walls. Upon
    opening the tank, an explosimeter reading may again indicate a
    near zero vapor concentration. Man-entry at this point may ex-
    pose workers to concentrations that exceed the Short Term Expo-
    sure Limit.

   At any given time, vapor concentrations in a tank are a function of
many variables and their interactions. Two mathematical models were devel-
oped to aid in identifying the predominant variables that control the gas
freeing process. The first model simulated dilution ventilation in the pre-
sence of evaporation of residual liquid cargo from the tank walls and bottom.
The second model simulates the vapor concentrations that could occur in the
corner of a tank as a result of mucking residual cargo. The remainder of this
section includes the derivation of the model equations, the assumptions that
were made, model limitations, examples of computer-generated concentration
predictions, and the results of a model sensitivity analysis.

69

Tank Ventilation With Evaporation

Assume that a chemical cargo has been discharged from a tank and that dilution ventilation gas-freeing is to be initiated. The physical model for this scenario is shown in Figure III.12. The tank is modeled as a rectangular parallelepiped of dimensions L, W and H. All that remains of the previous cargo is a thin film of chemical, t_{film}, on the vertical walls and a residual layer, t_{pool}, on the tank bottom. The model assumes that the vertical wall temperature varies with depth, y, and that opposing parallel walls have the same temperature distribution. Thus, $T_{yz}(y)$ may be different than $T_{xy}(y)$. This profile permits the tank bottom temperature, T_0, to approach water temperature and the tank top to be influenced by ambient and/or radiation heating. The initial concentration in the tank is C_0, and after the blower of flow rate Q is activated, the concentration varies with time, C(t), but is independent of space. Liquid may evaporate locally at a rate $\dot{m}_{g\ell}$. At this point, the important assumptions are:

o   The vapor in the tank is uniformly mixed. Thus, vapor concentrations vary only with time. A consequence of this assumption is that the inlet and exhaust locations do not affect formulation of the model.

o   The evaporation process reflects the presence of a single component, pure chemical. This assumption neglects the mixing of pure chemical with the washing solution (water) prior to ventilation.

o   The interior surfaces of the tank are perfectly smooth. This assumption limits the evaporation process to what is known as the "constant rate period" of drying and neglects the "falling rate period" of the drying process. This falling rate period is governed by the roughness of the tank walls.

o   Liquid film on the vertical walls does not flow under gravity.

o   Vapor concentration is zero in the blower-supplied ambient air.

o   The tank is free of internal structures such as webframes and stringers.

o   Wall temperatures vary with distance below deck but are independent of time.

o   Tank bottom temperature is constant in time.

Based on these assumptions, a simple mass balance in the tank states that

$$\dot{m}_G - \dot{m}_E = \dot{m}_A \qquad\qquad (III-1)$$
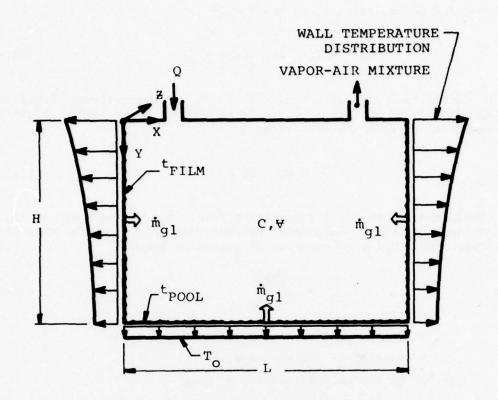
where $\dot{m}_G$ = total evaporation rate, i.e., the integral of $\dot{m}_{g\ell}$ over the tank interior surfaces (excluding the top)

$\dot{m}_E$ = mass rate of vapor discharged from the tank

$\dot{m}_A$ = mass rate of vapor accumulation within the tank.

70

t_{FILM} = THICKNESS OF CHEMICAL FILM ON VERTICAL WALLS

t_{POOL} = THICKNESS OF CHEMICAL FILM ON TANK BOTTOM

C_O = INITIAL WELL-MIXED VAPOR CONCENTRATION AT BEGINNING OF VENTILATION

C = AVERAGE WELL-MIXED VAPOR CONCENTRATION AT TIME, t

Ω = VENTILATION FLOW RATE

W = TANK WIDTH

$\forall$ = TANK VOLUME; LHW

$\dot{m}_{gl}$ = LOCAL LIQUID EVAPORATION RATE

$T_{yz}(y)$ = TEMPERATURE DISTRIBUTION ON WALLS PARALLEL TO Y-Z PLANE

$T_{xy}(y)$ = TEMPERATURE DISTRIBUTION ON WALLS PARALLEL TO X-Y PLANE

T_O = UNIFORM TANK BOTTOM TEMPERATURE $[T_O = T_{yz}(H) = T_{xy}(H)]$

FIGURE III.12.   ELEVATION VIEW OF A WELL-MIXED TANK WITH
WALL EVAPORATION

71

The exhaust and accumulation terms are simply

$$\dot{m}_E = QC(t) \quad \text{and} \quad \dot{m}_A = \Psi \frac{dC}{dt} \qquad \text{(III-2)}$$

where C is the mass concentration, and Ψ is the tank volume. Combining Equations (III-1) and (III-2) yields a first order, linear, ordinary differential equation for tank concentration;

$$\Psi \frac{dC}{dt} = \dot{m}_G - CQ \qquad \text{(III-3)}$$

Estimates of the local evaporation rate, $\dot{m}_{g\ell}$, were based on the model developed by Gray.[*] This model assumes the validity of the Maxwell steady-state equation for evaporation of liquid in ducts.

$$\frac{d\dot{m}}{dA} = \frac{DPMP_d}{RT_GFP_m} \qquad \text{(III-4)}$$

where
$d\dot{m}$ = incremental mass evaporation rate, gm/sec

dA = element of surface area, cm^2

D = diffusion coefficient, cm^2/sec

P = total atmospheric pressure, mm Hg

M = liquid molecular weight, gm/mole

P_d = driving force pressure, mm Hg

R = universal gas constant, $6.2358 \times 10^4 \frac{cm^3 - mm\ Hg}{mole - °K}$

T_G = gas temperature, °K

F = air-vapor film thickness, cm

P_m = mean partial pressure of gas above the liquid, mm Hg.

The important assumptions that are contained in Equation (III-4) are:

o a uniform concentration profile exists above the liquid surface, thus vapor mixing is instantaneous and uniform,

o the air-vapor mixture within the film thickness, F, is stagnant,

o mass transfer with the film is controlled by molecular diffusion,

o flow velocity profiles are laminar, and

o a single component liquid evaporates into a mixture of its own vapor and air.

---

[*] Gray, D. C. "Solvent Evaporation Rates," American Industrial Hygiene Association Journal, November 1974.

72

The driving force pressure, P_d, and the mean partial pressure in the vapor space, P_m, can be estimated from the following equations.

$$P_d = \left[(P_v-P_i)\ (P_v-P_i-P_s)\right]^{\frac{1}{2}} \qquad \text{(III-5)}$$

$$P_m = \left[(P-P_i)\ (P-P_i-P_s)\right]^{\frac{1}{2}} \qquad \text{(III-6)}$$

where P_i = partial pressure of the vapor in the air at upwind end of the liquid surface element,

P_v = vapor pressure of liquid at temperature, T_L

P_s = partial pressure of the evaporated vapor.

Within a relatively narrow range of liquid temperatures, the liquid vapor pressure can be estimated as

$$\log_{10}P_v = a + bT_L \qquad \text{(III-7)}$$

where   a   and   b   are constants and T_L is the liquid temperature. At this point, simplifying assumptions were introduced.

o   The elements of liquid surface are continually presented with fresh, uncontaminated air. This assumption implies that P_i equals zero.

o   The moles of liquid evaporated per unit time are negligible compared to the number of moles of air that sweep the liquid surface per unit time. The result of this assumption is that

$$P_s = P\ \frac{N_L}{N_A} = \text{Order } (0) \qquad \text{(III-8)}$$

where N_L = molar rate of liquid evaporation

N_A = molar rate of air movement.

With these assumptions,

$$P_d = P_v \qquad \text{(III-9)}$$

$$P_m = P \qquad \text{(III-10)}$$

and Equation (III-4) takes the form

$$\frac{d\dot{m}}{dA} = \frac{DMP_v}{R\ T_G\ F} \qquad \text{(III-11)}$$

Calculation of the diffusion coefficient, D, is based upon Gray's empirical correlation of physical constants,

$$D = \frac{0.425\ T_G^{3/2}}{P(MT_b/G)^{\frac{1}{2}}}$$ (III-12)

where $\quad T_b\ =\ $ liquid boiling point at atmospheric pressure, °K

$\qquad\quad G\ =\ $ liquid surface tension at 20°C, dynes/cm.

Finally, an empirical film thickness was also described by Gray;

$$1/F = 0.217\ S_c^{-0.9}\ (S_cU)^{0.625}\ S_c^{0.3}$$ (III-13)

where $\quad S_c\ =\ $ Schmidt number, D/ν

$\qquad\quad \nu\ =\ $ kinematic viscosity of air, cm^2/sec

$\qquad\quad U\ =\ $ effective air velocity over the liquid surfaces, cm/sec.

The wall velocity, U, is a function of blower flow rate, tank geometry and the density of the vapor/air mixture in the tank. Two methods of estimating U were employed.

Method I - The first method of estimating U was utilized on all analytical predictions up to and including a sensitivity analysis that will be discussed later. This method was based upon an extension of the work of Wolfshtein.[*] That extension consisted of redefining a control volume to include a two-dimensional enclosure with an inlet and an exhaust port. The governing differential equations were solved numerically for the stream function and vorticity fields that resulted from a submerged jet whose origin was located at the inlet port. Differentiation of the stream function yielded the local components of velocity parallel to the tank walls. These local wall velocities were then averaged in the rms sense to generate a first approximation to U as a function of Q.

Method II - Subsequent to the sensitivity analysis, the predictive model for U was modified and was used exclusively in theoretical/experimental comparisons that appear in Section VII. This second model is based on the work of Hrycak, et al.[**] and consists of a submerged jet impinging normally onto a flat plate. In the application of this model to the current problem, flow field modifications due to the presence of vertical tank walls were neglected. The model assumes a submerged air jet, and thus neglects the presence of a second component-chemical vapor. Following impingement of the jet on the tank bottom, the maximum air velocity, V_m, parallel to the impingement surface increases linearly with distance, r, from the stagnation point. This relationship applies throughout the "jet deflection" region whose boundary has been experimentally defined to be 0.3H where H is the tank depth. Thus,

---

[*] Wolfshtein, M., "Some Solutions of the Plane Turbulent Impinging Jet," Journal of Basic Engineering, Transactions of the ASME, December 1970.

[**] Hrycak, P., Lee, D. T., Gauntner, J. W., and Livingood, J. N. B., "Experimental Flow Characteristics of a Single Turbulent Jet Impinging on a Flat Plat," NASA TN D-5690, March 1970.

$$V_{m,jd} = Kr, \quad 0 \leq r \leq 0.3H \quad\quad\quad \text{(III-14)}$$

where K is a constant. In this region, viscous effects are negligible. Immediately downstream of the "jet deflection" region is the "wall jet" region. This region is characterized by self-similar velocity profiles that also exhibit a maximum velocity, $V_{m,wj}$. This maximum velocity parallel to the tank bottom separates the boundary layer zone from a free jet zone. Experimental and theoretical studies substantiate that $V_{m,wj}$ decays monotonically.

$$V_{m,wj} = \frac{1.4 \, U_o}{(r/d)^{1.12}} \quad \text{for} \quad r \geq 0.3H \quad\quad\quad \text{(III-15)}$$

where U_o = average jet velocity based on blower flow rate, Q, and jet inlet diameter, d.

The effective wall velocity, U, along the tank bottom was obtained by integrating these maximum velocity expressions radially outward from the stagnation point.

$$Ur_2 = \int_0^{0.3H} r \, dr + \int_{0.3H}^{r_2} \frac{C}{r^n} \, dr \quad\quad\quad \text{(III-16)}$$

where
$$C = 1.4 \, U_o d^{1.12}$$
$$n = 1.12$$
r_2 = an arbitrary distance that was taken to be the radial distance from the stagnation to the farthest vertical tank wall.
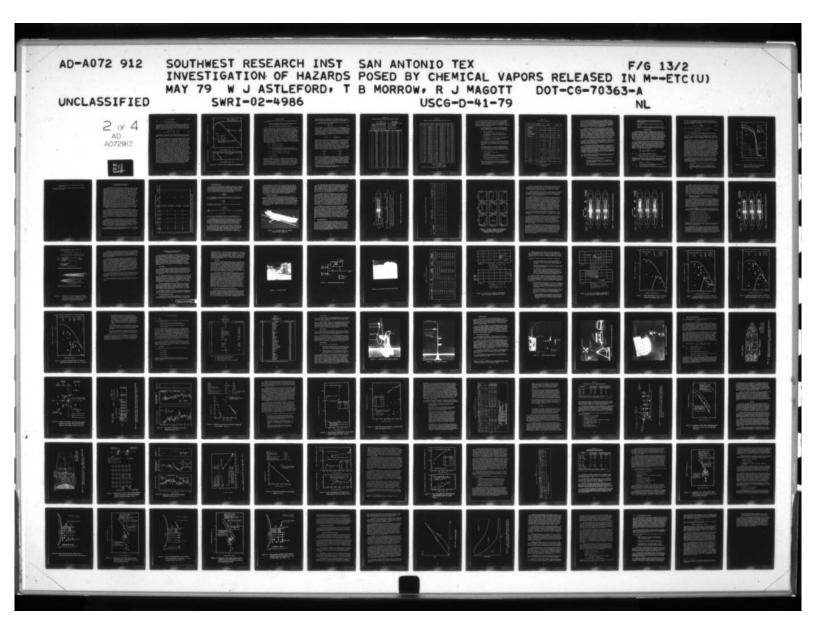
Carrying out the integration yields
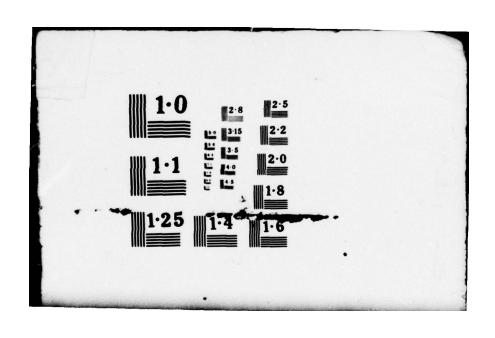
$$U = \frac{K}{2} \frac{(0.3H)^2}{r_2} + \frac{C}{1-n} \, r_2^{-n} \left[1 - \left(\frac{r_1}{r_2}\right)^{1-n} \right] \quad\quad\quad \text{(III-17)}$$

An expression for the constant, K, was obtained by matching the velocity profiles at the boundary, 0.3H.

$$K = \frac{C}{(0.3H)^{n+1}} \quad\quad\quad \text{(III-18)}$$

The governing equations for the evaporation/ventilation process were programmed in FORTRAN IV for solution on a CDC Cyber 74 System. A listing of the program is contained in Appendix D. In the program logic, the governing equations are applied locally on the tank walls to calculate local evaporative mass flux rates, $d\dot{m}_{g\ell}/dA$, and the local time available for constant liquid evaporation. These latter times, τ_ℓ, are obtained from expressions of the form

$$\tau_\ell = t\rho_F/(d\dot{m}_{g\ell}/dA) \qquad\qquad (III-19)$$

where τ_ℓ = local evaporation time

t = an initial liquid thickness.

In these calculations, local liquid and wall temperatures are assumed to be equal and constant with time. As such, the model does not directly reflect evaporative cooling. At each instant of time, local mass flux rates are integrated over the tank surfaces to obtain the instantaneous total evaporation rate. Variations in evaporation rate due to temperature profiling are taken into account at the local level.

$$\dot{m}_{g\ell} = \begin{Bmatrix} \dot{m}_{g\ell} & \text{for} & \text{time} \leq \tau_\ell \\ 0 & \text{for} & \text{time} > \tau_\ell \end{Bmatrix} \qquad (III-20)$$

A Runge-Kutta-Gill routine was used to numerically integrate the governing linear differential equation for the well-mixed, tank concentration history, $C(t)$.

Figure III.13 illustrates two concentration-time histories that were generated by the evaporation-dilution ventilation computer program. The responses are presented in terms of nondimensional concentration as a function of nondimensional time or number of tank turnovers. These concentration-time histories differ as a result of constraints that were placed on the evaporation process. All other conditions, such as tank geometry, flow rate, temperature profiles, initial concentration, etc., are common to both runs. The upper curve demonstrates the concentration response that might be expected if there were an unlimited supply of acetone on the tank walls and bottom. While this condition is not likely to occur in practice, it does demonstrate that the integration of local evaporation mass flux rate over the tank walls results in a time-independent evaporation rate. Furthermore, the vapor concentration in the tank increased to an asymptotic level that is less than the saturation concentration for the prescribed temperatures. The asymptotic value indicates that vapor is being discharged from the tank at the same rate that it is being generated. Obviously, the evaporation process will have a finite duration because of the limited supply of liquid film on the tank surfaces. The lower curve in Figure III.13 demonstrates the concentration response when the liquid film thickness is restricted to 0.2 cm on the tank walls and bottom. A finite film thickness together with the prescribed surface temperature profiling results in a time-dependent local cessation of evaporation and, hence, a time-dependent total evaporation rate. For this more realistic condition, evaporation continues until the liquid film on all surfaces has been consumed. Following total cessation of evaporation, the well-mixed tank concentration falls exponentially with time as predicted by the governing differential equation. Also shown in Figure III.13 are the calculated evaporation rates. A complete computer printout for the time-dependent evaporation case is contained in Appendix D.
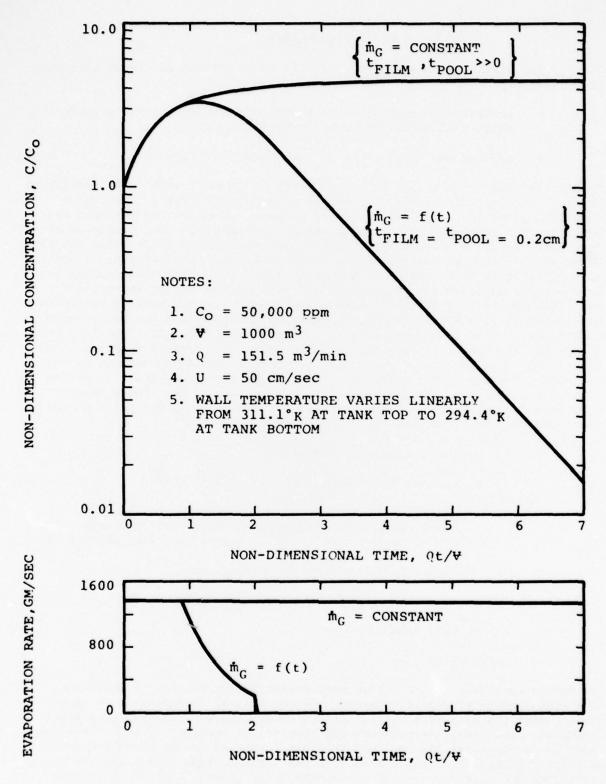
FIGURE III.13. EFFECT OF LIQUID THICKNESS ON TANK CONCENTRATION

Sensitivity Analysis

The liquid evaporation/tank ventilation model was developed with the objectives of

- o providing an analytical tool that can predict conditions under which a flammability/toxicity hazard may exist, and

- o guiding the development of experimental procedures.

To achieve these objectives, it is necessary to identify which model variables or their combinations have a dominant or subordinate effect on creating a hazardous situation. Identification of dominant variables and variable combinations was accomplished through a sensitivity analysis that consisted of a Fractional Factorial Design (FFD) followed by an Analysis of Variance (ANOVA). Given an experimental test plan that contains M independent variables, and each variable is to be tested at N levels, a full factorial experimental program would require N^M independent tests. This full factorial approach is not likely to be very efficient when a large number of independent variables are involved. The FFD technique, on the other hand, permits the experimentalist to define, on a rational basis, a subset of the total test matrix. Execution of this subset of experiments is essentially a screening process that identifies those factors or variables that have a significant effect on the outcome of the experiment. Based on this information, additional selective testing can be conducted if warranted. With respect to the liquid evaporation/tank ventilation model, the experiment is a computer run. The model contains seven independent variables.

- o C_o - initial tank concentration

- o T - tank surface temperature

- o Q,U - blower flow rate and air velocity over the liquid. These two parameters are considered together because U is dependent upon Q and cannot be specified separately.

- o t_F - liquid film thickness on vertical wall

- o t_P - thickness of liquid pool on tank bottom

- o V - tank volume

- o Chemical Species.

To reduce the number of variables to a manageable level, tank volume and chemical species were held constant. Based on field observations of chemical tankers, a 40 x 40 x 40-foot (12.2m cube) tank was selected as a representative tank size. Acetone was the chemical of choice. If each variable were to assume three levels, then the full factorial design would require a matrix of 3^5 or 243 computer runs. In the FFD technique, which was employed, this complete matrix was partitioned into three groups, each of which contained 3^4 or 81 statistically chosen combinations. Statistically, the

78

same model sensitivity information would be obtained regardless of which group of 81 computer runs was selected. The rational for selecting the combinations in the one-third factorial was based upon the work of Davies, et al.[*]

The combinations of five independent variables at three levels can be described by the following expression:

$$c^a Q^b t_F{}^c t_P{}^d T^e \qquad (III-21)$$

where a through e take on values of 0, 1, or 2. The superscripts 0, 1, and 2 correspond to a low, medium, or high level for the magnitude of a given variable. If a through e take on all values 0, 1, or 2, there will be 243 combinations. A criterion was needed to permit selection of the appropriate 81 combinations for the FFD. The criterion was that all main effects and two-factor interactions are clear of one another. Higher order interactions are assumed to be negligible. The consequence of this criterion is that there is but one defining contrast or algorithm that can be used to select the combinations. That algorithm is

$$a + b + c + d + e = \begin{Bmatrix} 0 \\ 1 \\ 2 \end{Bmatrix} \text{Modulo 3} \qquad (III-22)$$

Modulo 3 is dictated by the FFD and the requirement for three numerical levels of each variable. The term in the brackets indicates that there are three choices for the righthand side of the defining contrast. Each choice will result in one of the three groups of 81 combinations. A righthand side of zero was chosen. From this point, the mechanics are straightforward. The procedure is to search for combinations of a through e that sum to 0 (Modulo 3) when a through e take on values 0, 1, and 2. Table III-2 summarizes the combinations that satisfy the defining contrast and the numerical values that were selected for the three levels of each independent variable. Method I, which was described earlier, was used to predict values of wall velocity, U, that correspond to the three blower flow rates.

Q (m^3/min)	U (cm/sec)
75	56.5
151	113.0
302	226.0

All 81 FFD runs were subsequently processed on the computer. To determine which variables or combinations of variables have a statistically significant impact on liquid evaporation and tank ventilation, a performance criterion was needed. The selected criterion was the predicted length of time to evaporate the liquid and gas-free to an acetone concentration of 1% of the LEL, i.e., 260 ppm for an LEL of 2.6% by volume. This concentration level was chosen because chemical company operating procedures state that vapor levels at or below 1% LEL are safe for man and fire. The evaporation/ventilation times to 1% LEL are summarized in Table III-3.

---

[*] Design and Analysis of Industrial Experiments, Owen L. Davies, Editor, Second Edition, Hafner Publishing Co., New York, 1967.

TABLE III-2

FRACTIONAL FACTORIAL DESIGN FOR IN-TANK SENSITIVITY ANALYSIS

	LEVEL		
	0	1	2
C(ppm)	10000	20000	50000
Q(m³/min)	75	151	302
t_F (cm)	0.1	0.2	0.3
t_P (cm)	1.0	2.0	3.0
T (°K)	277.8	294.4	311.1

<u>CODING SCHEME</u>

Run 55; $C^a Q^b t_F^c t_P^d T^e$ = 02112

$C = C^0$ = 10,000 ppm

$Q = Q^2$ = 302 m³/min

$t_F = t_F^1$ = 0.2 cm

$t_P = t_P^1$ = 2.0 cm

$T = T^2$ = 311.1 °K

RUN	COMBINATION	RUN	COMBINATION	RUN	COMBINATION
1	00000	28	10101	55	02112
2	12000	29	10110	56	21012
3	10200	30	10011	57	12120
4	10020	31	01011	58	12102
5	10002	32	22200	59	10212
6	01200	33	22020	60	01212
7	01020	34	22002	61	12012
8	01002	35	02220	62	12210
9	00120	36	02202	63	12201
10	00102	37	00222	64	10221
11	00012	38	20202	65	01221
12	21000	39	20220	66	12021
13	20100	40	20022	67	11220
14	20010	41	02022	68	11202
15	20001	42	22110	69	10122
16	02100	43	22101	70	01122
17	02010	44	20211	71	11022
18	02001	45	02211	72	21111
19	00210	46	22011	73	12111
20	00201	47	21210	74	11211
21	00021	48	21201	75	11121
22	11100	49	20121	76	11112
23	11010	50	02121	77	22221
24	11001	51	21021	78	21222
25	01110	52	21120	79	12222
26	01101	53	21102	80	22122
27	00111	54	20112	81	22212

TABLE III-3

SUMMARY OF ACETONE EVAPORATION/VENTILATION TIMES TO 1% LEL

Run*	t (1% LEL) min	Comb.	Run*	t (1% LEL) min	Comb.	Run*	t (1% LEL) min	Comb.
1	260.44	00000	28	210.09	10101	55	59.59	02112
2	79.39	12000	29	393.23	10110	56	113.41	21012
3	261.78	10200	30	268.37	10011	57	180.37	12120
4	526.23	10020	31	145.05	01011	58	49.86	12102
5	188.36	10002	32	79.43	22200	59	222.08	10212
6	142.85	01200	33	180.37	22020	60	114.27	01212
7	305.99	01020	34	49.23	22002	61	59.49	12012
8	95.10	01002	35	180.37	02220	62	129.89	12210
9	526.23	00120	36	50.66	02202	63	57.82	12201
10	192.70	00102	37	249.37	00222	64	329.86	10221
11	210.07	00012	38	198.16	20202	65	182.55	01221
12	142.55	21000	39	526.23	20220	66	102.94	12021
13	261.02	20100	40	248.61	20022	67	305.99	11220
14	393.23	20010	41	69.97	02022	68	99.05	11202
15	208.02	20001	42	129.89	22110	69	248.94	10122
16	79.41	02100	43	57.48	22101	70	131.09	01122
17	129.89	02010	44	268.90	20211	71	131.00	11022
18	57.05	02001	45	79.96	02211	72	145.14	21111
19	393.23	00210	46	79.95	22011	73	79.96	12111
20	212.89	00201	47	224.50	21210	74	145.19	11211
21	329.82	00021	48	109.88	21201	75	182.55	11121
22	142.64	11100	49	329.84	20121	76	113.77	11112
23	224.49	11010	50	102.94	02121	77	102.94	22221
24	107.91	11001	51	182.55	21021	78	131.27	21222
25	224.49	01110	52	305.99	21121	79	70.03	12222
26	108.91	01101	53	97.45	21102	80	70.00	22122
27	268.57	00111	54	220.90	20112	81	59.85	22212

Comb. $= C^a Q^b t_F^c t_P^d T^e$

Acetone LEL = 2.6% = 26000 ppm

1% LEL = 260 ppm

*See Table III.2 for ventilation conditions on each run.

Development of the FFD combinations was based on five independent variables. As such, there are five main effects and 10 two-way inter-actions. To determine the strength or significance of each variable and its two-way combinations, the data in Table III-3 was subjected to an Analysis of Variance. The results are presented in Table III-4. These data permit statements regarding the dominance or insignificance of the variables and their two-way combinations.

1. The following parameters and parameter combinations do not have a statistically significant effect on the evaporation/ventilation time required to achieve a 1% LEL concentration:

   a. initial concentration,

   b. initial liquid thickness on the vertical walls,

   c. the combination of initial concentration with either flow rate, residue thickness on the tank bottom, or wall temperature,

   d. the combination of flow rate and wall film thickness, and

   e. the combination of wall film thickness with either residue thickness, or wall temperature.

   Items 1a through 1e reflect those entries in Table III-4 that are marked NS. The NS designation implies that we accept the null hypothesis (at all meaningful levels of confidence) that those entries do not have a significant effect on evaporation/dilution.

2. The following parameters and parameter combinations do have a statistically significant effect (at a minimum confidence level of 99%, except Item 7 in Table III-4 which has a confidence level of 90%) on the evaporation/dilution time criterion:

   a. ventilation flow rate,

   b. residue thickness on tank bottom,

   c. wall temperature,

   d. the combination of initial concentration with wall film thickness (significant at 90% confidence level),

   e. the combination of ventilation rate and either pool depth or wall temperature, and

   f. the combination of pool depth and wall temperature.

   Thus, in Items 2a through 2f, we reject the null hypothesis and accept the alternative hypothesis (at the indicated confidence levels) that those entries do have a significant effect on evaporation/dilution time.

TABLE III-4

ANOVA TABLE FOR ACETONE FFD

Source of Variation	Degrees of Freedom	Sum of Squares	Mean Square	F	Significance
1. Initial tank concentration	2	0.623	0.312	0.002	NS
2. Dilution flow rate	2	583079.319	291539.660	1741.433	$p < .0001$
3. Wall film thickness	2	17.261	8.631	0.052	NS
4. Residue thickness on tank bottom	2	128474.727	64237.363	383.704	$p < .0001$
5. Wall temperature	2	198465.935	99232.968	592.741	$p < .0001$
6. 1 x 2	4	1.816	0.454	0.003	NS
7. 1 x 3	4	1640.880	410.220	2.450	$p < .10$
8. 1 x 4	4	1.937	0.484	0.003	NS
9. 1 x 5	4	3.474	0.868	0.005	NS
10. 2 x 3	4	9.320	2.330	0.014	NS
11. 2 x 4	4	19128.977	4782.244	28.565	$p < .0001$
12. 2 x 5	4	25623.996	6405.999	38.264	$p < .0001$
13. 3 x 4	4	17.461	4.365	0.026	NS
14. 3 x 5	4	10.113	2.528	0.015	NS
15. 4 x 5	4	46187.798	11546.949	68.973	$p < .0001$
Error	30	5022.411	167.414		
Total	80	1007686.048			

F = Calculated F Statistic

NS = Not Significant

83

It is not surprising that Q, t_P, and T independently have a significant influence on the evaporation/ventilation process. Increases in T and Q result in an increased evaporation rate (reduced time to cessation of evaporation) and an increase in the mass rate of vapor discharge from the tank. Variations in evaporation time are directly proportional to t_P, which is much larger than t_F in the examples chosen. Consequently, the length of time to evaporate film t_F is small compared to either the time to evaporate t_P or the total gas freeing time.

What may seem surprising is the fact that, for a single chemical, the initial tank concentration does not have a significant impact on the overall process. If there were no liquid evaporation, then a simple calculation would indicate that the ventilation time to 1% LEL from an initial concentration of 1, 2, or 5% would result in variations of the gas freeing time that are important. However, for the assumed tank conditions, the mass of liquid to be evaporated is far greater than the initial vapor mass in the ullage space. The duration of the overall process is controlled by the time required to transfer mass from the liquid to the vapor state plus the time to dilute the tank concentration at the end of evaporation down to 1% LEL. For acetone, with the residual cargo conditions evaluated, the net result is that C_o did not have a significant influence on the total process time.

Note that combinations of individually significant parameters are also significant, and that combinations involving nonsignificant parameters are insignificant, with the exception of the combination of $C_o t_F$ which is significant at the 90% confidence level. At the 99% confidence level, this combination would become insignificant.

In summary, statistical techniques were used in a sensitivity analysis of the in-tank model. The purpose of the sensitivity analysis was to indicate which variables and their combinations have a significant effect on the evaporation/dilution process, and, therefore, the variables that would need to be measured in a full-scale test. In the final analysis, all five independent variables should be measured. Where the analysis indicated that an independent variable was insignificant from a statistical or mathematical standpoint, it does not imply that the variable is also insignificant from an operational or practical standpoint.

Based on the results presented in this section and the comparison of theory with experiment in Section VII, the following modifications to the model should be considered and studied:

o   synthesize the delay time effects of tank internal structure on the evaporation/ventilation process,

o   incorporate into the description of the evaporating liquid the effect of solutions or mixtures of pure chemical and tank washing liquid,

o   modify the wall velocity predictor to reflect an air jet issuing into an air/vapor mixture whose density is greater than air,

o   Supplement the constant rate evaporation period with a
    description of the falling rate drying period due to tank
    surface roughness,

o   investigate the effect of evaporative cooling of the liquid
    film, and

o   determine the validity of modifying the evaporative driving
    pressure to reflect the instantaneous tank vapor concentration.

Dead Spot Model

During dilution gas freeing of a chemical tank, there are likely to
be regions of the tank, principally in corners and behind internal struc-
tures, such as webframes, where the air flow will have a minimal effect on
vapor removal. Consequently, vapor concentrations in these regions may be
substantially higher than in the bulk of the unstructured tank. Despite the
fact that concentrations in the bulk of the tank may be acceptable for man-
entry, workers entering these dead spots may be exposed to concentrations in
excess of hygienically-acceptable levels. In addition, hand mucking of
residual cargo in these locations would be expected to produce a further
increase in dead-spot concentration as a result of liquid surface agitation.

To study this problem, a model of the dead spot was formulated.
Assume that the dead spot region is defined by the surfaces of two concen-
tric octants of spheres having radii R_1 and R_o ($R_o > R_1$) and the sur-
faces defined by their intersection with the three orthogonal walls in the
corner of the tank. Further, assume that mass is transported only by pure
diffusion within this region and that concentrations vary only with the
radial coordinate and time, i.e., the concentration field is spherically
symmetric. Therefore, within the dead spot, the concentration field is
described by the unsteady diffusion equation

$$\frac{\partial C_d}{\partial t} = \frac{1}{r^2} \frac{\partial}{\partial r} \left(Dr^2 \frac{\partial C_d}{\partial r} \right) \quad \begin{array}{l} R_1 < r < R_o \\ t > o \end{array} \qquad \text{(III-23)}$$

where C_d = local dead spot concentration, $C_d(r,t)$

        r,t = radial coordinate and time, respectively

        D = diffusion coefficient calculated as in the evaporation model.

Two boundary conditions and one initial condition are needed to complete the
problem definition. Assume that the concentration at the boundary, R_o, is
a function of time and varies exponentially according to the following ex-
pression

$$C_d(R_o,t) = C_o e^{-Qt/\Psi}, \quad t > 0 \qquad \text{(III-24)}$$

where C_o = concentration in the well-mixed portion of the tank
                 when the worker enters the dead spot

        Q,Ψ = dilution ventilation flow rate and tank volume, respectively.

85

Next, assume that a source of vapor generation exists within the space $0 \leq r \leq R_1$. Let the generation rate be $\dot{m}$ in units of mass per unit time, i.e., mg/sec. Assume that this vapor generation is imposed as a flux boundary condition on the surface $r = R_1$. Then,

$$\dot{m} = -\tfrac{1}{2} \, \pi \, R_1{}^2 \, D \, \frac{\partial C_d(R_1, t)}{\partial r} \,, \quad t > 0 \tag{III-25}$$

An initial condition at some reference time $t = 0$ is needed.

$$C_d(r, 0) = C_o f(r), \quad R_1 < r < R_o \tag{III-26}$$

where C_o = same quantity as above
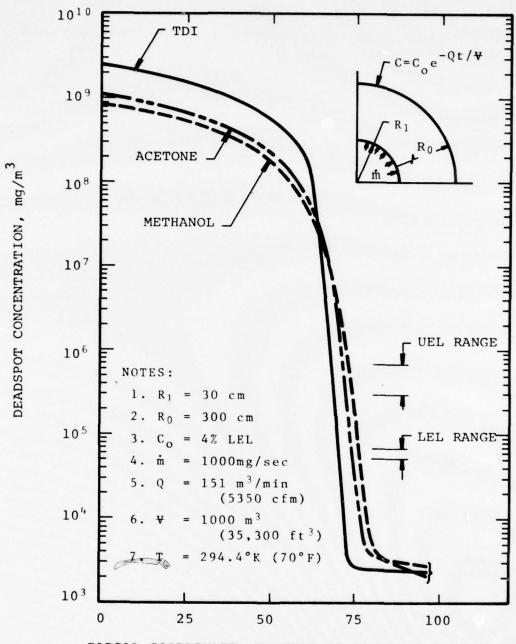
$f(r) = a + br + cr^2$, a second degree polynomial for the initial spatial variation of C_d such that $C_d = C_o$ at $r = R_o$.

In this model, $t = 0$ corresponds to the time when the worker enters the dead spot. This model was then programmed in FORTRAN IV for solution on the CDC Cyber 74 System. A listing of the program, entitled DSPOT, is contained in Appendix D.

An example of the results that were obtained with this model is shown in Figure III.14. For each of the three chemicals, an initial, uniform concentration of 4% LEL was assumed in the dead spot. According to certain corporate operating procedures, concentrations between 1% and 4% LEL are safe for man, but not for fire. Only in the case of acetone is 4% LEL less than the Short Term Exposure Limit (STEL) as proposed by the ACGIH. Therefore, at an initial 4% LEL concentration, it was assumed that some form of respiratory protection would be needed. The program results are presented for a 30-minute work time which approximates the available time with a Scott Air-Pac. After 30 minutes, the convective boundary condition at $r = R_o$ had influenced the vapor concentration in only roughly the outer 5% of the dead spot thickness. Conversely, the flux boundary condition at $r = R_1$ produced large accumulations in concentration in approximately the inner 75% to 80% of the dead spot thickness. The majority of the dead spot contained vapor concentrations that exceeded the UEL. Combustible concentrations between the UEL and LEL were confined to a relatively small portion of the dead spot thickness. However, following termination of vapor regeneration ($\dot{m} = 0$), an extended period of explosive concentrations would be expected as the vapors dilute through diffusion and their concentrations pass between the UEL and LEL.

This model is instructive in the sense that it illustrates that localized work in dead spot areas with vapor sources represent a potential flammability and toxicity hazard. However, in its present form, the model has limited applicability. To improve its applicability, the following improvements would be needed:

o a rational basis for estimating the localized evaporation rate, $\dot{m}$,

o a coupling of the magnitude of R_o with the flow rate Q since it is reasonable to expect that, because of mixing effects, the dead spot radius decreases with increasing flow rate,

FIGURE III.14. EFFECT OF CHEMICAL SPECIES ON DEAD SPOT
CONCENTRATION AFTER 30 MINUTES.

87

o   a method of estimating the initial dead spot concentration
     profile, $f(r)$.

For these reasons, a sensitivity analysis was not felt to be warranted at
this stage of development.

IV. SCALE MODEL VAPOR DISPERSION TESTS
IN A METEOROLOGICAL WIND TUNNEL

During loading of cargo tanks, the cargo displaces a mixture of cargo vapor and air (or inert gas if the tank was inerted). This mixture is emitted from ship tank vents at or above deck level as a plume that is bent over by the wind and dispersed by atmospheric turbulence. If cargo vapors are present near the deck and ship superstructure in either flammable or toxic concentrations, they pose a potential occupational health and safety hazard. Brummage (B-12) carried out extensive low speed wind tunnel experiments using 1/100th scale models of crude oil tanker ships to investigate the size and location of the region of flammable vapor concentration in plumes emitted from ship tank vents during simulated loading conditions. In the tests reported in (B-12), the wind tunnel model was placed on a false floor that allowed the tunnel wall boundary layer to pass beneath the model. In this manner, a range of low turbulence, uniform wind velocities were produced equivalent to from 1.1 m/s (2.5 mph) to 4.5 m/s (10 mph) in full scale. Propane and butane were emitted at vent locations in concentrations ranging from 25% to 100% by volume at model scale flow rates to simulate the emission of a tank atmosphere rich in crude oil vapor near to the end of cargo loading. A portable spark igniter was used to identify the combustible region of the plumes. These wind tunnel experiments provided data that was used to formulate guidelines for the minimum height of vent outlets above the deck to prevent flammable gas concentrations from reaching the deck, and for the minimum separation distance between the vent and the superstructure to eliminate the influence of the superstructure on plume dispersion.

The objectives of the wind tunnel experiments performed during the current project were (1) to provide guidance for the design of a vapor sampling plan for use during full scale tests on tanker ships, and (2) to provide concentration distribution data under controlled atmospheric conditions for improving the analytical plume modeling methods used in this program. For this purpose it was necessary to extend the range of concentration measurement below the flammable region investigated by Brummage, and to determine the effect of a realistic simulation of meteorological conditions including atmospheric stability on the level of vapor concentration at scale man height above the ship deck.

An extensive set of flow visualization experiments was also performed to supplement the vapor concentration measurements. The gas emitted from scale model vents was made visible by adding TiO_2 smoke to the gas stream. Smoke was emitted from seven different vents sequentially while the model was placed at yaw angles of 0°, 30°, 60°, 90°, 120°, 150°, and 180°. The behavior of the visible plumes was recorded photographically on 16mm movie film. The films have proved to be very useful for demonstrating the influence of deck structure and atmospheric stability on the plume path.

The sections that follow describe the vapor concentration measurements during simulated cargo loading conditions in the wind tunnel. The test matrix of model scale conditions appears in Table IV-1.

TABLE IV-1 WIND TUNNEL TEST MATRIX - MODEL SCALE TEST CONDITIONS

Test	Atms. Stbl.	Ri_B*	Wind+ Vel. m/s	Q Vent cm³/s	S.G. at Vent	Froude No.	Ship Angle To Wind	Profiles Vel.	Profiles Temp.	Smoke (S) or Concentration (C)
1.1	Neutral	0	0.15	0.85	1.50	2.95	0	X	X	S
1.2	"	"	"	"	"	"	30			S
1.3	"	"	"	"	"	"	60			S
1.4	"	"	"	"	"	"	90			S
1.5	"	"	"	"	"	"	120			S
1.6	"	"	"	"	"	"	150			S
1.7	"	"	"	"	"	"	180			S
1.8	"	"	"	"	"	"	0	X	X	C
2.1	Neutral	0	0.30	0.85	1.50	11.80	0	X	X	S
2.2	"	"	"	"	"	"	30			S
2.3	"	"	"	"	"	"	60			S
2.4	"	"	"	"	"	"	90			S
2.5	"	"	"	"	"	"	120			S
2.6	"	"	"	"	"	"	150			S
2.7	"	"	"	"	"	"	180			S
2.8	"	"	"	"	"	"	0	X	X	C
3.1	Stable	0.75	0.30	0.85	1.50	11.80	0	X	X	S
3.2	"	"	"	"	"	"	30			S
3.3	"	"	"	"	"	"	60			S
3.4	"	"	"	"	"	"	90			S
3.5	"	"	"	"	"	"	120			S
3.6	"	"	"	"	"	"	150			S
3.7	"	"	"	"	"	"	180			S
3.8	"	"	"	"	"	"	0	X	X	C
4.1	Unstable	-4.7	0.30	0.85	1.50	11.80	0	X	X	S
4.2	"	"	"	"	"	"	30			S
4.3	"	"	"	"	"	"	60			S
4.4	"	"	"	"	"	"	90			S
4.5	"	"	"	"	"	"	120			S
4.6	"	"	"	"	"	"	150			S
4.7	"	"	"	"	"	"	180			S
4.8	"	"	"	"	"	"	0	X	X	C

*Value of the bulk Richardson number to be determined from velocity and temperature measurements made at ship mast height and deck level, (5-1/2 inches and 3 inches above the tunnel floor).

+Wind velocity at deck level, 3 inches above the wind tunnel floor near to model location.

IV.1   Scaling Considerations

The similarity of the dispersion of gaseous effluents in an atmospheric boundary layer and in a laboratory scale boundary layer developed in a meteorological wind tunnel has been discussed by Cermak (B-138). Similarity of velocity and turbulence profiles may be achieved by assuring that the laboratory boundary layer is turbulent, rough and has a long development length. Similarity of atmospheric stability conditions within a layer ΔZ in height is provided by equality of the bulk gradient Richardson number.

$$ Ri = \frac{g \ (\Delta T/\Delta Z)}{T \ (\Delta U/\Delta Z)^2} $$

The trajectory of forced plumes emitted normal to the wind direction is known to depend upon the momentum ratio and the densimetric Froude number. The momentum ratio,

$$ J = \frac{\rho_j \ U_j^2}{\rho_a \ U_a^2} $$

influences the initial rise of the plume as it is turned over by the wind. The densimetric Froude number,

$$ F = \frac{\rho_a \ U_a^2}{(\rho_j - \rho_a) \ g \ d} $$

affects the rise or fall of the plume due to buoyancy. Also, the jet Reynolds number

$$ Re_j = \frac{U_j \ d}{\nu} $$

and the turbulence of the boundary layer affect the entrainment of ambient air by the plume and the dispersion of gaseous effluents in the plume.

Unfortunately, it was not possible to satisfy both Froude number similarity and Reynolds number similarity in the model experiments. Preference was given to exact modeling of momentum ratio and Froude number since it was believed that correct simulation of plume trajectory was most important in these tests. As a result, the plumes emitted from the vents were laminar, and plume dispersion was affected primarily by boundary layer turbulence.

Model scale and full scale values of wind speed are related by the Froude number, while values of venting rate are related by the momentum ratio. The model experiments were designed to simulate the emission of a plume with a high concentration of cargo vapor. This condition can occur near the end of loading when the tank gas atmosphere becomes saturated with cargo vapor. Many of the liquid cargos transported in marine carriers are volatile and have a molecular weight greater than air. Acetone with a molecular weight of

91

58 and a partial pressure of 185 mm Hg at 20°C was chosen as the basis for a full scale example. A typical value of ρ_j/ρ_a for a saturated mixture of acetone vapor in air is 1.25. Using Froude number similarity with a gas mixture having the same value of ρ_j/ρ_a in model scale and a length scale factor of 150, a full scale wind speed of 2.2 m/s corresponds to 0.18 m/s in the wind tunnel. However, it was necessary to maintain the wind tunnel air velocity at a speed of 0.3 m/s (1 ft/s) or higher at deck height for both the stable and unstable atmosphere simulations. Consequently, the value of ρ_j/ρ_a in model scale was increased to approximately 1.5 to give an equivalent full scale wind speed of 2.6 m/s (5.8 mile/hr).

IV.2   Experimental Arrangement

A series of wind tunnel experiments was planned to simulate the dispersion of plumes of heavier-than-air chemical vapor and air emitted from vents on a chemical tanker ship into an ambient wind of approximately 2.2 m/s (5 mile/hr) at deck level. The experiments were performed in the Meteorological Wind Tunnel at Colorado State University. Since current multi-product tanker ships are rather large, typically 183m (600 ft) and longer, a geometric scale of 1:150 was chosen to permit placing a 1.22m (4 ft) long model of a 183 meter ship at various orientations relative to the wind in the 2m (6.6 ft) wide tunnel test section. Figure IV.1 shows the ship model next to a model of a loading dock.
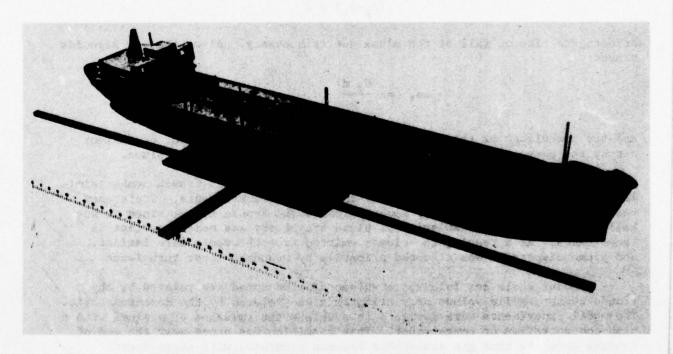
FIGURE IV.1. 1/150 SCALE MODEL OF A CHEMICAL
TANKER SHIP AND LOADING DOCK
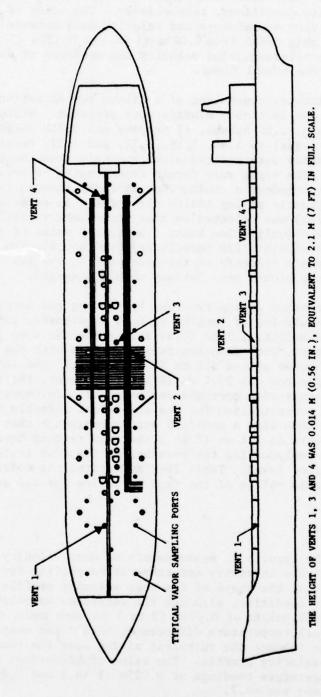
The tanker ship model was placed directly on the wind tunnel floor. A saw-tooth boundary layer trip at the head of the 22-meter long test section insured that the boundary layer ahead of the ship model was turbulent and rough. The wind tunnel floor was cooled and heated to stimulate stable and unstable atmospheric stability conditions, respectively. The value of Richardson number was based upon temperature and velocity measurements in the layer of air around the ship model from 0.025m (1 in.) to 0.127m (5.5 in.) above the tunnel floor. The reference wind velocity was measured at deck level, 0.076m (3 in.) above the tunnel floor.

Four separate gas mixtures consisting of a dilute concentration of a single hydrocarbon tracer gas in carbon dioxide were prepared. Mixture concentrations were 3% methane, 1.5% ethane, 1% propane and 0.75% butane in CO_2 giving values of ρ_j/ρ_a equal to 1.44, 1.51, 1.52, and 1.52, respectively. The tracer gas mixtures were emitted simultaneously from the four vents shown in Figure IV.2. The vents were formed from lengths of nominal 0.16 cm (0.063 in.) diameter hypodermic tubing that extended through the deck and were connected to plastic tubing inside the model. An emission rate of 51 cm^3/min (6.5 ft^3/hr) was selected to give good smoke visibility in the companion set of flow visualization tests. A typical value of full scale emission rate was 11.4 m^3/min (4290 barrels/hr) from a 0.25m (10 in.) diameter vent. Due to the small diameter of the model vents, the jet Reynolds number was 84, and the plumes were laminar when discharged.

Gas sampling was performed during two runs by drawing gas samples through 26 sampling ports consisting of lengths of 0.16 cm diameter tubing open to the air at scale man height, 1.1 cm (0.44 in.) above the ship deck. For the neutral stability tests, both sampling runs were made with the sampling ports arranged in 3 rows spaced 5.1 cm (2 in.) apart. The distance between sampling ports along a row was 10.2 cm (4 in.). However, the spatial resolution of the vapor concentration contours was marginal. To improve the spatial resolution of vapor concentration for the stable and unstable tests, the second sampling run was made with a modified port arrangement that reduced the spacing between ports to 5.1 cm (2 in.) apart in regions downwind of vents. Gas samples were analyzed for the presence of the four tracer gases, corrected for background level. Table IV-2 summarizes the model scale and equivalent full scale values of the test variables for all experiments.

IV.3   Experimental Results

Figure IV.3 shows the results of measurements of mean velocity profile, one-dimensional turbulence intensity and temperature profile for each stability condition. Note that the shape of the mean velocity profile is different for each stability condition, although the reference velocity was 0.30 m/s (1 ft/s) at ship deck height of 0.076m (3 in.) in each case. At this low wind tunnel speed, a small temperature difference, ∿2.6°C for unstable conditions, was sufficient to enhance the turbulent mixing near the tunnel floor and flatten the mean velocity profile. The value of Richardson number, based upon velocity and temperature readings at 0.025m (1 in.) and 0.076m (3 in.) above the tunnel floor was -4.7.

THE HEIGHT OF VENTS 1, 3 AND 4 WAS 0.014 M (0.56 IN.), EQUIVALENT TO 2.1 M (7 FT) IN FULL SCALE.

THE HEIGHT OF VENT 2 WAS 0.061 M (2.4 IN.), EQUIVALENT TO 9.2 M (30 FT) IN FULL SCALE.

THE HEIGHT OF THE VAPOR SAMPLING PORTS WAS 0.011 M (0.44 IN.), EQUIVALENT TO 1.7 M (5.5 FT) IN FULL SCALE.

FIGURE IV.2. VENT LOCATIONS ON SCALE MODEL OF TANKERSHIP

TABLE IV-2. MODEL AND FULL SCALE VALUES OF TEST VARIABLES

| VENT NO. | DIMENSIONLESS PARAMETERS | | MODEL SCALE VARIABLES | | | | | | FULL SCALE VARIABLES | | | | | |
	J	F	ρ_j/ρ_a	U_a m/s	(ft/s)	U_j m/s	(ft/s)	ρ_j/ρ_a	U_a km/hr	(mile/hr)	U_j m/s	(ft/s)
1	2.82	13.04	1.44	0.3	(1.0)	0.42	(1.4)	1.25	9.97	(6.20)	4.16	(13.6)
2	2.96	11.25	1.51	0.3	(1.0)	0.42	(1.4)	1.25	9.26	(5.75)	3.96	(13.0)
3	2.98	11.03	1.52	0.3	(1.0)	0.42	(1.4)	1.25	9.17	(5.70)	3.93	(12.9)
4	2.98	11.03	1.52	0.3	(1.0)	0.42	(1.4)	1.25	9.17	(5.70)	3.93	(12.9)
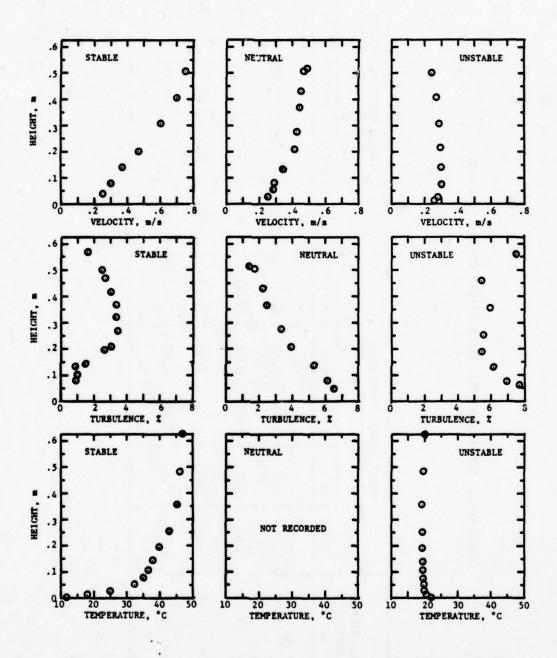
FIGURE IV.3. VELOCITY, TURBULENCE AND TEMPERATURE
PROFILES FOR STABLE, NEUTRAL AND UNSTABLE
ATMOSPHERIC STABILITY SIMULATIONS

There is a noticeable similarity between the mean velocity and turbu-
lence profiles for the neutral and the unstable atmospheric simulations in
the region of the ship deck 0.076m (3 in.). Note, the velocity at the top
of the superstructure 0.14m (5.5 in.) is about 10% higher for the neutral
simulation than for the unstable simulation.

The stable atmosphere simulation shows a strong suppression of boundary
layer turbulence in the 0 to 0.14m (5.5 in.) region when compared with either
the neutral or unstable atmosphere simulation. The value of Richardson num-
ber, based on velocity and temperature readings at 0.076m (3 in.) and 0.14m
(5.5 in.) above the tunnel floor was 0.75.

Figure IV.4 shows the contours of tracer gas concentration (based upon
the concentration measurements at the sampling ports) for gas emitted from
vent number 1, a low vent 0.014m (0.56 in.) above the deck near the bow of the
ship. The tracer concentration at the vent was 30,000 ppm of methane. The
shaded regions ranging from light to dark correspond to concentration levels
of 5 - 9.9 ppm, 10 - 19.9 ppm, 20 - 29.9 ppm and >30 ppm. The equivalent con-
centration ranges for full scale emission of a saturated mixture of acetone
vapor in air are 42 - 83 ppm, 84 - 161 ppm, 168 - 251 ppm and >252 ppm. Even
with the closer spacing of sampling ports in the unstable and stable atmo-
spheric simulations, the spatial resolution of concentration was inadequate
to resolve the peak concentration region near the vent. The highest measured
values of concentration were 139 ppm for the stable simulation and 149 ppm
for the unstable simulation at a sampling port placed only 2.5 cm (1 in.)
from the vent. However, the spatial resolution was sufficient to distinguish
the far field concentration distribution downwind of the vent.

Note that the stable atmospheric simulation gave the greatest area of
coverage and the highest values of concentration far away from vent 1. Note
also the similarity of concentration contours for the neutral and the unstable
simulations.

Vent number 2 was a high vent near the middle of the ship 0.061m (2.4
in.) above the deck, equivalent to 9.14m (30 ft) above the deck in full scale.
The tracer concentration at the vent was 15,000 ppm of ethane which gave a
gas chromatograph (GC) response equivalent to 28,143 ppm of methane. The
concentration of ethane was very low near deck level, less than 2 ppm of
equivalent methane at all sampling ports for all stability conditions. These
results confirm that an elevated vent is an effective method for preventing
vented chemical vapors from reaching deck level at wind speeds of 2.2 m/s
(5 mile/hr) and higher.

Figure IV.5 shows the tracer gas concentration for gas emitted from
vent number 3, a low vent 0.014m (0.56 in.) above the deck behind the loading
manifold piping near the middle of the ship. The tracer concentration at the
vent was 10,000 ppm of propane, giving a GC response equivalent to 27,473 ppm
of methane. The shaded regions ranging from light to dark correspond to the
same concentration levels of equivalent methane as in Figure IV.4. The high-
est measured values of concentration were 120 ppm for stable, 17.1 ppm for
neutral, and 54.3 ppm for unstable atmospheric stability simulations. For
this vent location, the concentration contours are similar in shape for all
three stability simulations.

97

CONCENTRATION RANGES

	5 - 9.9 ppm			20 - 29.9 ppm	
MODEL SCALE					>30 ppm
FULL SCALE	42 - 83 ppm	84 - 167 ppm	168 - 251 ppm		>252 ppm

VENT CONCENTRATION

30,000 ppm METHANE

251,700 ppm ACETONE

STABLE ATMOSPHERIC STABILITY SIMULATION

NEUTRAL ATMOSPHERIC STABILITY SIMULATION

UNSTABLE ATMOSPHERIC STABILITY SIMULATION
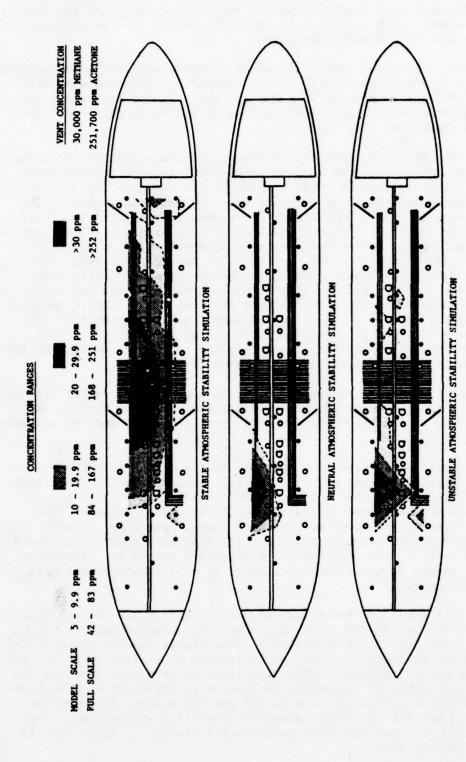
FIGURE IV.4. CONCENTRATION CONTOURS FOR VAPOR EMISSION FROM VENT 1

CONCENTRATION RANGES

MODEL SCALE | 5 – 9.9 ppm | 10 – 19.9 ppm | 20 – 29.9 ppm | >30 ppm
FULL SCALE | 42 – 91 ppm | 92 – 182 ppm | 183 – 274 ppm | >275 ppm

VENT CONCENTRATION

27,473 ppm METHANE
251,700 ppm ACETONE

STABLE ATMOSPHERIC STABILITY SIMULATION

NEUTRAL ATMOSPHERIC STABILITY SIMULATION

UNSTABLE ATMOSPHERIC STABILITY SIMULATION
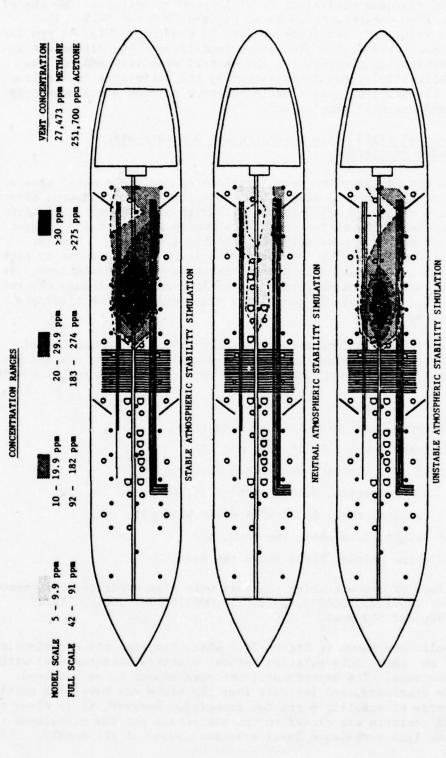
FIGURE IV.5.   CONCENTRATION CONTOURS FOR VAPOR EMISSION FROM VENT 3

Figure IV.6 shows the tracer gas concentration for gas emitted from vent number 4, a low vent 0.014m (0.56 in.) above the deck directly in front of the superstructure. The tracer concentration at the vent was 7500 ppm of butane, with a GC response equivalent to 27,174 ppm of methane. The shaded regions have the same interpretation as in Figures IV.4 and IV.5. The highest measured values of concentration were 35 ppm for stable, 44 ppm for neutral, and 39 ppm for unstable atmosphere conditions. The difference in location of concentration contours for the neutral stability and for the stable and unstable simulations is explained by the difference in sampling port location. The sampling port location closest to vent 4 was used only for the stable and unstable simulations.

IV.4 Comparison of 1/150 Scale Concentration Contours with Plume Model Predictions

Although the gas sampling port locations on the scale model gave a relatively poor resolution of concentration contours in the crosswind direction, a comparison of the experimental results with plume model predictions was undertaken. The concentration contours shown in Figure IV.4 for vapor emission from vent number 1 were selected for this comparison. Similar values of upstream wind velocity and turbulence level were measured at deck height for the neutral and unstable thermal stratification simulations. As a result, the contours of concentration are similar as well, though the resolution is better for the unstable simulation which employed two alternate sampling port arrangements.

Plume model computations were performed for the following set of full-scale conditions (equivalent to the wind tunnel conditions for emission from vent number 1). These computations were based on the Ooms-teRiele model.

o   neutral atmospheric stratification,

o   wind speed, 2.77 m/s at 11.4m elevation,

o   turbulence levels, 6, 10, 15, and 20%,

o   emitted gas, acetone vapor mixed with air,

o   vent concentration, 0.6093 kg/m^3 (251,700 ppm),

o   vent emission rate, 0.190 m^3/s (4290 bbl/hr),

o   vent height, 2.1m above the deck, and

o   prediction height, 1.68m above the deck.

Crosswind locations of concentration contours were also predicted for concentration levels of .000102, .000203, .000407, .000610, and .001210 kg/m^3 (42, 84, 168, 252, and 500 ppm).

The results are shown in Figure IV.7 which compares the experimental contours (based on linear interpolation between discrete measurements) with the predicted contours. The experimental contours appear to be inclined slightly towards starboard, and indicate that the plume may have been carried away from the array of sampling ports far downwind. However, it is clear that the experimental contours are closer to the prediction for 20% turbulence than for 6% turbulence (the turbulence level measured upwind of the model).

100
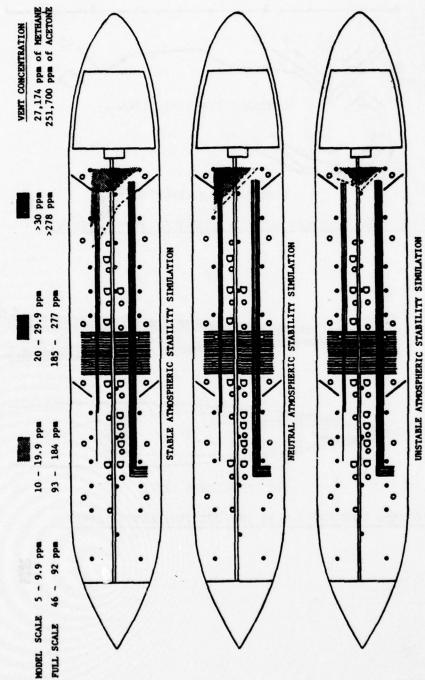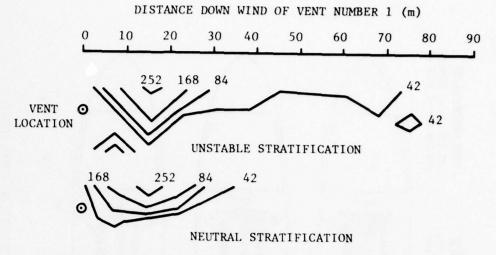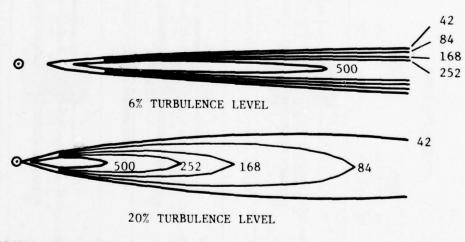
FIGURE IV.6. CONCENTRATION CONTOURS FOR VAPOR EMISSION FROM VENT 4

CONCENTRATION CONTOURS IN PPM OF ACETONE VAPOR

VENT CONCENTRATION 251,700 ppm

DISTANCE DOWN WIND OF VENT NUMBER 1 (m)

FIGURE IV.7. COMPARISON OF MEASURED CONCENTRATION CONTOURS
FOR NEUTRAL AND UNSTABLE ATMOSPHERIC STABILITY
SIMULATIONS WITH PLUME MODEL PREDICTIONS

102

Vent number 1 lay downwind and in the wake of the fore deck leading up to the bow. The flow visualization movies for 0° yaw angle show that the smoke plume emitted from vent number 1 changed direction rapidly, indicating that the airstream around the vent was highly unsteady. These considerations may explain why the experimental contours show a more rapid concentration decay and greater crosswind spread than predicted by the plume model for the correct 6% upwind turbulence level.

Another factor that deserves consideration is the influence of low frequency unsteadiness in wind tunnel speed on the experimental concentration measurements. Wind tunnel turbulence levels reported in Figure IV.3 were made by reading the hot-film anemometer voltage fluctuations on a true rms voltmeter. This instrument does not respond accurately to fluctuations with frequencies below 0.2 Hz. However, at the beginning of the wind tunnel test program, turbulence levels were also measured in the tunnel by sampling the anemometer voltage at a rate of 300 samples per second and computer averaging for periods of 10 and 60 seconds. The turbulence levels estimated by this method were consistently higher (turbulence levels up to 20-30%) than the levels estimated by the true rms voltmeter, presumably due to a low frequency unsteadiness in the tunnel speed. Since the gas concentration samples were drawn through the sampling ports and into bags over a period of from 3 to 5 minutes, the experimental results would be influenced by low frequency unsteadiness in wind direction and speed.

This comparison shows that the analytical plume model predicts spatial distributions of vapor concentration that are similar to experimentally determined concentration contours. The comparison also shows the need for careful determination of wind turbulence level in further model and full scale experiments.

A more comprehensive comparison of analytical predictions to experimental data are given for the 1/4 and full scale test results in Chapters V and VI.

V. DISPERSION OF HEAVIER-THAN-AIR VAPORS ON
A ONE-QUARTER SCALE SHIP DECK

The 1/150 scale model experiments of vapor dispersion reported in Section IV showed that a full-scale vapor sampling plan, based upon making concentration measurements at geometric grid locations spaced 7.6m or farther apart, would not give acceptable resolution of concentration contours within 10m of the vent. Further test work was required with closer grid spacing before undertaking full scale tests. Also, there was a need to train project personnel in the methods of data gathering and data analysis that would be used during full-scale tests. Therefore, it was decided to construct a simple 1/4 scale test facility that would be economical to use but large enough to allow the use of full size portable instrumentation. In the discussion that follows all dimensions are 1/4 scale dimensions unless otherwise noted.

V.1 The Facility

A 1/4 scale layout of a ship deck, complete with simulated superstructure and scale model vents, was constructed on the Institute grounds. The scaled deck plan of a 36,000 DWT chemical tanker was laid out directly on the ground. No attempt was made to simulate the elevation of an actual deck above the water line. The simulated deckhouse consisted of plywood panels nailed to a wooden framework to give a wind blockage effect similar to that experienced on a ship.

Two portable gas discharge vents were constructed. The first vent consisted of a 0.66m length of 6.4 cm I.D. PVC pipe representing a short discharge vent 2.4m tall and 26 cm I.D. connected to an expansion trunk on the ship deck. Screens were placed in the model vent to aid flow straightening and to promote gas mixing. The second vent consisted of a 2.3m length of 6.4 cm I.D. pipe representing a 9.2m tall, 26 cm I.D. vent that discharges vapor at a height above deck equal to one-third the ship beam dimension. Internal screens were not required due to the length of this vent model

A grid of gas sampling locations was superimposed onto the deck plan form. The initial distance between the nodes of the grid was 3.0m (longitudinal) by 1.7m (lateral, equal to 1/4 beam). Finer grid sizes were also used and evaluated during personnel training exercises. Also, 1/4 scale plume dispersion data was collected in the downwind direction, as indicated by the release of smoke, without reference to grid locations, for comparison with the analytical plume model predictions.

The presence and concentration of CH_4 tracer gas was determined by continuous sequential sampling at the center of grid panels or at predetermined downwind locations using an organic vapor analyzer described in Section VI.2.

V.2 Gas Mixing and Delivery Systems

A system was developed to supply a metered mixture of carbon dioxide (CO_2), methane (CH_4), and titanium dioxide (TiO_2) smoke to a 1/4 scale model vent for the simulation of cargo tank atmosphere venting during typical end

105

of loading conditions. Similarity requirements (discussed in Section IV) specified a CH_4 to CO_2 ratio of 1:100 and a total venting rate of 4180 cm^3/s. A photograph of the gas supply system is shown in Figure V.1, and a schematic drawing of the component arrangement appears in Figure V.2. The gas mixture emerging from the vent model was made visible as shown in Figure V.3 by passing a small portion of the CO_2 flow stream through a bottle containing titanium tetrachloride ($TiCl_4$) vapor. This vapor reacts with moisture to form a white smoke (TiO_2).

V.3   Test Program

A total of twelve tests were performed on the 1/4 scale facility as shown in Table V-1. Tests 1 through 4 served primarily as personnel training exercises during which project members gained experience with the vapor measuring instruments. The instantaneous tracer gas concentration was measured at a height of 41 cm above the ground at specified grid locations around the vent. Project personnel read the range and peak value of tracer gas concentration on the probe/readout assembly and recorded these values before moving to the next grid location. Wind velocity was measured with a hand-held hot-wire anemometer at a height of 1.68m above the ground. The range of wind velocity readings was recorded at several times during a run, and an average value of wind velocity was computed.

Tests 5 through 9 were designed specifically to collect time averaged gas concentration data for a direct comparison with predictions from the analytical plume model. For this purpose it was desired to collect data at vent height and at scale man height level along the plume centerline in a downwind direction from the vent. Accordingly, the concentration instrumentation was positioned at a specified distance downwind of the vent and the instantaneous concentration values were recorded for 90 seconds on a strip chart recorder. Measurements were made at several downwind locations at two heights, 41cm and 66cm, above the ground. Tests 5, 6, 8, and 9 used a gas mixture of 1 part CH_4 to 100 parts CO_2 giving a negatively buoyant plume with a value of $\bar{\rho} = 1.51$. Test 7 used a mixture of 1 part CH_4 to 100 parts N_2 giving a slightly positive buoyant plume with $\bar{\rho} = 0.96$. Tests 5, 6, 7, and 8 used a gas release rate of about 4180 cm^3/s, compared with 2088 cm^3/s for run 9. Tests 7, 8, and 9 were replicated in order to gain some indication of the consistency of the time average concentration measurements. Wind velocity was measured with a hand-held anemometer several times during a test, and an average value was computed.

V.4   Test Results and Comparison With Analytical Prediction

Figure V.4 (a) and (b) shows the peak concentration values (in units of mg/m^3) noted during the release of a CO_2/CH_4 mixture from the 66-cm high vent in Test 1, and from the 2.3m high vent in Test 2. The concentration values shown in the figure were measured at the center of each 3.05 x 1.71m grid panel at a height of 41 cm above the ground. Note that the concentration values downwind of the tall vent in Figure V.4(b) are an order of magnitude lower than those downwind of the short vent in Figure V.4(a).
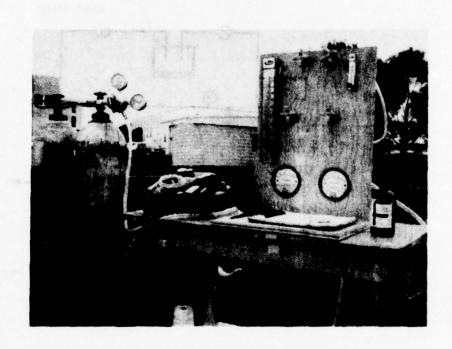
FIGURE V.1. GAS SUPPLY SYSTEM
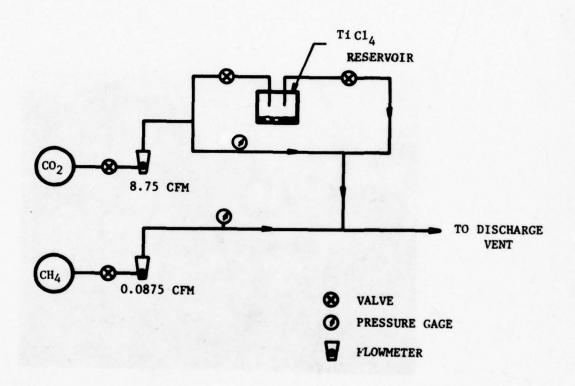
FIGURE V.2. GAS MIXING AND DELIVERY SYSTEM

FIGURE V.3. GAS SUPPLY SYSTEM AND VISIBLE PLUME

TABLE V-1

SUMMARY OF 1/4 SCALE TEST CONDITIONS

TEST NO.	GASES RELEASED	$\bar{\rho} = \frac{\rho_f}{\rho_a}$	WIND SPEED	SAMPLING ARRANGEMENT	VENT HEIGHT	CONCENTRATION MEASUREMENT
1	CO_2/CH_4	1.51	1.5 - 2.8 m/s	Grid, 3m x 1.7m	66 cm	Range and Peak Value
2	CO_2/CH_4	1.51	1.5 - 5.1 m/s	Grid, 3m x 1.7m	2.3 m	Range and Peak Value
3	CO_2/CH_4	1.51	2.5 - 7.6 m/s	Grid, 1.5m x 1.7m	66 cm	Peak Values
4	CO_2/CH_4	1.51	1.5 - 3.0 m/s	Grid, 1.0m x 0.85m	66 cm	Peak Values
5	CO_2/CH_4	1.51	Avg. 4.1 m/s	Downwind	66 cm	Average Values
6	CO_2/CH_4	1.51	Avg. 3.4 m/s	Downwind	66 cm	Average Values
7-1	N_2/CH_4	0.96	Avg. 2.1 m/s	Downwind	66 cm	Average Values
7-2	N_2/CH_4	0.96	Avg. 2.1 m/s	Downwind	66 cm	Average Values
8-1	CO_2/CH_4	1.51	Avg. 1.8 m/s	Downwind	66 cm	Average Values
8-2	CO_2/CH_4	1.51	Avg. 1.8 m/s	Downwind	66 cm	Average Values
9-1	CO_2/CH_4	1.51	Avg. 2.3 m/s	Downwind	66 cm	Average Values
9-2	CO_2/CH_4	1.51	Avg. 2.3 m/s	Downwind	66 cm	Average Values

a) TEST 1   WIND SPEED 1.52 - 2.79 m/s

         GRID DIMENSIONS 3.05m x 1.71m

         VENT HEIGHT 66cm

         TRACER CONCENTRATION UNITS mg/m^3

b) TEST 2   WIND SPEED 1.52 - 5.08 m/s

         GRID DIMENSION 3.05m x 1.71m

         VENT HEIGHT 2.3m

         TRACER CONCENTRATION UNITS mg/m^3

FIGURE V.4. PEAK VALUES OF TRACER GAS CONCENTRATION
FOR 1/4 SCALE MATRIX SAMPLING TESTS 1 AND 2
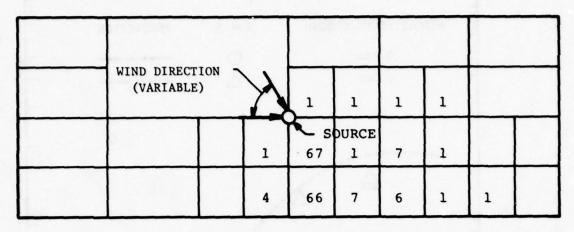
Figure V.5(a) and (b) shows the peak concentration values of CH_4 tracer (in units of mg/m^3) noted in Tests 3 and 4 at the center of grid panels with dimensions of 1.52 x 1.71m and 1.01 x 0.85m, respectively downwind of the short, 66 cm high vent. The improved resolution of concentration variation given by the finer grid spacing in Figure V.5(b) is readily apparent.

The key observations from Tests 1 through 4 may be summarized as follows:

o   The tall vent (height equal to one-third ship beam width) is noticeably more effective than the short vent (equivalent full scale height ~8 ft) in limiting vapor concentration near the ship deck.

o   Close grid spacing (equivalent to 3 to 4m or less in full scale) is necessary to adequately resolve the region of highest concentration downwind of a vent.

o   The instantaneous tracer gas concentration varies quite rapidly in time, and the average cannot be estimated by eye from an instrument readout. Therefore, for comparison with the predictions of time average concentration from the analytical plume model, the instantaneous concentration readings must be recorded and averaged using the procedure described in Section VI.2.

The results of Tests 5 through 9 are shown in Figures V.6 through V.9, which compare the values of tracer gas concentration downwind of the vent at 41 cm and 66 cm height (as predicted by the Ooms-teRiele model) with the actual time averaged concentration data. A turbulence level of 20% was used in all plume dispersion computations. In general, the agreement between prediction and experiment is fairly good. Key observations from Tests 5 through 9 are summarized below.

o   During the 90-second concentration recording time, the wind direction and wind velocity would change. As a result, it was impossible to assure that the concentration instrument was located downwind of the vent. Therefore, it would be expected that some of the concentration-time averages would be noticeably less than the predicted levels.

o   The time averaged concentration values do not exceed the predicted levels at 66 cm height, but they do exceed the predictions for 41 cm height in the region that is less than 2m downwind of the vent. There are two possible factors that may explain this behavior:

1.   When the wind speed falls to low values, <0.5 m/s, the plume trajectory drops close to the ground. A short period, perhaps 10 seconds, of low wind speed would greatly increase the time average concentration at locations believed to be below the plume.

112

WIND DIRECTION
(VARIABLE)

			1	1	1	1	
				SOURCE			
		1	67	1	7	1	
		4	66	7	6	1	1

a) TEST 3   WIND SPEED   2.54 - 7.62   m/s
                    GRID DIMENSIONS   1.52m x 1.71m
                    TRACER CONCENTRATION UNITS   mg/m^3
                    VENT HEIGHT   66cm

	16	32	55	48	57	52		
	13	35	48	55	61	52		
	0	20	44	48	5	5		
	0	21	46	59	61	2		

SOURCE

WIND DIRECTION
(VARIABLE)

b) TEST 4   WIND SPEED   1.52 - 3.05   m/s
                    GRID DIMENSIONS   1.01m x 0.85m
                    TRACER CONCENTRATION UNITS   mg/m^3
                    VENT HEIGHT   66cm

FIGURE V.5.   PEAK VALUES OF TRACER GAS CONCENTRATION
        FOR 1/4 SCALE MATRIX SAMPLING TESTS 3 AND 4
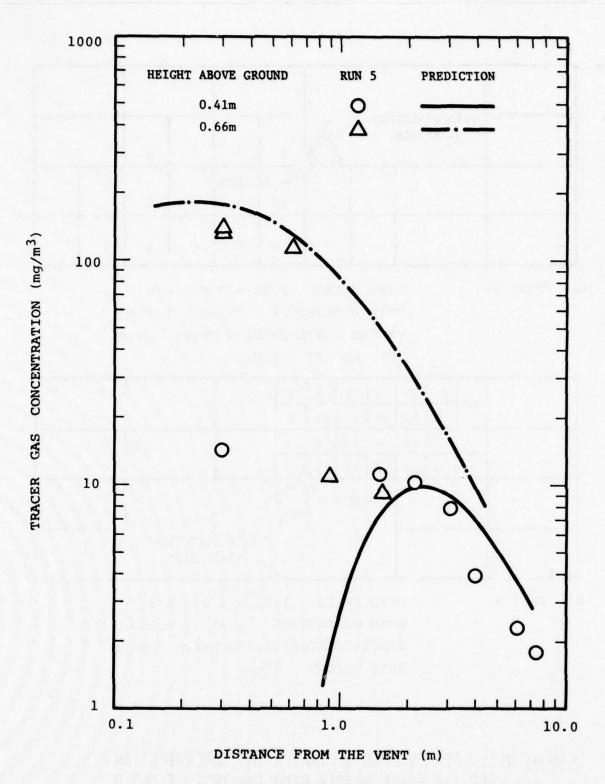
FIGURE V.6.   MEASURED AND PREDICTED VALUES OF TRACER GAS
CONCENTRATION DOWNWIND OF VENT. TEST 5.
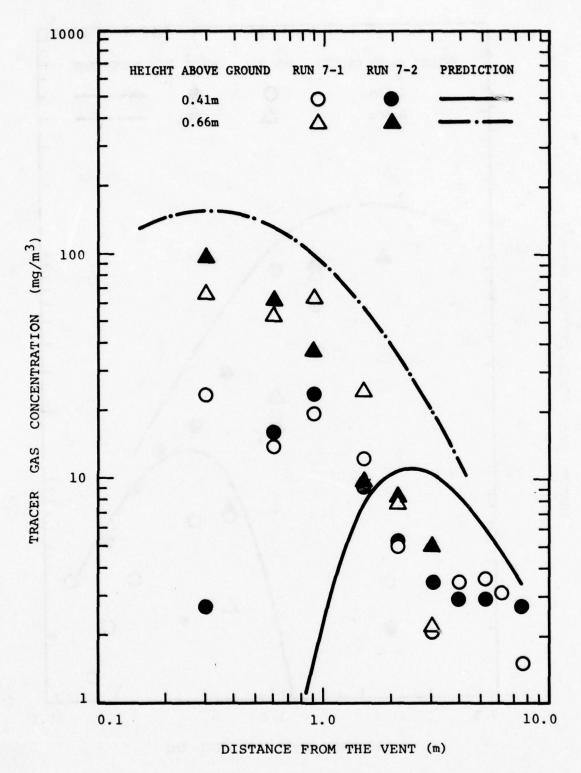
FIGURE V.7. MEASURED AND PREDICTED VALUES OF TRACER GAS CONCENTRATION DOWNWIND OF VENT. TESTS 7-I AND 7-2
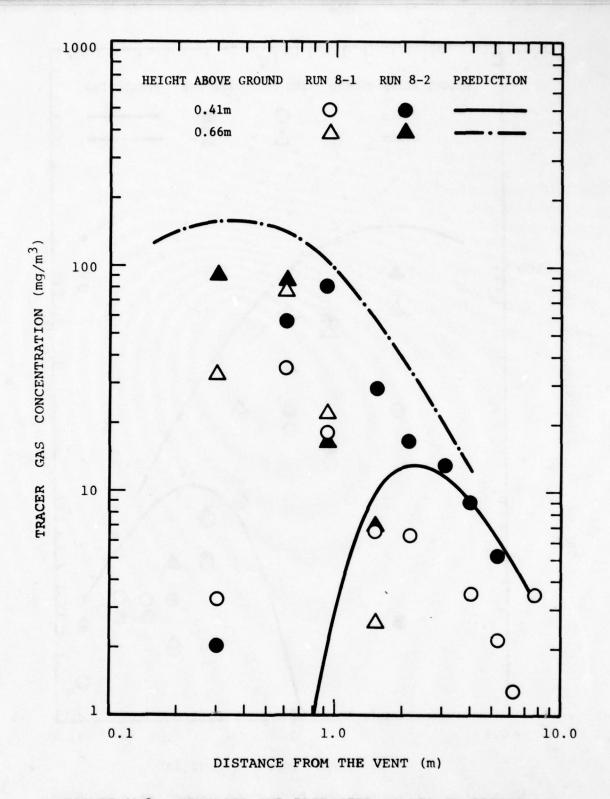
FIGURE V.8. MEASURED AND PREDICTED VALUES OF TRACER GAS CONCENTRATION DOWNWIND OF VENT. TESTS 8-1 AND 8-2

116
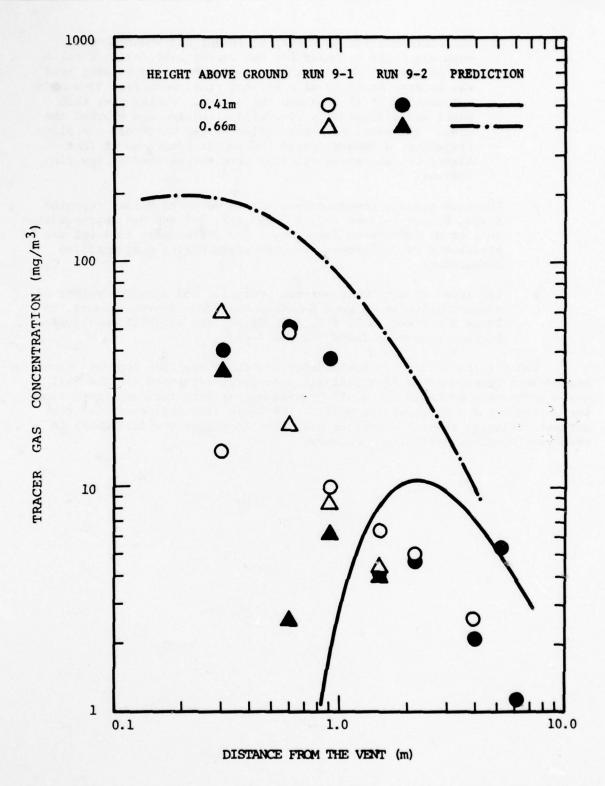
FIGURE V.9 MEASURED AND PREDICTED VALUES OF TRACER GAS
CONCENTRATION DOWNWIND OF VENT. TESTS 9-I AND 9-2.

117

2. The concentration measuring equipment was mounted on a moveable dolly designed for use during full scale tests. During the 1/4 scale tests, the concentration sensing head was located in front of a plywood panel measuring 33 x 55 cm and mounted at 70 cm above the ground. During use, this panel was aligned in a crosswind direction and blocked the wind. The panel may have deflected the airstream and plume trajectory downward toward the sensor locations so that higher concentration readings were encountered at low elevations.

o The time average concentration values measured during repeated tests, Number 7-1 and 7-2, 8-1 and 8-2, 9-1 and 9-2, agree rather well at most downwind locations. The differences in level can be attributed to differences in wind speed during concentration measurements.

o The level of agreement between predicted and measured values of concentration is as good for the negatively buoyant plumes, in Tests 5 and 8-1, 8-2, 9-1, 9-2, as for the slightly positively buoyant plumes in Tests 7-1 and 7-2.

The results of the 1/4 scale tests confirmed that the concentration measurement technique and data analysis procedures developed for the full scale tests were workable and would provide useful data for comparison with the analytical plume dispersion model. The tests also indicated that the natural variation in wind direction with time increases the difficulty in resolving plume concentration contours.

118

VI. FULL-SCALE TANKER TESTS

VI.1 Scope

Two full-scale tanker tests were conducted on this program. The objectives of these tests were to

o measure the vapor concentrations to which tankermen are exposed during the course of normal work activities, and

o collect vapor concentration data for use in validating analytical models.

Both tests involved loading of pure chemicals. Vapor concentration measurements were obtained in cargo tanks before commencement of loading and in the air above the ship deck during loading. Both tests were conducted aboard vessels that had been observed during the early stages of this program. Test No. 1 was conducted on a 36,000 DWT multi-cargo tanker (Appendix B, Terminal B, Observation 3). Test No. 2 involved a 28,000 DWT multi-product tanker (Appendix B, Terminal A, Observation 1). The cargo loading plan for each vessel is presented in Tables VI-1 and VI-2. Test No. 1 monitored the vapors that were vented from 3CP and 3S tanks during product loading. In addition, project and ship personnel entered 3CA and 3S tanks. The previous contents of these latter two tanks, which had been washed and ventilated at sea, were methyl isobutyl ketone (MIBK) and toluene, respectively. Test No. 2 monitored the vapors vented during the loading of 3C and 4C tanks.

On each of these tests, the chemicals of interest and the tanks into which they were to be loaded were identified prior to vessel docking. Final selection of the tank(s) to be monitored was influenced by an approximate tank loading sequence, which was, in all cases, developed at a preloading conference immediately following vessel tie-up.

VI.2 Air Sampling

Four classes of air sampling activities were conducted on both of these tests:

o Source Sampling

o Area Sampling

o Matrix Sampling

o Personal Sampling

Appendix E contains a detailed discussion of the sampling methodologies, the instrumentation that was used, the procedures that were followed, and the methods of analysis.

119

TABLE VI-1

TEST NO. 1

VESSEL LOADING PLAN
VOYAGE No. 321

Tank No.	Contents	Quantity (bbls)[4]
1P	(1)	
1C	(1)	
1S	(1)	
2P	(1)	
2CP	Cyclosol 33	6,600
2CS	Sol B	6,600
2CA	Sol 140	8,800
3P	Ethylene Glycol	11,600
3CP	Ethyl Alcohol-190	6,600
3CA	Epichlorohydrin	3,800
3CS	Methyl Ethyl Ketone	
3CF	Acetone	6,600
3S	Toluene	11,600
4P	(1)	
4C	VM&P Naphtha	10,000
4S	(1)	
5P	(2)	
5CA	Diala-A	8,800
5CF	HVI-100-MQ	13,200
5CP	LVI-65	6,500
5CS	HVI-250-tQ	6,500
5S	(2)	
5P	(3)	
6CA	Isopropyl Alcohol	6,100
6CF	(1)	
6S	(3)	

NOTES: (1) Unleaded gasoline, 115,000 bbl total

(2) Regular gasoline, 34,000 bbl total

(3) Aviation gas, 27,000 bbl total

(4) Scheduled quantity, actual delivery may differ.

TABLE VI-2

TEST NO. 2

VESSEL LOADING PLAN
VOYAGE No. 21

Tank No.	Contents	Quantity (bbls)[1]
1P	Coray-60	3,000
1CP	Necton-60	3,600
1CS	F-3262 W.O.B.	3,600
1S	Flexon 766	1,500
2P	L/P-100N	5,400
2C	Varsol-18	12,000
2S	L/P-100N	5,400
3P	HAN	6,000
3C	Hexane	12,000
3S	Aromatic-150	6,000
4P	Varsol-18	6,000
4C	Toluene	12,000
4S	VM&P	5,000
5P	Flexon-641	6,000
5C	F-3261 W.O.B.	8,000
5S	Necton-37	6,000
6PF	Necton-78	4,600
6CP	Insulating Oil	3,000
6CS	Insulating Oil	3,000
6SF	Coray-150	4,600
6PA	Bright Stock	1,500
6SA	Bright Stock	1,500
7P	Diluent Oil-F1503	2,000
7C	Diluent Oil-F1503	12,000
7S	Coray-1000	4,400
8P	Varsol-1	6,000
8C	Varsol-1	12,000
8S	Varsol-1	6,000
9P	Lops	5,000
9C	Toluene	12,000
9S	Isopar-G	6,000
10P	F-3268 W.O.B.	4,400
10C	Xylene	8,200
10S	F-3268 W.O.B.	4,400
11P	Coray-320	1,700
11S	Coray-220	3,000

NOTE: (1) Scheduled quantity, actual delivery may differ.

Source Sampling

The objective of the source sampling task was to continuously moni-
tor the concentration of chemical vapors that were discharged from a tank as
it was being loaded. Typically, monitoring began at tank farm pump startup
and continued through tank top-off.

Source and matrix vapor concentrations were obtained using the in-
strumentation that is shown in Figure VI.1. The sampling and analysis instru-
ment was a Century Systems Corporation Organic Vapor Analyzer (OVA Model
No. 108 with linear readout or OVA Model No. 128 with logarithmic readout).
These units and their accompanying strip chart recorders are certified by
Factory Mutual Research Corporation as intrinsically safe for use in Class I,
Division 1, Groups A, B, C, and D hazardous locations.

Area Sampling

The objective of the area sampling was to obtain time weighted
(30-min. period) vapor concentration samples at fixed locations on the ship
deck. This data could then be compared to the 3-min. averaged matrix vapor
concentration data and analytical plume model predictions.

Area sampling consisted of collecting vapor laden air in inert
bags at five on-deck sampling stations. Each sampling station was composed
of the apparatus that is shown in Figure VI.2. An MSA Model C-200 personal
sampling pump and accompanying bag was fastened to a weighted vertical boom.
Pump inlet was fixed at 5.5 ft (1.68m) above the deck, which closely approxi-
mates man's breathing level height. Several samples were collected at each
location with each sample (bag) being obtained over a 30-minute period.

Matrix Sampling

The objectives of matrix sampling were:

(1)   to provide an indication of the total hydrocarbon concen-
       tration as a function of space and time during tank loading.
       The resultant concentrations can be expressed as %LEL for
       methane, which is the basis for explosimeter readings.

(2)   to generate data for use in validating plume dispersion
       models assuming there is no vapor present from other tanks
       being loaded at the same time as the tank of interest.

Following identification of the tanks to be monitored, a matrix
of sampling points was marked on the ship's deck. This matrix extended down-
wind and crosswind of the vapor source. The purpose of this grid layout was
to define points on the deck where an OVA apparatus could be sequentially
positioned to record total hydrocarbon concentrations. To this end, two
mobile OVA units of the type that were shown in Figure VI.1 traversed the
matrix of points in a prescribed sequence with a 3-minute sampling duration
at each gridpoint. The sample inlet on the probe/readout assembly was again
positioned at a breathing level height of 5.5 ft (1.68m) above deck level. A
3-minute sampling duration was selected based on the results of scale model wind
tunnel vapor dispersion tests discussed in Section IV.

122
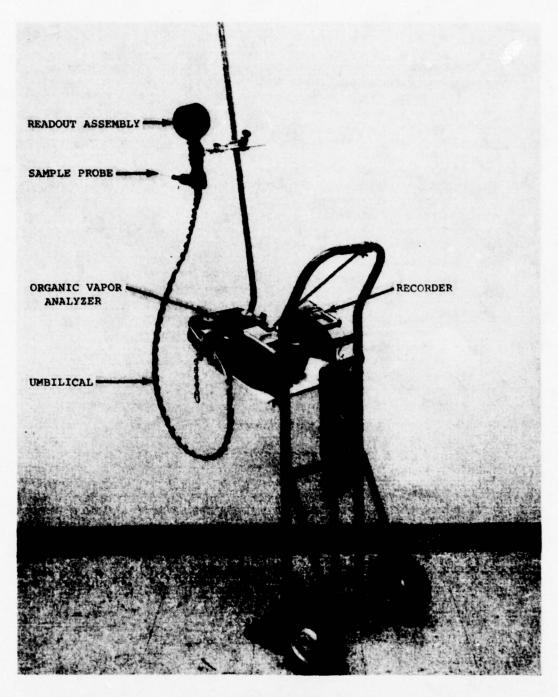
FIGURE VI.I   SOURCE AND MATRIX SAMPLING APPARATUS

123

LOCAL WIND
DIRECTION INDICATOR

SAMPLING PUMP

INERT LINE

INERT COLLECTION
BAG
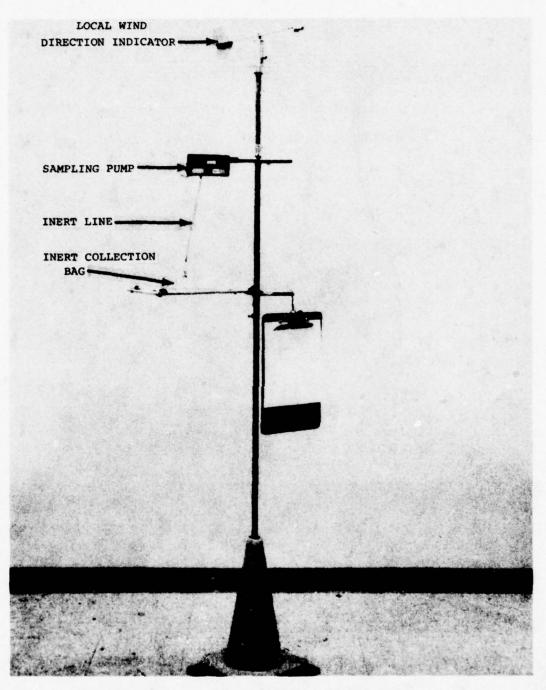
FIGURE VI.2   AREA SAMPLING APPARATUS

Personal Sampling

The objective of the personal sampling program was to ascertain the vapor concentration levels to which workers were exposed during their normal work routine. Both acute and chronic exposures were evaluated. In the former case, the data could be compared to Short Term Exposure Limits (STEL), while in the latter case, the data were compared to the prevailing 8-hour time-weighted average Threshold Limit Values (TLV), and additive exposure effects could also be assessed.

Selected crew members wore the sampling apparatus that is shown in Figure VI.3. Project personnel also wore the sampling equipment when they accompanied a ship's officer into an empty tank. The individual to be monitored wore a belt-mounted MSA Model C-200 portable pump and a lapel-mounted tube holder that housed an SKC Corp. charcoal sampling tube. These pumps are certified by Factory Mutual Research Corp. as intrinsically safe for use in Class I, Division 1, Groups C and D hazardous locations and non-incendive for use in Class I, Division 2, Groups A, B, C, and D hazardous locations as defined by the National Electrical Code.

VI.3   Meteorological Measurements

The meteorological parameters of wind speed, wind direction and atmospheric temperature were recorded during each experiment. The instrumentation is described in Appendix E and shown in Figures VI.4 and VI.5.

Prior to ship arrival, a shore-based meteorological tower was erected. The location of the tower was selected so as to minimize blockage or interference effects due to buildings, dock piping and above-ground storage tanks. Total tower height was 10.7m. Atop the tower was mounted a 4-blade Gill Propeller Vane (Model 35001, R. M. Young Co.) to provide continuous monitoring of wind speed and direction. Wind velocity is provided by a DC tachometer generator, and wind direction is obtained from a precision potentiometer. The generator and potentiometer electrical outputs were hard-wired into a ground-based power supply translator. Translator output was linked to a dual channel recorder as well as visual display indicators.

Air temperature was measured at 1m and 10m above ground level using a single sensor that was mounted on a pulley system that was attached to the tower. The measurement system was manufactured and certified by Omega Engineering, Inc.

By measuring wind velocity at one elevation and temperature at two elevations, an indicator of atmospheric stability class may be calculated following the method of Wang, et al.[*]

---

[*]Wang, I. T., Myers, R. L., McKinley, C. M., "Concerning the Use of Routine Meteorological Data in Estimating Atmospheric Diffusion Parameters," Journal of Applied Meteorology, Vol. 17, Feb. 1978, pp. 166-170.
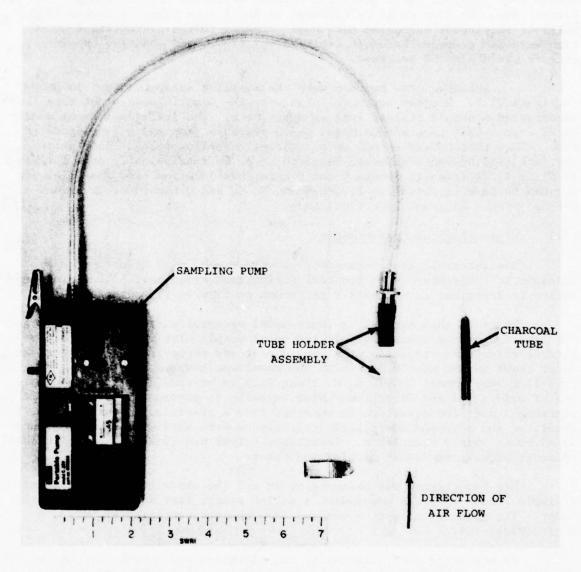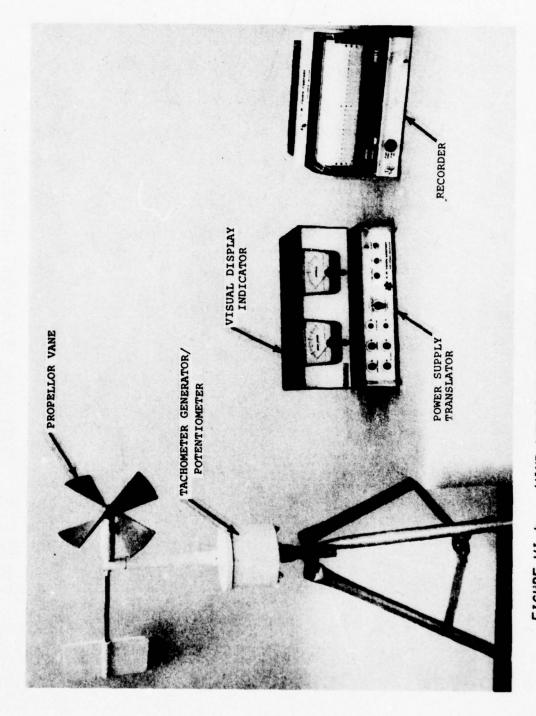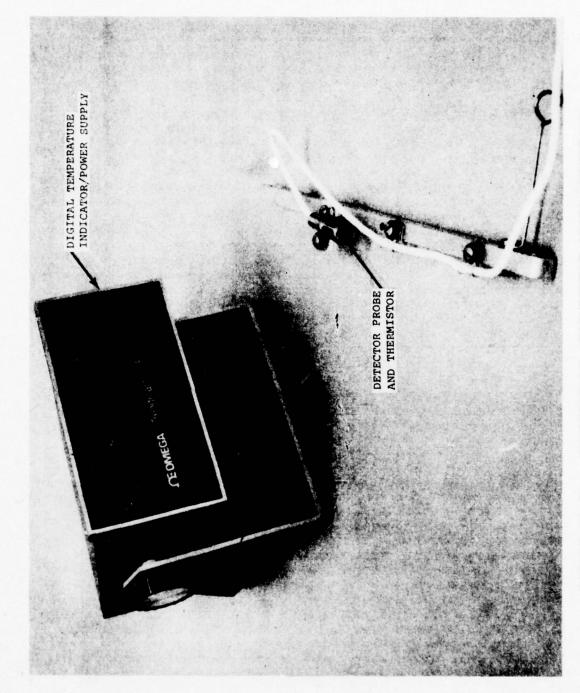
FIGURE VI.3   PERSONAL SAMPLING APPARATUS

126

PROPELLOR VANE

TACHOMETER GENERATOR/
POTENTIOMETER

VISUAL DISPLAY
INDICATOR

POWER SUPPLY
TRANSLATOR

RECORDER

FIGURE VI.4   WIND VELOCITY AND DIRECTION INSTRUMENTATION

127

DIGITAL TEMPERATURE
INDICATOR/POWER SUPPLY

DETECTOR PROBE
AND THERMISTOR

FIGURE VI.5 TEMPERATURE MEASUREMENT INSTRUMENTATION

128

VI.4   Summary of Significant Results

This section presents the source, area, matrix, and personal sampling data that were measured on full-scale Tests Nos. 1 and 2.

Test No. 1

This test consisted of monitoring the discharge and dispersion of vapors emitted during loading of ethyl alcohol and toluene tanks. Both tanks were open loaded with vapors vented through an open ullage port on the expansion trunk. The ullage port was approximately 3.5 feet (1.07m) above deck level. Figure VI.6 shows the position of these two tanks on the ship as well as the locations of the source, matrix, and area sampling stations. Figures VI.7 and VI.8 contain enlarged views of sampling stations for each tank. For reference, the wind velocity/direction and ambient temperature during the test are shown in Figure VI.9.

Loading conditions for the ethyl alcohol and toluene tanks are summarized in Figure VI.10. Variations in indicated ullage rates are due to differences in tank capacity and loading rate. On both tanks, product loading had commenced prior to initiation of data acquisition. Therefore, the loading rate for ethyl alcohol was calculated on the basis of quantity of product loaded, time at tank top-off, and a pump start-up time determined by linearly extrapolating the ullage/time history back to the maximum indicated ullage of 52.98 feet (16.15m). In the case of the toluene tank, the loading rate was increased at roughly 1130 hours. The higher toluene loading rate was calculated during the 2.5 hours that were required to reduce the indicated ullage from 41.5 ft (12.65m) to 10 ft (3.05m). That is,

$$\text{Toluene loading rate} = \left\{ \frac{\Delta_u}{U_{max} - [(1-\eta)(U_{max} - h) + h]} \right\} \frac{V}{\Delta t} \qquad \text{(VI-1)}$$

where Δ_u = change in ullage, 31.5 ft

   U_{max} = maximum indicated ullage, 51.95 ft
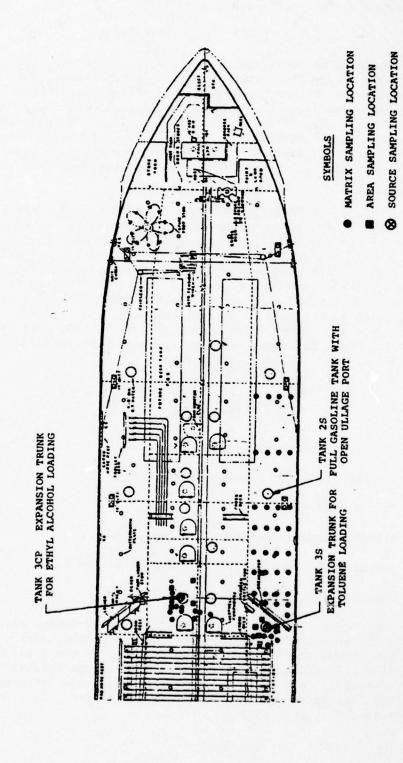
   η = fill fraction, 0.9859

   h = ullage standpipe height, 2.58 ft (31 in.)

   V = actual quantity of toluene delivered to the tank, 11,724 bbl

   Δt = loading time at high fill rate, 2.5 hrs.

This expression assumes that the number of barrels delivered during each foot of innage is constant. It neglects the thickness of the weather deck plating and deck camber. The denominator of the term in brackets is the final innage at 98.59% full. Using this expression, the calculated toluene loading rate was 3035 bbl/hr. At roughly 1400 hours the toluene loading was interrupted to permit a barge to pull alongside and load bunker fuel onto the ship. Data acquisition was terminated at that time.

129

TANK 3CP EXPANSION TRUNK
FOR ETHYL ALCOHOL LOADING

TANK 2S

TANK 3S
EXPANSION TRUNK FOR
TOLUENE LOADING

FULL GASOLINE TANK WITH
OPEN ULLAGE PORT

SYMBOLS

● MATRIX SAMPLING LOCATION
■ AREA SAMPLING LOCATION
⊗ SOURCE SAMPLING LOCATION

FIGURE VI.6.   PLANVIEW OF SHIP DECK FOR TEST NO. 1, SHOWING MATRIX, SOURCE AND AREA
SAMPLING LOCATIONS RELATIVE TO SOURCE TANKS 3CP AND 3S

130

	WIND SPEED			WIND DIRECTION	
hours	avg	σ		avg	σ
0930-1000	0.57 m/s	0.38 m/s		68°	81°
1000-1030	1.62 m/s	0.68 m/s		138°	30°

270°

1.65m

TANK 3CP EXPANSION TRUNK
FOR ETHYL ALCOHOL LOADING

STERN 180°

0° BOW

0930-1000 hrs
AVG. WIND DIRECTION

1000-1030 hrs
AVG. WIND DIRECTION

90°

SYMBOLS

○ MATRIX SAMPLING LOCATION

□ AREA SAMPLING LOCATION

⊗ SOURCE SAMPLING LOCATION
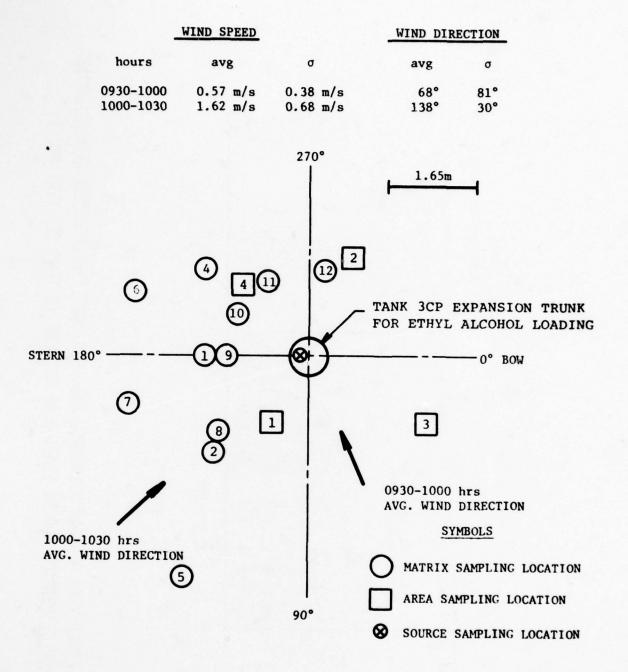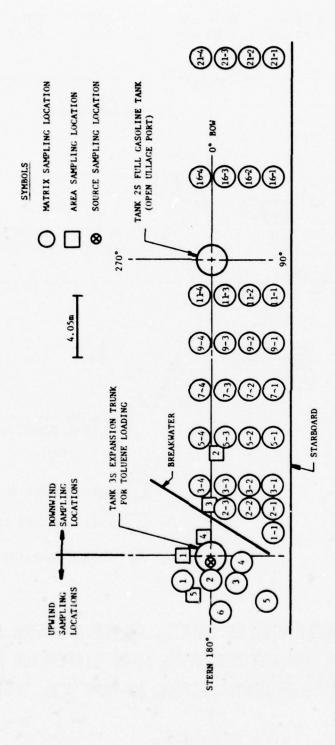
FIGURE VI.7 ENLARGED VIEW OF MATRIX, SOURCE AND AREA SAMPLING
LOCATIONS FOR MEASURING VAPOR DISPERSION DURING
LOADING OF ETHYL ALCOHOL IN TANK 3CP, TEST NO. I.

131

FIGURE VI.8. ENLARGED VIEW OF MATRIX, SOURCE AND AREA SAMPLING LOCATIONS FOR MEASURING VAPOR DISPERSION DURING LOADING OF TOLUENE IN TANK 3S, TEST NO. 1.

132
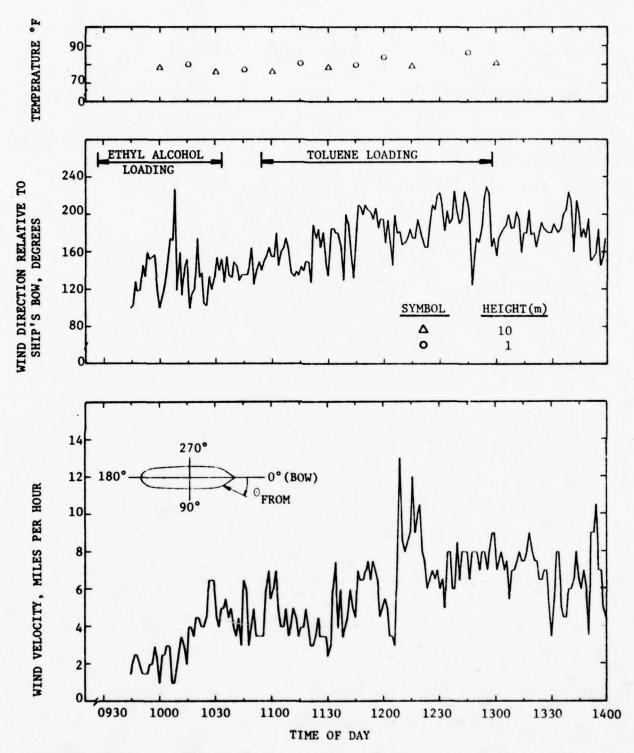
FIGURE VI.9   WIND VELOCITY, WIND DIRECTION AND AMBIENT
TEMPERATURE DURING TEST NO. I.

133

SYMBOL	O	□
TANK NO.	3CP	3S
PRODUCT	ETHYL ALCOHOL	TOLUENE
TANK CAPACITY (bbl)	6715	11,892
QUANTITY LOADED (bbl)	6645	11;724
% FULL	98.96	98.59
ULLAGE RATE (ft/hr , m/hr)	-37.2 , -11.3	-12.5 , -3.8 (linear range)
LOADING RATE (bbl/hr)	4833	3035 (linear range)
MAXIMUM INDICATED ULLAGE (ft, m)	52.98, 16.15	51.95, 15.83

NOTE: INDICATED ULLAGE AT STANDPIPE 31 in. (0.79m) ABOVE DECK LEVEL.
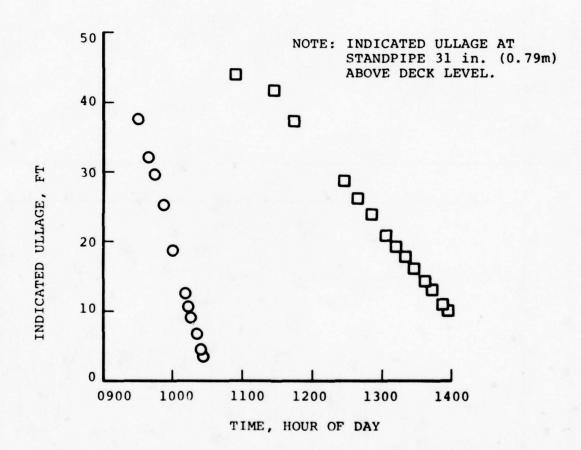
FIGURE VI.10 INDICATED ULLAGE VERSUS TIME FOR ETHYL ALCOHOL AND TOLUENE LOADINGS, TEST NO. I.

Figure VI.11 presents the concentration-time history for the ethyl alcohol vapors that were discharged from the open ullage port during loading of tank 3CP. Also shown in this figure are the ethyl alcohol concentrations that were obtained from the analysis of the bag samples at area stations A-1, 2, and 3. Comparable data for the loading of toluene in tank 3S are contained in Figure VI.12.

Loading of the ethyl alcohol tank took place quite rapidly. Consequently, there was insufficient time for development of a thick vapor blanket above the liquid surface and for concentrations in the blanket to approach a saturated or even an LEL condition. As a result, discharge concentrations rose appreciably only during the last 18 minutes of the 1.35 hour loading time. The ullage-time data suggest that the vapor blanket was of the order of 6.5 ft (1.98m) during the period of rapidly increasing discharge concentration. The constant source concentration prior to 1000 hours implies that concentration gradients in the tank were quite steep and were diffusion-controlled. A slower loading rate undoubtedly would have resulted in the development of a thicker vapor blanket, an earlier on-set of the rise in discharge concentration, and a higher final concentration. Ethyl alcohol vapors also diluted rapidly following discharge. Measured concentrations at the area sampling stations did not exceed 100 ppm at distances greater than approximately 4.9 ft (1.49m) from the ullage port.

By contrast, the toluene loading was much slower. During the slow loading rate that existed at the beginning of loading, the discharge concentration was essentially constant. Source concentration began to rise shortly after the loading rate was increased. As cited above, data acquisition was terminated prior to tank top-off. During the observation period, toluene vapor concentrations at the area sampling stations did not exceed 100 ppm at any time. The time history of toluene vapor concentration at area sampling stations A-2 and A-4 follows the trend at the discharge point, which indicates that these stations were within the plume boundary. Station A-2 was approximately 21 ft (6.4m) downwind of station A-4; hence, lower concentrations existed at A-2. Station A-3 was located intermediate to A-2 and A-4 and produced an intermediate concentration.

Three sets of personal sampling data were collected on this test.

o   The first set consisted of breathing zone vapor samples collected on three individuals (one ship's officer and two project personnel) during man-entry into an empty tank that had previously carried MIBK (methyl isobutyl ketone). These samples were designated PS-1, 2, and 3.

o   The second set of personal exposures was obtained for the same group of individuals, but during man-entry into a toluene tank. Sample numbers PS-4, 5, and 6 identify these samples.

o   Finally, vapor exposures were monitored on three deck officers during product loading, and their samples were identified as PS-7, 8, and 9.

135
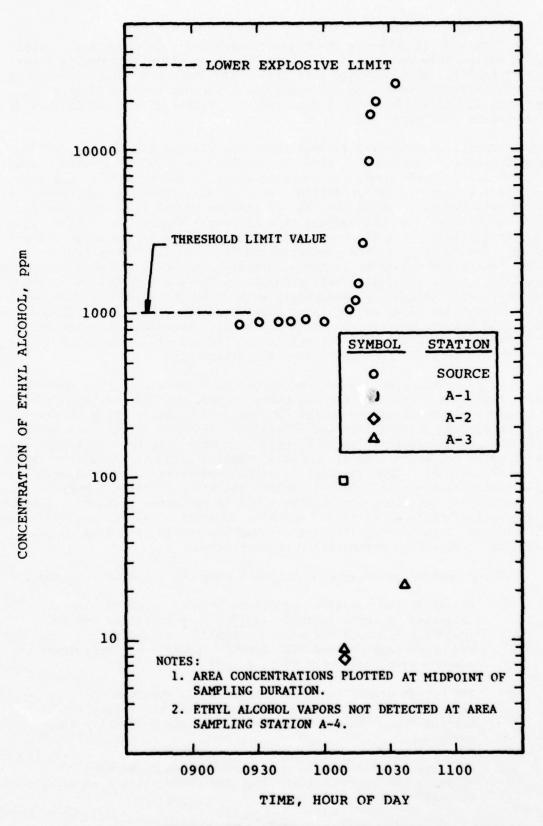
FIGURE VI.II   SOURCE AND AREA CONCENTRATIONS OF ETHYL ALCOHOL
MEASURED DURING TANK LOADING. TEST NO. I.
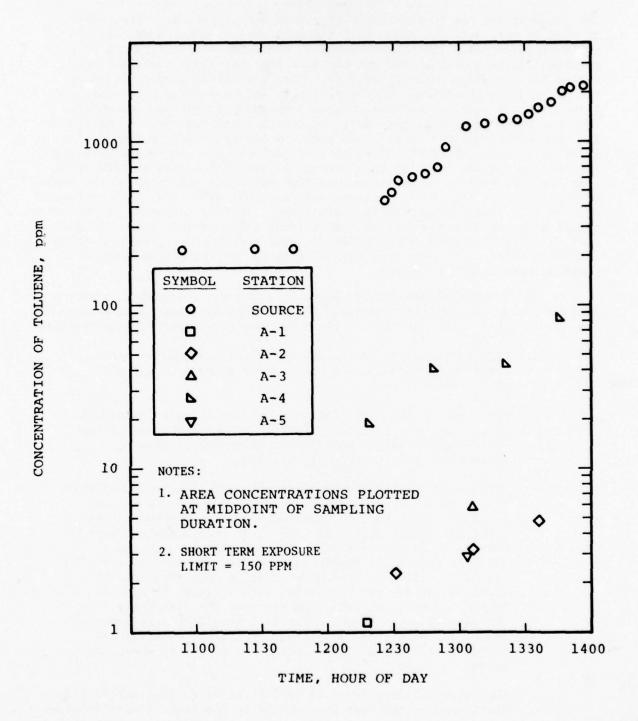
FIGURE VI.12   SOURCE AND AREA CONCENTRATIONS OF TOLUENE MEASURED
DURING TANK LOADING. TEST NO. I.

The scenario for the in-tank vapor exposures was as follows. The vessel arrived in port with two tanks that had been washed, ventilated, and manually cleaned during the ballast voyage. Other than identification of the previous contents of the tank and the fact that the clean tanks had been sealed for five days prior to docking, there was little documentation of the particulars of washing and ventilating. Before sealing the tanks, the Chief Mate had sampled the tanks with an explosimeter and had determined that the vapor concentrations were zero on the instrument scale. Upon opening, the tanks appeared to be clean and void of any liquid residual. The Chief Mate again tested the tanks with an explosimeter; the vapor sampling line was introduced into the tank through an open hatch, and it terminated near the tank bottom. A zero concentration was again indicated on the tanks of interest—one had carried toluene and the other MIBK. Two SwRI personnel entered both tanks along with the Third Mate. In both instances, each individual wore personal sampling equipment (pump and charcoal tube). In addition, a portable organic vapor analyzer (OVA) and recorder were also taken into each tank. SwRI personnel carried respiratory protection devices (organic vapor canister masks).

The results of monitoring personnel exposures to chemical vapors on Test No. 1 are summarized in Table VI-3. These data have been interpreted, and the following conclusions, observations, and/or comments are appropriate.

1. Chemical analysis indicated that there had been no vapor breakthrough into the backup charcoal section in any of the sampling tubes.

2. Men entering the MIBK tank were exposed to vapor concentrations that were less than the STEL. The definition of the STEL has been excerpted from the reference of Note 8, Table VI-3, and it is presented below.

    "Threshold Limit Value-Short Term Exposure Limit (TLV-STEL)— the maximal concentration to which workers can be exposed for a period up to 15 minutes continuously without suffering from 1) irritation, 2) chronic or irreversible tissue change, or 3) narcosis of sufficient degree to increase accident proneness, impair self-rescue, or materially reduce work efficiency, provided that no more than four excursions per day are permitted, with at least 60 minutes between exposure periods, and provided that the daily TLV-TWA also is not exceeded. The STEL should be considered a maximal allowable concentraton, or absolute ceiling, not to be exceeded at any time during the 15-minute excursion period. . . . . . ."

    The lower exposure level of PS-2 relative to PS-1 and PS-3 is attributed to the fact that, while in the tank, these personnel performed individual familiarization and inspection activities, but not as a group. This diversity of movement is reflected in the variation of exposure concentration. The OVA instrumentation that accompanied this man-entry recorded a mean MIBK concentration of 67 ppm with excursions to 47 and 96 ppm.

TABLE VI-3

SUMMARY OF PERSONAL SAMPLING ON FULL-SCALE TEST NO. 1

Sample No.	Personnel	Location	Chemical Vapors	Pump No.	Sampling Time (min)	Sampling Rate (ℓ/min)	V(ℓ)	W_V(μg) (2)	W_B(μg) (4)	M (5)	T(°C)	P (mm Hg)	Recovery Effic, n	C(ppm) (7)	TWA-TLV STEL (ppm) (8)
PS-1	SwRI	In-Tank	MIBK	10	20.48	0.099	2.028	341	Note 3	100.16	20.8	763	0.363	111	100/125
PS-2	SwRI	→	→	9	20.90	0.074	1.547	111	→	→	→	→		47	→
PS-3	3/M			5	21.45	0.264	5.660	733						85	
PS-4	SwRI		Toluene	10	37.28	0.099	3.690	2872		92.13			0.881	230	100/150
PS-5	SwRI			9	36.07	0.074	2.67	1775		→				197	→
PS-6	3/M-1		→	5	38.38	0.264	10.13	7850	→					229	
PS-7	C/M	On-Deck	EA-190 / Toluene	10	261.5	0.099	25.89	45.6 / 60.2	21.0 / Note 3	46.07 / 92.13	26.1	763.9	0.02 / 0.881	25 / <1	1000/— / 100/150
			MEK					<0.004 (3)		72.10			0.144	0(o)	200/250
PS-8	2/M2		EA-190 / Toluene	9	133.3	0.074	9.86	43.9 / 10.9	21.0 / Note 3	46.07 / 92.13	25.4	→	0.02 / 0.881	61 / <1	1000/1900 / 100/150
			MEK					<0.004 (3)		72.10			0.144	0(o)	200/250
PS-9	PRO (1)		EA-190 / Toluene	5	255.5	0.264	67.7	70.9 / 97.9	21.0 / Note 3	46.07 / 92.13	26.1	→	0.02 / 0.881	19 / <1	1000/1900 / 100/150
			MEK					2.6		72.10			0.144	<1	200/250

NOTES:

1. PRO = Port Relief Officer.
2. W_V = Weight of chemical solvent desorbed from primary charcoal section.
3. GC Detection Limit is 0.004 μg. Those entries bearing this note number were set equal to zero when calculating concentration.
4. W_B = Weight of chemical solvent desorbed from blank.
5. M = Molecular weight of liquid.
6. W_S = Weight of chemical solvent desorbed from secondary charcoal section. Analysis indicated $W_S = 0$ for all samples.

7. $C = \dfrac{(W_V + W_S - W_B)}{nV} \left(\dfrac{760}{P}\right) \left(\dfrac{T+273}{298}\right) \left(\dfrac{24.45}{M}\right)$

8. Threshold Limit Values for Chemical Substances in the Workroom, American Conference of Governmental Industrial Hygienists, 1977.

139

3. Pump No. 5 had a calibration slightly in excess of the recommended maximum level of 0.2 ℓ/min because a lower flow rate could not be obtained. This deviation is not believed to be significant in view of the fact that carbon saturation or breakthrough did not occur on the primary section of the sample tube.

4. Man-entry into the toluene tank indicated that all three personnel were exposed to vapor concentrations that exceeded the STEL by 46% on the average. The OVA instrumentation substantiated these levels with a mean recorded toluene concentration of 240 ppm and excursions to 200 and 273 ppm. These results are particularly interesting because concentration levels were apparently below the detection limit of the explosimeter whose readings are used as a basis for decisions regarding man-entry. In the case of this toluene tank, the explosimeter was insensitive to vapor concentrations that were hygienically significant.

5. On-deck monitoring of crew members during product loading indicated that personal exposures to individual chemical vapors were well below published TWA-TLV or STEL levels. In addition, exposure calculated on the basis of additive effects were also below the mixture TLV. That is,

$$\sum_{i=1}^{N} \frac{C_i}{TLV_i} << 1.0$$

Ethyl alcohol was included in the analysis plan because on the previous voyage that chemical had been carried in the tank that received MEK. Personal exposure samples PS-7, 8, and 9 reflect the fact that the majority of their deck watch time was spent upwind of the loading tanks in the vicinity of the manifold with brief excursions to gauge a tank, check valving, etc.

Vapor concentration data collected at matrix locations during the toluene loading was chosen for comparison with the analytical plume model. The matrix data taken during toluene loading is more extensive than the EA-190 matrix data, and the confined location of the EA-190 vent (surrounded by tall pump houses and pipe runs) was less likely to produce the regular type of plume dispersion that is modeled by the analytical method. Therefore, attention has been given first to the analysis of data expected to agree well with the analytical model.

The experimental conditions during the toluene loading were quite favorable. The tank atmosphere from tank 3S was vented at a constant rate of 1.134 m³/s through a 25-cm diameter vent located at 1.07m height above deck level on the 3S expansion trunk. There was little deck structure downwind of the vent to interfere with plume dispersion. Table IV-4 shows the values of average wind speed and direction that were recorded at the meteorological tower during matrix sampling. As the table shows, the wind speed increased significantly from a level of 2.5 m/s at 1130 to 1159 hours to over 3 m/s from 1200 hours onward. However, during the period of 1230 to 1340 hours, the wind

TABLE VI-4

METEOROLOGICAL DATA DURING TOLUENE MATRIX SAMPLING

TIME,HOURS	WIND SPEED (m/s)		WIND DIRECTION* (degrees)	
	Mean	Std.Dev.	Mean	Std.Dev.
1130 – 1159	2.49	0.68	184	24
1200 – 1215	3.26	1.46	176	14
1215 – 1230	3.42	0.70	190	20
1230 – 1340	3.12	0.59	189	21

*Angle of wind with respect to axis of ship. 0° indicates a wind from bow to stern, 90° a wind from starboard to port.
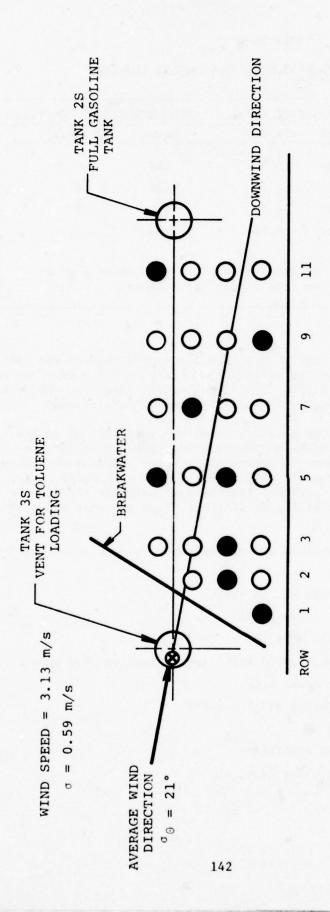
speed was relatively constant at 3.1 m/s, and the wind direction was inclined 10° to starboard which carried the vented vapor plume directly over the matrix locations as shown in Figure VI.13. Therefore, matrix data from this time period was chosen for comparison with analytical model predictions.

Since the matrix samples were collected sequentially, at different points in time, allowance has to be made for the time dependence of the vapor concentration at the vent source shown in Figure VI.12. The simplest procedure is to divide the time average concentration value, C, for each matrix point by the source concentration, C_o, recorded for the same point in time as the matrix point. The values of C/C_o at different distances from the vent are shown in Figure VI.14.

The plume model predictions of toluene vapor concentration level were computed for conditions of

o Wind speed, 3.13 m/s at 10m height

o Turbulence level, 10% and 20%

o Venting rate, 0.134 m^3/s

o Vent concentration, 0.0090 kg/m^3 (equivalent to 2400 ppm)

o Vent height above deck, 1.07m

o Matrix vapor measuring height, 1.68m

o Vent diameter, 25 cm

o Neutral atmosphere stability

o Deck height above water line, 9m.

141

WIND SPEED = 3.13 m/s

σ = 0.59 m/s

AVERAGE WIND DIRECTION

σ_θ = 21°

TANK 3S

VENT FOR TOLUENE LOADING

BREAKWATER

TANK 2S

FULL GASOLINE TANK

DOWNWIND DIRECTION

ROW 1 2 3 5 7 9 11

FIGURE VI.13 MATRIX LOCATIONS REPORTING HIGHEST VALUES OF DIMENSIONLESS CONCENTRATION, C/Co, DURING TOLUENE LOADING DURING FIRST FULL SCALE TEST.

142
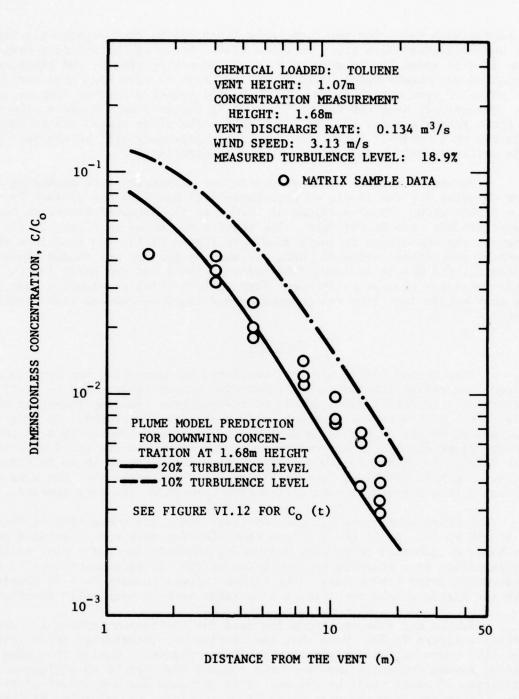
FIGURE VI.14 COMPARISON OF MATRIX SAMPLE CONCENTRATION DATA
FROM FIRST FULL SCALE TEST WITH PLUME MODEL
PREDICTIONS.

143

An approximate value for the turbulence level can be derived directly from the meteorological data given in Table VI-4. Dividing the standard deviation in wind speed by the mean wind speed and multiplying by 100 gives an estimated turbulence value of 18.9% for the 1230 to 1340 hour time period. The value of vent concentration, 0.0090 kg/m^3, selected for the computation was reached only near the end of the loading observation. However, the value of plume Froude number, 752, is too high for the plume trajectory to be much affected by buoyancy. Therefore, the plume trajectory will be the same for this and lower values of toluene vapor concentration.

Values of toluene vapor concentration at matrix vapor measuring height were computed for two levels of turbulence (10% and 20%) and divided by $C_O = 0.0090$ kg/m^3 to give values of C/C_O in the downwind direction for comparison with the matrix data. The results are shown in Figure VI.14. In general, the comparison is quite good. In Figure VI.13, the locations that measured the highest value of C/C_O in each matrix row are shaded black. Except for the single isolated data point in row 1 and the point in row 11 (this point was closest to the vent from tank 2S which was loading gasoline), the peak matrix locations are grouped around the time-average wind direction vector.
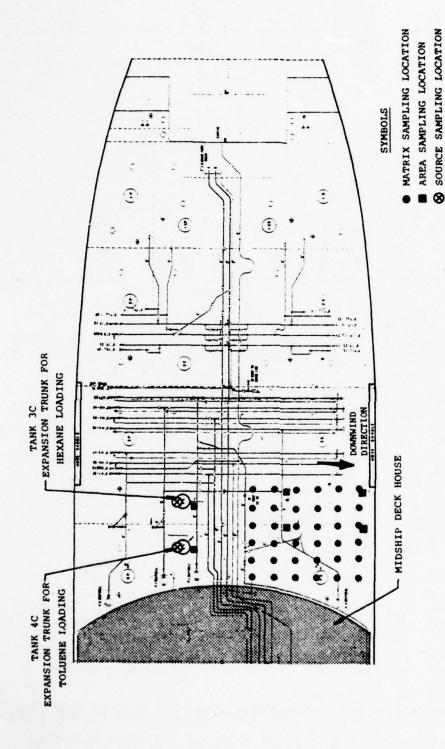
Test No. 2

This second full-scale test consisted of monitoring the loading of toluene and hexane into adjacent, equal size center tanks. Figure VI.15 illustrates the relationship of the matrix and area sampling locations relative to the source expansion trunks and other deck structures. On this ship, the readout on the tape gauging system was 2.75 ft (0.84m) above deck level, and the plane of ullage port on the expansion trunk was 3.4 ft (1.04m) above deck level. An enlarged view of the sampling locations is shown in Figure VI.16. The meteorological data in Figure VI.17 indicates that the wind was generally in a port-to-starboard direction throughout the tank loadings.

Loading conditions for each of these tanks are summarized in Figures VI.18 and VI.19. As in the previous test, loading rate was calculated on the basis of quantity of product delivered, top-off time and a flow initiation corresponding to a rearward extrapolation of the ullage time-history to the maximum indicated tank ullage. The higher toluene loading rate is consistent with the higher ullage rate, since both tanks were geometrically identical.

Source and area concentration data for the hexane loading are presented in Figure VI.20. Note that the loading was interrupted for slightly over five hours so that ship's trim could be adjusted. During that time period, source concentration rose from roughly 4000 ppm to an explosive concentration of nearly 2.5% by volume. This increase was the result of evaporation of chemical from the stationary liquid surface and molecular diffusion in the ullage space. Source vapor concentration remained in the explosive range for 5.5 hours (from 2313 to 0445 hours) after which the concentration exceeded the UEL.

The maximum recorded hexane concentration was 120,725 ppm. In the absence of a measured liquid temperature, it was assumed that this concentration represented a saturated condition. Using the vapor pressure equation

144

TANK 3C
EXPANSION TRUNK FOR
HEXANE LOADING

TANK 4C
EXPANSION TRUNK FOR
TOLUENE LOADING

DOWNWIND
DIRECTION

MIDSHIP DECK HOUSE

SYMBOLS

● MATRIX SAMPLING LOCATION
■ AREA SAMPLING LOCATION
⊗ SOURCE SAMPLING LOCATION

FIGURE VI.15. PLANVIEW OF SHIP DECK FOR TEST NO. 2 SHOWING MATRIX, SOURCE AND AREA
SAMPLING LOCATIONS RELATIVE TO SOURCE TANKS 3C AND 4C

145

TANK 4C
EXPANSION TRUNK FOR
TOLUENE LOADING

TANK 3C
EXPANSION TRUNK FOR
HEXANE LOADING

STERN ———————————————————————— BOW

2

1

SYMBOLS

◯ MATRIX SAMPLING LOCATION

▢ AREA SAMPLING LOCATION

⊗ SOURCE SAMPLING LOCATION

2.47m

(1-1) (1-2) (1-3) (1-4) (1-5) (1-6)

(2-1) (2-2) (2-3) (2-4) (2-5) (2-6)

(3-1) (3-2) (3-3) (3-4) (3-5) (3-6)
                        4   3

(4-1) (4-2) (4-3) (4-4) (4-5) (4-6)

(5-1) (5-2) (5-3) (5-4) (5-5) (5-6)

(6-1) (6-2) (6-3) (6-4) (6-5) (6-6)
                        5   5

A-5 LOCATION FOR
TOLUENE LOADING

A-5 LOCATION FOR
HEXANE LOADING
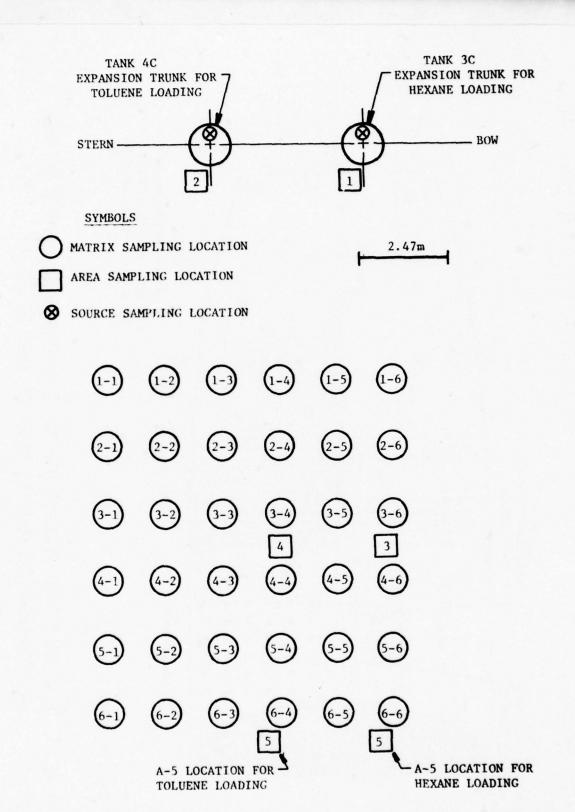
FIGURE VI.16 ENLARGED VIEW OF MATRIX, SOURCE AND AREA SAMPLING
LOCATIONS FOR MEASURING VAPOR DISPERSION DURING
LOADING OF HEXANE AND TOLUENE, TEST NO. 2.

146
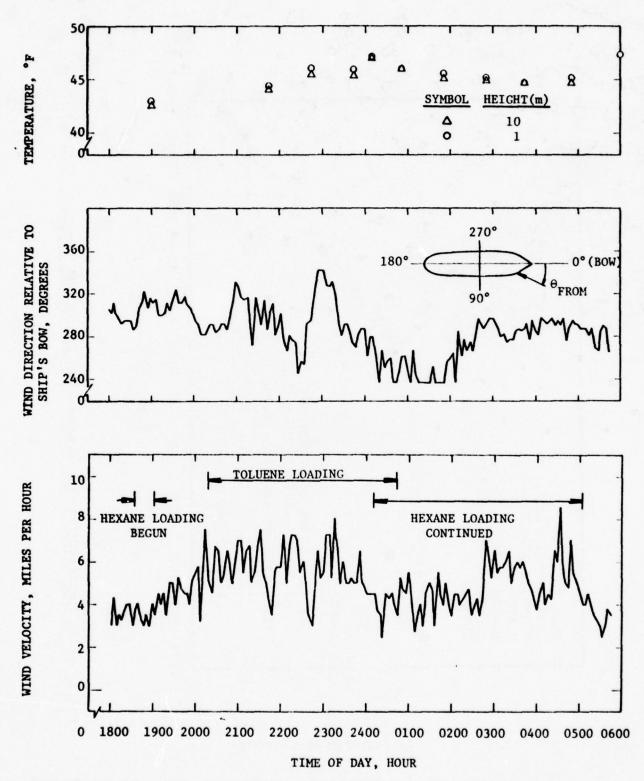
FIGURE VI.17 WIND VELOCITY, WIND DIRECTION AND AMBIENT
TEMPERATURE DURING TEST NO. 2.

147
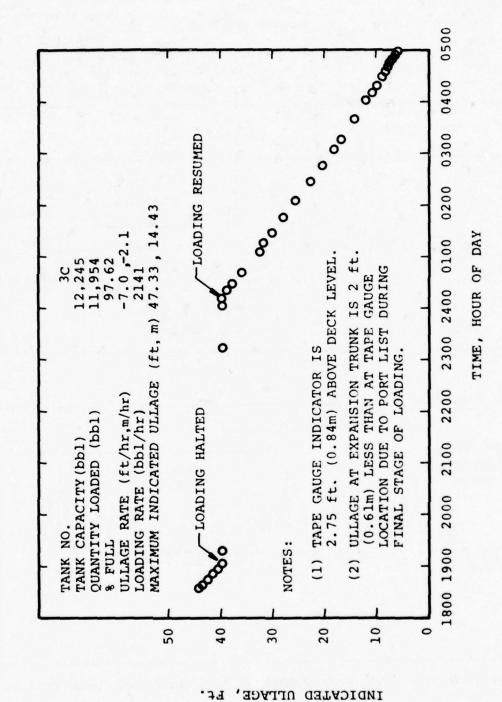
FIGURE VI.18 INDICATED ULLAGE VERSUS TIME FOR HEXANE LOADING. TEST NO. 2.

148

TANK NO.	4C
TANK CAPACITY (bbl)	12,245
QUANTITY LOADED (bbl)	11,959
% FULL	97.66
ULLAGE RATE (ft/hr, m/hr)	-9.2 ,-2.8
LOADING RATE (bbl/hr)	2600
MAXIMUM INDICATED ULLAGE (ft,m)	47.33 , 14.43

NOTES

1. TAPE GAUGE INDICATOR IS 2.75 Ft (0.84m) ABOVE DECK LEVEL
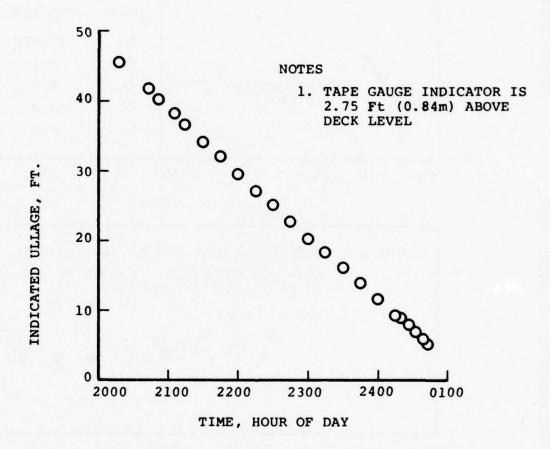
FIGURE VI.19 INDICATED ULLAGE VERSUS TIME FOR TOLUENE LOADING, TEST NO. 2.

149
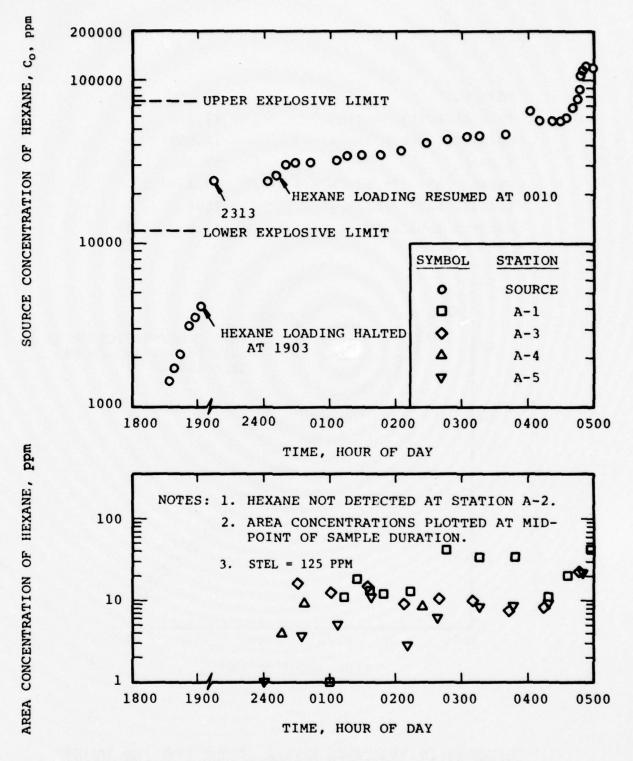
FIGURE VI.20 SOURCE AND DOWNWIND AREA CONCENTRATIONS OF HEXANE MEASURED DURING TANK LOADING, TEST NO. 2.

of Boublik[*] and the fact that, at saturation, the liquid vapor pressure is equal to the partial pressure of the vapor above the liquid surface, a pure n-hexane liquid temperature of 56.5°F (13.98°C) was calculated. This delivery temperature is entirely plausible because the thermal capacity of the shore-based storage tank plus the frictional heat of pumping could act to increase the liquid temperature above the ambient level of 45.1°F at 0451 hours. However, the liquid was a mixture of hexanes, and the extent to which hexane isomers would modify the n-hexane vapor pressure-temperature relationship was unknown. Therefore, the assumption of a saturated condition at top-off appears to be justified.

The 30-minute, time average hexane concentrations at area sampling stations, shown in Figure VI.20, indicate that the vent emissions were rapidly diluted, and that vapor levels at area sampling locations did not exceed 100 ppm at any time during the loading. While the concentration at area sampling location A-1 (see Figure VI.16) would be expected to be high due to its closeness to the vent, the sample point was probably not in the plume path. That is, the sample point either lay above the plume, or was not in the downwind direction during loading. Close to the vent, the plume dimensions are relatively small, and the probability of a stationary sampling point missing the plume is higher than it would be farther downwind where the plume dimensions are greater. For all of the sampling points, the variability in concentration reading with time is probably due to the unsteady ambient wind field (variable speed and direction) and local turbulence generated by the wake of deck structures (piping, etc.).

Loading of toluene was initiated shortly following the interruption of the hexane loading. Toluene loading proceeded continuously from pump start-up to tank top-off. Source and area concentrations of toluene vapor during loading are shown in Figure VI.21. Source concentration rose monotonically with time to a maximum concentration of 14,625 ppm. From this level, the concentration dropped and then increased to 11,700 ppm at top-off. The precise cause for this behavior is unknown. One possible explanation is that there was a reduction in pumping rate near top-off that could not be detected within the accuracy of the tape gauging system. An alternative explanation is that the tank breathing resulted in ingestion of ambient air, which diluted the vapors in the expansion trunk.

The maximum toluene concentration is not believed to represent a saturated vapor state. Based on the vapor pressure equations of Boublik, the toluene saturation concentration corresponding to the hypothesized hexane delivery temperature, was calculated to be 20,594 ppm. Thus, saturation is not indicated. Similarly, the calculated toluene saturation temperature corresponding to this maximum measured concentration was 45.98°F (8.1°C). Since this temperature is less than the measured vapor discharge temperature of 49°F at the ullage port, saturation is again not indicated.

The area sampling data generally follow the time trend of the source. Downwind toluene vapor concentrations at area sampling locations were less than 100 ppm with the exception of one sample at station A-4, which coincided with tank top-off.

---

[*]Boublik, T., et al., <u>The Vapor Pressures of Pure Substance</u>, Elsevier Scientific Publishing Co., 1973.
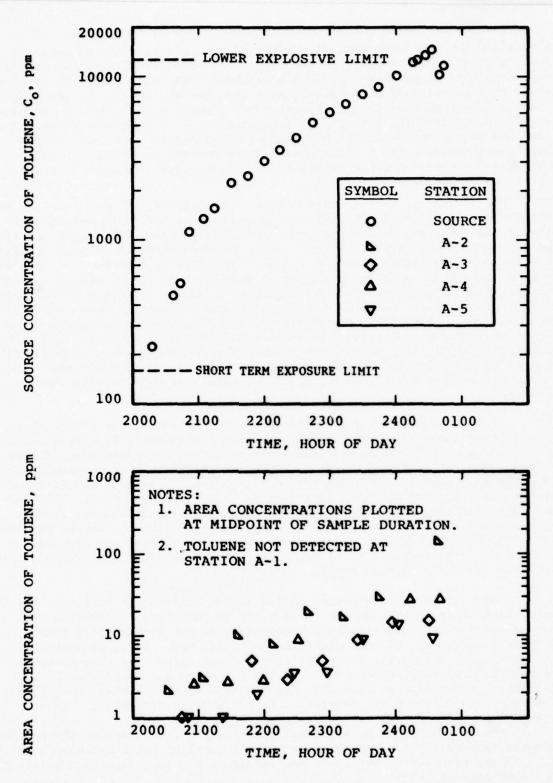
FIGURE VI.2I   SOURCE AND DOWNWIND AREA CONCENTRATIONS OF
TOLUENE MEASURED DURING TANK LOADING,
TEST NO. 2.

Personal sampling consisted of monitoring the vapor exposure of workers that were involved with topping-off chemical tanks. In this phase of the operation, the concentration of vapor that is discharged from an open ullage port on an expansion trunk increases rapidly and approaches a saturation level. During these latter stages of loading, a deck officer was assigned the responsibility of visually gauging the ullage depth through an open ullage port. If the ship has a list or pitch as a result of differential product loading, the deck officer may be assisted by a deckhand whose job is to call out indicated ullage from a tape gauging system that is located some distance from the expansion trunk. The perceived ullage is then a mean of the two indications.

The personal sampling activities can best be described with the aid of Figure VI.15. Shortly after hexane loading had commenced in Tank 3C, the shore-based pump was shut down. Loading of toluene in Tank 4C was initiated and proceeded without interruption to tank top-off. The topping operation was monitored continuously by the Third Mate beginning at an indicated tape ullage of 10 ft (3.05m) and ending at an approximate ullage of 4.5 ft (1.37m). Following top-off of Tank 4C, the hexane loading was completed. Since the ship had a port list, the Second Mate was assisted in the topping operation as described above. The exposure of both mates was monitored, as was the exposure of the deckhand at the tape gauging system which was located roughly 31 ft (9.45m) to the starboard from the Tank 3C expansion trunk. In Figure VI.15, this gauging system was located adjacent to area sampling station A-3, both of which were downwind of the source point. The duration of the personal samples coincided with the topping operations.

Both of these tanks were open loaded, but with vent covers on their pins. The hinge line was on the starboard side of the vent cover. This reduction of discharge area relative to a full open vent produced a jet of high velocity, high concentration vapor that was projected upwind at the mate when the vent cover was opened and reseated.

The results of the personal samples are presented in Table VI-5 and are interpreted below.

1. Sample Number PE-1 indicates that the Third Mate was exposed to toluene concentrations that exceeded the STEL by 33%. By comparison, the hexane exposure was detectable, but minimal.

2. The Mate in charge of topping Tank 3C was exposed to hexane concentrations that were 7.6 times larger than the STEL.

3. At roughly 30 ft downwind of the source, the hexane vapors had been sufficiently diluted such that the tape gauger's exposure was but 53% of the STEL.

Considerably more concentration data were collected at matrix locations during the second full-scale test than during the first. Except during the period from about 2400 to 0050 hours when toluene and hexane loadings were occurring simultaneously, the total hydrocarbon concentration data collected at matrix locations may be converted to equivalent concentrations of toluene vapor or hexane vapor. Inspection of the meteorological records shows that wind speed and direction were relatively constant for three periods listed in Table VI-6. From 2200 to 2400 hours during toluene loading, the wind speed was steady at about 2.57 m/s and the wind direction rather variable, but well directed to carry the vented plume past the matrix locations.

153

TABLE VI-5

SUMMARY OF PERSONAL SAMPLING ON FULL-SCALE TEST NO. 2

Sample No.	Personnel	Duties	Chemical Vapors	Pump No.	Sampling Time (min)	Sampling Rate (ℓ/min)	V(ℓ)	W_V(µg)	W_B(µg)	W_S(µg)	M	T(°C)	P (mm Hg)	Recovery Effic, η	C(ppm)	TWA-TLV STEL (ppm)
PE-1	3/M	Tank Top-Off	Toluene	9	35.37	0.092	3.25	1917	9	9	92.13	9.5	767.9	.739	199	100/150
			Hexane					30	5	0	86.17	9.5	767.9	.989	2	100/125
PE-4	A/B	Gauge Ullage	Hexane	10	40.75	0.092	3.75	912	0	0	86.17	9.8	766	.989	66	100/125
PE-5	2/M	Tank Top-Off	Hexane	9	34.93	0.092	3.21	11220	0	0	86.17	9.8	766	.989	944	100/125

NOTE: The nomenclature in this table is identical to that which was used in Table VI-3.

154

TABLE VI-6

METEOROLOGICAL DATA DURING MATRIX
SAMPLING FOR THE SECOND FULL-SCALE TEST

TIME,HOURS	WIND SPEED (m/s)		WIND DIRECTION* (degrees)	
	Mean	Std.Dev.	Mean	Std.Dev.
2200 - 2300	2.57	0.57	288	28
2300 - 2400	2.59	0.50	300	23
Two hour average	2.57	0.52	293	27
0100 - 0200	1.86	0.39	243	10
0300 - 0400	2.42	0.40	285	7
0400 - 0500	2.41	0.54	291	6
Two hour average	2.42	0.48	288	7

*Angle of wind with respect to axis of ship. 0° indicates a wind
from bow to stern, 90° a wind from starboard to port, etc.

The period from midnight to 0100 hours when both toluene and hexane
were being loaded was excluded from analysis due to the ambiguity in con-
verting the matrix values of total hydrocarbon concentration to equivalent
concentrations of hexane or toluene.

By 0100 hours, the wind speed had dropped. From 0100 to 0200 hours,
during the hexane loading, the wind speed averaged about 1.86 m/s and the
wind direction was shifted by 50° to 243°. Unfortunately, the wind shift
carried the hexane plume away from the matrix locations.

From 0200 to 0300 hours, the wind speed increased again, and from
0300 to 0500 hours, during hexane loading, the wind speed was relatively
steady at 2.42 m/s. The wind direction returned to about 288° close to the
293° direction recorded earlier from 2200 to 2400 hours. This direction would
be expected to carry the plume right through the matrix locations.

Due to the relative steadiness of both wind speed and direction during
these three periods of time, matrix data for toluene concentration from 2200
to 2400 hours, for hexane concentration from 0100 to 0200 hours, and hexane
concentration from 0300 to 0500 hours was selected for comparison with ana-
lytical model predictions.

155

Matrix locations were sampled sequentially, and the total hydrocarbon concentration was recorded for 3 minutes. The concentration records were later time-averaged and converted to an equivalent concentration of toluene vapor and air, or hexane vapor and air depending on the time of sampling. For comparison with model predictions, the average concentration value, C, for each matrix point was divided by the concentration measured at the vent, C_o, at the same time of sampling.

During the loading of toluene into the 4C tank and hexane into the 3C tank, the tank atmospheres were vented at constant rate through 25 cm diameter vents at 1.07m height above deck level located on the expansion trunks for these tanks. However, the ship's crew did not completely remove the vent cover from above the vent until the final 5 minutes of loading. Instead, it was their practice to raise the cover slightly and allow the cover latch to rest on top of the vent pin. This procedure of venting "on the pins" reduced the vent opening to a small slit, approximately 0.6 cm high, and extending about 120° around the perimeter of the vent cover. As a result, the vented tank atmospheres were emitted at high velocity (estimated velocity ∿68 m/s for toluene loading and ∿55 m/s for hexane loading) in a direction away from the matrix sampling locations. The practice of venting on the pins should increase the initial rate of dilution and limit the vertical rise of the plume compared to unrestricted vertical venting.

Plume model predictions of toluene vapor concentration level in a downwind direction were computed for conditions of

o   Wind speed, 2.57 m/s at 10m height

o   Turbulence level, 20%

o   Venting rate, 0.115 m^3/s

o   Vent concentration of toluene, 0.0400 kg/m^3 (equivalent to 10,000 ppm)

o   Vent height above deck, 1.07m

o   Vapor measuring height, 1.68m

o   Vent diameter, 25 cm (assumed fully open)

o   Neutral atmospheric stability

o   Deck height above water line, 9m.

The assumed value of turbulence level is supported by the meteorological data for wind velocity variation. Note that the plume computation assumed unrestricted vertical venting and did not model the actual "on the pins" vent configuration. Further analytical work is required to incorporate a non-circular vent model into the plume dispersion computation method.

Figure VI.22 shows the comparison of matrix data with model prediction for toluene loading between 2200 and 2400 hours. The agreement is surprisingly good considering the difference between model and actual vent configuration. The highest values of matrix concentration are clustered about the prediction line, which represents the concentration directly downwind of the vent. Of course, only a few matrix locations will be downwind of the vent

156
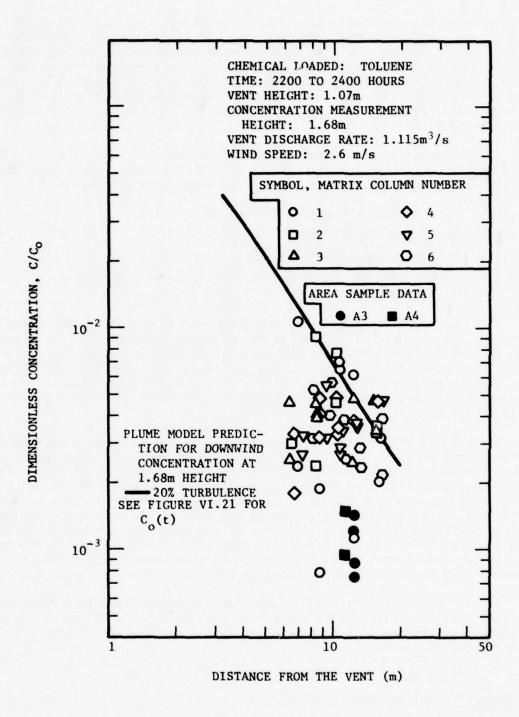
FIGURE VI. 22 COMPARISON OF MATRIX SAMPLE AND AREA SAMPLE
CONCENTRATION DATA FROM SECOND FULL SCALE TEST
WITH PLUME MODEL PREDICTION.

157

during concentration measurements. Other locations, away from the plume center-
line, are expected to indicate lower values of concentration. In Figure VI.23
the location of matrix points in each row that recorded the highest values of
concentration in Figure VI.22 are shaded black. As expected, the highest con-
centrations were found in an approximately downwind direction from the vent.
We should also note that the presence of the deck house probably influenced
the local wind field, turning it back towards 270° in the region of the matrix
columns 1 and 2.

Plume model predictions of hexane vapor concentration level in a down-
wind direction were made for the 0100 to 0200 hour period. Input conditions
were the same as for the toluene calculation with these exceptions:

o   Wind speed, 1.90 m/s at 10m height

o   Turbulence level, 20%

o   Venting rate, 0.094 m^3/s

o   Vent concentration of hexane, 0.1876 kg/m^3 (equivalent to
    50,000 ppm).

The assumed value of turbulence intensity is once again supported by
the meteorological data on wind speed variation in Table VI-6. The assumed
value of hexane concentration at the vent is about 50% too high for the 0100
to 0200 hour time period. However, the additional negative buoyancy afford-
ed by the higher concentration would only cause the plume to sink closer to
the deck and might better approximate the trajectory of the actual plume
vented on the pins.

Figure VI.24 compares the matrix data for hexane loading between 0100
and 0200 hours with the model prediction. Only three matrix data points ap-
proach the downwind concentration prediction line. Figure VI.25 shows that
these matrix points (shaded black) lie in column 6 and would be closest to the
center of the plume. For the observed wind direction shown in Figure VI.25,
many of the matrix locations would be in the wake of the deck house and be
somewhat sheltered from direct influence of the wind. In the wake, the wind
speed would be lower and the local wind direction much less regular and un-
predictable. Therefore, it is not surprising that some matrix points in
columns 1 or 2 recorded concentrations as high as points in columns 4 or 5.

Plume model predictions of hexane vapor concentration in a downwind
direction were also made for the period between 0300 and 0500 hours. Input
conditions were the same as for the other hexane calculations except for wind
speed and turbulence level,

o   Wind speed, 2.46 m/s at 10m height

o   Turbulence leven, 20% and 30%.

The meteorological data for wind velocity variation again supports a
value of turbulence intensity in the region of 20%. However, as shown in
Figure VI.26, the actual matrix data compare better to a prediction line of
30% turbulence than to 20%. Figure VI.27 shows that the matrix locations

WIND SPEED = 2.60 m/s
σ = 0.53 m/s

AVERAGE WIND DIRECTION
$\sigma_\theta = 27°$

TOLUENE VENT

ABOVE DECK PIPING

LADDER

DECK HOUSE

ROW
1
2
3
AREA SAMPLES
4

6

COLUMN   1 2 3 4 5 6
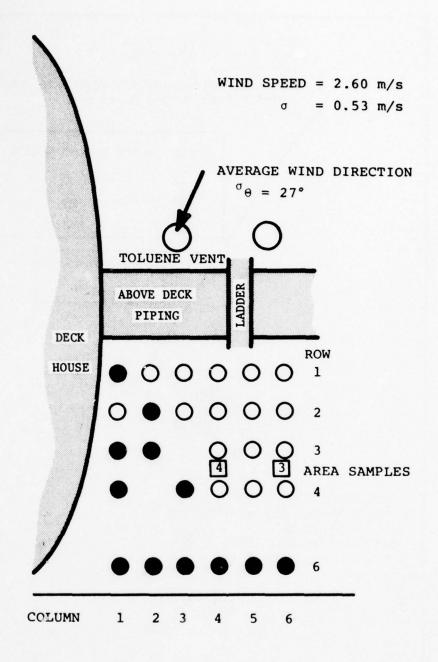
FIGURE VI.23 MATRIX LOCATIONS REPORTING HIGHEST VALUES OF CONCENTRATION DURING TOLUENE LOADING (SEE FIGURE VI.22)

159
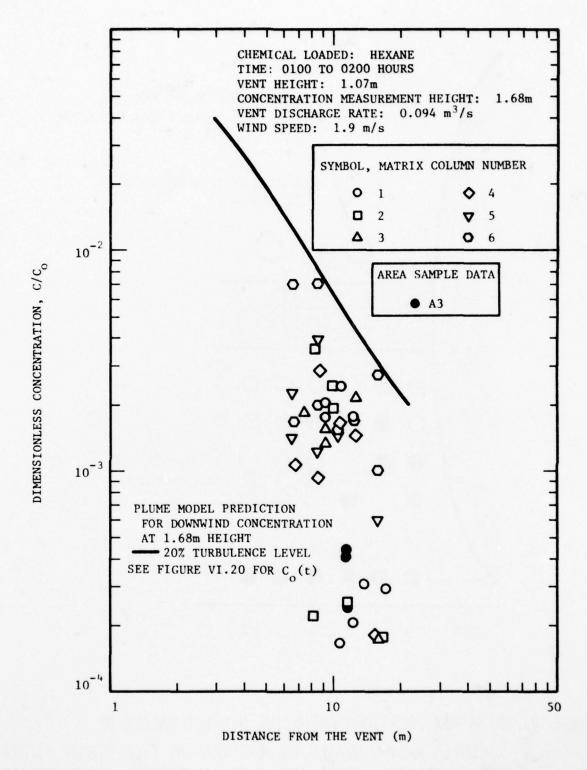
FIGURE VI. 24   COMPARISON OF MATRIX SAMPLE AND AREA SAMPLE
CONCENTRATION DATA FROM SECOND FULL SCALE TEST
WITH PLUME MODEL PREDICTION.

160

WIND SPEED = 1.88 m/s

σ = 0.39 m/s

AVERAGE WIND DIRECTION

$\sigma_\theta = 10°$
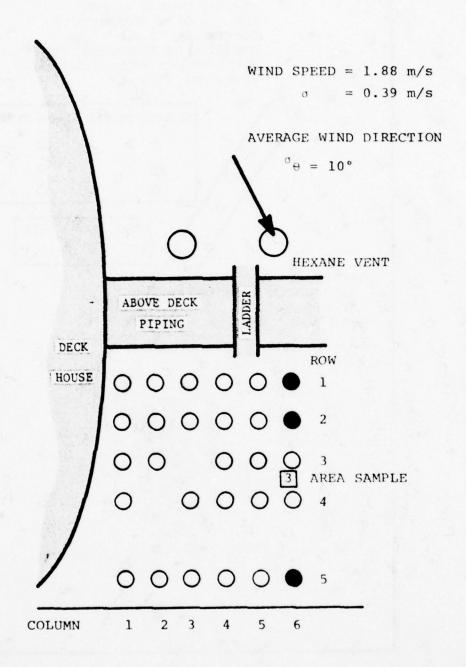
FIGURE VI.25 MATRIX LOCATIONS REPORTING HIGHEST VALUES OF
CONCENTRATION DURING INITIAL PERIOD (I TO 2 AM)
OF HEXANE LOADING (SEE FIGURE VI.24)

161
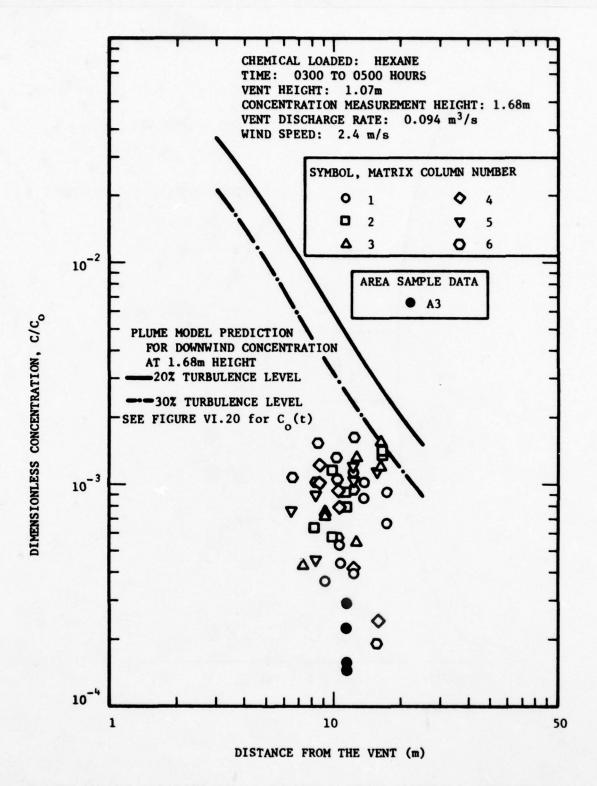
FIGURE VI. 26 COMPARISON OF MATRIX SAMPLE AND AREA SAMPLE
CONCENTRATION DATA FROM SECOND FULL SCALE TEST
WITH PLUME MODEL PREDICTION.

WIND SPEED = 2.41 m/s

σ = 0.47 m/s

AVERAGE WIND DIRECTION

$\sigma_\theta = 7°$

HEXANE VENT

ABOVE DECK PIPING

LADDER

DECK HOUSE

ROW
1
2
3
4
6

[3] AREA SAMPLE

COLUMN   1 2 3 4 5 6
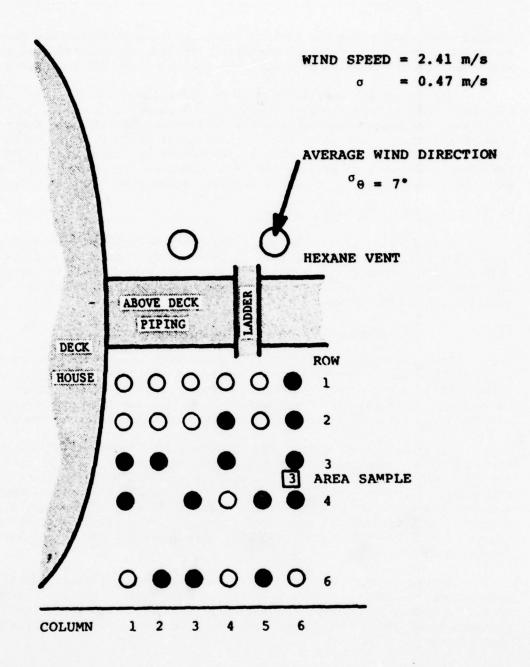
FIGURE VI. 27   MATRIX LOCATIONS REPORTING HIGHEST VALUES OF CONCENTRATION DURING LATER PERIOD (3 TO 5 AM) OF HEXANE LOADING (SEE FIGURE VI. 26)

163

(shaded black) recording the highest values of concentration were generally distributed around the observed downwind direction as expected, but the magnitude of concentration is lower than predicted for 20% turbulence level.

The reason for a higher degree of plume dispersion between 0200 and 0500 hours cannot be given with certainty. However, it is noted in Figure VI.27 that the ladder leading from the deck to the catwalk lies directly downwind of the vent. This fact, and the very small wind direction variation observed between 0300 and 0500 hours at the meteorological tower, suggests that the plume path was disrupted by the deck structure, increasing the mixing with the ambient wind, in a manner similar to increased wind turbulence.

VI.5   Toxicological Interpretation

This section draws some preliminary conclusions concerning the meaning of the results obtained to date in terms of the health of workers experiencing the exposures determined in the tests described. To understand and evaluate the results, some understanding of the broad principles of industrial toxicology is useful.

VI.5.1   Principles of Industrial Toxicology

The assessment of the health consequences of exposures to chemicals is in the province of toxicology. Despite the fact that toxicology is an old science with a very strong quantitative base, there is still a great deal of uncertainty regarding the consequence of chemical exposure. Some general discussion of basic toxicology is useful to understanding these uncertainties.

In terms of human exposure, three primary intoxication pathways can be distinguished: inhalation, ingestion, and skin contact. All of these contacts are still external to the organism, and the chemical must penetrate a barrier — pulmonary, gastrointestinal, or dermal — to enter the biochemical systems of the organism and produce intoxication. The efficiency of passage, i.e., absorption, is different for each of the pathways, and, therefore, the consequence of contact with a given quantity of a substance can vary substantially, depending on the pathway.

In the occupational situation, the most common contact is via the skin. Occupational dermatitis is the most common occupational disease. Inhalation is also a common occurrence. Ingestion is the least common; unsuspected ingestions occur among workers who smoke in environments where chemicals are also present.

The result of a contact with a chemical depends most strongly on the dose. Dose is defined as some function of the concentration to which exposed and the time duration of exposure. A closely related factor is the dosage, which is the rate of administration of the dose. A given quantity of chemical can exert vastly different effects depending on the rate of administration.

Chemical exposures may be of the acute or chronic type. An acute dose involves an exposure to a relatively high concentration over a relatively short period of time. In addition, there is generally a short time interval between exposure and outcome, which makes it relatively easy to associate the

164

insult and effect. The chronic dose is characterized by exposure to a relatively low concentration over a relatively long period of time, and, therefore, a long time interval between exposure and toxic manifestation. This makes it much more difficult to associate cause and effect.

Acute exposures most frequently involve accidents, again facilitating the establishment of a link between chemical and health effect. Chronic exposures occur in the everyday work situation, frequently without any awareness on the part of the worker or management. Consequently, the chronic exposure is the more insidious and difficult situation.

The major issue relating to chemical exposures deals with the dose-response or dose-effect relationship, which is illustrated by the two curves shown in Figure VI.28. The linear curve is the continuous relationship, which holds that there is some effect, whether or not it may be clinically discernible, from even the smallest contact. The "threshold" curve, frequently referred to as the "hockey stick" representation, indicates that there is a threshold value below which there is no effect whatever until a certainty dose (the threshold) is reached. This means that exposures to doses below the threshold produce no effect, whether or not clinically measurable. The logical consequence of a threshold dose-effect relationship is that exposures below the threshold are of no consequence whatever, and controls that are applied when concentrations are below the threshold produce no benefits in terms of human health.

The dose-response curve shown in Figure VI.28 holds for a single individual, whether it be the mouse, chimpanzee or human. When concern turns to large populations, where variations in susceptibility within that population come into consideration, a dose-response curve shown in Figure VI.29 would apply. In this illustration, the dose is the product of the two axes, and the effect is within the body of the plot. Obviously, the definition of the boundary between morbidity (illness) and mortality (death) is not a satisfactory basis for public health in the occupational or other situations. Rather, the need is to define the boundary between no effect and morbidity. It is this need that presents the greatest difficulty.

Most experts in toxicology accept the hypothesis that the human organism has a tolerance for many chemicals. We are, after all, chemical compounds and mixtures, functioning in a chemical environment, even when that environment is not contaminated by human and industrial activities. Therefore, there is a strong basis for maintaining that many chemicals behave in accordance with the threshold dose-response relationship. However, a view held by many experts is that chemicals capable of producing cancer or tumors — carcinogens and tumorigens — behave in accordance with the linear model. The consequence of holding to this view is that the only acceptable exposure to a carcinogen is zero; in practical industrial terms, this means the lowest detectable limit. Obviously, a related and very serious uncertainty concerns the arrival of the judgement as to what constitutes a carcinogen, i.e., what sort of experimental data provides an acceptable basis for designation as a cancer-causing chemical?

Historically, there have been four basic sources of toxicologic data: laboratory toxicologic studies, clinical exposure studies, data from occupational exposures, both controlled and otherwise, and epidemiologic investigations.

165
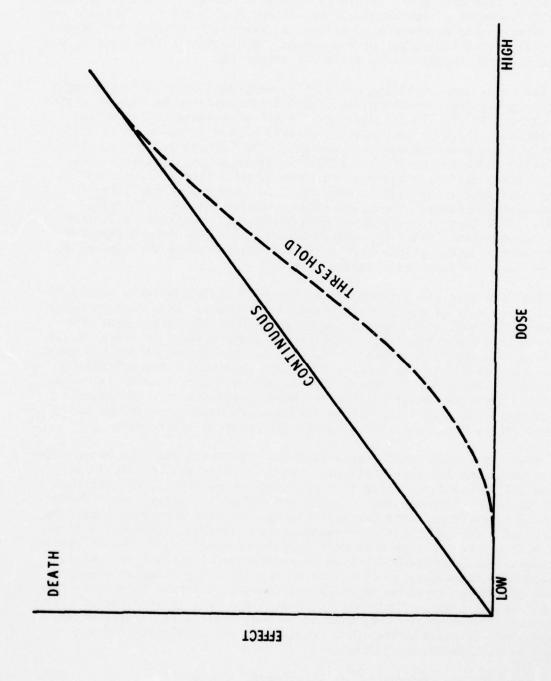
FIGURE VI.28. DOSE-RESPONSE CURBES
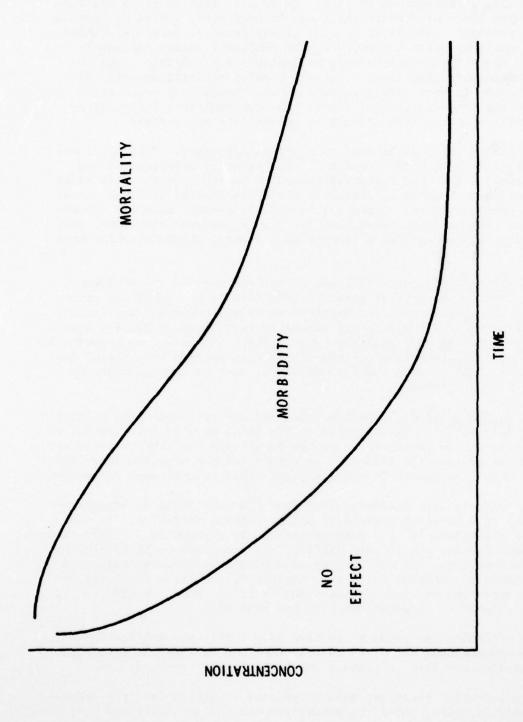
FIGURE VI.29. EFFECT OF EXPOSURE CONCENTRATION AND TIME ON THE BOUNDARIES BETWEEN MORTALITY, MORBIDITY AND NO EFFECT

167

Laboratory toxicologic studies employ experimental animals. Such studies allow for the use of relatively large numbers of animals at modest cost; this statement applies to rodents but is obviously less applicable to research involving chimpanzees or pigs. There are essentially no restrictions as to the types of studies which can be conducted, including testing to terminal outcomes. Excellent control of exposures is possible. Where necessary, multigenerational studies may be conducted within reasonable time spans. Complete histopathologic evaluations are possible. The obvious disadvantage is that there is always a major biologic question mark to data developed in such investigations because humans may react quite differently from the experimental animal that was employed; the applicability of extrapolations from animals to humans is never certain.

The biologic gap is bridged in clinical exposures. However, there are many disadvantages in such studies. The number of experimental subjects is generally very small and restricted to healthy adults. The range of experiments which can be conducted is obviously limited by legal, moral and ethical considerations. Costs are enormously greater than for laboratory studies. Current government restrictions on research with human subjects has virtually eliminated such work as a routine phase in toxicologic screening.

Occupational exposures do occur under both routine and accidental conditions. To the extent that health information is available and exposures can be quantified, such information can be quite germane and useful. Again, the experimental subjects are generally restricted to healthy adults. Retrospective epidemiologic evaluations of workers who have been chronically exposed to chemicals over long periods of time can provide very useful information, especially with respect to diseases, such as cancer, which exhibits long latency periods.

Epidemiologic studies, both prospective and retrospective, provide very useful information. When applied to the total population, such information is pertinent to community exposures to pollutants. When restricted to occupational groups, the data give important insight into the long-term effects of chronic exposures to chemicals and other occupational influences.

All epidemiologic studies suffer from the same basic disadvantage—the inability to accomplish control of all extraneous variables. In the occupational situation, it is a rare worker who is exposed to a single chemical or single insult. It is thus difficult to associate definitively the insult and the outcome. It can also be said with considerable confidence that no worker's environment is totally monitored, and there is always the danger of associating an exposure and a health effect when the effect may, in fact, be related to an agent which is not monitored.

The epidemiologic studies are also very costly and subject to long delays. In occupational terms, an adverse health effect may be discerned from such studies too late to protect the health of affected workers.

More recently, there has been a tendency to employ in vitro laboratory mutagenicity tests, under the assumption that mutagenicity and carcinogenicity have similar cytologic mechanisms, and therefore, if a substance

168

is mutagenic, there is a reasonable basis to fear carcinogenicity. This assumption is not universally accepted. Nonetheless, these tests, which employ bacteria, are exceedingly low in cost relative to other toxicologic evaluations and yield results in days or weeks. Tests may be run with simple bacterial systems with and without added experimental variables to simulate in vivo metabolism. Although these methods are generally regarded as useful in screening, they cannot be regarded as being definitive.

Even the most sophisticated toxicologic evaluations employing higher animals such as primates, produce results with sizeable areas of uncertainty. Questions such as dose, dosage, appropriateness of administration route, etc., render the data of uncertain significance in terms of human exposures. The closer the approach can be made to reality, the more confidence can be placed in the data, but such approaches to reality generally make for much more extended and costly investigations.

A major contributor to the uncertainty inherent in toxicologic data stems from the recognition that exposure to a single substance under carefully controlled conditions is generally most unrealistic. The average worker is likely to be exposed to many chemicals and other stress factors, in varying combinations and sequences, in the course of a normal day. This presents an experimental system offering almost an infinite number of variables. Consequently, relatively little is known about synergisms, antagonisms, simple additive and simple subtractive phenomena in producing toxic manifestations. More work is being done in this area, especially with respect to carcinogens, resulting from the acceptance of the fact that there are chemical agents which appear not to be carcinogenic themselves, but which seem to act as cocarcinogens when in the presence of another carcinogen. However, at this point, little can be said regarding the interactions among potentially toxic chemicals in either the occupational or community environments.

Another source of difficulty in determining the toxic properties of chemicals relates to the wide variety of toxic manifestations which can follow chemical exposures. The critical factor of time must also be considered, with some outcomes occurring within minutes, facilitating associations, and others taking years to develop, obscuring association. Some examples of chemical-related diseases, along with chemicals that produce them, are as follows; the list is in no sense exhaustive.

> Dermatitis: organic solvents
>
> Peripheral nervous system effects: hexane
>
> Narcosis: acetone
>
> Blood dyscrasias: benzene
>
> Cancer: vinyl chloride, benzene, polynuclear aromatic
> hydrocarbons, acrylonitrile
>
> Reproductive defects: dibromochloropropane.

Many other toxic effects and chemicals could be listed. Obviously a critical matter concerns the dose required to effect intoxication.

VI.5.2   Health Implications of Results

Workplace exposures to chemicals are regulated by means of a Threshold Limit Value. The TLV is that value to which a worker may be exposed for 8 - 10 hours per day, five days a week, 50 weeks a year for an entire working life of 40 years, and remain free of significant or irreversible adverse health effects. The TLV is most generally expressed as a Time Weighted Average (TWA), reflecting the fact that the concentration of a chemical in the workplace atmosphere is unlikely to remain at a constant level. For chemicals of significant acute toxicity, the exposure is also controlled with a Maximum Allowable Concentration (MAC) or peak or ceiling value, with the level permissible for a stated period of time, with a stated number of excursions to this level within a given time interval such as a normal shift. There is also the Short Term Exposure Limit (STEL) which has been referred to in Section VI.4.

TLVs are not immutable; they are frequently changed as additional information becomes available through toxicologic research or epidemiologic studies. The overall trend of changes has been in the downward direction, though there are some exceptions.

Based on the data from the two full scale tests, the following conclusions may be drawn:

1. Workers on occasion are exposed to chemical vapors at levels substantially in excess of the TLV, expressed as the time weighted average.

2. Workers may also be exposed to chemical vapor concentrations well in excess of the Short Term Exposure Limit.

3. The interpretation of the measured exposure is rendered more difficult by the unusual work schedules to which workers adhere during the loading and offloading operations.

Historically, the Threshold Limit Value was derived for the typical or usual work schedule of eight hours per day, five days per week. More recently, the TLV has come to be regarded as applicable to the eight or ten-hour work day, thus reflecting changes in work schedules. These altered work patterns are frequently designated "novel work schedules".

The formulation of the TLV implicitly makes certain assumptions relating to the exposure time being followed by a certain period for recovery (no exposure) and purging of the potential toxicant. If the relationship between exposure and recovery times is drastically altered, the TLV might require significant adjustment.

Among the shortcomings of the TLV that have been recently pointed out are the lack of attention to high risk groups, failure to take account of circadian rhythms, and, most recently, inadequate accounting for the phenomenon of carcinogenesis. The problem has not been totally ignored.

170

Brief and Scala[*] have devised a mathematical formula for the calculation of a TLV reduction factor to deal with some of the novel work schedule problems. The TLV reduction factor (RF) is defined as the effect of increased exposure time, multiplied by the effect of decreased exposure-free (recovery) time. The factor may be calculated as:

$$RF = 8/h \times (24 - h)/16$$

where h is the hours worked per day. The 8-10 hour TLV is then adjusted to the novel work schedule by the calculation:

$$\text{Novel work schedule TLV} = RF \times TLV$$

This formulation is probably not applicable to the extremely distorted work schedules of personnel aboard chemical tankers or barges who might work 12-48 hours under exposure conditions, followed by a long (relatively) period of many days without exposure when purging would be expected to occur. Further consideration of this subject is needed but may be complicated by factors such as those described below.
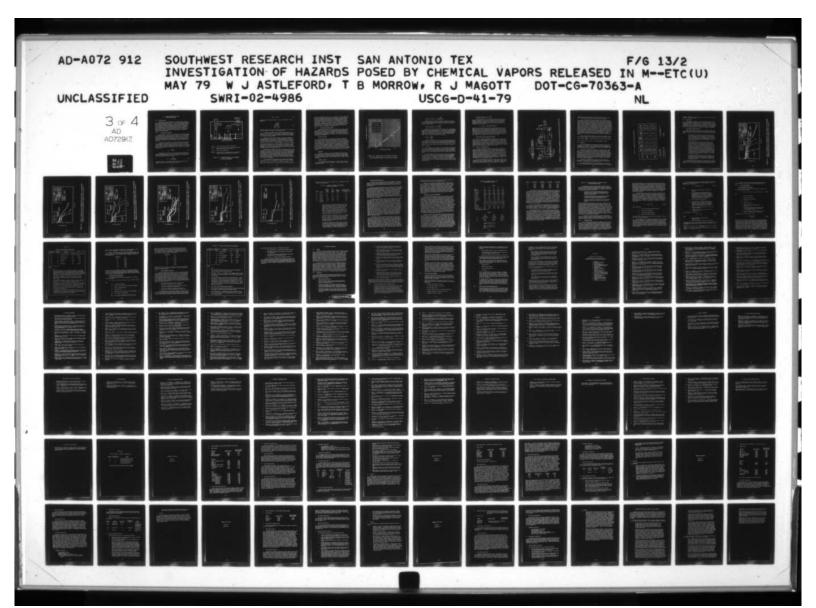
Neither the standard TLV nor the modified value for novel work schedules takes account of atypically high risk groups. Clearly there are wide variations within any population in risk from "ordinary" toxicants or cytotoxic chemicals. Risks may vary because of genetic factors, general state of health or disease, nutritional situation, development or aging phenomena, or behavioral characteristics. With growing recognition of the interplay between the organism and carcinogens, another element of variation is introduced. As sophistication grows in the understanding of the mechanisms of intoxication and oncogenesis, these factors may be taken into account, but the current state of knowledge does not allow for this.
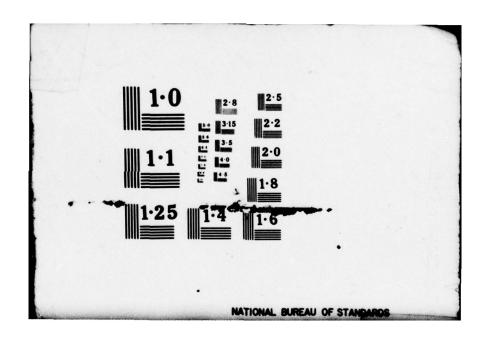
It is now generally accepted that the organism is governed by a series of regulatory mechanisms in the form of biological clocks with different periods. There are daily (circadian), monthly (circamensual) and annual (circannual) rhythms. Recent studies have shown that chemotherapeutic agents can vary dramatically in both efficacy and nature and extent of side effects depending on when the agent is administered relative to the rhythms, especially the circadian rhythm. The same phenomenon may be expected to be at play with respect to chemical toxicants. Yet, this phenomenon is not taken into account in the TLV. A given exposure at one point in the rhythm cycle might be quite safe, whereas the same quantity at another point in the cycle might be dangerous. It is questionable that this degree of sophistication can be added to the control of chemical exposures at the current level of understanding of the phenomenon. Clearly, additional research must be done on these matters, though such research is beyond the scope of this study.

---

[*]Brief, R. S. and Scala, R. A., "Occupational Exposure Limits for Novel Work Schedules," American Industrial Hygiene Association Journal, Vol. 36, August 1975.

4. Chemicals regarded as suspect carcinogens are transported by
   water, and workers are frequently exposed to levels which
   are extremely high relative to existing or proposed standards.

One of the major dilemmas existing with regard to chemical exposure concerns chemicals viewed as oncogenic, and focusses on the issue of whether there is a threshold dose for oncogens. The universal application of a no-threshold philosophy for oncogenic chemicals is probably unreasonable and unachievable, though it is certainly justified for those chemicals which have been shown to be human oncogens on a sound basis. Normal shipboard operations as currently practiced in the loading and offloading of chemicals are almost certainly not compatible with the attainment of zero exposure for suspect oncogens. Although beyond the scope of this study, the resolution of the threshold vs. no threshold dose-effect relationship for oncogens is a question of the highest priority.

VII. LABORATORY EXPERIMENTS OF LIQUID
EVAPORATION/GAS FREEING

VII.1   Scaling Criteria

Tank ventilation tests performed in the laboratory can be used to
predict full-scale tank behavior when the tests are performed in accordance
with accepted principles of similarity. In this section the important physi-
cal and chemical phenomena that take place during the gas exchange process
will be described. Then the significant physical and chemical variables
will be grouped into appropriate dimensionless parameters. To assure simi-
larity between model- and full-scale tank behavior, these dimensionless
parameters should have the same numerical values in model tests as in full-
scale operation. However, since exact similarity cannot be achieved for
some of the dimensionless parameters, the consequences of out-of-scale
parameters will be discussed.

VII.1.1   Description of Phenomena

Figure VII.1 is a sketch of a tank undergoing a gas exchange process
by the dilution method. Gas A is blown at high velocity into the tank where
it mixes with and dilutes the original tank contents, gas B. The diluted
tank contents leave the tank through an exit located in the tank top. Web-
frames and bulkheads (hereafter called tank internal structure) divide the
region near the tank bottom into compartments. Vapor and liquid cargo may
flow from one compartment into another through stringer penetrations in the
structure.
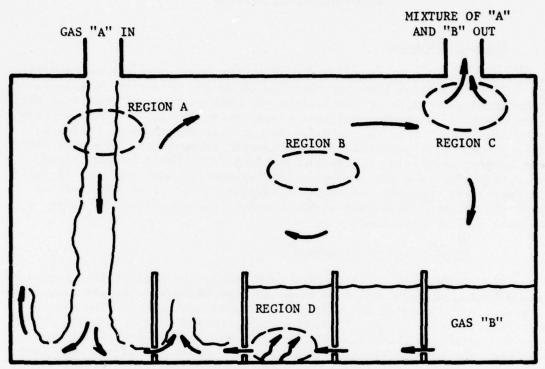
There are several regions in the tank where different flow phenomena
occur. In Region A of Figure VII.1, the inlet jet entrains gas from the
tank atmosphere and (ideally) reaches the bottom of the tank. The rate of
jet entrainment is higher for turbulent jets than for laminar jets, and rela-
tively constant for values of Reynolds number greater than 10^4. The Reynolds
number is a dimensionless ratio of dynamic forces to viscous forces and may
be written as

$$Re = \frac{V_A d_i \rho_A}{\mu_A} \tag{7.1}$$

The ability of the inlet jet to penetrate through the denser tank
gas atmosphere depends upon the ratio of jet momentum to the buoyancy force
exerted by the tank atmosphere. This ratio has been given the name densi-
metric Froude number and is usually written

$$Fr = \frac{\rho_A V_A^2}{(\rho_B - \rho_A)gH} \tag{7.1}$$

Reference J-52 gives a correlation of model- and full-scale data for jet
penetration distance versus a modified Froude number as

173

GAS "A" IN

MIXTURE OF "A" AND "B" OUT

REGION A

REGION B

REGION C

REGION D

GAS "B"

MASS TRANSFER FROM
EVAPORATING CARGO RESIDUE

REGION A - INERTIA AND BUOYANCY FORCES ARE PREDOMINANT.

REGION B - INERTIA AND BUOYANCY FORCES ARE PREDOMINANT WITH MUCH
LOWER INERTIA FORCES THAN IN REGION A.

REGION C - INERTIA FORCES PREDOMINATE.

REGION D - VISCOUS, BUOYANCY AND PRESSURE FORCES ARE PREDOMINANT.
DIFFUSION AND VAPOR REGENERATION ARE IMPORTANT.

FIGURE VII.1. IMPORTANT REGIONS OF GAS EXCHANGE
IN THE DILUTION METHOD

$$\frac{X}{d_i} = 1.85 \sqrt{F} \tag{7.2}$$

where X is the jet penetration depth, d_i is the inlet diameter, and F is defined as

$$F = \frac{V_A^2 \left(\frac{\rho_B}{\rho_A}\right)^{1.5}}{\left(\frac{\rho_B}{\rho_A} - 1\right) g \, d_i} \tag{7.3}$$

Equation 7.2 defines the value of F necessary for the inlet jet to reach the tank bottom when X is set equal to H_T, the tank height.

In Region B the convective gas velocities are much lower than in Region A. The buoyancy forces are also much lower because Region B consists of gas with nearly uniform (but time dependent) concentration and density. In regions where the gas is stagnant, molecular diffusion aids in homogenizing the concentration distribution.

In Region C inertia forces predominate as the flow accelerates in the neighborhood of the exit port. In shielded compartments between web-frames and bulkheads, such as Region D, the driving force for gas motion is the density difference between the gas in Region D and the gas in compartments that are diluted directly by the inlet jet. The flow rate of gas B toward the inlet will scale as $A_G \sqrt{(\rho_B - \rho_A) g H_G / \rho_A}$ where H_G is the height of the shielded compartment and A_G is the open area in webframes and bulkheads near to the tank bottom. As time continues, the density of the gas in Region D decreases. This will cause a decrease in the flow rate out of the region, but the gravity flow process will continue until the gas density in Region D is equal to the density of gas A.

Evaporation mass transfer (also called vapor regeneration) may occur in Region D from pools of liquid cargo residue. The mass flow rate of evaporated vapor will depend upon the liquid pool area, the local mass transfer coefficient, g_i' (a function of the local gas flow velocity and the physical-cal-chemical properties of the gases involved), and the vapor concentration C(t) in Region D. In compartments shielded by tank internal structure, molecular diffusion aids the transfer of gas B (and cargo vapor) from regions of high concentration to regions of lower concentration. The molecular diffusion rate depends upon the value of diffusion coefficient and the local concentration gradient.

In an ideal dilution gas exchange process, without vapor regeneration, the tank contents are homogeneous at any instant of time, and the concentration of gas B in all parts of the tank falls as $C(t)/C_o = e^{-Qt/V}$ where Q is the flow rate of gas A into the tank, V is the tank volume, and

175

C_o is the concentration of gas B at $t = 0$. Actually, the tank contents are generally not homogeneous for a real dilution process. Internal tank structure delays the gas exchange process in shielded compartments between webframes and bulkheads, as explained above. The additional number of tank volume turnovers required to reduce the gas B concentration in all regions of the tank to a desired level, say $0.2\ C_o$, can be expressed as a gas exchange delay, τ, which is a function of the ratio of the time required to drain shielded compartments by gravity flow to the time required for a tank volume turnover. This ratio is called the tank drainage number, N_d, and Figure VII.2 shows a correlation of τ as a function of N_d obtained from laboratory scale tests described in Reference J-53.

VII.1.2   Important Dimensionless Terms

A dimensionless modeling law can be postulated that relates a dependent variable of interest (such as the concentration of hydrocarbon vapor at some point in a tank) to a set of independent dimensionless variables. Although the form of the model law is unknown, exact similarity of the independent dimensionless variables is expected to assure similar behavior of the prototype and a geometrically scaled model. The important dimensionless parameters are listed below.

Concentration, C/C_o

For a prototype tank, the concentration of interest might be the oxygen concentration, the total hydrocarbon concentration, the concentration of one or more hydrocarbon vapor constituents, or the concentration of a toxic chemical vapor. The concentration will be a function of time during a gas exchange process. Therefore, the concentration may be made dimensionless by dividing by the initial concentration, C_o, present in the tank at the start of the gas atmosphere procedure. The dimensionless concentration, C/C_o, is often the dependent variable of the dimensionless model law. When the replacement gas contains a component which is to be removed from the tank (such as O_2 in inert gas), then C/C_o is replaced by $(C - \overline{C})/(C_o - \overline{C})$ where $\overline{C}$ is the concentration of the gas of interest which is present in the replacement gas (gas A). In the limit, the final concentration can never be lower than $\overline{C}$.

Time, Qt/Ψ

The time, t, from the start of a gas atmosphere procedure may be made dimensionless by multiplying by the gas A flow rate, Q, and dividing by the tank volume, Ψ. Since Ψ/Q is equal to the time required to blow into the tank an amount of gas equal to the tank volume, the dimensionless term Qt/Ψ is often referred to as "tank turnover time" or "number of tank changeovers."

Length, $\lambda = \ell_P/\ell_M$

It is assumed that the model tank is an accurate scale replica of the prototype tank with a ratio of lengths, λ. Typical values of λ range from about 8 to 50.
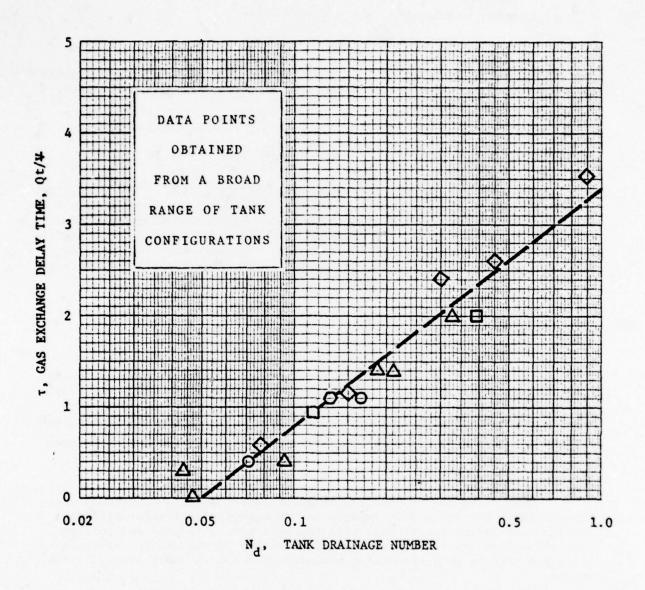
FIGURE VII.2. CORRELATION OF GAS EXCHANGE TIME DELAY, τ
WITH TANK DRAINAGE NUMBER FOR DILUTION GAS EXCHANGE

$$\text{Buoyancy and Inertia,} \quad Fr = \frac{\rho_A V_A^2}{g\, H_T\, (\rho_B - \rho_A)}$$

Reproducing the dual effects of buoyancy and inertia is critical for the correct simulation of tank ventilation. The ratio of gas A inertia to gas B buoyancy forces produces the dimensionless parameter called the densimetric Froude number.

$$\text{Viscosity and Inertia,} \quad Re = \frac{V_A d_i \rho_A}{\mu_A}$$

The ratio of inertia to viscous effects gives rise to the dimensionless parameter called the Reynolds number. In general it is not possible to satisfy both Froude number similarity and Reynolds number similarity simultaneously in a reduced scale experiment. In this case Reynolds number similarity can be relaxed since it is sufficient to ensure that the Reynolds number is large ($> 10^4$) enough for the jet to be fully turbulent to give similar rates of inlet jet entrainment and spreading.

$$\text{Diffusion,} \quad \frac{D_{AB}\, V}{H_T^2\, Q}$$

The ratio of time since the start of a gas exchange process to the time necessary for diffusion to mix two gases together is a convenient diffusion parameter. Actual time may be represented by the time for a tank volume turnover, V/Q, and the diffusion time may be determined by the tank height, H_T^2, or webframe height, H_G^2, divided by the diffusion coefficient, D_{AB}, i.e., H_T^2/D_{AB}.

This parameter is also impossible to model exactly in reduced scale experiments. Reference J-53 considered the effect of molecular diffusion in tank ventilation experiments with internal tank structure and concluded that the use of the liquid analogy was necessary to prevent out-of-scale diffusion effects from disguising structure effects in small scale ($\lambda = 50$) models.

When gases must be used (as to study the effect of vapor regeneration from cargo residue), it is recommended that the diffusion parameter should have a value of 0.005 or less. This may be achieved by reducing the scale factor, λ. For example, the diffusion factor is 0.00016 for a full scale tank with $V = 500,000 \text{ ft}^3$, $H_T = 100$ ft, and $Q = 4000$ cfm. A scale model with $\lambda = 10$ gives a diffusion factor of 0.0051, which is acceptable, but a model with $\lambda = 50$ gives a diffusion factor of 0.056, which is not acceptable.

Tank Internal Structure, $\quad N_d \approx \dfrac{t_G Q}{\mathcal{V}}$

The principal effect of tank internal structure (webframes, bulk-heads) is to delay the end of the gas atmosphere procedure by obstructing the forced ventilation of regions near the tank bottom. These shielded regions are eventually ventilated by the gravity flow of the denser gas through holes in the structure. A time scale for gravity drainage of the shielded regions may be written as

$$ t_G = \mathcal{V}_G/Q_G = \mathcal{V}_G / \left(A_G \sqrt{(\rho - 1) g H_G} \right) $$

where $\mathcal{V}_G$ is the volume of gas contained in shielded compartments, A_G is the open area for flow through webframes and bulkheads near the tank bottom, and Q_G is the flow rate of dense gas through these holes. Then a nondimensional parameter, N_d, may be formed as the ratio of t_G to the tank turnover time $\mathcal{V}/Q$. N_d is given the name "tank drainage number" because it relates the time required to gravity drain heavy gas from the tank bottom to the time for a tank turnover. For small values of N_d, the tank internal structure is not restrictive to efficient forced ventilation of the tank.

Mass Transfer (Vapor Regeneration), $\dot{m}_G/QC_o$

The ratio of the vapor regeneration rate, $\dot{m}_G$, to the initial vapor efflux, QC_o, is a convenient dimensionless parameter for vapor regeneration studies. Another useful parameter is the Stanton number, $St = g_i/\rho V$, where g_i is the local value of mass transfer coefficient ($g_i = \dot{m}_G/(C - C_o)$) and ρV is the mass flux of gas moving past the surface. The utility of the Stanton number with Reynolds number and Schmidt number may be found in mass transfer texts (see Reference J-54, for example) that will provide guidance in scaling model scale vapor regeneration results up to full scale.

VII.2   Facility and Instrumentation

Two series of tests were conducted to investigate the effects of chemical evaporation and tank internal structure on the concentration-time history in a small scale tank that was gas freed by the dilution method. The test facility is shown schematically in Figure VII.3. The first series of tests was designed to study only the effect of liquid evaporation. Consequently, the simulated webframes (internal structure) were not utilized. Vapor concentration was monitored at the tank discharge port, and liquid temperature was monitored at thermocouple station No. 2. The second series of tests was designed to investigate the combined effect of evaporation and internal structure. The complete experimental arrangement in Figure VII.3 was employed on this latter group of tests.

The tank was constructed of plywood, and the internal surfaces were coated with a chemical-resistant epoxy paint. Tank internal length, width, and depth were 2.372 m, 0.3048 m, and 1.213 m, respectively. Overall dimensions of the eight webframes were 0.3048 m by 0.3048 m. Each webframe

179
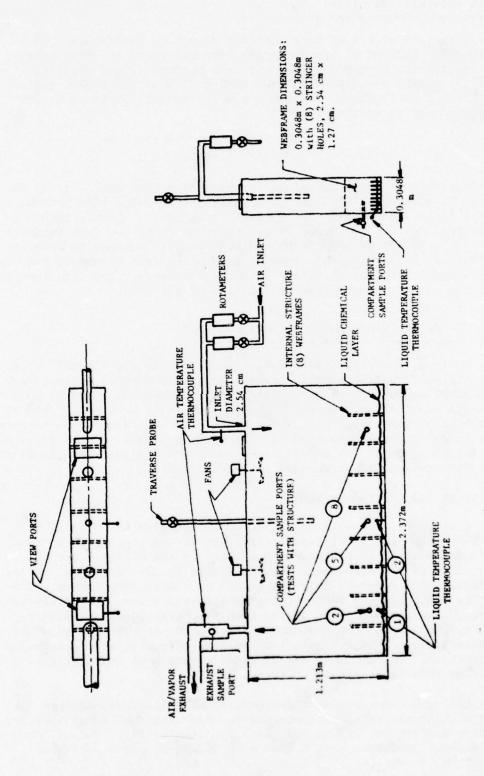
FIGURE VII.3. EXPERIMENTAL ARRANGEMENT FOR EVAPORATION/DILUTION VENTILATION TESTS

contained eight equally-spaced cutouts that simulated stringer hole openings. The stringer holes measured 2.54 cm high by 1.27 cm wide.

Prior to the start of a ventilation test, the liquid chemical was introduced onto the floor of the tank. With the tank top, inlet and exhaust ports sealed, the liquid was allowed to evaporate until a predetermined uniform vapor concentration had been achieved in the ullage space. Two internal fans located on the topside of the tank were used to expedite the mixing process and, thereby, minimize the time needed to arrive at a uniform concentration. Vertical traverses of the ullage space were made with a sampling probe centered on the tank top. Vapor samples were extracted at predetermined distances below the tank top; and these samples, as well as the samples collected during the ventilation tests, were analyzed by a Century Systems Model 108 Organic Vapor Analyzer. When the concentration in the vapor space had reached the desired degree of homogeneity and level, the mixing fans were turned off, and the ventilation test was initiated. Jet impingement on the liquid surface and subsequent drying patterns were observed through two viewing ports on the tank top. Temperatures were measured with a multipoint, digital thermocouple indicator, and rotameters were used to monitor ventilation flow rates.

Tank size and webframe dimensions were selected to minimize out-of-scale diffusion effects on the gas freeing process. For all tests, the diffusion parameter, $\dfrac{D_{AB} \Psi}{H_T^2 Q}$, that was discussed in Section VII.1 was calculated to be less than 0.002, well under the recommended maximum of 0.005.

VII.3 Test Plan

Table VII-1 summarizes the evaporation/ventilation tests that were conducted in the small-scale tank. Test Series I and II were designed to investigate (1) the effect of liquid evaporation and (2) the combined effect of evaporation and internal structure on the concentration-time history during the gas freeing process, respectively.

Test Series I consisted of six tests that included different chemicals, ventilation flow rates, and thicknesses of liquid film on the tank bottom. Two test combinations (I.2 and I.5) and (I.4 and I.6) were selected to demonstrate the impact of liquid volatility on the evaporation process. Test pairs (I.1 and I.3) and (I.4 and I.5) reflect the effects of ventilation rate. Finally, the combination of Tests I.1 and I.2 incorporates the effect of liquid thickness. In all tests, the densimetric Froude number exceeded 50, which is an adequate value to ensure that the ventilating jet penetrates to the bottom of the tank and that the vapor concentration in the ullage space is well-mixed or homogeneous.

Test Series II consisted of five tests with internal structure. Each test in this sequence can be compared directly with its unstructured counterpart in Test Series I, e.g., I.1 and II.1, etc.

It should be emphasized that the facility and the tests that were conducted were designed to provide an improved understanding of two phenomena.

TABLE VII-1. SUMMARY OF GAS FREEING TEST CONDITIONS

Test Series	Test No.	Chemical Liquid in Tank	P_v Vapor Pressure mm Hg @ 20°C	Nominal Vent Flow Rate m^3/min	Nominal Chemical Liquid Thickness mm	Initial Chemical Concentration % v/v	$\bar{\rho}$ $\dfrac{\rho_{tank}}{\rho_{air}}$	Froude Number, Fr
I Without Structure	I.1	Acetone	176	0.2	2.7	5.99	1.060	59.5
	I.2	Acetone	176	0.2	1.35	6.22	1.062	57.6
	I.3	Acetone	176	0.37	2.7	6.48	1.065	189.5
	I.4	Toluene	23.8	0.37	1.35	0.99	1.022	560
	I.5	Toluene	23.8	0.20	1.35	1.32	1.029	127.5
	I.6	Isopropyl Alcohol	31.0	0.37	1.35	3.96	1.042	293
II With Structure	II.1	Acetone	176	0.2	2.7	5.31	1.053	67.4
	II.2	Acetone	176	0.2	1.35	6.38	1.064	55.8
	II.3	Acetone	176	0.37	2.7	7.11	1.071	173.5
	II.4	Toluene	23.8	0.37	1.35	1.09	1.024	513
	II.5	Toluene	23.8	0.20	1.35	1.37	1.030	123

$$\bar{\rho} = \frac{\dfrac{C_o}{100} M_b + \left(1 - \dfrac{C_o}{100}\right) M_a}{M_a}$$

M_b = molecular weight of chemical

M_a = molecular weight of air

v_a = inlet velocity based on flow rate and jet inlet diameter

$$Fr = \frac{v_a^2}{(\bar{\rho} - 1) g H}$$

Therefore, extrapolation of the test results to a full-scale chemical tank is neither intended nor implied.

VII.4   Test Results
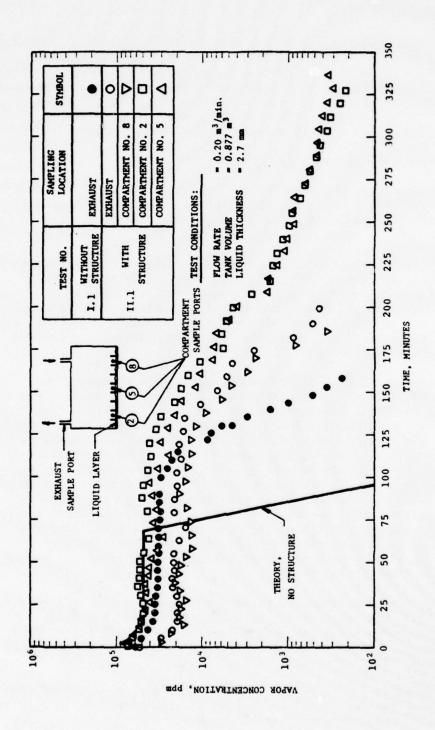
The experimental results of the evaporation/ventilation tests are presented in Figures VII.4 through VII.9. The first five figures contain concentration data for companion tests with and without structure. Theoretical predictions of the in-tank model are also included where appropriate. The remainder of this section includes a discussion of the evaporation/ventilation tests without structure followed by a discussion of the apparent effects of structure, and finally a comparison of theory with experiment.

Tests Without Internal Structure

The evaporation/ventilation process in an unstructured tank can be divided into a constant rate drying phase which is followed sequentially in time by a falling rate period of drying and an ideal dilution gas freeing phase.
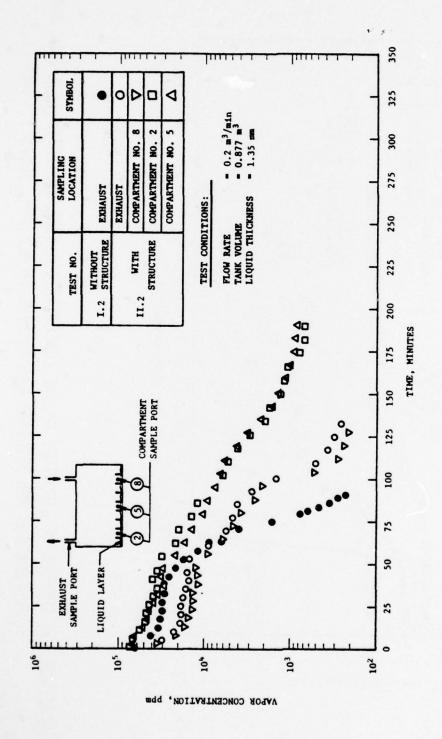
o   The constant rate drying phase is encountered shortly after test initiation, and it is characterized by the discharge of a time-independent vapor concentration at the tank exhaust. During this initial plateau, the evaporation rate is constant and is in equilibrium with the mass discharge rate, CQ. All tests in Series I exhibited, to varying degrees, a constant rate drying period.

o   If the tank bottom were perfectly level and smooth, the constant drying rate period would be followed immediately by the ideal dilution gas freeing phase. The transition would occur when all of the liquid had evaporated at a constant rate. Realistically, both large and small scale tank bottoms will be rough and uneven to some degree. Surface roughness and unevenness give rise to the second phase of drying—the falling rate period. Localized pooling of chemical and accumulation of liquid between roughness elements results in a time-dependent reduction in liquid surface area and evaporation rate. The experimental data indicate that, as evaporation rate decreases with time, there is a gradual roll-off of discharge concentration beginning at the end of the constant rate period.

o   The ideal dilution gas freeing phase begins when all of the liquid has evaporated. From that point, the discharge concentration falls exponentially with time. All tests, with the exception of Test No. I.6, approached or exhibited this ideal dilution phase.

The apparent duration of the constant rate drying period provides a measure of the effect of liquid volatility, ventilation rate, and liquid thickness on the evaporation/ventilation process. The duration of this
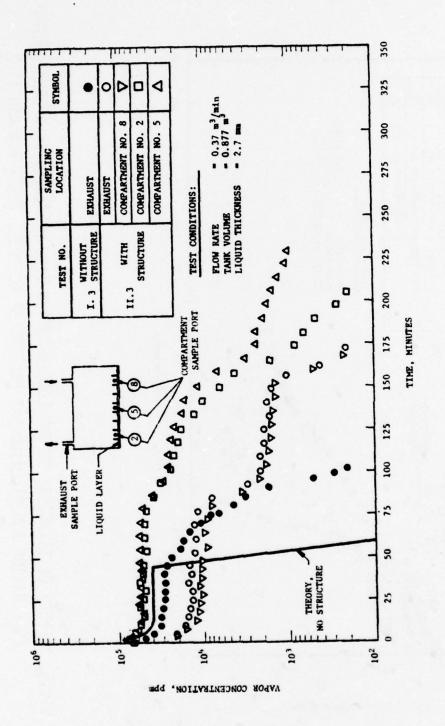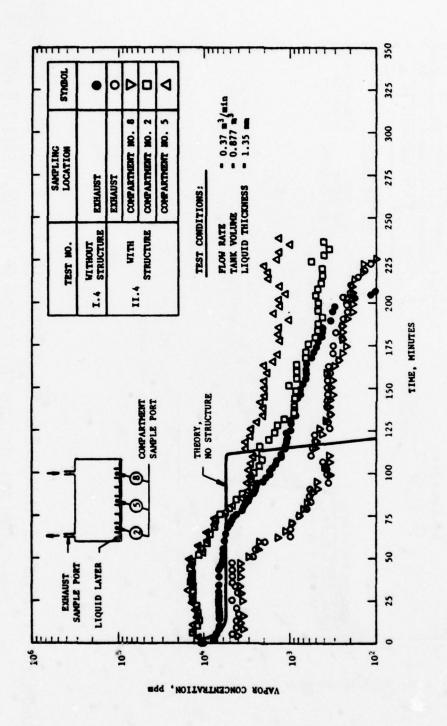
FIGURE VII.4. EFFECT OF STRUCTURE ON THE CONCENTRATION-TIME HISTORIES IN A TANK DURING EVAPORATION AND DILUTION GAS FREEING OF ACETONE, TESTS I.1 AND II.1
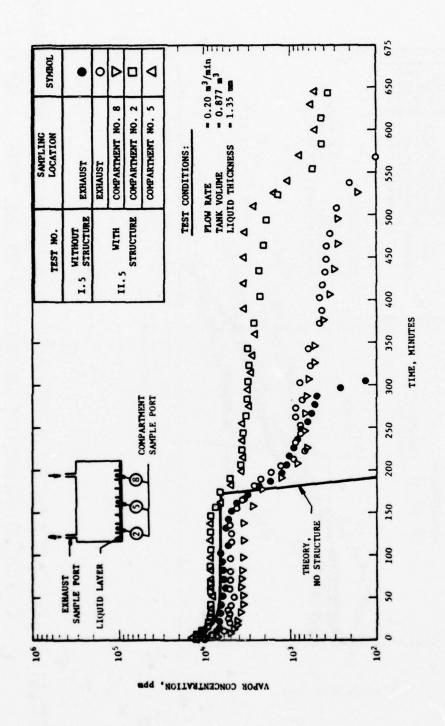
FIGURE VII.5. EFFECT OF STRUCTURE ON THE CONCENTRATION-TIME HISTORIES IN A TANK DURING EVAPORATION AND DILUTION GAS FREEING OF ACETONE, TESTS I.2 AND II.2

185
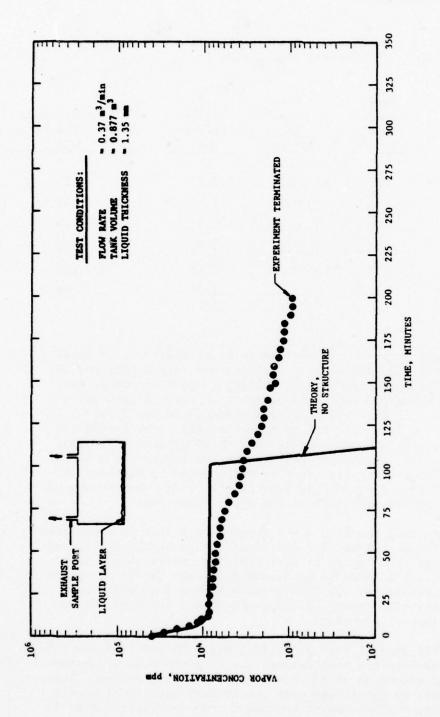
FIGURE VII.6. EFFECTS OF STRUCTURE ON THE CONCENTRATION-TIME HISTORIES IN A TANK DURING EVAPORATION AND DILUTION GAS FREEING OF ACETONE. TESTS I.3 AND II.3

186

FIGURE VII.7. EFFECT OF STRUCTURE ON THE CONCENTRATION-TIME HISTORIES IN A TANK DURING EVAPORATION AND DILUTION GAS FREEING OF TOLUENE, TESTS I.4 AND II.4

FIGURE VII.8. EFFECT OF STRUCTURE ON THE CONCENTRATION-TIME HISTORIES IN A TANK DURING EVAPORATION AND DILUTION GAS FREEING OF TOLUENE, TESTS I.5 AND II.5

TEST CONDITIONS:

FLOW RATE = 0.37 m³/min
TANK VOLUME = 0.877 m³
LIQUID THICKNESS = 1.35 ▬

EXHAUST
SAMPLE PORT

LIQUID LAYER

THEORY,
NO STRUCTURE

EXPERIMENT TERMINATED

VAPOR CONCENTRATION, ppm

TIME, MINUTES

FIGURE VII.9. EXHAUST CONCENTRATION-TIME HISTORY FOR ISOPROPYL ALCOHOL DURING EVAPORATION AND DILUTION GAS FREEING IN A TANK WITHOUT INTERNAL STRUCTURE, TEST I.6

period, as interpreted from the experimental data, is summarized in Table VII-2 and is discussed below.

TABLE VII-2. DURATION OF CONSTANT RATE EVAPORATION
PERIOD FOR TEST SERIES I

Test No.	Chemical	Vapor Pressure, mmHg @ 20°C	Vent Flow Rate, m^3/min	Liquid Thickness mm	Constant Rate Evaporation Period, min
I.1	Acetone	176	0.2	2.7	~100
I.2	Acetone	176	0.2	1.35	~ 37.5
I.3	Acetone	176	0.37	2.7	~ 40
I.4	Toluene	23.8	0.37	1.35	~ 42.5
I.5	Toluene	23.8	0.20	1.35	~107
I.6	Isopropyl Alcohol	31.0	0.37	1.35	~ 38

o   On the basis of vapor pressure as an indicator of vola-
    tility, the duration of the constant rate drying period
    varies *inversely with volatility*. Under identical test
    conditions of ventilation rate and liquid thickness, a
    change of test liquid from acetone (Test No. I.2) to
    toluene (Test No. I.5) produced nearly a three-fold in-
    crease in the duration of the drying period while vapor
    pressure at standard temperature was reduced by a factor
    of 7.4. A similar trend is to be noted in the case of
    Test Nos. I.4 and I.6, but the effect is less pronounced
    due to the proximity of the vapor pressures.

o   Increasing the liquid thickness by a factor of two between
    Test Nos. I.1 and I.2 increased the constant rate drying
    period by a factor of 2.7. Ideally, there should have
    been a 1:1 increase in drying time with liquid thickness.
    The reason for the 70% increase beyond that which was
    anticipated cannot be explained on the basis of the ex-
    perimental procedure.

o   In the case of test pairs (I.1 and I.3) and (I.4 and I.5),
    increasing the ventilation flow rate produced a substan-
    tial reduction in the constant rate drying period. This
    result is consistent with the in-tank analytical sensi-
    tivity analysis which concluded that ventilation rate is
    a dominant variable in controlling evaporation time.

190

Tests with Internal Structure

In Test Series II, vapor concentrations were measured in compartment numbers 2, 5, and 8 between webframes and at the tank exhaust. The concentration responses at these sampling locations are presented in Figures VII.4 through VII.8 together with the data from the companion tests without internal structure.

A review of these data indicates that in all Series II tests the vapor concentrations in compartment number 8 were virtually identical to the exhaust concentrations throughout the duration of the tests. This result was anticipated. The ventilation jet penetrated to the tank bottom and impacted onto the liquid surface in compartment number 8, which was located directly beneath the ventilation inlet port. As liquid evaporated from that compartment, the vapors were transported by forced convection into the free space above the webframes where they mixed thoroughly with the tank atmosphere. This mixing and subsequent entrainment of vapors by the ventilating jet equalized the vapor concentrations in compartment number 8 and the tank exhaust, the latter being representative of the concentration in the well-mixed free space above the webframes.

For other than compartment number 8, the webframes shield the liquid from the convective flow field that is created by the ventilating jet and the exhaust flow. Hence, in these compartments, mass transfer of vapor by forced convection is minimal, and gas freeing is controlled by the slower mechanisms of molecular diffusion and gravity drainage of vapor. The test data indicate that compartment numbers 2 and 5 gas free much slower than compartment number 8, and, hence concentrations at any time are greater than those in either compartment number 8 or the tank discharge. In all cases, the vapor concentrations in these two shielded compartments are essentially equal throughout all or part of the testing period. Over the time period where their concentrations coincide, gas freeing is controlled by molecular diffusion and gravity drainage. At some point in time, it is hypothesized that the vertical concentration gradients in the shielded compartments approach zero, and vertical molecular diffusion ceases. Beyond that time, vapors tend to flow under gravity through the stringer hole openings from regions of high vapor concentration or high mixture density (compartment numbers 2 and 5) to regions of low concentration (compartment number 8). This drainage phenomenon results in compartment number 2 being gas freed ahead of compartment number 5.

These small scale tests indicate that internal structure acts to increase the length of time to gas free a tank relative to a tank with no structure. To illustrate this result, compare the exhaust concentration profiles from Series I with the companion concentration-time histories for the regions between webframes that are unaffected by forced ventilation. Since Froude number was chosen to yield a well-mixed vapor space, the exhaust concentration in Series I is identical to the concentration at a location in the unstructured tank that is equivalent to, say, compartment number 2 in the tank with structure. Based on this analogy, the incremental time required to gas free these shielded regions to a given concentration, i.e., the time delay, can be of the order of the time to gas free the tank without structure to the same level. Stated differently, these tests

indicate that structure can result in a doubling of the time to gas free to a predetermined level relative to an unstructured tank.

Recall that these tests were conducted using pure chemicals that were not diluted by any simulated tank washing liquids. If this procedure were to be applied to full-scale chemical tanks, it would result in an excessive number of tank turnovers to achieve a gas free condition. Industry has realized this, and, in practice, liquid chemical tanks are normally washed with hot and/or cold water, stripped and then ventilated, thus greatly reducing tank turnaround time. However, even when the residual product is diluted with wash water, the tank ventilated to "safe" conditions based on explosimeter readings and batted down before man entry, residual product remains on the tank structure to outgas and create potential safety hazards. The full-scale in-tank measurements reported in VI.4 confirm this statement.

Comparison of Theory with Experiment

The in-tank analytical model in Section III.2 was used to predict the concentration-time histories for selected tests in which there was no tank internal structure. Input data for each prediction consisted of a combination of experimentally measured parameters, chemical property data, and empirically derived quantities. These inputs are summarized in Table VII-3. TPOOL, the liquid thickness on the tank bottom, was derived from the initial chemical volume and the internal floor area. Vapor temperature in the tank, TGAS, was assumed equal to the mean measured gas discharge temperature. During the tests, the effect of evaporative cooling was determined by measuring liquid film temperature. Since the model does not include evaporative cooling, this effect was taken into account by assuming that the wall temperature and, hence, liquid temperature, could be approximated by the mean liquid test temperature. This effect is reflected in the values of ALPHA and ZETA in the table. Due to a malfunction of the potentiometer system on Test No. I.1, the gas and liquid temperatures from Test No. I.3 were used in the analysis of Test No. I.1 with the realization that some discrepancy would result from the difference in ventilation flow rates. The effective evaporation velocity for these tests was calculated from the jet impaction and turning model in Section III.2.

Model predictions of the well-mixed concentration-time histories for Test Nos. 1, 3, 4, 5, and 6 in Series I are presented in Figures VII.4 and VII.6 through VII.9, respectively. In each of these figures, the predicted concentration-time histories compare quite favorably with the experimental results during the constant rate drying period. This constant rate drying period is characterized by both a constant evaporation rate and tank concentration. Since the model describes only the constant rate period, tank concentration falls exponentially with time following cessation of evaporation. A comparison of theoretical and experimental evaporation rates and air velocities during this constant rate period is presented on the next page. The subscripts T and E denote theoretical and experimental quantities, respectively. The experimental values of $\dot{m}_E$ were calculated from the product of ventilation flow rate and the mass concentration of vapor during the constant rate period. Using these values, the evaporation air velocities, U_E, were obtained by applying Gray's evaporation model.

TABLE VII-3. SUMMARY OF INPUT DATA FOR
IN-TANK MODEL PREDICTIONS

	TEST NO.				
	I.1	I.3	I.4	I.5	I.6
Chemical	ACT	ACT	TOL	TOL	IPA
TPOOL (cm)	0.2692	0.2692	0.1346	0.1346	0.1346
TFILM (cm)	0.0	0.0	0.0	0.0	0.0
Q (m^3/min)	0.1982	0.3681	0.3681	0.1972	0.3681
C_o (ppm)	59,900	64,800	9,900	13,200	39,600
P (mm Hg)	760	760	760	760	760
TB (°K)	329.3	329.3	383.8	383.8	355.5
G (dynes/cm)	23.7	23.7	29.0	29.0	21.7
M (gm/mole)	58.08	58.08	92.14	92.14	60.1
L (m)	$\longleftarrow$		2.372		$\longrightarrow$
W (m)	$\longleftarrow$		0.3048		$\longrightarrow$
H (m)	$\longleftarrow$		1.213		$\longrightarrow$
U (cm/sec)	17.1	31.75	31.75	17.1	31.75
TGAS (°K)	293.9	293.9	294.2	292.8	295.8
ALPHA, ZETA (°K)	281.9	281.9	290.0	290.3	291.1

BETA, GAMMA, ETA, THETA $\equiv$ 0.0

CHEMICAL

	ACT	TOL	IPA
A	-0.284603	-3.08731	-3.05262
B	2.30536×10^{-2}	0.031389	0.038514
C_1	51.875	56.231	50.956
C_2	-0.0375	-0.0308	-0.0289

KINEMATIC VISCOSITY OF AIR

DELTA = 1.16714×10^{-4}

EPSILON = 6.57143×10^{-7}

PHI = 0.0

Test No.	$\dot{m}_T$ (gm/sec)	$\dot{m}_E$ (gm/sec)	U_T (cm/sec)	U_E (cm/sec)
1	0.378	0.255	17.10	7.53
3	0.579	0.435	31.75	27.30
4	0.127	0.160	31.75	33.70
5	0.082	0.0815	17.10	13.70
6	0.125	0.115	31.75	26.70

The model tends to predict a short-term, initial rise in concentration from the starting value following which the concentration decreases to a steady-state value. Conversely, the experimental data do not exhibit this initial rise; concentration decreases monotonically to a constant level. The initial predicted rise in concentration is the result of two modeling assumptions. The first assumption is that dissipation of air jet momentum by the dense, heavier-than-air vapor in the tank can be approximated by the dissipative effects of an air into air jet. A corollary to this assumption is that the radial velocity distribution over the liquid surface in the jet turning and wall jet regions is unaffected by the vapor state in the tank. In the second and companion assumption, all elements of the liquid surface are swept by fresh, uncontaminated air at all times, thus maximizing the evaporative contribution to tank concentration. Based on the level of agreement between theory and experiment, these assumptions appear to be valid during the constant rate period.

However, in the initial period following ventilation startup, the evaporation rate is not likely to be a step function to a constant value as the modeling assumptions dictate. During this period, evaporation rate will increase with time to a constant level as jet momentum dissipation effects become less dominant and the fresh air assumption is approached.

The experimental data for the tank without internal structure suggest that liquid evaporation from other than perfectly smooth surfaces includes the conventional constant rate drying period followed by the addition of a falling rate period. In the falling rate period, wall roughness acts to extend the total time to gas free to a given tank concentration relative to that which would be expected for perfectly smooth walls. As can be seen, the time delay during the falling rate period is significant and can exceed the duration of the constant rate period. The surfaces of full size chemical tanks contain rust and scale; hence, the evaporation process in these tanks should also exhibit the falling rate drying period. These observations indicate that there is a need to include a mathematical description of surface roughness in the evaporation model.

TABLE VIII.   STATISTICAL DESIGN FOR AN EXPANDED (PHASE II)
HAZARD ASSESSMENT PROGRAM

An experimental, full-scale, vapor sampling program of limited
scope was conducted aboard marine chemical carriers. The test data indi-
cate that the vapor concentration environment on a chemical tanker may pose
a hazard to ship's personnel and equipment. This statement is based upon
the experimental results which revealed that

   o   workers entering an empty and presumably safe tank, as
        determined by vapor testing with an explosimeter, were
        exposed to vapor concentrations that exceeded the Short
        Term Exposure Limit (STEL);

   o   tankermen were exposed to vapor concentrations in excess
        of the STEL while continuously gauging liquid ullage
        through an open ullage port during tank top-off;

   o   explosive concentrations of chemical vapor are discharged
        through open ullage ports during the latter stages of
        loading.

The data supporting these statements are valid, but the data base is not
yet broad enough to determine if the results represent isolated cases or
if they are statistically significant for the industry as a whole. The
obvious approach is to conduct an expanded test program that will provide
the data which are needed to resolve the issue. For the results to be sta-
tistically significant, all of the variables that are known to affect vapor
concentrations must be considered in the experimental design. The design
must indicate the number of tests that are to be conducted and the level of
confidence that can be placed on the results at the end of the program.
These ground rules have greater impact on a field test program than on a
series of carefully controlled laboratory experiments because of the plan-
ning, logistics, and timing that are associated with executing a full-scale
tanker test in an uncontrollable environment.

     To this end, statistical methods were utilized to design an ex-
panded test program. The data from that program will be statistically sig-
nificant at the 95% confidence level and 85% probability level. The sta-
tistical techniques and test size estimation are discussed in this section.

VIII.1   Statistical Tools

     There are many factors to consider in designing a full-scale test
program. First, a controlled experiment, where rigid selection criteria
are chosen, is not possible due to the inability to provide adequate con-
trol over such random variables as wind speed and direction, atmosphere
stability, vent height, and mass concentration of discharged vapor (gov-
erned by variable loading rates and chemicals). The only alternative is
to run a non-controlled type of experiment. The objective of a statistical
estimation of sample size is to predict the number of independent realiza-
tions or observations that are needed to ensure that the results are

195

statistically significant at a prescribed confidence level and probability level. Based on this objective, a single tanker loading may yield a variable number of realizations. The minimum number of realizations per tanker loading would be one, and this situation would occur if the combination of variables remained invariant between the loading of individual tanks. On the other hand, multiple observations would occur if the loading, venting, and atmospheric conditions varied from tank to tank. The following discussion describes the statistical technique that has been used to predict the required number of independent observations (independent of the number of tanker/barge dockings).

The statistical approach that has been used is to formulate a prediction equation for vapor concentration using as predictors the measured parameters. Thus, regression techniques, in contrast to analysis of variance methods, are utilized. Each predictor is examined to determine its influence and predictive power on vapor concentration. In this manner, it is possible to predict levels of concentration for ships not included in the study as well as for settings where conditions vary from those measured in the observations. The adequacy of this approach depends on the ability of the chosen parameters to predict concentration. For example, an equation of the form

$$C = b_o + \sum_{i=1}^{N} b_i P_i \qquad\qquad \text{(VIII-1)}$$

may be sought where

$$C \quad = \quad \text{vapor concentration (dependent variable)}$$

$$b_i \quad = \quad \text{correlation coefficients}$$

$$b_o \quad = \quad \text{intercept or background level}$$

$$P_i \quad = \quad \text{measured independent variables.}$$

The coefficients b_i indicate the contribution of each parameter to the prediction of the vapor concentration.

The determination of the appropriate sample size to use in this study is contingent on several factors. These center mainly on what is the chief objective of the experiment. Assuming that one desires to estimate the regression coefficients, b_i, accurately so that one can effectively evaluate the parameters that are most important to the prediction of concentration, then it is necessary to specify or estimate the error in measuring concentration, the error in evaluating b_i, the smallest value of b_i that will be detected as significant at a given probability level, and the number of coefficients of interest.

196

The method that has been used to estimate sample size was developed by Wheeler.[*] To estimate the sample size for each coefficient, b_i, the following equation is applied:

$$n = d^2 \sigma^2 X_{ii}^{-1} (V_1 + 1)/\Delta^2 \qquad \text{(VIII-2)}$$

where

n = sample size for estimating the coefficient of interest;

d = value determined from tables and graphs[†] by specifying the level of confidence, the number of coefficients, the probability of detecting a difference in b_i equal to Δ, and V_2 (degrees of freedom for error = $n - V_1 - 1$). These charts are variously termed Pearson and Hartley charts for the power of the F-Test or Fox Charts;

σ^2 = error variance for concentration;

X_{ii} = sum of squares of the values of the measured parameter. Since the results of the tests are not known a priori, this input can be approximated by the sums of squares of the anticipated maximum and minimum values of the parameter.

V_1 = number of regression coefficients to be estimated (excludes intercept);

Δ = smallest value of b_i that we want to detect as a significant result.

If Δ is difficult to evaluate, let

$$\Delta^2 = \gamma^2/p^2 \qquad \text{(VIII-3)}$$

where

p = range of values of measured parameter (maximum-minimum)

γ = smallest difference of interest in concentration.

The magnitude of n_i is calculated for each regression coefficient, b_i, and the required test sample size is largest value of n in the ensemble of n's.

---

[*] Wheeler, R. E., "Portable Power," _Technometrics_, Vol. 16, No. 2, May 1974.

[†] Scheffe, H., _The Analysis of Variance_, John Wiley and Sons, Inc., New York, 1959.

The number of on-deck and in-tank realizations were calculated using this method. The results are presented in Section VIII.2.

VIII.2   Test Size Estimation

On-Deck Measurement Requirements

The on-deck vapor concentration was assumed to be represented by the following regression equation.

$$C = b_o + b_1 F + b_2 H + b_3 S + b_4 A + b_5 D + b_6 \overline{\theta} + b_7 \overline{X} \qquad (VIII-4)$$

where

C = concentration on-deck

F = vapor mass discharge rate

H = discharge height above deck

S = wind speed

A = atmosphere stability

D = distance from vapor discharge point to measurement point

$\overline{\theta}$ = included angle defined by the wind vector and a line connecting the vapor discharge point to the measurement point

$\overline{X}$ = distance from the vapor discharge point to the location of maximum on-deck concentration.

The approximation for Δ was assumed. Thus,

$$n \doteq \frac{d^2 \sigma^2 (V_1 + 1) p^2}{\gamma^2 X_{ii}} \qquad (VIII-5)$$

The inputs to this equation and their justification are given in Table VIII-1. The error variance on concentration was estimated assuming that measurements are in a steady-state plume and that the variance is due to instrument sensitivity and not plume variability or instability. Thus, σ, the standard deviation was taken to be the organic vapor analyzer sensitivity, i.e., $\pm 2\%$ of full scale. It is anticipated that most downwind plume concentrations will be less than 1000 ppm. Therefore, on a 0.0 to 1000 ppm scale, the standard deviation will be ± 20 ppm, which for an acetone plume converts to ± 47.4 mg/m^3. Thus, σ^2 is equal to 2248 (mg/m^3)^2. The smallest difference of interest in concentration, γ, is difficult to predict precisely. However, from the standpoint of plume tracing or area

198

TABLE VIII-1.

INPUTS TO ON-DECK SAMPLE SIZE CALCULATION

Coefficient	Parameter	Min/Max	p	X_{11}
b_1	F	0 to 102,707 mg/sec	102,707 mg/sec	1.055×10^{10}
b_2	H	1 to 10 m	9	101
b_3	S	0 to 4.47 m/sec	4.47	19.98
b_4	A	-0.6 to +0.6	1.2	1.44
b_5	D	0 to 100 m	100	10^4
b_6	$\overline{\theta}$	0 to π^r	π^r	π^2
b_7	$\overline{X}$	1m to 100m	99	10,001

Notes:

1. $V_1 = 7$

2. Vapor mass discharge is zero at beginning of loading. The maximum rate shown is based upon a saturation concentration of 25% (592,653 mg/m^3) for acetone, which has the highest vapor pressure of any liquid observed to date, plus a discharge flow rate of 0.1733 m^3/sec which corresponds to a loading rate of roughly 3000 bbl/hr (F = CQ).

3. Wind velocity is expected to vary from 0 to 10 mph (4.47 m/sec). Above 10 mph, the plume will dilute to neutral buoyancy and not return to deck.

4. The range for A represents the range of Richardson numbers needed to describe stable to unstable atmospheric stability classes.

5. The distance, D, may vary from 0.0m at the ullage port to 100m, which is approximately one-half of the length of the tankers seen to date.

6. $\overline{\theta}$ varies from 0° for measurements along the downwind axis of the plume to 180° for the case of quartering winds that transport vapor upstream of the discharge port.

7. $\overline{X}$ is expected to vary from 1.0m for discharge points from 1.0 to 2.0 meters above deck to roughly 100m for discharge points 10m above deck. A neutrally-stable atmosphere has been assumed.

toxicity levels, a resolution in concentration of 20 ppm appears to be adequate. For an acetone plume, γ^2 is then equal to 2248 $(mg/m^3)^2$

Based on a confidence level (CL) of 95% and a probability level (PL) of 85%, a value of $d = 1.72$ was obtained from the indicated references. The estimated sample size for each coefficient that is required to achieve the stated CL and PL is

Coefficient	n_1
b_1	23.68
b_2	18.99
b_3	23.68
b_4	23.68
b_5	23.68
b_6	23.68
b_7	23.20

The maximum value of these numbers rounded to the nearest whole number is 24, which is the required sample size or number of realizations for on-deck testing. These same procedures indicated that a probability level of 90% can be achieved by incorporating the data from the first two full-scale tests of this project into the total data base.

In-Tank Measurement Requirements

The following regression equation was postulated for the in-tank vapor concentration.

$$C = a_o + a_1 T_S + a_2 S + a_3 C_o + a_4 Q + a_5 T_p + a_6 P_v + a_7 (Qt/\Psi) \quad \text{(VIII-6)}$$

where

T_S = tank surface temperature

S = effect of internal structure on dilution ventilation

C_o = initial tank concentration

Q = blower flow rate

T_p = thickness of the chemical pool on the tank bottom

P_v = vapor pressure of the chemical

$\dfrac{Qt}{\Psi}$ = tank turnovers (nondimensional ventilation time)

The inputs to this equation and their justification are given in Table VIII-2. The values of γ and σ that were used to estimate the on-deck sample size were applied to the in-tank problem as well. Since the number of coefficients is seven, the magnitude of d remains unchanged, i.e., 1.72. Thus, for a CL and PL of 95% and 85%, respectively, the sample size for each coefficient was calculated as shown below.

Coefficient	n_i
a_1	0.15
a_2	21.31
a_3	23.68
a_4	12.59
a_5	9.47
a_6	23.62
a_7	23.68

The maximum value of the n_i's is 24 (rounded to the nearest whole number). Therefore, 24 in-tank realizations are needed to achieve the required confidence and probability levels.

VIII.3   Hazard Assessment Methodology

The work reported herein represents a major step toward developing a hazard assessment algorithm that can be utilized to assess the vapor hazards during marine terminal and shipboard operations. A hazard algorithm for on-deck vapor dispersion should predict the location and area covered by concentrations of chemical vapors that exceed the LEL and the TLV. The in-tank hazard algorithm should predict the vapor concentration level in either a washed or unwashed tank after ventilation at a given air flow rate for a predetermined time. To assess the toxicity hazards associated with both the on-deck and in-tank problems, a team of toxicologists should provide input to the hazard assessment algorithm. The toxicologists should indicate health hazards as they relate to

o   the additive or synergistic effects of sequential or simultaneous multiple chemical vapor exposure,

o   the role of time-weighted average Threshold Limit Values as applied to abnormal work schedules, and

o   the effect of exposure to nonchemical vapors either sequentially or simultaneously with pure chemical vapors.

A hazardous chemical vapor assessment handbook for marine tank vessels should be generated. The purpose of this handbook would be to provide the U. S. Coast Guard Hazardous Material Specialist with a method of assessing the hazard potential of different preselected operational scenarios for

TABLE VIII-2. INPUTS TO IN-TANK SAMPLE SIZE CALCULATION

Coefficient	Parameter	Min/Max	p	X_{11}
a_1	T_S	278 to 311°K	33	174,005
a_2	S	0.05 to 1.0	0.95	1.0025
a_3	C_O	$\sim$0 to 11,877 ms/m³	11,877	1.41×10^8
a_4	Q	75 to 302 m³/min	227	96,829
a_5	T_P	0.1 to 0.3 m	0.2	0.1
a_6	P_v	0.186 to 191 min Hg	190.8	36,481
a_7	Qt/V	0 to 10	10	100

Notes:

1. $V_1 = 7$

2. Deck and water temperatures may result in tank wall temperatures that vary between 40 and 70°F (Kelvin shown).

3. The range of values of S correspond to tank drainage number for which the presence of internal tank structure is known to retard the ventilation process.

4. C_O is the initial tank concentration following off-loading. Assume off-loading of a 98% full tank that had a saturated vapor in the 2% ullage volume. The resulting well-mixed concentration, C_O, of a low vapor pressure liquid such as 2EH would be essentially zero. However, a saturated acetone vapor in the ullage volume would ideally dilute to 5000 ppm (11,877 ms/m³).

5. The values of T_P are engineering best estimated.

6. Vapor pressures correspond to 2EH and acetone, the most and least difficult liquids to evaporate based on observations to date.

7. Ten tank turnovers is a reasonable upper limit for dilution ventilation. The lower limit, zero, would represent entry into a tank that had not been gas-freed.

both on-deck and in-tank activities. The manual should identify

o   input information that is required for the hazard analysis,

o   input default options that are available if certain data
     are unobtainable,

o   a step-by-step procedure for hazard assessment computation
     and guidance for its interpretation, and

o   an example of a complete hazard assessment computation.

The hazard assessment algorithms can be based upon either the analytical models developed in this project or linear regression models developed through the data obtained in the recommended experimental program. The final choice of models will depend upon their accuracy of prediction compared to actual data and their potential for extrapolation to conditions not encountered.

IX.   SUMMARY AND CONCLUSIONS

IX.1   Summary

This Phase I study has identified several potential hazards that arise from the exposure of shipboard and marine terminal workers to chemical vapors during routine operations on bulk chemical carriers. Two operations with possibly the greatest potential for human exposure to concentration levels that exceed presently defined safe limits are the venting of tank gas atmospheres from low level vents near the deck during cargo loading of chemical tankers and barges and man-entry into empty tanks for inspection or work. Analytical models have been developed to provide the basic tools for estimating the level of chemical vapor concentration in the air downwind of ship tank vents during cargo loading, and in a nearly empty tank as it is ventilated with fresh air. Predictions obtained from the analytical models show good agreement with experimental data taken in both model and full scale.

The objective of both the analytical model development and the experimental model validation activities has been the ultimate development of reliable chemical vapor hazard predictive techniques. These methods will predict vapor concentrations as a function of actual operating conditions for various marine terminal and shipboard scenarios. These concentration predictions, when compared with existing toxicity and flammability limits, can subsequently be used to assess hazards. A comprehensive full scale, Phase II, measurement activity has been defined that will permit the validation of the analytical models for a wide range of operating conditions and assure the accuracy and reliability of the hazard predictive techniques.

IX.2   Conclusions

There are many important observations and conclusions that may be drawn from the background study, the analytical modeling effort, and the model and full scale vapor concentration measurement activities. The most significant items are listed below.

IX.2.1   Marine Terminal Observation

o   Worker activities in marine terminals during cargo transfer are rather unstructured due to the work task flexibility required by the loading operation.

o   Typically, from three to seven terminal workers and two to five ship crew members are involved in dockside and shipboard activities during tankership loading. Barge loading typically requires fewer terminal workers and one independent tankerman.

o   A qualitative assessment of work exposure and potential health hazards has been made. Sources of cargo liquid and vapor exposure (and the anticipated health hazard to workers) include the following:

(1) visual and manual gauging of cargo ullage through open hatches and ullage ports during loading of barges and tankers (acute respiratory exposure),

(2) visual observation of product level through open hatches during the lattermost stages of cargo discharge on barges (acute respiratory exposure),

(3) swabbing of tank bottoms on barges using long-handled mops with eventual manual wringing of product into buckets (skin contact and acute respiratory exposure),

(4) exposure to the general background concentration of vapors on the deck of barges and tankers (chronic respiratory exposure),

(5) exposure to multiple chemical cargo vapors (unknown additive, synergistic, etc. effects of multiple respiratory insult),

(6) presence of undiluted, raw product in drip pans on the dock and on the decks of barges and tankers (chronic respiratory exposure). A low flow rate water flush would promote dilution and transport of product to slop tanks or a water treatment plant,

(7) product leaks at the valves on the dock manifold (chronic respiratory exposure),

(8) discharge of large volumes of raw product into the dock drip pans when the flange blind is removed from a valve that does not have a positive seal against product bypass (acute respiratory and skin contact exposure), and

(9) descent into an empty but not completely gas-freed tank (acute respiratory exposure).

These observations are made under the assumption that respiratory equipment and protective clothing are not worn. Also, it is re-emphasized that the above conditions may or may not present a health hazard, depending on the degree of exposure (concentration level and time of exposure) which must be quantified.

IX.2.2   Review of Regulations and Technical Literature

o   Current and proposed federal regulations relating to the transfer of hazardous chemical cargos are given by the Coast Guard, and OSHA. In addition, state and international agencies and groups are formulating regulations dealing with chemical cargo handling. The U. S. Coast Guard regulations are more specific on the chemical cargo transfer activities as related to this project than are those of other agencies. Coast Guard regulations set many operational and equipment requirements which are related to the hazard studies herein.

206

o   OSHA is contemplating an expansion of regulations into the areas
    of interest to the project. There does not appear to be a con-
    flict of regulations, although jurisdictional conflicts between
    regulatory agencies may occur. Also, there is significant activity
    by most of the major oil and chemical companies as coordinated by
    the American Petroleum Institute to generate full scale vapor
    emissions data to allow an assessment of both environmental pollu-
    tion and health-related problems.

o   A review of the literature reveals that previous work on in-tank
    vapor hazards has been experimental in nature with emphasis
    placed on design and operational procedures to eliminate flammable
    atmospheres. Experimental studies to determine vapor concentra-
    tion data for the purpose of evaluating potential toxicity hazards
    in a shiptank appear nonexistent. Also, no comprehensive analyt-
    ical efforts on in-tank hazardous vapor removal have been under-
    taken.

o   Problems associated with hazardous vapors exterior to the ship-
    tank have received little analytical or experimental attention.
    Experimental wind tunnel studies have been conducted with the
    primary objective of studying the flammability hazards associated
    with open venting during loading.   No experimental studies asso-
    ciated with evaluating toxicity hazards were uncovered. A few
    analytical methods have been developed for predicting vapor plume
    trajectory and dispersion as applied to ambient air pollution
    problems. No analytical work specific to vapor hazards associated
    with negatively buoyant chemical vapor plumes on a ship deck
    (either near or far field) has been performed.

IX.2.3   Analytical Model Development

o   An analytical model based on the work of Ooms for forced plume
    dispersion, and the work of teRiele for gaseous dispersion from
    ground level sources, provides the capability for predicting the
    spatially dependent concentration field downwind of vents on ships
    and barges during cargo loading.

o   Based upon an evaluation of parameters used in this model, the
    vapor concentration level at man-height downwind of a vent depends
    primarily on

    -    the vapor concentration at the vent,

    -    the vent height, diameter and geometry,

    -    the cargo loading rate,

    -    the wind velocity, direction and turbulence intensity,

    -    turbulence produced by on-deck structure, and

    -    atmospheric stability conditions.

207

o Based on analytical model predictions, the conditions that cause high levels of vapor concentration at man-height downwind of a vent are

- low vent height, typical of a vent on an expansion trunk,

- low wind speed and low turbulence intensity as could occur with stable atmospheric stability, and

- high vapor concentration at the vent and low vent velocity.

o An analytical in-tank model allows the prediction of vapor concentration levels during cargo tank ventilation in the presence of vapor regeneration from pure chemical cargo residue.

o Based on analytical model predictions, significant periods of time are required to ventilate a tank to safe levels of vapor concentration. Parameters shown to be important for the in-tank ventilation problem include:

- blower capacity,

- residual cargo thickness,

- tank wall temperature, and

- tank volume.

o When even small amounts of pure product remain in a shiptank, large ventilation times are required to evaporate the residual liquid and remove the hazardous vapors. The total ventilation time is governed by the time required to evaporate the liquid residue and discharge the resultant vapor. This time may be much larger than the time to ventilate the tank based upon ideal dilution without evaporation.

o A localized model was developed to predict vapor concentrations in shielded areas of a cargo tank during manual activities such as the mucking of residual cargo. Liquid surface agitation may increase the evaporation rate and produce vapor concentrations that exceed safe levels because convection and diffusion are relatively ineffective in removing vapors from the shielded work area.

IX.2.4   Model and Full Scale Experimental Studies

o Scale model wind tunnel tests showed that stable thermal stratification (atmospheric stability) of the wind reduced the dispersion of vapor plumes emitted from shiptank vents. On the other hand, the interference of on-deck structure increased the turbulence of the air stream and increased vapor plume dispersion.

o   A comparison of vapor concentration data, both in full scale and
    model scale, to values predicted from the analytical plume model
    shows reasonably good agreement between analytical model and
    experiment.

    -    These comparisons confirmed the need for careful selection
         of vapor sampling locations, sampling methods, and meteoro-
         logical data gathering methods so that variations in wind
         speed and direction may be accounted for in the analysis
         of experimental data.

    -    The best procedure for vapor sampling appears to be simul-
         taneous sampling at a matrix of locations, closely spaced
         in the crosswind direction and logarithmically spaced in the
         downwind direction.

o   Continuous cargo loading appears to reduce the vapor concentration
    at the vent, and it is advantageous to load without interruption
    from pump startup to tank top-off. The interruption of loading
    allows diffusion to increase the concentration in the ullage space,
    giving higher vent concentrations when loading is resumed.

o   Full scale tests confirmed several of the hazards that were postu-
    lated in the background study.

    -    A previously ventilated tank that was considered to be safe
         for man-entry, based on explosimeter readings, had vapor
         concentration levels that exceeded the STEL.

    -    For some tank loading conditions, respirable vapor concentra-
         tions (i.e., personal exposures) exceeded the STEL during
         tank top-off.

    -    Vapor concentrations at the vent and in the neighborhood of
         the vent were within the explosive range during some load-
         ing conditions.

o   Laboratory scale in-tank ventilation tests with vapor regeneration
    confirm that small amounts of cargo residue and tank internal
    structure significantly increase the length of time needed to gas
    free a tank to low concentration levels.

o   A broad experimental plan has been developed to acquire the data
    needed to validate the current analytical models. The experi-
    mental program has been designed on a statistical basis. The
    successful completion of the proposed experiments and subsequent
    validation and revision of the analytical models will provide the
    necessary tools to form accurate hazard predictive techniques.

APPENDIX A

CATEGORIZED BIBLIOGRAPHY

"INVESTIGATION OF THE HAZARDS POSED BY
CHEMICAL VAPORS RELEASED IN MARINE OPERATIONS"

A - TOXICITY
B - PLUME AND PLUME MODELS
C - REGULATIONS
D - SAMPLING PROCEDURES
E - MARINE TERMINAL EMISSIONS STUDY
F - BUILDING MATERIALS AND SHIP
    CONSTRUCTION
G - EXPLOSION MODELS
H - CONTROL OF HYDROCARBON
    EMISSIONS
I - HAZARD ASSESSMENT MODELS
    AND CLASSIFICATION
J - SHIPTANK GAS ATMOSPHERE CONTROL
K - REACTIVITY OF HAZARDOUS CARGOS
L - SAFETY ASPECTS OF TRANSPORTING
    HAZARDOUS CARGOS
M - DISCHARGING OF HAZARDOUS
    WASTES FROM SHIPS
N - TANKER CLEANING OPERATIONS
O - ANALYSIS OF MAJOR HAZARDOUS
    ACCIDENTS
P - DISPOSAL OF TOXIC CHEMICALS

A. TOXICITY

1. "Acrylonitrile and Human Cancer...", _American Industrial Hygiene Association Journal_, Vol. 38, August 1977.

2. Adams, W. G. F., "Long-Term Effects on the Health of Men Engaged in the Manufacture of Tolylene Di-Isocyanate," _British Journal of Industrial Medicine_, Vol. 32, p. 72-78, 1975.

3. Bustueva, K. A. and Roscin, A. V. "Safe Levels of Biological Exposure to Chemicals in the Air of Industrial Premises and in the Atmosphere," World Health Organization, 1975.

4. Carpenter, C. P., Kinkead, E. R., Geary, D. L., Sullivan, L. J. and King, J. M., "Petroleum Hydrocarbon Toxicity Studies, V. Animal and Human Responses to Vapors of Mixed Xylenes," _Toxicology Applied Pharmacology_, Ser. 33, Issue 3, 1975.

5. Carpenter, C. P., et. al., "Petroleum Hydrocarbon Toxicity Studies, VI. Animal and Human Responses to Vapors of 60 Solvent," _Toxicology Applied Pharmacology_, Ser. 34, Issue 3, 1975.

6. Carpenter, C. P., et. al., "Petroleum Hydrocarbon Toxicity Studies, VII. Animal and Human Response to Vapors of 70 Solvent," _Toxicology Applied Pharmacology_, Ser. 34, Issue 3, 1975.

7. Carpenter, C. P., et. al., "Petroleum Hydrocarbon Toxicity Studies, VIII. Animal and Human Response to Vapors of 140 Deg. Flash Aliphatic Solvent," _Toxicology Applied Pharmacology_, Ser. 34, Issue 3, 1975.

8. Carpenter, C. P. et. al., "Petroleum Hydrocarbon Toxicity Studies, IX. Animal and Human Response to Vapors of 80 Thinner," _Toxicology Applied Pharmacology_, Series 36, Issue 3, 1976.

9. Carpenter, C. P., et. al., "Petroleum Hydrocarbon Toxicity Studies, X. Animal and Human Response to Vapors of 50 Thinner," _Toxicology Applied Pharmacology_, Series 36, Issue 3, 1976.

10. Carpenter, C. P., et. al., "Petroleum Hydrocarbon Toxicity Studies, XIII. Animal and Human Response to Vapors of Toluene Concentrate," _Toxicology Applied Pharmacology_, Series 36, Issue 3, 1976.

11. Clark, L. H., Noble, M., Oloffs, P. C. and Szeto, S. Y., "Inhalation Chamber for Administering Volatile Compounds to Animals Performance Using Carbon Tetrachloride," _Canadian Journal of Zoology_, Vol. 51, Issue 3, 1973.

12. Cohen, Steven R., and Maier, Albert A., "Occupational Health Case Report No. 2 Toluene Diisocyanate," _Journal of Occupational Medicine_, Vol. 16, No. 2, February 1974.

13. Davis, Richard A., Terpolilli, Ralph N., and Back, Kenneth C., "Toxic Point Determination of Selected Hazardous Materials," Final Report Medical Research Laboratory, Wright-Patterson A.F.B., for Department of Transportation.

14. Degesero, R. A., "The Evaluation and Control of Chemicals in Polystyrene Manufacturing," Annals of Occupational Hygiene, Vol. 17, 1974.

15. DiVincenzo, G. D., Yanno, F. F., Astill, B. D., "Exposure of Man and Dog to Low Concentrations of Acetone Vapor," American Industrial Hygiene Association Journal, Series 34, Issue 8, August 1973.

16. Foder, G., Noxious Vapors, Verein Deut. Ing., Duesseldorf, Germany.

17. Gerarde, Horace W., "Noxious Gases and Vapors, II. Hydrocarbons and Hydrocarbon Mixtures," Pharmacology in Medicine, 4th Edition, McGraw-Hill Book Co., N. Y., N. Y.

18. Gerarde, Horace W., "Noxious Gases and Vapors. III. Carbon Tetrachloride," Pharmacology in Medicine, 4th Edition, McGraw-Hill Book Co., N. Y., N.Y.

19. Holland, Dewey and Rooney, Terrance, "TDI Vapor Concentrations," Letter to the Editor, Journal of Occupational Medicine, Vol. 19, No. 4, April 1977.

20. Hunter, C. G. and Blair, D., "Benzene: Pharmacokinetic Studies in Man," Annals of Occupational Hygiene, Series 15, Issue 2-4, 1972.

21. Jones, Allan R. and Brief, Richard S., "Evaluating Benzene Exposures," American Industrial Hygiene Association Journal, Vol. 32 No. 9, 1971.

22. Matsushita, Arimatsu, Y., and Veda, A., "Hematological and Neuro-Muscular Response of Workers Exposed to Low Concentration of Toluene Vapor," Industrial Health, Series 13, Issue 4, Mar. 1975.

23. Mikulski, P., Wiglusz, R., Bublewska, A. and Uselis, J., "Investigations on Exposure of Ship Painters to Organic Solvents," Bulletin of the Institute of Marine Medicine in Gdansk, Vol. 23, 1-2, 1975.

24. National Research Council, Medical and Biological Effects of Environmental Pollutants – Vapor Phase Organic Pollutants, National Academy of Sciences, Washington, D. C., 1976.

25. Posner, H. S., "Biohazards of Methanol in Proposed New Uses," Journal of Toxicology and Environmental Health, Vol. 1, No. 1, Sept. 1975.

26. Ross, David S., "Acute Acetone Intoxication Involving Eight Male Workers," Annals of Occupational Hygiene, Vol. 16, 1973.

27. Runion, Howard E., "Benzene in Gasoline II," Journal of the American Industrial Hygiene Association, No. 38, August 1977.

28. Schwardzmann, Kutscha, "Accidental Styrene Poisoning," Research in the Life Sciences, Vol. 19 No. 3, 1971.

29. "Scientific and Technical Data Base for Criteria and Hazardous Pollutants," Yearly Review, Health Effects Research Laboratory, Research Triangle Park, N. C., May 1976.

30. Sherwood, R. J., "Evaluation of Exposure to Benzene Vapor During the Loading of Petrol," British Journal of Industrial Medicine, Series 29, Issue 1, 1972.

31. Sherwood, R. J. and Carter, F. W. G., "Measurement of Occupational Exposure to Benzene Vapor," Annals of Occupational Hygiene, Ser. 13,I. 2, 1970.

32. Silverstein, L. G., "Validation of Abcor Gasbadge^{TM} for Acrylonitrile and Improved Desorption Efficiency," Journal of the American Industrial Hygiene Association, Vol. 38, August 1977.

33. Smith, Darrell B. and Henderson, Richard, "TDI Vapor Concentrations," Letter to the Editor, Journal of Occupational Medicine, Vol. 17, No. 7, July 1975.

34. Steinman, George C., "Maritime Administration Bulk Chemical Carrier Construction Program," Environmental Activities Group, Maritime Administration, Final Report, 1974.

35. Swinyard, Ewart A., "Noxious Gases and Vapors," The Pharmacological Basis of Therapeutics, 5th Edition, MacMillan Co., New York, N. Y., 1975.

36. Thomas, Vera, "Biological-Mathematical Modeling of Chronic Toxicity," Final Report, University of Miami School of Medicine for Air Force Systems Command, Wright-Patterson Air Force Base, January 1975.

37. Wegman, D. H. and Peters, J. M., "Epidemiology of Toluene Diisocyanate - Induced Respiratory Disease," Environmental Health Perspectives, Vol. 11, June 1975.

38. Winek, C. L., Collom, W. D., and Davis, E. R., "Accidental Solvent Fatality," Clinical Toxicology, Vol. 6, Issue 1, 1973.

39. Zedda, S., Cirla, A., Aresini, G. and Sala C., "Occupational Type Test for the Etiological Diagnosis of Asthma Due to Toluene Diisocyanate," Respiration, Vol. 33, 1976.

B. PLUME AND PLUME MODELS

1. American Gas Association, "Evaluation of Models for Predicting Atmospheric Dispersion from Gas Compression Models."

2. American Society of Mechanical Engineers, "Cooling Tower Plume Modeling and Drift Measurement" ASME Review.

3. Augustine, Frank E., and Boubel, Richard W., "Particle Size Distributions of Kraft Paper Mill Aerosols Obtained by Airborne Sampling," Journal of the Air Pollution Control Association, Vol. 25, No. 6, June 1975.

4. Barad, Morton L., and Haugen, Duane A., "A Preliminary Evaluation of Sutton's Hypothesis For Diffusion from a Continuous Point Source," Journal of Meteorology, Vol. 16, February 1959.

5. Berlyand, M. E., Editor, Air Polution and Atmospheric Diffusion, John Wiley and Sons, Pub., Israel Program for Scientific Translation.

6. Bjorklund, J. R. and Dumbauld, K., "User's Instructions for the Volume Source Diffusion Models Computer Program," H. E. Cramer Co., November 1975.

7. Bosanquet, C. H., "The Rise of a Hot Waste Gas Plume" Journal of the Institute of Fuel, June 1957.

8. Bowne, N. E., "Diffusion Rates," Journal of the Air Pollution Control Association, Vol. 24, No. 9, Sept. 1974.

9. Briggs, Gary A., "A Plume Rise Model Compared with Observations," Journal of the Air Pollution Control Association, Vol. 15, No. 9, September 1965.

10. Briggs, Gary A., "Some Recent Analyses of Plume Rise Observation," Second International Clean Air Congress.

11. Briggs, Gary, "Chimney Plumes in Neutral and Stable Surroundings," Atmospheric Environment Vol. 6, pp. 507-510.

12. Brummage, K. G., "The Dispersion of Hydrocarbon Gas During the Loading of Tankers," Gas Evolution: Tanker and Terminal Safety, Institute of Petroleum Special Publication Series No. 1, 1971.

13. Carpenter, S. B., et al., "Full-Scale Study of Plume Rise at Large Coal-Fired Electric Generating Stations," Journal of the Air Pollution Control Association, Vol. 18, No. 7, July 1968.

14. Carpenter, S. B., et al., "Principal Plume Dispersion Models: TVA Power Plants," Journal of the Air Pollution Control Association, Vol. 21, No. 8, August 1971.

15. Carson, James E., and Moses, Harry, "The Validity of Several Plume Rise Formulas," Journal of the Air Pollution Control Association, Vol. 19, No. 11, Nov. 1969.

16. Chou, J. H.,et. al., "An Analytical Investigation of Fluid Cargo Vapor Dispersion," University of Washington, August 1974.

17. Colbaugh, Wm. C., et. al., "Investigation of Cooling Tower Plume Behavior."

18. Cramer, Harrison E., "Engineering Estimates of Atmospheric Dispersal Capacity" Industrial Hygiene Journal, June 1959.

19. Cramer, H. E., "A Practical Method for Estimating the Dispersion of Atmospheric Contaminants," National Conference on Applied Meteorology, American Meteorology Society, 1957.

20. Cramer, H. E., "A Brief Survey of the Meteorological Aspects of Atmospheric Pollution," Bulletin of the American Meteorology Society, Vol. 40, No. 4, April 1959.

21. Csanady, G. T., "Bent-Over Vapor Plumes," Journal of Applied Meteorology, Vol. 10, Feb. 1971.

22. Csanady, G. T., "Some Observations on Smoke Plumes," International Journal of Air and Water Pollution, Vol. 4 No. 1 and 2, pp. 47-51.

23. Csanady, G. T., "Turbulent Diffusion of Heavy Particles in the Atmosphere," Journal of the Atmospheric Sciences, Vol. 20, May 1963.

24. Davies, D. R., "On Diffusion from a Continuous Point Source at Ground Level into a Turbulent Atmosphere," Quarterly Journal Mechanical and Applied Mathematics, Vol. VII, Part 2, 1954.

25. Deland, Raymond J., "Notes on Estimation of Plume Rise for Large Thermal Sources," Journal of the Air Pollution Control Association, Vol. 23, No. 4, April 1973.

26. E G and G. Inc., "Potential Environmental Modifications Produced by Large Evaporative Cooling Towers," Final Report for the Environmental Protection Agency Water Quality Office.

27. England, Walter G., et.al., "A Measurement Program to Determine Plume Configurations at the Beaver Gas Turbine Facility, Port Westward, Oregon," Journal of the Air Pollution Control Association, Vol. 26, No. 10, October 1976.

28. Ensor, D. S., et. al., "Calculation of Smoke Plume Opacity from Particulate Air Pollution Properties," Journal of the Air Pollution Control Association, Vol. 21, No. 8, August 1971.

29. Environmental Protection Agency, Workbook of Atmospheric Dispersion Estimates.

30. Fay, James A., et.al., "A Correlation of Field Observations of Plume Rise," _Journal of the Air Pollution Control Association_, Vol. 20, No. 6, June 1970.

31. Fox, Douglas G., "Forced Plume in a Stratified Fluid," _Journal of Geophysical Research_, Vol. 75, No. 33, Nov. 20, 1970.

32. Franconer, Peter and Kaplan, Lawrence, "Determination and Evaluation of Stack Emissions from Municipal Incinerators," _Journal of the Air Pollution Control Association_, Vol. 26, No. 9, September 1976.

33. Gifford, F. A., Jr., "Atmospheric Dispersion Calculations Using the Generalized Gaussian Plume Model. _Nuclear Safety_.

34. Gifford, F. A., Jr., "Use of Routine Meteorological Observations for Estimating Atmospheric Dispersion" _Nuclear Safety_.

35. Gifford, F. A., Jr., "Peak to Average Concentration Ratios According to a Fluctuating Plume Dispersion Model," _International Journal of Air Pollution_, Vol. 3, No. 4, pp. 253-260.

36. Gifford, F. A., Jr., "Statistical Properties of a Fluctuating Plume Dispersion Model," Final Report, U. S. Weather Bureau Office, Oak Ridge, Tennessee.

37. Guzewich, David C. and Pringle, Wm. J. B., "Validation of the EPA-PTMTP Short Term Gaussian Dispersion Model," _Journal of the Air Pollution Control Association_.

38. Hall, W. A., "Cooling Tower Plume Abatement," Final Report, Atlantic Richfield Company.

39. Halow, John S. and Zeek, Susan J., "Predicting Ringlemann Number and Optical Characteristics of Plumes," _Journal of the Air Pollution Control Association_, Vol. 23, No. 8, August 1973.

40. Hanna, Steven R., "A Simple Method of Calculating Dispersion from Urban Area Sources," _Journal of the Air Pollution Control Association_, Vol. 21, No. 12, December 1971.

41. Hanna, Steven R., "Meteorological Effects of the Mechanical-Draft Cooling Towers of the Oak Ridge Gaseous Diffusion Plant," Final Report, Air Resources Atmospheric Turbulence and Diffusion Laboratory, Oak Ridge, Tennessee.

42. Hanna, Steven R., "Rise and Condensation of Large Cooling Tower Plumes," _Journal of Applied Meteorology_, Vol. 11, August 1972.

43. Hay, J. S., and Pasquill, F., "Diffusion from a Continuous Source in Relation to the Spectrum and Scale of Turbulence," Final Report, Meteorological Office and Chemical Defense Experimental Establishment, Porton, England.

44. Hay, J. S. and Pasquill, F., "Diffusion From a Fixed Source at a Height of a few Hundred Feet in the Atmosphere," Final Report, Meteorological Office and Chemical Defense Experimental Establishment, Porton, England.

45. Hewson, E. W., "Stack Heights Required to Minimize Ground Concentrations," Transactions of the ASME, October 1955.

46. Hindman, Edward E., II, Hobbs, Peter V. and Radke, Lawrence F., "Airborne Investigations of Aerosol Particles from a Paper," Journal of the Air Pollution Control Association, Vol. 27, No. 3, March 1977.

47. Homolya, James B., "Current Technology for Continuous Monitoring of Gaseous Emissions," Journal of the Air Pollution Control Association, Vol. 25, No. 8, August 1975.

48. Hoult, David P., Fay, James A. and Forney, Larry J., "A Theory of Plume Rise Compared with Field Observations," Journal of the Air Pollution Control Association, Vol. 19, No. 8, August 1969.

49. Hoult, D. P., et.al., "Turbulent Plume in a Turbulent Cross Flow: Comparison of Wind Tunnel Tests with Field Observations," Journal of the Air Pollution Control Association, Vol. 27, No. 1, January 1977.

50. Hosler, C. L., "Wet Cooling Tower Plume Behavior."

51. Isyumov, N., Jandali, T. and Davenport, A. G., "Model Studies and the Prediction of Full Scale Levels of Stack Gas Concentration," Journal of the Air Pollution Control Association, Vol. 26, No. 10, October 1976.

52. Jacko, Robert B., Nevendorf, David W. and Yost, Kenneth J., "Trace Metal Samples Collected in the Front and Back Halves of the EPA Stack Sampling Train," Journal of the Air Pollution Control Association, Vol. 25, No. 10, October 1975.

53. Johnson, Morris C., "Methodology for Chemical Hazard Prediction."

54. Kaylor, F. B., Petrillo, J. L. and Tsai, Y. J., "Prediction and Verification of Visible Plume Behavior."

55. Knettig, P. and Meisen, A., "A New Method for Determining the Contribution of a Refinery to Local SO_2 Levels in an Industrial Region," Journal of the Air Pollution Control Association," Vol. 27, No. 7, July 1977.

56. Knox, Joseph P., "Numerical Modeling of the Transport Diffusion and Deposition of Pollutants for Regions and Extended Scales," Journal of the Air Pollution Control Association, Vol. 24, No. 7, July 1974.

57. Leavitt, Jack M., George, Lawrence A., and Clark, Robert E., "Sulfur Dioxide Emission Limitation (SDEL) Program at TVA Power Plants," Journal of the Air Pollution Control Association, Vol. 26, No. 12, December 1976.

58. Lucas, D. H., Moore, D. J. and Spurr, G., "The Rise of Hot Plumes from Chimneys," International Journal of Air and Water Pollution, Vol. 7, 1963.

59. Lyons, Walter A. and Olsson, Lar E., "Mesoscale Air Pollution Transport in the Chicago Lake Breeze," Journal of the Air Pollution Control Association, Vol. 22, No. 11, November 1972.

60. McKee, Herbert C., and Childers, Ralph E., "Estimation of Additive Effects from Multiple Sources," Journal of the Air Pollution Control Association, Vol. 22, No. 10, October 1972.

61. Milford, S. N., McCoyd, G. C., Aronowitz, L., Scanlon, J. H., and Simon, C., "Developing A Practical Dispersion Model for an Air Quality Region," Journal of the Air Pollution Control Association, Vol. 21, No. 9, September 1971.

62. Montgomery, Thomas L., et.al., "Results of Recent TVA Investigations of Plume Rise," Journal of the Air Pollution Control Association, Vol. 22, No. 10, October 1972.

63. Montgomery, Thomas L., et.al., "A Simplified Technique Used to Evaluate Atmospheric Dispersion of Emissions from Large Power Plants," Journal of the Air Pollution Control Association, Vol. 23, No. 5, May 1973.

64. Moore, D. J., "Physical Aspects of Plume Models," Air and Water Pollution, Vol. 10, 1966.

65. Moore, D. J., "The Prediction of the Rise of Cooling Tower Plumes," Atmospheric Environment, Vol. 8, 1974.

66. Morton, B. R., "Buoyant Plumes in a Moist Atmosphere," Department of Mathematics, University College, London, September 1956.

67. Morton, B. R., "The Choice of Conservation Equations for Plume Models," Journal of Geophysical Research, October 1971, Vol. 76, No. 3.

68. Moses, Hardy and Carson, James E., "Stack Design Parameters Influence Plume Rise," Journal of the Air Pollution Control Association, Vol. 18, No. 7, July 1968.

69. Moses, Harry and Kraimer, Martin, "Plume Rise Determination--A New Technique Without Equations," Journal of the Air Pollution Control Association, Vol. 22, No. 8, August 1972.

70. Moses, Harry and Strom, Gordon, "A Comparison of Observed Plume Rises with Values Obtained from Well-Known Formulas," Journal of the Air Pollution Control Association, Vol. 11, No. 10, October 1961.

71. Moses, Harry, Strom, Gordon and Carson, James E., "Effects of Meteorological and Engineering Factors on Stack Plume Rise," Nuclear Safety, Vol. 6, No. 1.

72. Moyer, William W. and Osman, Fred P., "A Microprocessor-Based Air Quality Monitoring System," _Journal of the Air Pollution Control Association,_ Vol. 25, No. 11, Nov. 1975.

73. Nagy, G., "A Mathematical Model for Building Height Limitations Imposed by Multiple Plume Effects," _Journal of the Air Pollution Control Association_, Vol. 27, No. 4, April 1977.

74. Nagy, G., "A Plume Management Model," _Journal of the Air Pollution Control Association_, Vol. 26, No. 7, July 1976.

75. Novak, J. H. and Turner, D. B., "An Efficient Gaussian-Plume Multiple-Source Air-Quality Algorithm," _Journal of the Air Pollution Control Association_, Vol. 26, No. 6, June 1976.

76. Ooms, G., "A New Method for the Calculation of the Plume Path of Gases Emitted by a Stack," _Atmospheric Environment_ Vol. 6, 1972.

77. Overcamp, Thomas, and Hoult, David, "Precipitation in the Wake of Cooling Towers," _Atmospheric Environment_, Vol. 5, 1971.

78. Padmanabhamurty, B., "The Role of Wind in Pollution Dispersion," _Journal of the Air Pollution Control Association_, Vol. 25, No. 9, September 1975.

79. Pasquill, F., _Atmospheric Diffusion_, Ellis Horwood Ltd, 1974.

80. Pasquill, F., "Atmospheric Dispersion of Pollution," _Quarterly Journal of the Royal Meteorological Society_, Vol. 97, No. 414, October 1971.

81. Pasquill, F., "Lagrangian Similarity and Vertical Diffusion from a Source at Ground Level," _Quarterly Journal of the Royal Meteorological Society_, Vol. 92, No. 392, April 1966.

82. Pasquill, F., "The Estimation of the Dispersion of Windborne Material," _The Meteorological Magazine_, Vol. 90, No. 1063, February 1961.

83. Pennsyle, Ronald O., "A Mathematical Model for the Atmospheric Dissemination of Evaporating Aerosol Clouds."

84. Priestley, C. H. B., "A Working Theory of the Bent-Over Plume of Hot Gas," Division of Meteorological Physics, Commonwealth Scientific and Industrial Research Organization, Victoria, Australia.

85. Rao, K. S., Nee, V. W. and Vang, K. T., "Mass Diffusion from a Point Source in a Neutral Turbulent Shear Layer," AIAA/ASME Thermophysics and Heat Transfer Conference, July 19-17, 1974 Boston, Mass.

86. Richards, J. M., "The Stability of Wet and Dry Bent-Over Plumes," _Journal of Applied Meteorology_, Vol. 12, Feb. 1973.

87. Roffman, Amiram and Van Vleck, Lowell D., "The State-of-the-Art of Measuring and Predicting Cooling Tower Drift and Its Deposition," _Journal of the Air Pollution Control Association,_ Vol. 24, No. 9, September 1974.

88. Root, Barry D., Bach, Willfrid and Daniels, Anders, "Spatial Distribution of Particulates from Sugar-Cane Fires in Hawaii: Measurements and Calculations," _Journal of the Air Pollution Control Association_, Vol. 25, No. 6, June 1975.

89. Samson, Perry J., Neighmond, Garry, and Yencha, Andrew J., "The Transport of Suspended Particulates as a Function of Wind Direction and Atmospheric Conditions," _Journal of the Air Pollution Control Association_, Vol. 25, No. 12, December 1975.

90. Scorer, R. S., "The Rise of Bent-Over Hot Plumes," Department of Mathematics, London, England.

91. Sheih, C. M., "A Puff-Grid Model for Predicting Pollution Transport Over an Urban Area," _Journal of the Air Pollution Control Association_, Vol. 27, No. 8, August 1977.

92. Shum, Y. S., Loveland, W. D. and Hewson, E. W., "The Use of Artificial Activable Trace Elements to Monitor Pollutant Source Strengths and Dispersal Patterns," _Journal of the Air Pollution Control Association_, Vol. 25, No. 11, November 1975.

93. Siewart, R. D., "A Method for Defining Down-wind Evacuation Areas for Transportation Accidents Involving Toxic Propellant Spills," NASA Report, 1972.

94. Sklarew, R. C., Fabrick, A. J. and Wilson, J. C., "GEM/GEMGAR: Gaussian Evaluation Models," Ralch C. Sklarew, Consultant.

95. Slawson, P. R., "Buoyant Moist Bent-Over Plumes," University of Waterloo.

96. Slawson, P. R. and Csanady, G. T., "On the Mean Path of Buoyant, Bent-Over Chimney Plumes," _Journal of Fluid Mechanics_, Vol. 28 Part 2.

97. Slawson, P. R., and Csanady, G. T., "The Effect of Atmospheric Conditions on Plume Rise," _Journal of Fluid Mechanics_, Vol. 47, Part 1, 1971.

98. "Stack Design and Air Pollution Disperson," Chapter 10, _Pollution Engineering Practice Handbook_.

99. Stephen, D. W., and Moroz, W., "Plume Rise from Wet Cooling Towers in Strong Winds," Engineering Research Bulletin, B-107, 1972, College of Engineering, Pennslyvania State University.

100. Strom, G. H., Hackman, M., and Kaplin, E. J., "Atmospheric Dispersal of Industrial Stack Gases Determined by Concentration Measurements in Scale Model Wind Tunnel Experiments," _Journal of the Air Pollution Control Association_, Vol. 7, No. 3, 1957.

101. Sutton, O. G., "A Theory of Eddy Diffusion in the Atmosphere."

102. Sutton, O. G., _Micrometeorology_, McGraw-Hill Book Co. Inc. 1953.

103. Sutton, O. G., "The Problem of Diffusion in the Lower Atmosphere."

104. Thomas, F. W., Carpenter, S. B. and Colbaugh, W. C., "Plume Rise Estimates for Electric Generating Stations," _Journal of the Air Pollution Control Association_, Vol. 20, No. 3, March 1970.

105. Ti-3 Petroleum Committee, "Control of Atmospheric Emissions from Petroleum Storage Tanks," _Journal of the Air Pollution Control Association_, Vol. 21, No. 5, May 1971.

106. Turner, J. S., "Buoyant Plumes and Thermals," University of Cambridge.

107. Wang, I. T. and Rote, D. M., "A Finite Line Source Dispersion Model for Mobile Source Air Pollution," _Journal of the Air Pollution Control Association_, Vol. 25 No. 7, July 1975.

108. Weddendorf, William K., "A Computer Program for Processing Stack Sampling Data," _Journal of the Air Pollution Control Association_, Vol. 25, No. 9, September 1975.

109. Weil, Jeffrey C., "The Rise of Moist, Buoyant Plumes," _Journal of Applied Meteorology_, Vol. 13, June 1974.

110. Wessels, H. R. A. and Wisse, J. A., "A Method for Calculating the Size of Cooling Tower Plumes," _Atmospheric Environment_ Vol. 5, 1971.

111. Wigley, T. M. L., "Condensation in Jets, Industrial Plumes and Cooling Tower Plumes," _Journal of Applied Meteorology_, Vol. 14, Feb. 1975.

112. Wigley, T. M. L. and Slawson, P. R., "A Comparison of Wet and Dry Bent-Over Plumes," _Journal of Applied Meteorology_, Vol. 11, March 1972.

113. Wigley, T. M. L. and Slawson, P. R., "On the Condensation of Buoyant, Moist Bent-Over Plumes," _Journal of Applied Meteorology_, Vol. 10, April 1971.

114. Wilson, David J. and Netlerville, D. J., "Influence of Downwind High-Rise Buildings on Stack Design," _Journal of the Air Pollution Control Association_, Vol. 26, No. 10, October 1976.

115. Wolff, George T., Wight, Gregory D. and Pasceri, Ralph E., "Aerial Investigation of the Ozone Plume Phenomenon," _Journal of the Air Pollution Control Association_, Vol. 27, No. 5, May 1977.

116. Yamartino, R. J., Jr., "A New Method for Computing Pollutant Concentrations in the Presence of Limited Vertical Mixing," _APCA Notebook_, Vol. 27, No. 5, May 1977.

117. Fay, James A., "Buoyant Plumes and Wakes," _Annual Review of Fluid Mechanics_, Vol. 5, 1973.

118. Kamotani, Y. and Greber, I., "Experiments on a Turbulent Jet in a Cross Flow," _AIAA Journal_, Vol. 10, No. 11, November 1972.

119. Wu, J., "Near Field Trajectory of Turbulent Jets Discharged at Various Inclinations into a Uniform Crossflow," _AIAA Journal_, Vol. 11, No. 11, November 1973.

120. Morton, B. R., "Forced Plumes," _Journal of Fluid Mechanics_, Vol. 5, 1959.

121. Turner, J. S., "Buoyant Plumes and Thermals," _Annual Reviews of Fluid Mechanics_, Vol. 1, 1969.

122. Turner, J. S., "Jets and Plumes with Negative or Reversing Buoyancy," _Journal of Fluid Mechanics_, Vol. 26, 1966.

123. Shirazi, M. A. and Davis, L. R., "Analysis of Buoyant Surface Jets," _Journal of Heat Transfer_, August 1976.

124. Sklarew, R. C., Wilson, J. C., and Fabrick, A. J., "DEPICT/IMPACT Grid Models of Point Source Emissions, Chemical Reactions and Winds in Complex Terrain," Ralph C. Sklarew, Consultant.

125. Trent, D. S. and J. R. Welty, "Numerical Computation of Momentum Jets and Forced Plumes," _Computers and Fluids_, Vol. 1, 1973.

126. Gibson, M. M. and Launder, B. E., "On the Calculation of Horizontal, Turbulent, Free Shear Flows Under Gravitational Influence," _Journal of Heat Transfer_, February 1976.

127. Bergeles, G., Gosman, A. D. and Launder, B. E., "The Near Field Character of a Jet Discharged Normal to a Main Stream," _Journal of Heat Transfer_, August, 1976.

128. Touma, J. S., "Dependence of the Wind Profile Law on Stability for Various Locations," _Journal of the Air Pollution Control Association_, Vol. 27, No. 9.

129. "Airborne Problems Associated with Spills," presented at the National Conference on Control of Hazardous Material Spills, San Francisco, California Aug. 25-28, 1974.

130. Cavanaugh, E. C. et.al., "Atmospheric Pollution Potential from Fossil-Fuel Resource Extraction, On-Site Processing and Transportation," Final Report, Radian Corporation for the Environmental Protection Agency, March 1976.

131. Church, Hugh W., "The Atmospheric Dispersion Model as Used in the Reactor Safety Study," <u>Third Symposium on Atmospheric Turbulence Diffusion and Air Quality</u>, Raleigh, N. C., October 19-22, 1976.

132. Demerjian, Kenneth L., "Photochemical Diffusion Models for Air Quality Simulation: Current Status," Environmental Protection Agency, 1976.

133. Murray, F. W., "Atmospheric Dispersion of Vaporized Liquefied Natural Gas," Final Report, Rand Corporation, February 1975.

134. Brummage, K. G., "The Evolution and Dispersal of Hydrocarbon Gas on Tankers," appearing as Chapter II in the <u>International Oil Tanker and Terminal Safety Guide</u>, Second Edition, 1974, Halsted Press.

135. Burgess, D., Biordi, J., and Murphy, J., "Hazards of Spillage of LNG Into Water," U.S. Bureau of Mines, Report PM SRC 4177 (AD 754-498), September 1972.

136. Keffer, J. F., and Baines, W. D., "The Round Turbulent Jet in a Cross-Wind," <u>Journal of Fluid Mechanics</u>, Vol. 15, No. 4, 1963.

137. Ooms, G., Mahieu, A. P., Zelis, F., "The Plume Path of Vent Gases Heavier Than Air," Proceedings of the First International Symposium on Loss Prevention and Safety Promotion in the Process Industries, Delft, 1974.

138. Cermak, J. E., "Laboratory Simulation of the Atmospheric Boundary Layer," <u>AIAA Journal</u>, Vol. 9, September 1971, pp. 1746=1754.

138. teRiele, P. H. M., "Atmospheric Dispersion of Heavy Gases Emitted at or Near Ground Level," Second International Symposium on Loss Prevention and Safety Promotion in the Process Industries, Heidelberg, September 5-9, 1977.

140. Bodurtha, F. T., "The Behavior of Dense Stack Gases," <u>Journal of the Air Pollution Control Association</u>, Vol. 11, p. 431, (1961).

C. REGULATIONS

1. Breidenbach, A. W., "Dealing with Toxic Substances," *Pollution Engineering*, Vol. 8 No. 12, December 1976.

2. Burklin, C. E., Cavanaugh, E. C., Dickman, J. C. and Fernandes, S. R., "A Study of Vapor Control Methods for Gasoline Marketing Operations, Vol. 1, Industry Survey and Control Techniques," Final Report Radian Corporation for the Environmental Protection Agency, April 1975.

3. Burklin, C. E., Cavanaugh, E. C., Dickman, J. C. and Fernandes, S. R., "A Study of Vapor Control Methods for Gasoline Marketing Operations, Vol. II, Industry Survey and Control Techniques," Final Report Radian Corporation for Environmental Protection Agency, April 1975.

4. Ember, L. R., "TOSCA: Paves the Way for Controlling Toxic Substances," *Environmental Science and Technology*, Vol. 11 No. 1, January 1977.

5. Environmental Protection Agency, "Activities of Federal Agencies Concerning Selected High Volume Chemicals," Final Report, February, 1975.

6. Murry, Chris, "Chemical Firms Wary Over Toxic Substances Law," *Chemical and Engineering News*, Jan. 3, 1977, Vol. 55, No. 1.

7. National Research Council, "Decision Making for Regulating Chemicals in the Environment," National Academy of Sciences, 1975.

8. Ordway, G. L. and Druley, R. M., *The Toxic Substances Control Act*, Bureau of National Affairs, Washington, D. C., 1977.

9. Ricci, Larry J., "U. S. Toxic-Substances-Control Law: Real Impact Fuzzy Until 1980," *Chemical Engineering*, Vol. 83, No. 25, November 22, 1976.

10. Ricci, Larry J., "OSHA's Morton Corn Tells of Plans to Upgrade the Agency," *Chemical Engineering*, Vol. 83, No. 18, August 30, 1976.

11. Steinman, George C., "Maritime Administration Bulk Chemical Carrier Construction Program," Environmental Activities Group, Maritime Administration, Final Report, 1974.

12. Steymann, Edward H., "Industry's Views Regarding Pollution-Control Laws," *Chemical Engineering*, Vol. 83 No. 22, October 18, 1976.

13. "Toxic Substances Control Act" House Committee on Interstate and Foreign Commerce Hearings, 94th Congress, Serial 94-41, June 16, July 9-11, 1975.

14. Train, Russell E., "Approval and Promulgation of Implementation Plans, Ship and Barge Vapor Recovery," *Federal Register*, 40(198): 47765, October 10, 1975.

15. Train, Russell E., "Approval and Promulgation of Implementation Plans, Ship and Barge Vapor Recovery," Federal Register, 40(198): 47765, October 10, 1975.

16. Zarytkiewicz, E. D., "Federal Environmental Laws and Regulations," Chemical Engineering, Vol. 82, No. 21, October 6, 1975.

D. SAMPLING PROCEDURES

1. Corn, Morton and Sansone, Eric B., "Assessment of Inhalation Hazards Aboard Inland Towboats," American Industrial Hygiene Association Journal, Vol. 32, May 1971.

2. Johnson, Morris C., "Methodology For Chemical Hazard Prediction," Report from Department of Defense Explosives Safety Board, Washington, D. C., October 1974.

3. Kalliokoski, P., "Charcoal Sampling Method for Determining the Concentration of Styrene in Air," Scandinavian Journal of Work Environmental Health, Vol. 1 No. 3, 1975.

4. Tomkins, Frederick C., Jr. and Goldsmith, Robert L., "A New Personal Dosimeter for the Monitoring of Industrial Pollutants," Journal of the American Industrial Hygiene Association, No. 38, August 1977.

E. MARINE TERMINAL EMISSIONS STUDY

1. Burklin, C. E., Colley, J. D. and Owen, M. L., "Background Information on Hydrocarbon Emissions from Marine Terminal Operations, Vol. I-Discussion," Final Report Radian Corporation for Environmental Protection Agency, Nov. 1976.

2. Burklin, C. E., Colley, J. D. and Owen, M. L., "Background Information on Hydrocarbon Emissions from Marine Terminal Operations, Vol. II-Appendices," Final Report Radian Corporation for Environmental Protection Agency, November 1976.

3. Cooper, Hal B., and Mahdi, Chassan M., "Air Pollution Impact of Maritime Shipping Operations in the Port of Houston," <u>Coastal Zone Management Journal</u>, Vol. 1 No. 4, 1974.

F. BUILDING MATERIALS AND SHIP CONSTRUCTION

1. Anonymous, "Building Materials, Chemicals Help Provide the Answer,"
    Marine Engineering Log., Vol. 78 No. 2, February 1973.

2. "Post Challenger--The First Purpose-Built Chemical Parcel Tanker for
    Panocean," Shipbuilding and Marine Engineering International, Vol. 96
    (1163), February 1973.

3. Rogers, J., "Tank Coatings for Chemical Cargoes, "Transactions of In-
    stitute of Marine Engineers, London, Vol. 83, No. 5, 1971.

4. Steinman, George C., "Maritime Administration Bulk Chemical Carrier
    Construction Program," Environmental Activities Group, Maritime Ad-
    ministration, Final Report, 1974.

G. EXPLOSION MODELS

1. Anderson, R. P. and Armstrong, D. R., "Comparison Between Vapor Explosion Models and Recent Experimental Results," AIChE Symposium Series No. 70, 1974.

2. Coevert, K., Groothuizen, Th. M., Pasman, H. J. and Trense, R. W., "Explosions of Unconfined Vapor Clouds," 1st International Loss Prevention Symposium, 1974.

H.   CONTROL OF HYDROCARBON EMISSIONS

1.   Burklin, C. E., Cavanaugh, E. C., Dickerman, J. C., Fernandes, S. R. and Wilkins, G. C., "Control of Hydrocarbon Emissions from Petroleum Liquids," Radian Corporation, Final Report for Environmental Protection Agency, September 1975.

2.   Geiger, James H. and Charrington, Peter R., "Gasoline Vapor Recovery Efficiency Testing at Bulk Transfer Terminals," Final Report, Betz Environmental Engineers, Inc., 1976.

3.   Light, E., "Unregulated Air Pollutants: The Chemical Industry," West Virginia-Citizen Action Group, Charleston, W. Virginia 1976.

4.   Neligan, R. E., "Emission Modifications: Overview," National Environmental Protection Administration Research Center Report, April 1975.

5.   Pellizzari, E. D., Bunch, J. E., Berkley, R. E. and McRae, J., "Determination of Trace Hazardous Organic Vapor Pollutants in Ambient Atmospheres by Gas Chromatography/Mass Spectrometry/Computer," _Analytical Chemistry_, Series 48 Issue 6, 1976.

6.   Tamura, M., Fujiike, H. and Uda, K., "Technical Development Trends for Vapor Recovery System," _Chemical Economy and Engineering Review_," Series 8 Issue 11, 1976.

7.   Walker, D. C., Husa, H. W. and Ginsburgh, I., "Demonstrations of Reduced Hydrocarbon Emissions from Gasoline Loading Terminals," Research and Development Department, Amoco Oil Co. Naperville, Ill., 1975.

8.   Astleford, W. J., "Development of Criteria for the Recirculation of Exhaust Air," Final Report, NIOSH Contract No. CDC-99-74-96, SwRI Project 02-4011, 1975.

I. HAZARD ASSESSMENT MODELS AND CLASSIFICATION

1. Affens, W. A. and Lange, E. A., "Ignition of Flammable Gases in Crude Oil Tanks as a Result of Metal Fracture," Naval Research Laboratory Report 8013, June 29, 1976.

2. Raj, Phani, Kalelkar, and Ashok, S., "Assessment Models in Support of the Hazard Assessment Handbook," Final Report by Arthur D. Little Co. for Department of Transportation, January 1974.

3. "System for Classification of the Hazards of Bulk Water Transportation of Industrial Chemicals," Committee on Hazardous Materials, National Academy of Sciences, September 1975.

J. SHIPTANK GAS ATMOSPHERE CONTROL

1.   American Bureau of Shipping, "Guide for Inert Gas Installations on Vessels Carrying Oil in Bulk," 1973.

2.   B. P. Tanker Company, Ltd., The Inert Flue Gas System, Operational Instructions, July 1968.

3.   Horne, G. H., "Inert Gas Blanketing for Tankers," Engineering Department, Standard Oil of California, August 6, 1970.

4.   Hosie, R. M., and Sommer, P. H. J., "The Ventilation of Cargo Spaces in Oil Tankers," British Ship Research Association Report N.S. 164, 1967.

5.   Keeling, H. W., Jr., and Stewart, W. P., "Use of Dry Flue Gas to Retard Internal Corrosion and Prevent Explosion in Clean Products Tankers," Soc. Naval Architects and Marine Engineers Trans., 61, 718-42 (1953).

6.   Laidlaw, D. K., Spencer, S. F., and Ayers, E. B., "Gas Concentrations in Cargo Tank of Refined Product Carriers," paper presented at Annual Tanker Conference of the American Petroleum Institute, May 6-8, 1963.

7.   Laskey, N. V., "Displacement Gas-Freeing in King Alexander the Great," Tanker and Bulk Carrier, June 1971, pp 15-22.

8.   Muir, J. B., and Stanford, A. E., "Experiments with Flue Gas Inerting and Fresh Air Tank Venting," paper presented at API Meeting, May 1963.

9.   Stanford, A. E., "Is 'Inerting' the Complete Answer to Tanker Explosions?," The Motor Ship, 52 (15), 321 (1971).

10. Stanford, A. E., "Inert Gas - A Survey," Tanker and Bulk Carrier, November 1972.

11. Johnstone, H. F., and Roberts, M. H., "Deposition of Aerosol Particles from Moving Gas Streams," Ind. Eng. Chem., 41, 2417-23 (1949).

12. Day, C. F., Platt, E. H. W., Telfer, I. E., and Petreau, R. P., "The Development and Operation of an Inert Gas System for Oil Tankers," The Naval Architect, Jour. of the Royal Inst. of Naval Architects, No. 1, January 1972, pp 33-72.

13. "Is the Cost of an Inert Gas System Justified?," IMCO recommendations and the operation of the BP System, The Naval Architect, Jour. of the Royal Inst. of Naval Architects, No. 2, July 1971, pp 34-35.

14. Franklin, T., "Inert-Gas Systems for Tankers: What They Are, How They Work," Marine Engineering/Log, January 1975, pp 48-52.

15. Hosie, R. M., "On Ventilating and Purging Ships' Compartments," The Naval Architect, Jour. of the Royal Inst. of Naval Architects, No. 4, October 1972, pp 90-91.

16. "Explosions in Tankers - Some Methods of Prevention Including Gas-Freeing and Venting," Shipping World and Shipbuilder, Vol. 163, No. 3843, March 1970, pp 421-424.

17. Aitken, W. H., "Nitrogen for Inerting," Tanker and Bulk Carrier, Vol. 20, No. 7, November 1973.

18. Rutherford, D. M. M., "An Introduction to Inert Gas," Tanker and Bulk Carrier, July 1974.

19. Wilson, S., "Foam Gas Inert Systems," Tanker and Bulk Carrier, Vol. 20, No. 7, November 1973.

20. Canton, A. T., "A Marine Flue Gas Scrubber," Tanker and Bulk Carrier, Vol. 20, No. 7, November 1973.

21. "Inert Gas Control and Monitoring," Tanker and Bulk Carrier, Vol. 20, No. 7, November 1973.

22. Riksheim, J. B., "Investigation Into Inert Gas Systems for Crude Oil Carriers," Veritas, No. 84, Oslo, July 1975.

23. Porter, J. F., "Marine Inert Gas Systems," Petroleum Review, June 1974.

24. Hemeon, W. C. L., Plant and Process Ventilation, Industrial Press, Inc., 1963.

25. Inter-Governmental Maritime Consultative Organization (IMCO), Addendum No. 1, "Gas-Freeing" (Re: Memorandum dated October 29, 1970).

26. Inter-Governmental Maritime Consultative Organization (IMCO), Addendum No. 2, "Pertinent IMCO Activities" (Re: Memorandum dated October 29, 1970).

27. "A Report on Simulated Gas-Freeing Tests with the CAMAT System on Board the 227,506 D.W.T.S.T. 'King Alexander the Great'," CAMAT International Transportation Consultants, Ltd., Technical Report No. 14-120/A, June 23, 1970.

28. Logan, A., "Experience with Gas Control in Crude Oil Carriers," Paper presented to the American Petroleum Institute Tanker Conference, May 4-8, 1963, Transactions, The Institute of Marine Engineers, Vol. 76, No. 2, February 1964.

29. Logan, A., and Drinkwater, J. W., "Gas Concentrations in the Cargo Tanks of Crude Oil Carriers," Transactions of the Royal Institution of Naval Architects, Vol. 103, 1961, pp 67-89.

30. "A CAMAT System for Gas Freeing by Displacement," _The Motor Ship_, Vol. 51, No. 604, November 1970, p 367.

31. "Tanker Tank Cleaning Research Program," Phase I Final Report, MSAR 74-36, U.S. Dept. of Commerce Maritime Adm., Contract 2-36279, March 1974.

32. "Gas Evolution: Tanker and Terminal Safety," edited by Peter Hepple, Special Publications Series No. 1, Proceedings of a Symposium organized by the Institute of Petroleum and held at the Mount Royal Hotel, London, March 5, 1971.

33. Rutherford, Capt. D. L. C., "Inert Flue Gas Systems for Tankers," The Nautical Institute, London Branch Seminar, London, October 2, 1975.

34. Logan, A., and Drinkwater, J. W., "Gas Concentrations in the Cargo Tanks of Crude Oil Carriers," _Shipbuilding and Shipping Record_, May 19, 1960.

35. "The Moss 'Package' for Flue Gas Inerting," _Shipbuilding and Shipping Record_, April 28, 1972.

36. Witze, P. O., "Centerline Velocity Decay of Compressible Free Jets," _AIAA Journal_, 12, April 1974, pp 417-418.

37. Kleinstein, G., "Mixing in Turbulent Axially Symmetric Free Jets," _AIAA Jour. Spacecraft/Rockets_, 1, July-August 1964, pp 403-408.

38. Schlichting, H., _Boundary Layer Theory_, Chapter 23, McGraw-Hill Book Co., New York, 1960.

39. Baker, W. E., Westine, P. S., and Dodge, F. T., _Similarity Methods in Engineering Dynamics_, Spartan Books, Washington, D. C., 1973.

40. Holman, J. P., _Heat Transfer_, 3rd edition, pp 221-222, McGraw-Hill Book Co., New York, 1972.

41. Gordier, R. L., "Studies on Fluid Jets Discharging into Moving Liquid," St. Anthony Falls Hydraulic Laboratory, Technical Paper No. 28, Series B, Univ. of Minnesota, Minneapolis, 1959.

42. Albertson, M. L., Dai, Y. B., Jensen, R. A., and Rouse, H., "Diffusion of Submerged Jets," _Trans. ASME_, _115_, pp 639-697.

43. Viktorin, K., "Investigation of Turbulent Mixing Processes," NASA TM 1096, 1946.

44. Grossman, G., "Model Tests for Gas Exchange in Cargo Tanks," _HANSA-Schiffahrt-Schiffbau-Hafen 110_, November 1973, pp 1935-1940.

45. Grossman, G., "Research on Inert Gas Systems," _HANSA-Schiffahrt-Schiffbau-Hafen - 111_, Nr. 22, 1974, pp 1915-1920.

46. Confidential Company Report.

47. Lange, R. F., "Gas Concentration and Static Electrification Studies During Tank Washing on the S/S Mobil Pegasus," Mobil Research and Development Corp. Report No. 72.6-GSD, May 1, 1972.

48. Barstad, J., Boler, J. B., Hjorteland, O., and Solum, E., "Variations in Hydrocarbon Gas Concentration During Supertanker Cleaning Operations," Nature, Vol. 241, No. 5386, pp 196-197, January 19, 1973.

49. Aitken, W. H., "Nitrogen for Inerting," Tanker and Bulk Carrier, Vol. 20, No. 7, November 1973.

50. Bass, R. L., Owen, T. E., and Dodge, F. T., "Bulk Carrier Operations Safety Enhancement Project, Final Report-Phase I," MA-RD-920-76057, U.S. Dept. of Commerce Maritime Adm., SwRI Project 02-4317, June 7, 1976.

51. Gray, D. C., "Solvent Evaporation Rates," American Industrial Hygiene Association Journal, November 1974.

52. Johannessen, T., Rieksheim, J., "Exchange of Atmosphere in Cargo Oil Tanks by Using the Mixing Method," Norwegian Maritime Research, No. 3, 1977.

53. Bass, R. L. and Morrow, T. B., "Bulk Carrier Safety Enhancement Project - Vol. I, Tank Atmosphere Control," Phase II Final Report, U. S. Maritime Administration Contract No. 5-38044, October 1978.

54. Spalding, D. B., Convective Mass Transfer, McGraw-Hill, 1963.

K. REACTIVITY OF HAZARDOUS CARGOES

1. Askheim, N. E., Steensland, O. and Vossgaard, R., "Reactivity Between Chemical Cargoes," Norwegian Maritime Research, Vol. 2 No. 2, 1974.

2. Hunter, T. F., Rumbles, D., and Stock, M. G., "Photo-Oxidation of Vapor-Phase Benzene," Chemistry Physics Letter, Series 45 Issue 1, 1977.

3. Noweir, Madbuli, Pfitzer, Emil, and Hatch, Theodore, "Thermal Decomposition of Carbon Tetrachloride Vapors at its Industrial Threshold Limit Concentration," Journal of the American Industrial Hygiene Association, Series 34, Issue 1, 1973.

4. "Scientific and Technical Data Base for Criteria and Hazardous Pollutants," Yearly Review, Health Effects Research Laboratory Research, Triangle Park, N. C., May 1976.

L. SAFETY ASPECTS OF TRANSPORTING HAZARDOUS CARGOES

1.   Walmsley, F. H., "Safety Aspects of Transport of Hazardous Chemicals," _Chemical Engineer_, February 1973.

2.   Welker, J. R. et.al., "A Survey of the Effectiveness of Control Methods for Fire in some Hazardous Chemical Cargoes," Final Report, University Engineers, Inc., for United States Coast Guard Office of Research, March 1976.

M. DISCHARGING OF HAZARDOUS WASTES FROM SHIPS

1. Lakey, Robert J., "The 1973 Marine Pollution Convention's Impact on Ships Transporting Hazardous Materials," Journal of Hazardous Material, Vol. 1, No. 2, January 1976.

N.   TANKER CLEANING OPERATIONS

1.   Barstad, J., Boeler, J. B., Hjorteland, O. E. and Solum, E., Varia-
     tions in Hydrocarbon Gas Concentration During Supertanker Cleaning
     Operations," Nature, No. 241, January 19, 1973.

2.   Ball, John, et.al., "Management of Tank Washings in Marine and Coastal
     Commerce," Final Report for Office of Sea Grant-NOAA, Report No.
     TAMU-SG-74-221, Contract No. OSG-04-3-158-18, February 1975.

3.   American Petroleum Institute, "Recommended Practice for Cleaning Petroleum
     Storage Tanks," API RP 2015, 1968.

4.   Bustin, W. M., "Water Slug Formation During Tank Washing," Second half
     of API Statics Research Program, Exxon Research and Engineering Company,
     Florham Park, N.J., 1973-1974.

5.   Cates, M. F., "Cargo Tank Cleaning and Vapor Concentration Studies, S.S.
     Ralph B. Johnson," Chevron Research Company, July 27, 1970.

6.   "Explosions in Tankers," International Chamber of Shipping Report, and
     "Details of a New Tank Cleaning Method," Shipping World and Shipbuilder,
     Vol. 16, No. 3851, November 1970, pp 1545-1548.

7.   International Chamber of Shipping, "Cleaning of Structural Members in
     the Tanks of Very Large Tankers," Maritime Safety Committee, MRT/32,
     October 10, 1969.

8.   International Chamber of Shipping - Oil Companies International Marine
     Forum, Clean Seas Guide for Oil Tankers, 1973.

9.   Klaver, R. F., "Tank Washing Safety on Board S.S. Mangelia," Chevron
     Research Company, March 1970.

10. Lloyd's List, "Cleaning Tankers--With Oil," September 13, 1973.

11. Shewmaker, J. E., "Waterless Washing of Tankers," Esso Research and Engi-
     neering Company, January 16, 1973.

12. International Chamber of Shipping - Oil Companies International Marine
     Forum, Clean Seas Guide for Oil Tankers, The Operation of Load on Top,
     ICS-OCIMF, 1973.

13. Lockweed, W. H., "Use of a Gravity Type Oil Separator for Tanker Opera-
     tions," Tanker and Bulk Carrier, February 1972.

14. Wiley, W. O., "Tank Cleaning Methods and Their Application to Service
     Conditions," The Motor Ship, May 1972, pp 91-93.

15. "Tanker Tank Cleaning Research Program," Phase I Final Report, MSAR
     74-36, U.S. Dept. of Commerce Maritime Adm., Contract 2-36279, March
     1974.

16. Reif, R. B., and Hawk, S. A., "Review and Evaluation of the Literature on Electrostatic Generation in Tank Cleaning," Report No. CG-D-76-74, February 1974.

17. Murakami, Mitsukiyo, and Katayama, Kinji, "Discharge Coefficients of Fire Nozzles," *Journal of Basic Engineering*, December 1966, pp 706-716.

18. Castaldi, G., and Powll, W. J., "Crude Washing Guidelines," Interim Report on Task 1 of Contract No. C-5-38000, April 1975.

19. "Cleaning Unit for OBO Wing Tanks," *Shipbuilding and Shipping Record*, January 29 and February 5, 1971.

20. "Tank Cleaning VLCC's Using Crude Oil," *Shipbuilding and Shipping Record*, December 14, 1973.

21. Maybourn, R., "Crude Oil Washing," Paper No. 4, Session 1, Safety Standards and Pollution Control, International Tanker Safety Conferdnce, Bergen, Norway, October 1975.

22. Wilhelmsen, J, Jr., "Tank Cleaning and Load-On-Top," Paper No. , Session 1, Safety Standards and Pollution Control, International Tanker Safety Conference, Bergen, Norway, October 1975.

23. Bass, R. L., Owen, T. E., and Dodge, F. T., "Bulk Carrier Operations Safety Enhancement Project, Final Report-Phase I," MA-RD-920-76057, U.S. Dept. of Commerce Maritime Adm., SwRI Project 02-4317, June 7, 1976.

O.   ANALYSIS OF MAJOR HAZARDOUS ACCIDENTS

1.   "S. S. V. A. Fogg, Sinking in the Gulf of Mexico, February 1, 1972 with
     Loss of Life," United States Coast Guard Marine Casualty Report, September 1974.

2.   "S. S. William T. Steele: Death of Three Ships' Officers at Guayanilla,
     Puerto Rico on November 18, 1972," United States Coast Guard Marine
     Casualty Report, September 1974.

3.   "Marine Casualty Report Tank Barge OCEAN 80 Fire and Explosions, Carteret,
     New Jersey, October 25, 1972," United States Coast Guard May 2, 1975.

P. DISPOSAL OF TOXIC CHEMICALS

1. Hansen, Arthur G., "The Need of Academic Support for Establishing Reason-
   able Environmental Standards," Proceedings of the Third Symposium on
   Hazardous Chemicals Handling and Disposal 1972, Indianapolis, Indiana,
   April 11-13, 1972.

APPENDIX B

DETAIL SUMMARY OF TERMINAL OBSERVATIONS

TERMINAL	OBSERVATION NO.	VESSEL
A	1	28,125 DWT multi-cargo tanker
A	2	75,649 DWT gasoline tanker
B	3	36,600 DWT multi-cargo tanker
B	4	Three 10,000 bbl barges
C	5	10-barge integrated tow

DISCUSSIONS WITH CHEMICAL TERMINAL AND SHIP PERSONNEL

SUMMARY OF SITE VISIT

Terminal A

Observation 1

1. Vessel Description – 28,125 DWT, 40-tank multi-cargo tanker

2. Cargos Loaded

Chemicals	Quantity (bbl)	Average Loading Rate (bbl/hr)
Heptane	8,000	860
Toluene	6,000	2,260
Acetone (discharged)	8,000	--
MEK (discharged)	7,000	1,230

Mixtures		
Laktane (aliphatic solvent)	6,000	1,390
VM&P	8,000	1,240
Varsol 18	18,000	1,750
Isopar H	2,500	1,200
HAN (high aromatic naptha)	5,000	1,350
Isopar M	3,000	1,210
LOPS (low odor petroleum solvent)	6,000	1,570
Varsol 1	24,000	1,420

Other		
Heating oil	32,000	6,150
Insulating oil	3,000	2,080
White oil	10,000	1,500
B-Lube (Hydraulic Oil)	1,500	1,730
(Necton 37)	3,600	1,640
E-Lube (Bright Stock)	8,000	1,070
F-Lube (L/P 100)	12,000	1,860
I-Lube (diluent oil)	18,000	1,570
H-Lube (Coray 22)	8,000	1,460
(Coray 60)	4,400	1,350
(Coray 150)	3,000	850
(Coray 220)	4,700	830

3. Static Electricity Accumulators

Varsol 1 and 18, Isopar M and H, HAN, and LOPS are classified as static electricity accumulator cargos. To minimize the possibility of an arc discharge in the cargo vapor, no object is to be inserted into these product tanks during loading, e.g., hand operated ullage tapes or product sample lines. To minimize aerosolization of the product, initial loading is by gravity until an 18-in. innage is reached.

4.   Electrostatic Grounding System

The vessel is grounded for static charge buildup through the first load-ing hose that is connected to the ship's manifold. This hose has an electrical-ly conductive element incorporated into the hose laminations. The major con-cern is the condition of this conductor because repeated flexing of the hose could cause a break in the conductor which would go unnoticed and would nullify the grounding system. However, it is unlikely that the hose would deteriorate to the point where all bonding wires broke without the hose being removed from service for other reasons.

5.   Cargo Loading Method

Each product was loaded into its respective tank by the open drop technique. With this method there is no below deck distribution of product from a common source line to a given tank as in the closed drop method. Rather, each tank has a permanently installed, dedicated delivery line that begins at the ship's manifold, descends vertically into the tank, and termi-nates approximately 18 to 24 in. above the tank bottom. In addition, all loading was performed with open ullage caps and flame screens in place.

6.   Cargo Gauging Technique

During loading, the height of the ullage space above the liquid sur-face was monitored with the aid of a deck-mounted, automatic tape gauging system. This system, which is physically separated from the hatches, uti-lizes a calibrated tape that is attached to a float that rises with the liquid level. Periodically, deck hands would remove the flame screens to visually observe the liquid level after the tape gauge had been read. Co-ordination of ullage readings with the loading plan was accomplished using walkie-talkies. After each tank was topped, the final ullage was read manu-ally with a Lufkin tape inserted through the ullage port. A flashlight was used to observe contact of the tape bob and the liquid surface.

7.   Vent System Configuration

Each cargo tank was serviced by a separate hatch. Vapors were vented through the open ullage ports (hatch openings closed) as well as a common vent riser system. This system consisted of individual vapor discharge lines at deck level from each hatch. These lines terminated in a common vent line approximately 6 to 8 ft above deck level. Each of these individ-ual vapor discharge lines contained a P/V valve with flame screen, which was set for 3 psig pressure and 2 psig vacuum, just upstream of the junction with the common vapor line. Vapors in the common header could then be vent-ed to the atmosphere through either of two forward or two aft vent risers. These risers terminate with flame screens approximately 30 to 40 ft above the deck. The pump room was ventilated via bow facing, deck mounted air intake, and discharge ducts.

8.   Atmospheric Conditions

        Air temperature – 70 to 84°F
        Barometric pressure – 30.5 in. Hg
        Wind direction – variable to 5.5 mph (midship bridge and deck)
        Wind speed – port to starboard
        Weather – heavy cloud cover and rain interspersed with sunlight

9.   Photographic Documentation

    A 16-mm motion picture camera with a 75-mm zoom lens was set up on
the levy alongside of the dock. The viewing angle was adjusted to include
the main product manifold and deck structure located between the fore and
aft deck houses. Footage included both stop action at 12 frames/minute as
well as a 16 fps pan of the entire ship.

10.   Measured Concentrations

    A company-owned Scott D-16 Vapotester was used to estimate vapor con-
centrations at various locations. The calibration date of the instrument
was unknown. Some indication of concentration was gained from the use of
this instrument even though the device was calibrated against hexane, which
will produce a response that is somewhat different than calibration against
specific cargo vapors. The results of these cursory tests are summarized
below.

Tank No.	Contents	Ullage (ft)	Concentration (% LEL)	Location
4S	Toluene	4' 5"	40	ullage port
9P	Varsol 18	9' 10"	16	ullage port
7C	Diluent oil	41'	0	inside hatch
1CS	Necton 37	13' 0"	0.2	ullage port
3C	Acetone	18' 4"	>100	ullage port
4C	MEK	Empty tank	30	ullage port
		being blown	1.0	ullage port-- 3 ft upwind of hatch
			0.8	10 ft downwind of hatch at deck level
			1.0	10 ft downwind of hatch, 3 ft above deck level

11.   Safety and Health Precautions

    Safety and health precautions were not observed to be posted in either
the deck house or on the ship. The following precautions were documented
by question and observation:

a. Long sleeve shirts and boots (no canvas tennis shoes) were required.

b. Rubber gloves were available aboard ship for protection against liquid-skin contact, but they were not worn.

c. MSA fresh air masks (BuMines approval 1905A) with diaphragm pumps were housed in boxes on deck.

d. Entry hatches to deckhouses are closed during loading.

e. Radio telephone equipment is not to be operated during loading or discharging of cargo. The concern is that an electrically charged antenna may constitute a potential ignition source.

f. See Item No. 3.

g. Man entry into tanks would be permitted by Chief Mate if vapor concentration is less than or equal to 2% LEL.

h. Crew relies heavily on vapor odor and their own feeling of well-being as early warning devices.

i. All cargo pumps are steam operated, i.e., no electric or hydraulic pumps.

j. Drip pans are located below the on-deck product manifolds.

k. Hammer blinds are used on those ships' product lines that carry liquids which will leak past conventional blind flange or valve seat.

l. Loading is terminated if the ship is light and a substantial wind comes up. The concern is that the mooring lines become taut.

m. High temperature, high humidity, and no wind create the worst on-deck vapor conditions (subjective comment of crew).

12. Personnel

On this vessel there was a Chief Mate, one Second Mate, and two Third Mates. Theoretically, with this staffing, the C/M does not stand watch. However, in addition to the typical water personnel during loading, which included one deck officer, two able-bodied seamen, one ordinary seaman, and one pumpman, the C/M was on-duty at all times. Thus, there were six crew members that could be on deck at a given time, and all of these personnel were randomly involved with cargo gauging. When not gauging or under direct order from the C/M, personnel were free to move about on the deck. Crew members were observed to congregate near open ullage ports, and no attempt was made to avoid vapor exposure by standing downwind of ullage ports.

SUMMARY OF SITE VISIT

Terminal A

Observation 2

1.   Vessel Description - 75,649 DWT, 21-tank gasoline tanker

2.   Cargos Loaded

Product	Quantity (bbl)	Average Loading Rate (bbl/hr)
Unleaded gas	98,000	11,200
Regular gas	123,000	9,300
Premium gas	56,000	10,500
Kerosene	36,000	4,400
Heating oil	115,000	16,700
No. 2 Diesel	75,000	8,400
Turbo Fuel A	36,000	7,300

3.   Electrostatic Grounding System

See Item 4 under Terminal A - Observation 1.

4.   Cargo Loading Method

This observation represents an extreme with respect to dock and ship
operations during loading. In Terminal A-Observation 1, the flexible load-
ing hoses were moved about by winches and cranes, and the hose flanges were
manually bolted to the deck and dock manifolds. During this observation,
hydraulically-operated, automatic loading arms on the deck were remotely
manuevered into position in front of the deck flange. A chuck on the termi-
nal end of the arm gripped the deck flange, thus sealing the flange inter-
face. On the ship, a closed drop loading system distributed the various
product grades to their designated tanks. In this system, products are de-
livered to the level of the tank bottom via five drops or downcomers. These
downcomers connect to common distribution lines. Through a series of valves,
product grades are segregated and delivered to each tank. This closed drop
system is not generally suited for loading of chemical cargos where product
contamination, due to sequential loading, is to be avoided. All product
loading activities were monitored and controlled remotely using three con-
soles in a control room. These activities included automatic, remote posi-
tioning of below-deck valves and gauging. Loading was accomplished with
open ullage ports and flame screens in place.

5.   Cargo Gauging Technique

Cargo gauging was accomplished using two techniques. Both of these
methods provided a visual indication of ullage depth to deck personnel. In
addition, each method was instrumented to provide a continuous indication
of ullage depth to supervisory personnel in the control room so that loading rate
could be remotely controlled. The first method, a flotation tape gauging
system, was basically the same as the device described in Terminal A-Obser-
vation 1 with the exception that the tape rewind had been modified to provide
an output analog signal from a Wheatstone bridge which was proportional to

B-8

ullage depth. It was this analog signal that was displayed in the control
room. This system was in use throughout loading. The second system operated
during the latter stages of loading when the ullage depth fell between 5 and
14 ft. In addition to a visual readout of ullage depth on deck and in the
control room, this system activated a low level alarm in the control room
at 14 ft and a high level alarm at 5 ft. The method of transducing the ul-
lage depth on this system, which was manufactured by De Laval, was not
available. Because of the highly automated nature of the ships' loading
and gauging systems, there was minimal deck activity, and hand gauging
through open ullage ports was not observed.

6.   Vent System Configuration

This vessel did not have the familiar common mast riser, vapor dis-
charge system. The vessel had recently undergone modification to remove
all above deck vent piping from the individual lines that serviced each
hatch through the common vent manifold. The mast risers remained in place,
but the inlet opening was sealed with a flange. Also, the exhaust opening
on each hatch was similarly sealed. A new high speed pressure/vacuum re-
lief valve manufactured by Press-Vac Engineering, Ltd., in Allerod, Den-
mark, was installed on each tank. Rising from the deck to a height of
roughly 8 ft was an 8-in. I.D. standpipe which was open to the tank vapors.
Atop the standpipe was a tear-drop shaped weight. During non-venting this
weight rested on a machined seat on the standpipe, thus sealing the vent
system. When tank pressure built up to 1.5 psig, the weight became un-
seated and rose vertically 3 inches. In so doing, the pressure in the
tank was relieved, and the vapors were vented to the atmosphere. The up-
ward motion of the weight was guided by vanes and was limited by stops on
the vanes and the slotted guideways on the inside surface of the vent pipe.
The frequency and duration of venting were a function of the tank ullage.
Timed estimates of the duty cycle are as follows:

Ullage (ft)	Venting Duration (sec)	Off Time (sec)	Period (sec)
35' 6"	40	65	105
7' 11"	8	15	23

Based on an assumed loading rate of 11,200 bbl/hr, and discharge through an
annulus whose diameters are 8 and 10 in., it was estimated that the vapor
efflux velocities were of the order of 90 ft/sec. During loading, several
ullage hatches were resting on their pins. A calculation of the efflux ve-
locity under this condition produced 100 ft/sec, which is consistent with
the calculation made on the high speed vent system. Vacuum relief, if needed
during discharging of cargo, is provided by a side branch relief valve which
is set for -0.5 psig. During venting, the vapors were observed to be pro-
jected several feet above the top of the vent. Upon seating of the weight,
the vapors appeared to disburse laterally and then descend to deck level. It
was also observed that the weight did not necessarily seat properly and that
vapors could be discharged continuously at low levels.

B-9

7. Atmospheric Conditions

> Air temperature – 55 to 67°F
> Barometric pressure – 30.5 in. Hg
> Wind direction – port to starboard
> Wind speed – 1 to 6 knots (on bridge)
> Relative humidity – 40 to 25%

8. Photographic Documentation

Several rolls of 16-mm movie footage were taken from the ship's flying bridge. Time lapse photography was not attempted for safety reasons because the timer utilizes a 12-volt battery that could generate a spark. The footage that was obtained illustrates the gasoline tanker's venting system, deck configuration, control room, and the dock automatic loading arms as well as a more conventional ventilation system on a chemical tanker in an adjacent berth, i.e., similar to the tanker in Terminal A-Observation 1.

9. Measured Concentrations

A Scott D-16 Vapotester was again used to estimate vapor concentrations. Limited data were obtained due to malfunction of the device. The data which were obtained are summarized below.

Tank No.	Contents	Ullage (ft)	Concentration (% LEL)	Location
5C	gasoline	35' 6"	2	3 ft above vent outlet
5C	gasoline	25' 6"	2.8	at nozzle exit

10. Safety and Health Precautions

The following safety and health items are germane to this observation. For supplementary information, see Terminal A-Observation 1.

a. Deck and dock areas are classified as Class 1, Group D, Division 1 areas per IOTTSG.

b. Drip pans on dock are continually flushed with water.

c. The dock area had one vapor detector and alarm system. The single sensor was located behind the dock office at ground level. At this location, the sensor was roughly 150 yards from the loading manifold area.

d. The dock incorporated a cathodic protection system.

e. During loading, a tethered, emergency shutdown switch is placed on the ship deck. This switch can be used to close all motor operated loading valves on the dock.

f. Two compressed air packs were located on a dock that can berth roughly an 800-ft ship. The dock operating manual requires only one pack.

g. The odor of gasoline vapors could be detected at various points on deck. The vapors appeared to be concentrated in pockets in the vicinity of the high speed pressure/vacuum relief valves. Thus, there were also areas of minimal vapor odor.

h. This company has conducted in-house industrial hygiene vapor exposure studies. Personal samplers operating at 0.1 ℓ/min. draw vapors through a charcoal tube that is attached to the individual's lapel. Eight-hour time-weighted average samples are analyzed by gas chromatography. Desorption efficiency varies between 85 and 95%. Test results are not yet available.

11. Personnel

Listed below are some general observations of worker activity on the dock and tanker.

a. Hookup or disconnecting of the automatic loading nominally requires four workers. One worker controls the motion of the arm from an elevated control room. The remaining three workers are congregated around the chuck-deck flange interface to effect hookup. Following loading, the arms are not gravity drained into the tank, but, rather, they are cleared by a siphon back into the main distribution line. Hence, there is minimal opportunity for worker contact with bulk liquid during hookup or disconnect of the loading arms. Any leakage at the chuck/flange interface is collected in a drip pan.

b. As mentioned previously, there is negligible crew activity on the deck of vessels having automatic loading and gauging systems. However, as observed on this vessel and Observation 1, there is considerable deck activity on the part of contract workers who are loading stores for the voyage.

SUMMARY OF SITE VISIT

Terminal B

Observation 3

1. Vessel Description – 36,600 DWT, 27-tank, multi-cargo tanker

2. Cargos Loaded

Chemicals	Quantity (bbl)	Average Loading Rate (bbl/hr)
Toluene	8,000	2,180
DMK (acetone)	11,600	2,180
MEK	6,500	2,187
ECH (Epichlorohydrin)	3,800	1,041
Ethyl Alcohol (190)	6,500	4,610
2EH (ethyl hexanol)	6,500	2,175*
Glycerine	3,600	1,050
Tolusol 5	11,600	1,290

Mixtures		
VM&P	6,500	1,755
Sol 71	6,500	760
Sol 340	22,000	1,305

Other		
Aviation gas	23,000	2,329
Lube oils (LVI 200)	6,500	843
(LVI 750)	6,500	1,797
(HVI 100 TQ)	8,800	983
Bright stock	10,000	1,830
Premium gas	90,000	4,100

*Rates based on loading log from previous voyage

3. Electrical Ground System

One method of electrostatically grounding a tanker was outlined in Terminal A–Observation 1. At this terminal, vessels were grounded with a conventional static discharge line. A coated copper wire is secured to a convenient bolt on a butterworth opening. The other end of the wire is attached to a breaker box on the dock, one side of which is grounded. Up to this point, the contacts in the breaker box are open. The breaker switch is then closed, thus completing the grounding circuit.

4. Cargo Loading Method

The open drop method that was described earlier was also employed on this tanker. All chemicals with the exception of glycerine were loaded into the Nos. 2 and 3 sections of the ship. Each of these sections was segregated into multiple tanks. Glycerine was loaded into the aftmost tank in No. 6 section. All communications were accomplished without the aid of walkie-talkies.

5. Cargo Gauging Technique

Product levels were not gauged through open ullage ports. Rather, each tank was fitted with a 10-in. ID standpipe that extended from 8 in. above tank bottom through the deck to 31 in. above the deck. Manual gauging was accomplished through these standpipes using a Lufkin tape. As a result of the minimal liquid free surface area in the standpipe, the quantity of vapors to which a worker is exposed during gauging should be significantly less than for the case of gauging through an ullage port. On this vessel, the Chief Mate performed all of the gauging of all chemical tanks. Other deck hands gauged the non-chemical products. Presumably this situation resulted from a deck spill that had occurred. All standpipes were fitted with flame screens.

6. Vent System Configuration

Loading of all products, with the exception of epichlorohydrin, was performed with the ullage hatches on their pins (open ullage). Thus, vapors were discharged through the open ullage ports roughly 3 ft above deck level. Excess vapors were vented through a P/V valve approximately 8 ft above deck level. The P/V valves were connected to individual hatches via a 6-in. ID pipe. As on all of our tanker observations, the ullage ports are nominally 10 in. in diameter, and all were fitted with flame screens. On the observation, the flame screens had two layers--the bottom layer was a 30-mesh screen topped by a screen having 1/4-inch square openings. Epichlorohydrin was close loaded (closed ullage ports). The tank for this product was the only tank on the ship that had a dedicated vent riser which was located midship. This dedicated vent system, which also included a P/V valve and flame screens, consisted of approximately 140 to 150 ft of 6-in. ID pipe, 30 ft of which extended upward from the deck. The remainder of the piping was horizontal run, 5 ft above deck. Deckhouse ventilation inlet and exhaust ducts were located on the poopdeck of the wheelhouse.

7. Atmospheric Conditions

        Air temperature = 68°F
        Relative humidity = 75°F
        Barometric pressure = 30.6 in. Hg
        Wind conditions (ship's bridge) = variable 5 to 16 mph,
            bow to stern; shifting to 11 to 20 mph, starboard
            to port

8. Photographic Documentation

Several 100-ft rolls of 16-mm movie film were shot from the flying bridge to document the deck and dock structures and worker activity. Time lapse photography was not attempted.

9. Measured Concentrations

The ship's MSA Explosimeter (Model 2A) was used to estimate vapor concentrations.

Tank No.	Contents	Ullage (ft)	Concentration (% LEL)	Location
3CP	Ethylalcohol	45' 3"	5	Ullage port
3CP	Ethylalcohol	10' 7"	5	Gauging stand-pipe downwind of hatch
5CA	HVI lube oil	5' 2"	no response	12 ft downwind of hatch
1S	Gasoline	4' 4"	10-25	Above ullage port

10. Safety and Health Precautions

The following items pertain to this terminal observation:

a. See writeup in body of report pertaining to workers' activities during deck and dock hose hookup.

b. All deck and dock piping and valves for epichlorohydrin bore the warning POISON--CAUTION.

c. Posted in the berth office on the deck was a notice to the effect that personnel must wear respirators, slicker suits, goggles, and rubber boots and gloves when gauging, sampling, or connecting/disconnecting hoses of products such as ethylene dichloride, epichlorohydrin, and chemical slops. Respirators were also required when handling benzene, toluene, or xylene. Employees did not adhere to this company directive in any respect when handling epichlorohydrin or toluene on this voyage.

d. Respiratory equipment in the dock foreman's office included three cannister masks for use with acid gases, ammonia, organic vapors and particulates, and two Scott Air Packs.

e. Shipboard respiratory and protective equipment was stowed in the ship's office and included two MSA air or O_2 masks with 30-min limit, two MSA gas masks (Type N, Model SW) for use with acid gases, organic vapors, ammonia, CO, and particulates, one Chemox unit having a 1-hr duration and two emergency outfits

that included a hardhat, VAP knee-length protective coat, one pair each of rubber boots and gloves, and a flashlight.

11.   Personnel

During hose hookup, four workers were needed to secure the dockside flange and three workers were needed to bolt the hose flange to the deck manifold. The dockside hookup took roughly 30 minutes per hose. Two product samples are taken—one at the beginning of flow and one after the tank has been topped. It was observed that the worker drawing the sample would check it for color and smell and then feel the liquid with his fingers. A typical deck watch consisted of one deck officer, one able-bodied seaman, and two ordinary seamen.

SUMMARY OF SITE VISIT

Terminal B

Observation 4

1.   Vessel Description – three 10,000-bbl chemical barges

2.   Cargos Loaded

Product	Quantity (bbl)	Average Loading Rate (bbl/hr)
Sol 140	2,900	~490
Cyclo Sol 53	2,600	~2,080
Tolusol 5	3,450	~1,800
Benzene	~20,000	

3.   Electrostatic Grounding System

The electrical grounding for all barges was the same as described in Terminal B–Observation 3.

4.   Cargo Loading Method

The products loaded were accomplished by the open drop method of loading. One barge accepted the first three products mentioned in the above list, while the remaining two barges took on benzene. The three-product barge had three separate product valves. Each product pipe branched off to port and starboard tanks. The single product barge had a single product valve and piping which also branched off into port and starboard tanks. The internal piping dropped down to within 1/2 in. of the bottom of each tank. Initially the products were pumped in by gravity until the outlet was submerged, at which time the shore pumps were started. Both hose connections on barge and dock had drip pans located beneath them to catch any spills. Dock side valves were initially bled of pressure prior to removal of blind flanges for hose connection by opening a bleed valve located between valve stem and blind flange. After the tanks are filled, the dock product valves were closed and the same bleed valves were opened to allow the remaining product in the hose to siphon into the barge tank. The barge valve was then closed and the hose disconnected. Any unsiphoned liquid remaining in the hose was drained through the dock bleed valve by raising the detached end of the hose with a boom. The dock disconnection was made and the hose positioned along the dock.

5.   Cargo Gauging Techniques

As was done in Terminal C–Observation 5, sight checking without tapes was performed on these barges through the ullage ports (8 in. ID) to determine approximate ullages. Communication between the barge tankerman and the dock supervisor occurred periodically to assure that loading proceeded properly. In fact, the reason for the slow loading rate of the Sol 140 was determined in this way. By notifying the tank farm, the normal loading rate was established and filling continued. During the loading, samples on the dock side, as well as on barge, were taken at the start and end of

loading. The sampling location on the dock was through the dock product bleed valve. Product samples were obtained on the barge by filling a 2-gallon container that was lowered into the tank by a chain. Final ullages were taken using a Lufkin tape through the ullage port.

6.   Vent System Configuration

Atop each tank was an ullage dome containing the ullage port hatch and a P/V valve. During loading, venting was through the ullage port with the flame screen in place. The elevation of the ullage port above the deck was approximately 3 ft.

7.   Measured Concentrations

No vapor concentrations were monitored during this observation. However, it was mentioned by the dock personnel that another independent research group and an individual from the Terminal B environmental section had taken some air samples on a barge that had been loading benzene during the previous day.

8.   Safety and Health Precautions

The following items pertain to this terminal observation.

a.   A letter describing protective equipment to be worn during loading of toxic chemicals was displayed in the dock office.

b.   A list of emergency equipment was displayed in the dock office. Fresh air masks were not listed, and none were found in boxes marked for their storage.

c.   Dockmen boarding the barge wore life jackets. The tankermen did not.

d.   Dockmen operating the dock benzene loading valve to load the two benzene barges wore cannister-type respirators and goggles, but not rubber gloves. The barge tankerman did not wear a respirator or rubber gloves even when gauging tanks that were nearly full.

e.   Two mechanics worked on the diesel engine onboard the benzene barges during filling without life jackets, respirators, or rubber gloves.

f.   After one barge was filled with benzene, the double length hose (~60 ft long) was suspended in the air and drained through the pressure bleed valve into the open drip pan. Benzene was observed draining for several minutes, but men on the dock (including SwRI personnel) were not instructed to wear respirators. A steady flow (perhaps >1 gal/minute) of benzene was observed again through the pressure bleed valve during loading of the second barge. Since the hose was not disconnected from the

B-21

dock loading valve, after loading the first barge, the pressure bleed valve may have remained open after the connection to the second barge loading valve was made and the tank farm pumps were started.

g.   Tankermen usually obtain chemical safety cards from the Terminal B office that give information on the chemicals to be loaded. These cards are usually displayed on a vertical board on the barge deck, but none were displayed on any of the barges being loaded.

9.   Personnel

During loading, the following personnel are present on the dock or barge:

a.   Tankerman: Works for an independent tankerman service; not a Terminal B employee. He supervises loading, sees that samples of cargo are taken, gauges depth of cargo by sight (no tape). His work station is usually on board the barge, but he crosses the gangway to the dock from time to time. He is present in the dock area at all times.

b.   Dockman: Terminal B employee. He supervises the dockside activities and operates the boom during hookup and disconnection. He contacts the tank farm to start and stop loading. His work station is on the dock at all times.

c.   *Cargo Inspector:* Terminal B employee. He took samples of the cargo onboard the barge just after pumping began (one sample of each product in a 2-gallon can). The can was lowered with a chain through an opened ullage hatch into the cargo and was brought up again when full. Filling procedure required the hatch to be open (~1 minute) and took another set of samples when the tanks were fully loaded. He was present in the dock area only for cargo inspection.

d.   Two Dockhands: Terminal B employees. They board the barge to connect and disconnect the hoses to the loading valves. They remove the blind flanges from the dock loading valves, open the pressure bleed valve, operate the compressed air torque wrenches that open the dockside valves, and take 1-quart samples of each product through the pressure bleed valves for analysis. Once their services were no longer required, these men left for another dock area.

B-22

SUMMARY OF SITE VISIT

Terminal C

Observation 5

1.   **Vessel Description** - a ten-barge integrated tow, five barges long and two abreast. The four end barges contained ten tanks, and the six middle barges contained eight tanks.

2.   **Cargos Loaded**

Product	Quantity (bbls)	Average Loading Rate (bbls/hr)
Unleaded gas		
Heating oil	(Quantity and rate data not available	
Turbo fuel	as of publication date)	
Diesel oil		

3.   **Electrostatic Grounding System**

Each individual barge was electrostatically connected through each of its loading hoses. Those barges which were on the outboard side were connected to the dock side barge via loading hose and crossover piping on dock side barge.

4.   **Cargo Loading Method**

The products were loaded by closed drop system similar, but on a smaller scale as mentioned in Terminal A-Observation 2. There were two drops per barge which descended to about 5 ft below the deck and ran fore and aft of the barge, then branched off to respective tanks. Each tank had its own main product valve and stripping line valve accessible on the deck. Dock hoses were connected between dock and dock side barge. Outboard barges were loaded through dock hoses which connected to inboard barge piping (separate from inboard barge product line) which crossed over to another loading hose which was connected to the outboard barge. All communications were done by yelling to dock personnel, and if none were visible, a pull activated buzzer accessible to the barge crew on the side of the dock would be sounded if the barge crew needed assistance. This, in fact, was used to alert dock crew of a particular leak that had developed between a loading hose area and a product valve flange. After subsequent stoppage of product flow, a gasket was replaced and pumping of product resumed. Leakage during disconnection flowed into a 4 ft x 8 ft x 1 ft drip pan located beneath the flanges.

5.   **Cargo Gauging Techniques**

Gauging on the barges was done by draft. There was no use of tapes or other mechanical devices except at the end of the loading. Periodic sight checking by barge crew through open ullage ports and, in some cases, open hatch, was done by relating ullage with some internal tank component (i.e., rung of a ladder). At the end of loading, refinery personnel would

come aboard the barge and obtain final tank ullage by introducing a Lufkin
tape into a 3-in. I.D. standpipe which ascended about 3 ft above each tank.
Also at this time, samples of the product and its temperature would be tak-
en and recorded.

6.   Vent System Configuration

Each tank had its own P/V valve which extended off the side of the
ullage dome and vertically up to a height of about 7 ft. However, during
loading, venting was accomplished through ullage ports (9-3/8 in. ID), and
on some barges through the ullage hatch, which is oval shaped and has a
total cross-section area of approximately 450 square inches. The ullage
port contained single layer flange screens which at various times were not
set properly in place. There were no flame screens over the ullage hatch.
On one occasion, venting velocity through one ullage port was taken with a
torsional anemometer.

7.   Atmospheric Conditions

> Air temperature = 59°F to 65°F
> Relative humidity = 76 to 66%
> Water temperature = 45°F
> Wind speed = variable 13-18 mph to 5 mph
> Wind direction = starboard to port and stern to bow
> Weather = partly cloudy to clear

8.   Photographic Documentation

A 16-mm motion picture camera having a 75-mm lens was set up atop an
elevated dock house which was approximately 300 to 400 ft in front of the
nearest barge. Both time lapse (12 frames per minute) and normal 24 fps
filming was done during the observation period. Filming was directed to-
ward barge crew activity during loading. Also, a pan of the dock and dock
activity was accomplished.

9.   Safety and Health Precautions

The following items pertain to this terminal observation:

a.   All dock workers wore gloves, hard hats, and safety glasses
      while performing hose hookup and disconnection.

b.   All deck workers wore gloves and life jackets. No hard hats
      or safety glasses were worn.

c.   Emergency pump shutdown switches were accessible both on the
      dock and a portable connection on the tow barge deck/

d.   Numerous unused dock product valves were leaking either past
      the blind flanges on the valve or through the stem of the
      valve into the dock drip pan.

10. **Personnel**

   a.   Dock personnel activity usually occurred during hose hookup or disconnection. In addition, during our visit, a change of grade and a repair of a leaking connection were observed. For hose connection, three dock workers are involved, one working a boom and the other two flanging up the hoses. Disconnection of a hose was observed during a change of grade. The same number of personnel were involved. On this particular occasion, the hose was in previous use transferring a different product. Upon final unbolting of the flange, approximately 5 gallons of gasoline gushed out of the hose onto the dock. Although the dock product valve contained a bleed valve that could have drained this spilled liquid into a drain pan, it was not opened. While the other product valve blind was being removed and prepared for this hose, it was observed to have a continual leak past the valve while the hose was being flanged up to it. Another observation was made of a repair of a leaky flange connection on the barge deck. Again, a total of three dock workers were involved.

   b.   Barge crew activity consisted primarily of sight checking of product level during loading. A total of one chief mate, two tankermen, and four unlicensed seamen were involved. The C/M and two tankermen had responsibility for three barges each. (The tenth barge had been towed to the shipyards for further cleaning since it had not passed inspection.) In addition to checking the product level, another task that was performed was the winching of slack lines between adjacent barges as they were being filled. While the barge crew was not performing one of the above duties, they would usually sit down in the vicinity of where their last task was performed, and more often than not this location would be within a 2-3 ft distance downwind of the venting vapors.

DISCUSSIONS WITH CHEMICAL TERMINAL AND SHIP PERSONNEL

During visits to the various chemical terminals, both for general discussions and for observation of cargo transfer activities, discussions were held with supervisory personnel and with the dock and ship's crew responsible for the cargo transfer operations. It is to be noted that nearly all of these individuals were cooperative and expressed a willingness to work with us on this project. Individual opinions on what was believed to be the most hazardous aspects of the chemical terminal and tanker (barge) operation were also provided.

Several recurring comments were given by company management personnel in each of several chemical terminals. These comments included the following.

o   In the history of the company, they were not aware of any health problems resulting in permanent disability to any terminal employees as a result of vapor exposure. They indicated that company records would substantiate these claims; however, such health data could not be released due to legal implications.

o   Because of the recent government (Coast Guard, EPA) emphasis on reducing spills to zero levels and the associated penalties, there is a greater tendency on the part of tanker personnel to stick their heads in hatches to observe the ullage during tank filling. Therefore, a greater exposure to chemical vapors is being experienced by tankermen today than before the spill concern evolved. Personnel in several companies believed that while the problems associated with liquid cargo spills have been reduced, the exposure of tankermen to chemical vapors has been increased. As a result, one problem has been reduced at the expense of increased tankerman exposure.

o   Several members of chemical company management believe that one of the more difficult problems in operating a terminal was correct training and supervision of dock and ship's crew. They stated that the level of education of these people was low and, therefore, training was a problem. They stated that the equipment and rules for terminal transfer operations were sufficient to ensure that a safe operation could be undertaken; however, because of the problems with personnel, many times operating procedures were ignored or mental mistakes occurred which created unsafe conditions.

o   Another problem that was pointed out by terminal management was the fact that in many cases tanks are gauged by independent tankermen not under the jurisdiction of company rules and practices. These people often work extended periods of time loading as many as 2 to 6 barges (tankers) in succession in a terminal before quitting work. A typical operation can involve a tankerman being on duty as long as 48 hours taking only short periods to sleep between tanker loadings, usually in the back seat of his car. Because of this practice, numerous instances were reported from various terminals where tankermen had fallen asleep while on the job. In one instance it was
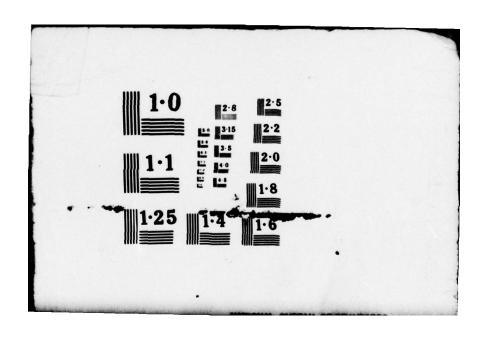
o   reported that a tankerman went to sleep leaning against an
     expansion trunk while the cargo overflowed onto his feet
     and the deck, thus waking him up.

o   It was pointed out that some ships now have a 2-inch lip
     welded around the perimeter of the shipdeck to contain any
     spilled cargo. While this reduces the possibility for an
     official spill, the spill would cover a portion of the deck
     with ship's cargo which workers must then mop up and remove.
     Therefore, workers are once again unduly exposed to chem-
     icals and other petroleum products in an attempt to elim-
     inate spills.

o   In all terminals, company management was asked about the his-
     tory of fires resulting from the loading of chemicals and/or
     petroleum products on tankers and barges. In most of the
     terminals visited, some type of fire had occurred during the
     history of terminal operation. These fires ranged from minor
     to catastrophic with significant loss of property and injury
     to workers. In each case, fires were attributed to improper
     application of operating procedures or equipment malfunctions,
     and in several instances were related to spills during loading.
     It was stated that, considering the few fires that had occurred
     over the time frame in which the terminals had operated, the
     potential for flammability hazards had effectively been re-
     duced as much as practicable through proper operational pro-
     cedures, associated safety equipment, and the limiting of
     potential ignition sources.

Several interesting comments were also obtained from dock and ship's
crew in chemical terminals. These include the following:

o   One dock worker who had worked in the same terminal for over 30
     years, indicated that he was not aware of any dock workers who
     had ever had a permanent disability or serious health incident
     from exposure to vapors while working in the terminal. He was
     aware of some exposure to chemicals due to spills and other im-
     proper handling; however, as far as he was aware, these workers
     recovered with no serious side effects or permanent disabilities.

o   One dock worker indicated that company safety rules on the use
     of respirators and gloves were often ignored at the discretion
     of the individual worker. In the case of some chemicals, the
     workers felt that they were dangerous enough that respirators
     and gloves should always be worn; however, for certain other
     chemicals, gloves and respirators were worn only on certain
     occasions. He indicated this was general operational practice
     for all the workers in that dock area.

o   Ship's crew indicated the same response that management indicated
     with regard to the emphasis on reducing spills. They also stated
     that they spend more time now observing cargo ullage during filling
     and the Chief Mates take a much greater role in the gauging of
     cargo tanks than prior to the time when spills were of such great

significance. They also indicated that they believe that this practice results in a greater exposure to chemical vapors.

o   Ship's crew also indicated that tank entry provides a situation in which extremely dangerous vapors can exist. Several experiences were related about men becoming unconscious in tanks and having to be hauled to the surface by co-workers. All shipboard workers indicated that they did not like to enter tanks unless absolutely necessary.

o   Workers also told of mopping and mucking tanks when a change of cargo grade was to be made. Mops tied to ropes were lowered from the deck into the tank. After the mops had absorbed residual cargo on the tank bottom, they were withdrawn from the tank, and the chemical was manually squeezed from the mop into a bucket. They indicated that this practice provided enough exposure that they became "drunk" from the vapors.

APPENDIX C

ANALYTICAL PLUME RISE
AND
PLUME DISPERSION METHODS

ANALYTICAL PLUME RISE AND PLUME DISPERSION METHODS

o   Turner's (B-122) correlation for rise height of negatively buoyant jets in quiescent surroundings is

$$Z_m = CM^{3/4} F_2^{-1/2} = C(\pi r^2 u^2)^{3/4} (\pi g \frac{(\rho-\rho_1)}{\rho_1} r^2 u)^{-1/2}$$

$$= C\pi^{-3/4} V \Delta^{-1/2} r^{-3/2} \qquad\qquad (C.1)$$

where

Z_m = maximum rise height

M = jet momentum flux

F_2 = buoyancy flux

C = numerical constant

u = jet velocity

$V = \pi r^2 u$ = volumetric flow rate

$\Delta = g (\rho-\rho_1)/\rho_1$

r = jet radius

g = gravitational constant

ρ, ρ_1 = density at jet exit and at rest, respectively.

Turner gives a value of 1.85 (dimensionless) to C, but this value does not fit the data reported in Figure 5 of his paper, which appears to support a value of $C = 3.1$. Equation (C.1) should be used with caution until this discrepancy is resolved.

o   Kamotani and Greber's (B-118) correlation for rise height of a
        turbulent jet in cross flow.

This correlation takes the simple form

$$Z_v/d = a_v(x/d)^{b_v} \qquad \text{(C.2)}$$

where

Z_v is the jet centerline elevation,

d   is the vent or nozzle diameter,

x   is the downstream location, and

a_v and b_v are functions of momentum ratio given in
        graph form for values of   J   from 4 to 570.

J   is the ratio of jet momentum to crossflow momentum

$$J = (\rho u^2)_{jet}/(\rho u^2)_o$$

where

u   is the velocity, and

ρ is the density.

Over the limited range of $15 \leq J \leq 60$ and $0 \leq x/D \leq 20$, the data
can be represented by the equation

$$\frac{Z_v}{d} = 0.89 \ J^{0.47} \ (x/d)^{0.36} \qquad \text{(C.3)}$$

It may be expected that Kamotani and Greber's correlation will predict
the initial rise of forced plumes up to a maximum downstream distance
of $x/d \sim 20$.   After that, buoyancy effects will begin to dominate.

o   Briggs' (B-10) plume rise equation when both momentum and buoyancy are significant.

$$Z = 3^{1/3} \left\{ \left[F_m x / (\tfrac{1}{3} + R^{-1})^2 u^2 \right] + \left[Fx^2 / 2(0.5)^2 u^3 \right] \right\}^{1/3} \qquad (C.4)$$

In this equation,

Z is the plume rise height

$$F_m = \frac{\pi/4 \; d^2 \; \rho_j \; u_j^2}{\pi \rho} \qquad \text{is the momentum flux, and}$$

$$F = g \frac{d^2}{4} \; u_j \; \frac{(\rho - \rho_j)}{\rho} \qquad \text{is the buoyancy flux .}$$

Also, u =   wind velocity

u_j =   jet velocity

d =   orifice diameter

R =   velocity ratio = u_j/u

Z =   plume centerline elevation

x =   downwind distance

ρ =   atmospheric density

ρ_j =   jet density.

Equation (II.4) applies to plume rise in unstratified surroundings and uses empirical guidance for the entrainment of surrounding air by the plume. In the first stage of rise, the characteristic plume radius is assumed proportional to height, $r = \gamma z$ and $\gamma = \tfrac{1}{3} + R^{-1}$. For the second, buoyant, stage of growth, there is no evidence that γ depends on R, so a constant value $\gamma = 0.6$ is used. Note that for a plume having negative buoyancy, F becomes negative and acts to reduce the height below that predicted by the momentum term alone.

o   Hoult, Fay and Forney's (B-48) method for numerically com-
     puting plume development

A system of differential equations for conservation of mass,
momentum and energy (or chemical species) are solved simultaneously
to predict plume development. It is assumed that the *actual velocity*,
density and/or concentration profiles in the plume are geometrically
similar along the plume axis and can be replaced by equivalent
"*top hat*" profiles (constant average value across the plume width).
The differential equations are

$$\frac{d}{ds} (\pi b^2 u \rho) = 2\pi b \alpha \rho_o \left| u - v \cos \theta \right| + 2\pi b \beta \rho_o \left| \sin \theta \right| \tag{C.5}$$

for conservation of mass, where the terms on the right represent en-
trainment due to parallel and cross-flow, respectively;

$$\frac{d}{ds} (\pi b^2 u^2 \rho) - v \cos \theta \frac{d}{ds} (\pi b^2 u \rho) = (\rho_o - \rho) \pi b^2 g \sin \theta \tag{C.6}$$

for the momentum equation in the s-streamwise direction;

$$\pi b^2 u^2 \rho \frac{d\theta}{ds} = -v \sin \theta \frac{d}{ds} (\pi b^2 u \rho) + (\rho_o - \rho) \pi b^2 g \cos \theta \tag{C.7}$$

for the momentum equation in the transverse direction.

An equation for buoyancy is still required, and it may take the
form of conservation of energy for thermally buoyant plumes, or con-
servation of chemical species together with an equation of state for a
chemical vapor and air mixture. Hoult, Fay and Forney replace the local
plume density ρ with the density at stack height, ρ_1, when calculat-
ing mass and momentum fluxes, and assume that temperature differences
are small so that $(\rho - \rho_o)/\rho_1 = (T_o - T)/T_1$ and write an equation for
conservation of energy as

$$\frac{d}{ds} \left[\pi b^2 u (\rho - \rho_o) g \right] = -\pi b^2 u g (d \rho_o^* / dz) \sin \theta \tag{C.8}$$

where $b(s) =$ plume radius

         $u(s) =$ plume velocity

         $v =$ wind velocity

$$\alpha \;=\; \text{entrainment parameter} = 0.12 \text{ for top hat profiles}$$

α = entrainment parameter = 0.12 for top hat profiles

β = entrainment parameter = 0.60 for top hat profiles

$\rho(s)$ = plume density

ρ_0 = atmospheric density at altitude z

ρ_0^* = potential density of the atmosphere

$\left(\dfrac{d\rho_0^*}{dz} = 0 \text{ for neutrally stable atmosphere} \right)$

θ = tangent angle between plume axis and horizon.

The height and downstream location of the plume center are calculated as

$$z = \int_0^s \sin\theta \; ds \tag{C.9}$$

$$x = \int_0^s \cos\theta \; ds \tag{C.10}$$

These equations must be integrated on a computer. However, the authors state that the solution requires that the plume trajectory be parabolic near a stack ejecting finite amounts of mass, momentum and energy into a neutral atmosphere with no wind shear. Then

$$Z = [R/(\beta + \alpha R)]^{\frac{1}{2}} \; (\ell_m x)^{\frac{1}{2}} \tag{C.11}$$

where ℓ_m is a momentum length scale $= b_i R = b_i \dfrac{u_i}{v_i}$. Far downstream, the solution of Equations (C.5) to (C.10) gives a plume rise obeying a 2/3 power law

$$Z = (3/2\beta^2)^{\frac{1}{3}} \; \ell_b^{\frac{1}{3}} \; x^{\frac{2}{3}} \tag{C.12}$$

where ℓ_b is a buoyancy length scale $= u_i \, b_i^2 \, [(T_i - T_1)/T_1]g/v^3$. Equation (C.12) can be shown to be identical (except for a constant factor) to the buoyancy dominant term in Briggs' Equation (C.4). Hence, it would be expected that numerical solutions to Equations (C.5) to (C.10) will approach Briggs' Equation (C.4) at some downstream location where momentum effects are negligible.

o   Ooms' (B-76) method for numerically computing plume devemopment.

Ooms' approach is similar to Hoult, Fay and Forney (B-48) as he derives a set of differential equations for conservation of mass, momentum and either chemical species or energy. Ooms also assumes that profiles of concentration, velocity defect and density are geometrically similar along the plume axis, but he gives the profiles a Gaussian Shape.

For concentration

$$C(s,r,\theta) = C^* \ e^{-r^2/\lambda^2 b^2} \quad , \tag{C.13}$$

for velocity defect

$$u(s,r,\theta) - U_a \cos \theta = u^* \ e^{-r^2/b^2} \quad , \tag{C.14}$$

and for density

$$\rho(s,r,\theta) = \rho^* \ e^{-r^2/\lambda^2 b^2} \quad , \tag{C.15}$$

where

    s   =   streamwise location along the plume centerline

    r   =   radial location normal to the plume centerline

    b(s) = characteristic plume width (the plume radius is defined
             arbitrarily as the value of $r = b\sqrt{2}$ where the velocity
             defect has a value equal to e^{-2} of the centerline value)

    λ^2 =   a turbulent Schmidt number which accounts for the small
             difference in plume radius between the velocity profile and
             the concentration or density profile.

    $C^*(s)$, $u^*(s)$, and $\rho^*(s)$ are values of concentration, velocity
                            defect, and density on the plume centerline

    U_a =   wind velocity

    θ =   tangent angle between the plume axis and the horizon.

Oom's equations are

$$\frac{d}{ds}\left(\int_0^{b\sqrt{2}} \rho u 2\pi r \ dr\right) = 2\pi b \rho_a \left\{\alpha_1 \left|u^*(s)\right| + \alpha_2 U_a \left|\sin \theta\right|\cos \theta \right.$$
$$\left. + \alpha_3 \ u^- \right\} \tag{C.16}$$

for mass conservation where the terms on the righthand side represent the entrainment due to shear between the plume and the wind, the entrainment typical for a line thermal, and the entrainment due to atmosphere turbulence;

$$\frac{d}{ds}\left(\int_{0}^{b\sqrt{2}} C u \, 2\pi r \, dr\right) = 0 \tag{C.17}$$

for conservation of chemical species;

$$\frac{d}{ds}\left(\int_{0}^{b\sqrt{2}} \rho u^2 \cos\theta \, 2\pi r \, dr\right) = 2\pi b \rho_a \, U_a \left\{\alpha_1 \left| u^* \right| + \right.$$

$$\left. + \alpha_2 \, U_a \left|\sin\theta\right| \cos\theta + \alpha_3 \, u^- \right\} + C_d \, \pi b \rho_a \, U_a^2 \left|\sin^3\theta\right| \tag{C.18}$$

for conservation of momentum in the x-direction, and

$$\frac{d}{ds}\left(\int_{0}^{b\sqrt{2}} \rho u^2 \sin\theta \, 2\pi r \, dr\right) = \int_{0}^{b\sqrt{2}} g(\rho_a - \rho) \, 2\pi r \, dr$$

$$\pm \, C_d \, \pi b \rho_a \, U_a^2 \, \sin^2\theta \, \cos\theta \tag{C.19}$$

for conservation of momentum in the y-direction. The + sign applies for $-\pi/2 \leq \theta \leq 0$, and the - sign for $0 \leq \theta \leq \pi/2$.

Values given for the entrainment constants are $\alpha_1 = 0.057$, $\alpha_2 = 0.5$, and $\alpha_3 = 1.0$ which are appropriate for Gaussian profiles. The drag coefficient C_d used to give the increase in impulse due to a drag force of the wind on the plume has a value of 0.3 which would be appropriate for flow over a circular cylinder, at a Reynolds number greater than 5×10^5.

The ambient density ρ_a can be varied with elevation as desired to simulate conditions of density stratification. Equations (C.16) through (C.19) may be integrated together with Equations (C.9) and (C.10) to obtain the plume trajectory.

o   teRiele's method (B-139) for numerically computing the atmospheric
         dispersion of gases emitted at or near ground level.

         teRiele's method was developed to predict the dispersion of gas
emitted from an area source at ground level. A set of differential equa-
tions is derived for conservation of mass and horizontal momentum. An
equation for conservation of vertical momentum is not employed, and
teRiele's method is restricted to plumes near the ground that do not rise
or fall. The method is used in conjunction with plume dispersion methods
to continue the computation of development for a negatively buoyant plume
that has fallen to ground level from an elevated source.

         teRiele assumes the shape of the concentration profile. Down-
wind of the area source this profile takes on the form

$$C = C_A \exp \left[- \left(\frac{z}{\sigma_z} \right)^s \right] \quad \text{for} \ |y| < b \tag{C.20}$$

and

$$C = C_A \exp \left[- \left(\frac{|y| - b}{\sigma_y} \right)^r - \left(\frac{z}{\sigma_z} \right)^s \right] \quad \text{for} \ |y| \geq b \tag{C.21}$$

where $C(x,y,z)$ is the value of concentration downwind of the
                       area source

          $C_A(x)$ is the value of concentration in the middle of
                       the plume $(y < b)$ at ground level $(z = 0)$

          $b(x)$ is the width of a constant concentration region
                       of the plume

          $\sigma_y(x)$ is a horizontal dispersion coefficient

          $\sigma_z(x)$ is a vertical dispersion coefficient

          r is a profile constant equal to 2

          s is a profile constant equal to $1 + 2\alpha$

          α is the exponent in the power law representation
                       of wind speed as a function of height above the
                       ground

$$u_x = u_o \left(\frac{z}{z_o} \right)^\alpha \tag{C.22}$$

         teRiele derives four mass and momentum balances which are solved
simultaneously for C_A, b, σ_y and σ_z at each X location.

$$\int_0^{y_L} \left[\frac{\partial}{\partial x} \left[\int_0^\infty cu_x \, dz \right] \right] dy = \left[\int_0^\infty K_y \frac{\partial c}{\partial y} \, dz \right]_{y = y_L} + \int_0^{y_L} Q^* \, dy \qquad (C.23)$$

$$\frac{d}{dx} \left[\int_0^\infty \int_0^\infty cu_x^2 \, dy \, dz \right] = \int_0^\infty \frac{c_{gr}}{\rho_{gr}} \cdot \tau_0 \, dy \qquad (C.24)$$

In relation (C.23) the integral limit y_L, may take three different values, resulting in three different mass balances

(a) $y_L < b$, giving the mass balance for the middle part of the concentration profile, which is independent of y. This mass balance is only valid for $b > 0$.

(b) $y_L \rightarrow \infty$, giving the total mass balance.

(c) $y_L = b + \frac{1}{2} \sqrt{2} \, \sigma_y$, giving the mass balance necessary for the determination of σ_y.

Other variables are

$u_x(z)$ the wind speed

$K_y(z)$ an atmospheric dispersion coefficient

Q^* the flux of gas taken up into the atmospheric flow field from the area source

c_{gr} concentration at ground level

ρ_{gr} density at ground level

τ_0 shear stress at ground level upwind of the area source.

For use in combination with Ooms' plume dispersion method, is it possible to set $b = 0$, and to compute downwind values of C_A, σ_y and σ_z.

o   Point Source Gaussian Diffusion Equation (B-29) and (B-79).

The Gaussian diffusion equation for the spread of pollutants from a point source located at $x = 0$, $y = 0$, and $z = H$ by the action of atmospheric turbulence is

$$X(x,y,z,H) = \frac{Q}{2\pi\sigma_y\sigma_z U} \exp\left[-\frac{1}{2}\left(\frac{y}{\sigma_y}\right)^2\right]\left\{\exp\left[-\frac{1}{2}\left(\frac{z-H}{\sigma_z}\right)^2\right]\right.$$

$$\left. + \exp\left[-\frac{1}{2}\left(\frac{z+H}{\sigma_z}\right)^2\right]\right\} \tag{C.25}$$

where $X(x,y,z,H)$ is the concentration at a point x,y,z in space from an elevated source at height H,

Q is the emission source strength,

σ_y, σ_z are standard deviations of the Gaussian distribution,

U is the wind velocity.

Briggs' Equation (C.4) is used to estimate the plume rise height above the vent height to give the proper value of H.

The values of σ_y and σ_z may be taken from the EPA Workbook (B-29) for six different classes of atmospheric stability and downstream distance from the source. Equation (C.25) includes the ground effect by adding a second image source at $z = -H$. *This effectively increases the vapor con-centration near the ground when σ_z is the same order as $z + H$.*

APPENDIX D

COMPUTER PROGRAMS

1. LISTING OF ONDEK COMPUTER CODE

2. LISTING OF INPUT DATA AND SAMPLE OUTPUT FOR ONDEK COMPUTER CODE

3. LISTING OF TANK3 AND RKLDEQ COMPUTER CODES

4. SAMPLE OUTPUT FOR TANK3 COMPUTER CODE

5. LISTING OF DSPOT COMPUTER CODE

LISTING OF

ONDEK

COMPUTER CODE

```
        PROGRAM ONDEK(INPUT,OUTPUT,TAPE1 = INPUT,TAPE3=OUTPUT)
C****
C     THIS PROGRAM COMPUTES THE TRAJECTORY AND CONCENTRATION DISTRIBUTION
C     OF BUOYANT PLUMES EMITTED INTO AN ATMOSPHERIC BOUNDARY LAYER BASED ON
C     OOMS' METHOD (REFERENCE, G. OOMS, 'A NEW METHOD FOR THE CALCULATION
C     OF THE PLUME PATH OF GASES EMITTED BY A STACK', ATMOSPHERIC ENVIRON-
C     MENT, VOL 6, 1972) AND TE RIELE'S METHOD (REFERENCE, P.M.M. TE
C     RIELE, 'ATMOSPHERIC DISPERSION OF HEAVY GASES EMITTED AT OR NEAR
C     GROUND LEVEL', 2ND INTERNATIONAL SYMPOSIUM ON LOSS PREVENTION AND
C     SAFETY PROMOTION IN THE PROCESS INDUSTRIES, SEPT. 1977)
C
C     INPUT VARIABLES
C        S = STARTING VALUE OF PLUME PATH INTEGRATION, M
C        H = INTEGRATION STEP SIZE, M
C     SMAX = TERMINATION VALUE OF PLUME PATH INTEGRATION, M
C      INT = NUMBER OF INTEGRATIONS BETWEEN PRINT-OUTS
C        N = NUMBER OF SIMULTANEOUS DIFFERENTIAL EQUATIONS
C    YR(1) = INITIAL VALUE OF CONCENTRATION, KG/M**3
C    YR(2) = INITIAL VALUE OF PLUME CHARACTERISTIC RADIUS, M
C    YR(3) = INITIAL VALUE OF PLUME VELOCITY - WIND SPEED COMPONENT, M/S
C    YR(4) = INITIAL VALUE OF PLUME ANGLE WITH RESPECT TO HORIZON, RADIANS
C    YR(5) = INITIAL VALUE OF X, HORIZONTAL DISTANCE FROM VENT, M
C    YR(6) = INITIAL VALUE OF Y, VERTICAL HEIGHT ABOVE DECK, M
C       WM = MOLECULAR WEIGHT OF EMITTED GAS
C       PO = ATMOSPHERIC PRESSURE, PSI.
C       TO = ATMOSPHERIC TEMPERATURE, DEG RANKINE
C       UR = REFERENCE VELOCITY AT YREF, M/S
C     YREF = REFERENCE HEIGHT, M
C      CMF = MASS FRACTION OF TRACER GAS IN EMITTED GAS
C      TLV = TURBULENCE LEVEL
C     YCON = CONCENTRATION MEASURE HEIGHT, M
C      ALF = WIND PROFILE SHAPE FACTOR DEPENDENT UPON STABILITY CLASS
C      GAM = GAMMA FUNCTION OF (1+2*ALF)**-1
C       IC = NUMBER OF CONCENTRATION VALUES FOR CONTOUR LINES, MAX=6
C     C(I) = CONCENTRATION VALUES FOR CONTOURS
C      DLA = CONSTANT FOR SIGMAY=DLA*X**BTA, FOR POINT SOURCE
C      BTA = CONSTANT FOR SIGMAY = DLA*X**BTA, FOR POINT SOURCE
C     YRUF = SURFACE ROUGHNESS PARAMETER, CENTIMETERS
      INTEGER COUNT, RUNGE, HAMING
      REAL APLACE(6),ADATE(3),ACLASS(5),AGAS(5)
      DIMENSION TE(6),YR(6),FR(6),Y(4,6),F(3,6),YRS(6),C(6),YC(6)
      COMMON/PHYS/DCDR,EPS,UPRI,ROA,ROE,G,YREF,UR,ALF,TAU,ZDECK,U10
      COMMON/CONS/IDECK,AF1,AF2,AF21,BTA,DLA,BT1,DBA,BM1,GAM
      COMMON/CON2/ROT
      G=9.80665
      DO 999 J1=1,5
C     ...... READ IN PARAMETERS AND INITIAL CONDITIONS .....
      READ(1,100) X,H,XMAX,INT,N,(YR(J),J=1,6)
      READ(1,110) (APLACE(J),J=1,6),(ADATE(J),J=1,3),(AGAS(J),J=1,5)
      READ(1,101) WM,PO,TO,UR,YREF,CMF,TLV,YCON
      READ(1,111) (ACLASS(J),J=1,5),ALF,GAM
      READ(1,112) IC,(C(J),J=1,IC)
      READ(1,113) DLA,BTA,YRUF,ZDECK
      UPRI=TLV*UR
      UA=UR
      DCDR=WM/(WM-28.96)
      ROA=PO*144.*28.96*16.0522/(1545.*TO)
```

```
      ROE=ROA*WM/28.96
      TRACON=YR(1)*CMF
      IDECK = 1
      CONH1=0.
      XCON=YR(5)
C***  COMPUTE SHEAR STRESS, TAUO - MAYBE ACCURATE FOR NEUTRAL FLOW ONLY
      U10=UR*((10.+ZDECK)/YREF)**ALF
      ZP= ALOG(1000./YRUF)
      TAU =0.16*U10*U10/(ZP*ZP)
C***  COMPUTE CONSTANTS FOR TE RIELE'S METHOD
      AF1=1.+ALF
      AF2=2*ALF
      AF21=1.+AF2
      BT1=1./BTA
      DBA=DLA**BT1
      BM1=1.-BT1
      ROT=(1.-ROA/ROE)/ROA
      TAUO=TAU*ROA
      GCON=0.8862269255*AF21/GAM
C     ..... PRINT PARAMETERS, HEADING AND INITIAL CONDITIONS .....
      WRITE(3,210) (APLACE(J),J=1,6),(ADATE(J),J=1,3)
      WRITE(3,211) P0,T0,UR,YREF,(ACLASS(J),J=1,5),ALF,TLV
      WRITE(3,212) (AGAS(J),J=1,5),CMF,WM,YR(1)
      WRITE(3,213) (C(J),J=1,IC),YCON
      WRITE(3,214) H,XMAX,INT
      WRITE(3,215)
      EPS=0.0000000001
C     ..... INITIALIZE STEP COUNTER AND FIRST ROW OF Y MATRIX .....
C     ..... SET INITIAL TRUNCATION ERRORS TO ZERO .....
      COUNT = 0
      DO 2 J=1,N
      TE(J) = 0.
    2 Y(4,J) = YR(J)
C     ..... CALL RUNGE TO INTEGRATE ACROSS FIRST THREE STEPS .....
    3 IF (RUNGE(N,YR,FR,X,H) .NE. 1) GO TO 4
      CALL RHS(YR,YRS)
      DO 91 K=1,4
   91 FR(K)=YRS(K)
      FR(5)= COS(YR(4))
      FR(6)= SIN(YR(4))
      GO TO 3
C     ..... PUT APPROPRIATE INITIAL VALUES IN THE Y AND F MATRICES .....
    4 COUNT = COUNT + 1
      ISUB = 4 - COUNT
      DO 5 J=1,N
    5 Y(ISUB,J) = YR(J)
      CALL RHS(YR,YRS)
      DO 93 K=1,4
   93 F(ISUB,K)=YRS(K)
      F(ISUB,5)= COS(YR(4))
      F(ISUB,6)= SIN(YR(4))
C     ..... PRINT SOLUTIONS AFTER EVERY INT STEPS .....
    6 CONTINUE
      IF (Y(1,6).LT.0.) GO TO 500
      IF (COUNT/INT*INT .NE. COUNT) GO TO 7
      IF (COUNT.LE.3) GO TO 7
      TRACON = Y(1,1)*CMF
C****
```

```
C      COMPUTE CONH1
       B2=Y(1,2)*Y(1,2)*1.35
       CR1=Y(1,6)-YCON
       CZ1=CR1*CR1/B2
       IF (CZ1.GT.13.81) GO TO 50
       CR2=Y(1,6)+YCON
       CZ2=CR2*CR2/B2
       XCON=Y(1,5)
       CONH1=Y(1,1)*CMF*( EXP(-CZ1) + EXP(-CZ2))
       GO TO 51
   50  XCON = Y(1,5)
       CONH1=0.
   51  CONTINUE
       CALL CONT(C,YC,Y,1,IC,0.,0.,0.,0.,YCON)
       IF (COUNT.GT.3) WRITE(3,216) X,Y(1,5),Y(1,6),Y(1,1),CONH1,XCON,
      1(YC(I),I=1,6),Y(1,2),Y(1,3),Y(1,4)
C      ..... IF X EXCEEDS XMAX, TERMINATE INTEGRATION .....
    7  IF (X.GT.XMAX-H/2.) GO TO 999
C      ..... CALL RUNGE OR HAMING TO INTEGRATE ACROSS NEXT STEP .....
       IF ( COUNT.LT.3 ) GO TO 3
C      ..... CALL HAMING (PREDICTION OR CORRECTION) .....
    8  M = HAMING(N,Y,F,X,H,TE)
       DO 94 K=1,4
   94  YR(K)=Y(1,K)
       CALL RHS(YR,YRS)
       DO 95 K=1,4
   95  F(1,K)=YRS(K)
       F(1,5)= COS(Y(1,4))
       F(1,6)= SIN(Y(1,4))
       IF (M.EQ.1) GO TO 8
C      ..... INCREMENT STEP COUNTER AND CONTINUE INTEGRATION .....
       COUNT = COUNT + 1
       GO TO 6
  500  CONTINUE
C***   TRANSITION TO TE RIELE'S METHOD
       IDECK = 0
C      Y(1,1)=2*Y(1,1)...CA=2*C ON PLUME CENTER LINE
       YR(1) = 2*Y(1,1)
C      Y(1,2)=1.161895*Y(1,2)...SIGMAY=LAMDA*PLUME CHARACTERISTIC WIDTH
       YR(2) =1.161895*Y(1,2)
C      Y(1,3)=Y(1,2)*GCON...SIGMAZ=SIGMAY*GCON
       YR(3) =Y(1,2)*GCON
       IDECK=0
       WRITE(3,217)
       COUNT = 0
       DO 502 J=1,3
       TE(J) = 0.
  502  Y(+,J) = YR(J)
C      ..... CALL RUNGE TO INTEGRATE ACROSS FIRST THREE STEPS .....
  503  IF (RUNGE(3,YR,FR,X,H) .NE. 1) GO TO 504
       CALL RHS(YR,YRS)
       DO 591 K=1,3
  591  FR(K)=YRS(K)
       GO TO 503
C      ..... PUT APPROPRIATE INITIAL VALUES IN THE Y AND F MATRICES .....
  504  COUNT = COUNT + 1
       ISUB = 4 - COUNT
       DO 505 J=1,3
```

```
  505 Y(ISUB,J) = YR(J)
      CALL RHS(YR,YRS)
      DO 593 K=1,3
  593 F(ISUB,K)=YRS(K)
C     ..... PRINT SOLUTIONS AFTER EVERY INT STEPS
  506 IF (COUNT/INT*INT .NE. COUNT) GO TO 507
      CALL CONT(C,YC,Y,0,IC,2.,ALF21,Y(2),Y(3),YCON)
      IF (COUNT.GT.3) WRITE(3,218) X,(Y(1,J),J=1,3),(YC(K),K=1,6)
C     ..... IF X EXCEEDS XMAX, TERMINATE INTEGRATION
  507 IF (X.GT.XMAX-H/2.) GO TO 999
C     ..... CALL RUNGE OR HAMING TO INTEGRATE ACROSS NEXT STEP
      IF ( COUNT.LT.3) GO TO 503
C     ..... CALL HAMING (PREDICTION OR CORRECTION) .....
  508 M= HAMING(3,Y,F,X,H,TE)
      DO 594 K=1,3
  594 YR(K)=Y(1,K)
      CALL RHS(YR,YRS)
      DO 595 K=1,3
  595 F(1,K)=YRS(K)
      IF (M.EQ.1) GO TO 508
C     ..... INCREMENT STEP COUNTER AND CONTINUE INTEGRATION .....
      COUNT = COUNT + 1
      GO TO 506
  999 CONTINUE
C     ..... FORMATS FOR INPUT AND OUTPUT STATEMENTS .....
  100 FORMAT( 5X, F10.4, 10X, F10.6, 12X, F10.4/ 5X, I5, 15X, I2/
     1   (20X, 4F12.5))
  101 FORMAT(5X,F7.3,5X,F6.3,5X,F5.1,5X,F6.3,7X,F5.2,6X,F8.6,5X,F5.3/
     1 7X,F6.4)
  110 FORMAT(10X,6A4,6X,3A4,8X,5A4)
  111 FORMAT(16X,5A4,12X,F5.2,15X,F12.9)
  112 FORMAT(4X,I2,1X,6(4X,F8.6))
  113 FORMAT(25X,F9.7,6X,F9.7,6X,F7.3,7X,F6.2)
  210 FORMAT(1H1, 7H PLACE=,6A4,6H DATE=,5A4//)
  211 FORMAT(30H0    METEOROLOGICAL CONDITIONS//7X,22H0 BAROMETRIC PRESS
     1URE=,F7.3,25H PSIA    AIR TEMPERATURE=,F5.1,6H DEG R/7X,22H0   AVER
     2AGE WIND SPEED=,F7.3,25H M/S AT REFERENCE HEIGHT=,F7.3,2H M/7X,22H
     30     STABILITY CLASS=,5A4,12HWIND FACTOR=,F6.2/7X,22H0    TURBULE
     4NCE LEVEL=,F6.2//)
  212 FORMAT(28H   VAPOR VENTING CONDITIONS//7X,22H0         EMITTED GA
     1S=,5A4,26H TRACER GAS MASS FRACTION=,F9.6/7X,22H0    MOLECULAR WEI
     2GHT=,F7.3,24H OF GAS AND AIR MIXTURE/7X,22H0  VENT CONCENTRATION=
     3,F10.6,15H KG/CUBIC METER//)
  213 FORMAT(61H    VALUES OF CONCENTRATION CHOSEN FOR CONCENTRATION CON
     1TOURS//7X,10H0    C1 =,F10.6/7X,10H0    C2 =,F10.6/7X,10H0     C
     23 =,F10.6/7X,10H0    C4 =,F10.6/7X,10H0    C5 =,F10.6/7X,10H0
     3  C6 =,F10.6/7X,29H0   PREDICTED FOR A HEIGHT OF,F6.3,24H METERS A
     4BOVE DECK LEVEL//)
  214 FORMAT(30H    NUMERICAL INTEGRATION DATA//7X,14H0    STEP SIZE=,F7.
     14,38H METERS,    MAXIMUM DOWNWIND DISTANCE=,F7.2,7H METERS/7X,50H0
     2    NUMBER OF INTEGRATION STEPS BETWEEN PRINT OUT=,I3)
  215 FORMAT(1H1,56H   BEGIN PLUME COMPUTATION THROUGH THE AIR ABOVE THE
     1DECK/1H0,4H   S,7X,3HXCL,6X,3HZCL,7X,3HCCL,8X,5HCZCON,6X,4HXCON,3X
     2,60H0Y C1    YC2     YC3     YC4     YC5     YC6      B    U*    THETA/1
     3H ,120H METERS    METERS    METERS   KG/M**3    KG/M**3    METERS
     4METERS METERS METERS METERS METERS METERS METERS M/S   RADIAN/)
  216 FORMAT(/F7.2,2(2X,F7.2),2(2X,E10.4),1X,F7.2,7(1X,F6.2),2(1X,F6.3))
  217 FORMAT(//43H   CONTINUE PLUME COMPUTATION ALONG THE DECK//98H X(MET
```

D-5

```
     1ERS) CA(KG/M3) SIGMAY(M) SIGMAZ(M) Y1(M)    Y2(M)     Y3(M)     Y
    24(M)     Y5(M)     Y6(M)  )
218 FORMAT(F7.2,3X,F9.6,1X,F7.3,7(3X,F7.3))
    END
```

```
      INTEGER FUNCTION HAMING( N,Y,F,X,H,TE)
      LOGICAL PRED
      DIMENSION YPRED(20), TE(N), Y(4,N), F(3,N)
      DATA PRED / .TRUE. /
C
C     ..... IS CALL FOR PREDICTOR OR CORRECTOR SECTION .....
      IF (.NOT.PRED) GO TO 4
C
C     ..... PREDICTOR SECTION OF HAMING .....
C     ..... COMPUTE PREDICTED Y(J) VALUES AT NEXT POINT .....
      DO 1 J=1,N
    1 YPRED(J) = Y(4,J) + 4.*H*(2.*F(1,J) - F(2,J) + 2.*F(3,J))/3.
C
C     ..... UPDATE THE Y AND F TABLES .....
      DO 2 J=1,N
      DO 2 KS=1,3
      K = 5 - KS
      Y(K,J) = Y(K-1,J)
    2 IF (K.LT.4) F(K,J) = F(K-1,J)
C
C     ..... MODIFY PREDICTED Y(J) VALUES USING THE TRUNCATION ERROR
C     ..... ESTIMATES FROM THE PREVIOUS STEP.  INCREMENT X VALUE
      DO 3 J=1,N
    3 Y(1,J) = YPRED(J) + 112.*TE(J)/9.
      X = X + H
C
C     ..... SET PRED AND REQUEST UPDATED DERIVATIVE VALUES .....
      PRED = .FALSE.
      HAMING = 1
      RETURN
C
C     ..... CORRECTOR SECTION OF HAMING
C     ..... COMPUTE CORRECTED AND IMPROVED VALUES OF THE Y(J) AND SAVE
C     ..... TRUNCATION ERROR ESTIMATES FOR THE CURRENT STEP .....
    4 DO 5 J=1,N
      Y(1,J) = (9.*Y(2,J)-Y(4,J) + 3.*H*(F(1,J)+2.*F(2,J)-F(3,J)))/8.
      TE(J) = 9.*(Y(1,J) - YPRED(J))/121.
    5 Y(1,J) = Y(1,J) - TE(J)
C
C     ..... SET PRED AND RETURN WITH SOLUTIONS FOR CURRENT STEP .....
      PRED = .TRUE.
      HAMING = 2
      RETURN
      END
```

```fortran
        INTEGER FUNCTION RUNGE(N,Y,F,X,H)
        DIMENSION PHI(50), SAVEY(50), Y(N), F(N)
        DATA M/0/
C
        M = M + 1
        GO TO (1,2,3,4,5), M
C
C       ..... PASS 1 .....
    1   RUNGE = 1
        RETURN
C
C       ..... PASS 2 .....
    2   DO 22 J=1,N
        SAVEY(J) = Y(J)
        PHI(J) = F(J)
   22   Y(J) = SAVEY(J) + 0.5*H*F(J)
        X = X + 0.5*H
        RUNGE = 1
        RETURN
C
C       ..... PASS 3 .....
    3   DO 33 J= 1,N
        PHI(J) = PHI(J) + 2.0*F(J)
   33   Y(J) = SAVEY(J) + 0.5*H*F(J)
        RUNGE = 1
        RETURN
C
C       ..... PASS 4 .....
    4   DO 44 J= 1,N
        PHI(J) = PHI(J) + 2.0*F(J)
   44   Y(J) = SAVEY(J) + H*F(J)
        X = X + 0.5*H
        RUNGE = 1
        RETURN
C
C       ..... PASS 5 .....
    5   DO 55 J = 1,N
   55   Y(J) = SAVEY(J) + (PHI(J) + F(J))*H/6.0
        M = 0
        RUNGE = 0
        RETURN
        END
```

```fortran
      REAL FUNCTION SIMUL(N,A,X,EPS,INDIC,NRC)
      DIMENSION IROW(15),JCOL(15),JORD(15),Y(15),A(NRC,NRC),X(N)
C
      MAX=N
      IF (INDIC.GE.0) MAX=N+1
C     ...BEGIN ELIMINATION PROCEDURE...
      DETER=1
      DO 18 K=1,N
      KM1=K-1
C     ...SEARCH FOR THE PIVOT ELEMENT...
      PIVOT=0.
      DO 11 I=1,N
      DO 11 J=1,N
C     ...SCAN IROW AND JCOL ARRAYS FOR INVALID PIVOT SUBSCRIPTS...
      IF (K.EQ.1) GO TO 9
      DO 8 ISCAN=1,KM1
      DO 8 JSCAN=1,KM1
      IF (I.EQ.IROW(ISCAN)) GO TO 11
      IF (J.EQ.JCOL(JSCAN)) GO TO 11
    8 CONTINUE
    9 IF ( ABS(A(I,J)).LE. ABS(PIVOT)) GO TO 11
      PIVOT=A(I,J)
      IROW(K)=I
      JCOL(K)=J
   11 CONTINUE
C     ...INSURE THAT SELECTED PIVOT IS LARGER THAN EPS...
      IF ( ABS(PIVOT).GT.EPS) GO TO 13
      WRITE(3,202)
      SIMUL=0.
      RETURN
C     ...UPDATE THE DETERMINANT VALUE...
   13 IROWK=IROW(K)
      JCOLK=JCOL(K)
      DETER=DETER*PIVOT
C     ...NORMALIZE PIVOT ROW ELEMENTS...
      DO 14 J=1,MAX
C     ...CARRY OUT ELIMINATION AND DEVELOP INVERSE...
   14 A(IROWK,J)=A(IROWK,J)/PIVOT
      A(IROWK,JCOLK)=1./PIVOT
      DO 18 I=1,N
      AIJCK=A(I,JCOLK)
      IF (I.EQ.IROWK) GO TO 18
      A(I,JCOLK) = -AIJCK/PIVOT
      DO 17 J=1,MAX
   17 IF (J.NE.JCOLK) A(I,J)=A(I,J)-AIJCK*A(IROWK,J)
   18 CONTINUE
C     ...ORDER SOLUTION VALUES (IF ANY) AND CREATE JORD ARRAY...
      DO 20 I=1,N
      IROWI=IROW(I)
      JCOLI=JCOL(I)
      JORD(IROWI)=JCOLI
   20 IF (INDIC.GE.0) X(JCOLI)=A(IROWI,MAX)
C     ...ADJUST SIGN OF DETERMINANT...
      INTCH=0
      NM1=N-1
      DO 22 I=1,NM1
      IP1=I+1
```

```
      DO 22 J=IP1,N
      IF (JORD(J).GE.JORD(I)) GO TO 22
      JTEMP=JORD(J)
      JORD(J)=JORD(I)
      JORD(I)=JTEMP
      INTCH=INTCH+1
   22 CONTINUE
      IF (INTCH/2*2.NE.INTCH) DETER=-DETER
C     ...IF INDIC IS POSITIVE RETURN WITH RESULTS...
      IF (INDIC.LE.0) GO TO 26
      SIMUL=DETER
      RETURN
C     ...IF INDIC IS NEGATIVE OR ZERO, UNSCRAMBLE THE INVERSE
C         FIRST BY ROWS...
   26 DO 28 J=1,N
      DO 27 I=1,N
      IROWI=IROW(I)
      JCOLI=JCOL(I)
   27 Y(JCOLI)=A(IROWI,J)
      DO 28 I=1,N
   28 A(I,J)=Y(I)
C     ...THEN BY COLUMNS...
      DO 30 I=1,N
      DO 29 J=1,N
      IROWJ=IROW(J)
      JCOLJ=JCOL(J)
   29 Y(IROWJ)=A(I,JCOLJ)
      DO 30 J=1,N
   30 A(I,J)=Y(J)
C     ...RETURN FOR INDIC NEGATIVE OR ZERO..
      SIMUL=DETER
      RETURN
  202 FORMAT(37H0SMALL PIVOT - MATRIX MAY BE SINGULAR)
      END
```

```
      SUBROUTINE RHS(Y,C)
      DIMENSION Y(6),A(5,5),B(4,4),C(4),D(3)
      COMMON/PHYS/DCDR,EPS,UPRI,ROA,ROE,G,YREF,UR,ALF,TAU,ZDECK,UIN
      COMMON/CONS/IDECK,AF1,AF2,AF21,BTA,DL1,BT1,DRA,BM1,GAM
C*** TEST IDECK
C        IDECK=1, PLUME CENTERLINE ABOVE DECK...USE OOMS' EQUATIONS
C        IDECK=0, PLUME IS ON THE DECK...USE TE RIELE'S EQUATIONS
      IF (IDECK.EQ.0) GO TO 100
C*** OOMS EQUATIONS FOR GAUSSIAN PROFILES AND VARIABLE DENSITY
      ST= SIN(Y(4))
      ST2=ST*ST
      CT= COS(Y(4))
      CT2=CT*CT
      UA=UR*((Y(6)+ZDECK)/YREF)**ALF
      UA2=UA*UA
      UACT=UA*CT
      UAST=UA*ST
      Y12=Y(1)*Y(2)
      Y33=Y(3)*Y(3)
      ROC=Y(1)/DCDR
      ROCA=ROC/ROA
      AC1=0.772699*UACT+0.412442*Y(3)
      AC2=(1.043144*UACT + 0.556796*Y(3))/ROA
      AC3=(1.043144*UACT*UACT + 1.113593*UACT*Y(3) + 0.363346*Y33)/ROA
      AM1=2.*UACT*UACT + 1.729329*UACT*Y(3) + 0.490842*Y33
      AM2=Y(2)*(1.729329*UACT+0.991684*Y(3)+ROCA*(1.113593*UACT
     1    +0.726692*Y(3)))
C*** CONSERVATION OF SPECIES
      A(1,1)=Y(2)*AC1
      A(1,2)=2.*Y(1)*AC1
      A(1,3)=0.412442*Y12
      A(1,4)=-0.772699*Y12*UAST
      A(1,5)=0.
C*** CONSERVATION OF MASS
      A(2,1)=Y(2)*AC2/DCDR
      A(2,2)=2.*(2.*UACT + 0.864665*Y(3) + ROC*AC2)
      A(2,3)=Y(2)*(0.864665 + 0.556796*ROCA)
      A(2,4)=Y(2)*UAST*(-2. -1.043144*ROCA)
      A(2,5)=2.*(0.052* ABS(Y(3)) + 0.5*UACT* ABS(ST) + UPRI)
C*** CONSERVATION OF X-MOMENTUM
      A(3,1)=Y(2)*AC3*CT/DCDR
      A(3,2)=2.*(AM1 + AC3*ROC)*CT
      A(3,3)=CT*AM2
      A(3,4)=Y(2)*ST*(-4.*UACT*UACT-3.458658*UACT*Y(3)-0.490842*Y33
     1   -ROCA*(3.129432*UACT*UACT+2.227186*UACT*Y(3)+0.363346*Y33))
      A(3,5)=UA*A(2,5)+0.3*UA2* ABS(ST*ST*ST)
C*** CONSERVATION OF Y-MOMENTUM
      A(4,1)=Y(2)*ST*AC3/DCDR
      A(4,2)=2.*ST*(AM1 + AC3*ROC)
      A(4,3)=ST*AM2
      A(4,4)=Y(2)*(2.*UA2*CT*(1.-3.*ST2)+1.729329*UA*Y(3)*(CT2-ST2)
     1       +0.490842*Y33*CT + ROCA*(1.043144*UA2*CT*(1.-3.*ST2)
     2       +1.113593*Y(3)*(UA*(CT2-ST2) + 0.363346*Y33*CT))
      IF (ST.LT.0.) GO TO 40
      SIG=-1.
      GO TO 45
40    SIG=1.
```

```
   45 CONTINUE
      A(4,5)=-1.043144*ROCA*Y(2)*G + SIG*0.3*UAST*UAST*CT
C***     SIMUL USED FOR MATRIX INVERSION
      DETER=SIMUL(4,A,C,EPS,1,5)
      RETURN
  100 CONTINUE
C***  TE PIELE'S EQUATIONS FOR PLUME DEVELOPMENT ALONG THE DECK
      Y12=Y(1)*Y(2)
      Y13=Y(1)*Y(3)
      Y23=Y(2)*Y(3)
C***  MASS CONSERVATION EQUATION, YL=INFINITY
      B(1,1)=Y23
      B(1,2)=Y13
      B(1,3)=AF1*Y12
      B(1,4)=0
C***  MASS CONSERVATION EQUATION, YL=Y(2)*.7071
      B(2,1)=0.605009*Y23
      B(2,2)=0.176127*Y13
      B(2,3)=0.605009*Y12*AF1
      B(2,4)=-0.4288819*DBA*BTA*Y13*(Y(2)**BM1)
C**** MOMENTUM CONSERVATION EQUATION
      CALL CSUM(Y(1),CSUM1)
      CL=(U10*U10/AF21)*((0.01*Y(3))**AF2)
      CR=Y12*TAU*CSUM1
      B(3,1)=CL*Y23
      B(3,2)=CL*Y13
      B(3,3)=CL*Y12*AF21
      B(3,4)=CR
C***     SIMUL USED FOR MATRIX INVERSION
      DETER=SIMUL(3,B,D,EPS,1,4)
      DO 110 I=1,3
  110 C(I)=D(I)
      RETURN
      END
```

```
      SUBROUTINE CONT(CC,YC,Y,IDECK,INUM,PR,PS,SIGY,SIGZ,YCON)
      DIMENSION CC(9),YC(9),Y(4,6)
C*** THIS SUBROUTINE COMPUTES THE Y-LOCATIONS OF CURVES OF CONSTANT
C      CONCENTRATION CC1 THROUGH CC9.
      DO 9 I=1,INUM
    9 YC(I)=0.
C
C      FIRST TEST TO DECIDE WHETHER OOMS OR TE RIELES MODEL WILL BE USED
C
      IF (IDECK.EQ.0) GO TO 100
C          OOMS' MODEL FOR CONCENTRATION PROFILE
      ZS = Y(1,6) - YCON
      ZSQ = ZS*ZS
      YLM2 = 1.35*Y(1,2)*Y(1,2)
      ZSA = ZSQ/YLM2
      IF (ZSA.GT.13.91) GO TO 95
      ZI = Y(1,6) + YCON
      ZIQ = ZI*ZI
      ZIA = ZIQ/YLM2
      DK =  EXP(-ZSA) +  EXP(-ZIA)
      DO 90 I=1,INUM
C*** TEST WHETHER CC(I) IS GREATER THAN MAX CONCENTRATION AT MAN HEIGHT
      CRAT = CC(I)/(Y(1,1)*DK)
      IF (CRAT.GE.1.0) GO TO 90
C*** COMPUTE Y-LOCATION OF CONTOUR
      YCSQ = - YLM2  * ALOG(CRAT)
      YC(I) =  SQRT(YCSQ)
   90 CONTINUE
   95 RETURN
  100 CONTINUE
C*** TE RIELE'S MODEL FOR CONCENTRATION PROFILE
      RV=1/PR
      ZPW=(YCON/SIGZ)**PS
      IF (ZPW.GT.13.81) GO TO 950
      DO 900 I=1,INUM
C*** TEST WHETHER CC(I) IS GREATER THAN CONCENTRATION AT MAN HEIGHT
      CRAT = CC(I)/(Y(1,1)*EXP(-ZPW))
      IF (CRAT.GE.1.0) GO TO 900
C*** COMPUTE Y-LOCATION OF CONTOUR
      YC(I) = SIGY * ((- ALOG(CRAT))**RV)
  900 CONTINUE
  950 RETURN
      END
```

```
      SUBROUTINE CSUM(CA,SUM1)
C***  THIS SUBROUTINE COMPUTES THE SUM OF A SERIES THAT ARISES IN
C     TE RIFLE'S CONSERVATION OF MOMENTUM EQUATION.
      COMMON/CON2/ROT
      SUM=1.
      I=1
      A=ROT+CA
      XO=-1.+A
      X1=1.
    1 CONTINUE
      X1=X1*XO
      I=I+1
      ANUM=1./SQRT(1.*I)
      X=X1*ANUM
      SUM1=SUM+X
      IF (ABS(X).LT.0.000001) GO TO 3
      SUM=SUM1
      IF (I.GT.50) GO TO 2
      GO TO 1
    2 WRITE(3,10)
    3 RETURN
   10 FORMAT(32H  NUMBER OF TERMS IN CSUM EXCEEDED 50)
      END
```

LISTING OF INPUT DATA

AND SAMPLE OUTPUT FOR

ONDEK

COMPUTER CODE

LIST OF INPUT DATA FOR ONDEK

Variable Name	Format	Purpose	Units
S	F10.4	Starting value of plume path integration	m
H	F10.6	Integration step size	m
SMAX	F10.4	Termination value of plume path integration	m
INT	I5	Number of integrations between printouts	--
N	I2	Number of simultaneous differential equations	--
YR(1)	F12.5	Initial value of concentration	kg/m^3
YR(2)	F12.5	Initial value of plume characteristic radius	m
YR(3)	F12.5	Initial value of plume velocity minus wind speed component	m/s
YR(4)	F12.5	Initial value of plume angle with respect to the horizon	radians
YR(5)	F12.5	Initial value of x, horizontal distance from vent	m
YR(6)	F12.5	Initial value of y, vertical height above deck	m
APLACE	6A4	Place name	--
ADATE	3A4	Date	--
AGAS	5A4	Composition of vent gas mixture	--
WM	F7.3	Molecular weight of vent gas mixture	kg/mole
PO	F6.3	Atmospheric pressure	psia
TO	F5.1	Atmospheric temperature	°R
UR	F6.3	Reference wind velocity at YREF	m/s
YREF	F5.2	Reference height for UR	m
CMF	F8.6	Mass fraction of tracer gas in vent gas mixture	--
TLV	F5.3	Turbulence level	--
YCON	F6.4	Concentration measurement height above the deck	m

LIST OF INPUT DATA FOR ONDEK

Variable Name	Format	Purpose	Units
ACLASS	5A4	Atmospheric stability class	--
ALF	F5.2	Wind profile power law exponent-depends on stability class	--
GAM	F12.9	Gamma function-depends on stability class	--
IC	I2	Number of concentration values for contour lines, max = 6	--
C(1)...C(IC)	F8.6	Values of concentration for contour lines	kg/m^3
DLA	F9.7	Constant for point source dispersion coefficient-depends on stability class	--
BTA	F9.7	Constant for point source dispersion coefficient-depends on stability class	--
YRUF	F7.3	Surface roughness parameter	cm
ZDECK	F6.2	Height of deck above shore line	m

SAMPLE DATA CARDS FOR ONDEK

S =   0.0000   H =   0.050000   SMAX =   35.0000

INT =   6   M =   6

YR(1)...YR(2)=   0.19764   0.10027   2.09374   1.06656

YR(5)...YR(6)=   0.07620   1.41300

PLACE NAME VARIATION TEST 1   DATE MAR 16.1979 VENT GAS HEXANE VAPOR/AIR

WM=   31.830 FC= 14.700 TC= 505.0 UR=   1.119 YREF= 10.00 CMF= 1.000000 TLV= .200

YCON= 1.6764

STABILITY CLASS   NEUTRAL   WIND PROFILE 0.14 GAMMA FUNCTION 1.19997434C

IC= 6   C1=0.091881 C2=0.003753 C3=0.001979 C4=0.000379 C5=0.000199 C6=0.000039

DISPER PARAMETERS.DELTA= 0.176918 BETA=0.911794 YRUF= 1.000 ZDECK= 10.00

VALUES OF WIND PROFILE AND DISPERSION COEFFICIENTS

USED IN ONDEK

Stability Class	ALF	GAM	DLA	BTA
(A) Unstable	0.02	1.02372 0105	0.781212	0.862711
(D) Neutral	0.14	1.18597 4340	0.176877	0.911784
(F) Stable	0.28	1.40211 3754	0.090873	0.907854

LIST OF OUTPUT DATA FOR ONDEK

Variable Name	Purpose	Units
S	Distance along plume path	m
XCL	Horizontal location of plume centerline	m
ZCL	Vertical location of plume centerline above deck	m
CCL	Concentration on plume centerline	kg/m^3
CZCON	Concentration at concentration measurement height downwind of vent	kg/m^3
XCON	Location downwind of vent where CZCON is estimated	m
YC1... YC6	Crosswind location where concentration is equal to C1...C6 at concentration measurement height	m
B	Plume characteristic radius	m
U*	Value of plume velocity minus wind speed component	m/s
THETA	Plume angle with respect to horizon	radians

SAMPLE OUTPUT FROM ONDEK

(on following pages)

PLACE= VARIATION TEST 1   DATE=MAR 16,1979
    METEOROLOGICAL CONDITIONS

        0 BAROMETRIC PRESSURE= 14.700 PSIA   AIR TEMPERATURE=505.0 DEG R
        0 AVERAGE WIND SPEED= 1.118 M/S AT REFERENCE HEIGHT= 10.000 M
        0   STABILITY CLASS=   NEUTRAL   WIND FACTOR=   .14
        0   TURBULENCE LEVEL=   .20

VAPOR VENTING CONDITIONS

        0   EMITTED GAS= HEXANE VAPOR/AIR   TRACER GAS MASS FRACTION= 1.000000
        0   MOLECULAR WEIGHT= 31.830 OF GAS AND AIR MIXTURE
        0 VENT CONCENTRATION= .187640 KG/CUBIC METER

VALUES OF CONCENTRATION CHOSEN FOR CONCENTRATION CONTOURS

        0   C1 =   .04128
        0   C2 =   .003753
        0   C3 =   .001876
        0   C4 =   .000375
        0   C5 =   .000188
        0   C6 =   .000038
        0   PREDICTED FOR A HEIGHT OF 1.676 METERS ABOVE DECK LEVEL

NUMERICAL INTEGRATION DATA

        0   STEP SIZE= .0500 METERS,   MAXIMUM DOWNWIND DISTANCE= 25.00 METERS
        0   NUMBER OF INTEGRATION STEPS BETWEEN PRINT OUT= 6

BEGIN PLUME COMPUTATION THROUGH THE AIR ABOVE THE DECK

S METERS	XCL METERS	ZCL METERS	CCL KG/M**3	CZCON KG/M**3	XCON METERS	YC1 METERS	YC2 METERS	YC3 METERS	YC4 METERS	YC5 METERS	YC6 METERS	B METERS	U* METERS M/S	THETA RADIAN
.30	.30	1.60	8.3730E-02	7.4005E-02	.30	.16	.37		.49	.52	.58	.18	.304	.443
.50	.59	1.70	5.1394E-02	5.1056E-02	.59	.13	.45	.49	.61	.66	.74	.24	.055	.248
.90	.88	1.76	3.6594E-02	3.9391E-02	.88	0.00	.49	.56	.70	.75	.86	.28	.001	.196
1.20	1.18	1.80	2.8039E-02	2.5100E-02	1.18	0.00	.52	.61	.77	.83	.96	.32	.015	.227
1.50	1.47	1.83	2.2471E-02	1.9533E-02	1.47	0.00	.54	.64	.84	.91	1.05	.36	-.019	.094
1.80	1.77	1.86	1.8564E-02	1.5483E-02	1.77	0.00	.56	.68	.89	.97	1.14	.40	-.020	.075
2.10	2.07	1.88	1.5581E-02	1.3321E-02	2.07	0.00	.57	.70	.95	1.04	1.22	.43	-.020	.062
2.40	2.37	1.90	1.3422E-02	1.1828E-02	2.37	0.00	.57	.73	1.00	1.10	1.29	.47	-.018	.050
2.70	2.67	1.91	1.1732E-02	9.9711E-03	2.67	0.00	.57	.75	1.05	1.16	1.37	.50	-.017	.044
3.00	2.97	1.92	1.0330E-02	8.8155E-03	2.97	0.00	.57	.77	1.10	1.21	1.44	.53	-.016	.037
3.30	3.27	1.93	9.1288E-03	7.8755E-03	3.27	0.00	.56	.79	1.14	1.27	1.51	.56	-.015	.032
3.60	3.57	1.94	8.2202E-03	7.0958E-03	3.57	0.00	.55	.80	1.19	1.32	1.58	.60	-.013	.028
3.90	3.87	1.95	7.4113E-03	6.9386E-03	3.87	0.00	.54	.81	1.23	1.37	1.65	.63	-.012	.024
4.20	4.17	1.96	6.7214E-03	5.8771E-03	4.17	0.00	.51	.82	1.27	1.42	1.72	.66	-.011	.022
4.50	4.47	1.96	6.1274E-03	5.3920E-03	4.47	0.00	.48	.83	1.31	1.47	1.78	.69	-.011	.020
4.80	4.77	1.97	5.6116E-03	4.9489E-03	4.77	0.00	.44	.83	1.35	1.52	1.85	.72	-.010	.018
5.10	5.07	1.97	5.1605E-03	4.5969E-03	5.07	0.00	.39	.82	1.38	1.56	1.91	.75	-.009	.016
5.40	5.37	1.98	4.7474E-03	4.2625E-03	5.37	0.00	.33	.81	1.42	1.61	1.97	.78	-.008	.015
5.70	5.67	1.98	4.4112E-03	3.9739E-03	5.67	0.00	.23	.80	1.45	1.65	2.04	.81	-.007	.014
6.00	5.97	1.99	4.0986E-03	3.7110E-03	5.97	0.00	0.00	.78	1.48	1.69	2.10	.84	-.006	.013
6.30	6.27	1.99	3.8185E-03	3.4743E-03	6.27	0.00	0.00	.76	1.51	1.73	2.16	.87	-.006	.012
6.60	6.57	1.99	3.5649E-03	3.2602E-03	6.57	0.00	0.00	.74	1.54	1.77	2.21	.90	-.005	.011
6.90	6.87	1.99	3.3338E-03	3.0659E-03	6.87	0.00	0.00	.71	1.57	1.81	2.27	.93	-.005	.010
7.20	7.17	2.00	3.1342E-03	2.8890E-03	7.17	0.00	0.00	.67	1.60	1.85	2.33	.96	-.005	.009
7.50	7.47	2.00	2.9494E-03	2.7272E-03	7.47	0.00	0.00	.63	1.63	1.89	2.39	.99	-.005	.008
7.80	7.77	2.00	2.7771E-03	2.5790E-03	7.77	0.00	0.00	.58	1.65	1.92	2.44	1.02	-.005	.007
8.10	8.07	2.00	2.6214E-03	2.4424E-03	8.07	0.00	0.00	.43	1.67	1.96	2.50	1.05	-.005	.006
8.40	8.37	2.00	2.4786E-03	2.3173E-03	8.37	0.00	0.00	.58	1.70	1.99	2.55	1.08	-.005	.005

LISTING OF

TANK3 AND RKLDEQ

COMPUTER CODES

```
      PROGRAM TANK3(INPUT,OUTPUT,TAPE10=INPUT,TAPE6=OUTPUT)
      REAL NU,MDOTB,M,MDOTHL,MDOTHW,MDOTG,MDOTXY,MDOTZY,MDOTXZ,L
      DIMENSION MDOTXY(900),MDOTZY(900),TAUXY(900),TAUZY(900),MDOTG(900)
     *,MDOTHL(900),MDOTHW(900),TIME(900),C(900),MDOTB(900)
C INPUT QUANTITIES AND DIMENSIONS
C      CO = INITIAL CONCENTRATION,PPM
C      L,W,H =LENGTH,WIDTH AND HEIGHT OF TANK IN METERS IN THE X,Y AND Z
C               DIRECTIONS, RESPECTIVELY
C      Q = DILUTION FLOW RATE,M3/MIN
C      M = LIQUID MOLECULAR WEIGHT,GM/MOLE
C      P = MEAN TANK PRESSURE,MM HG
C      TB = LIQUID BOILING TEMPERATURE,K
C      G = LIQUID SURFACE TENSION,DYNES/CM AT 20C
C      U = AIR VELOCITY ACROSS WALLS,CM/SEC
C      R = UNIVERSAL GAS CONSTANT,(CM3-MM HG)/(MOLE-K)
C      A,B = CURVE FIT COEFFICIENTS FOR LIQUID VAPOR PRESSURE AS A
C               FUNCTION OF TEMP. LN(PV)=A+BT, T(F),PV(PSIA)
C      ALPHA,BETA,GAMMA = CURVE FIT COEFFICIENTS ON WALL TEMP FOR WALLS
C               PARALLEL TO X-Y PLANE
C               TWALL(K)=ALPHA+BETA(Y)+GAMM(Y2), Y IN M
C      ZETA,ETA,THETA = CURVE FIT COEFFICIENTS ON WALL TEMP FOR WALLS
C               PARALLEL TO Y-Z PLANE
C               TWALL(K)=ZETA+ETA(Y)+THETA(Y2), Y IN M
C      TFILM = LIQUID CHEMICAL FILM THICKNESS ON VERTICAL WALLS, CM
C      TPOOL = THICKNESS OF LIQUID LAYER ON TANK BOTTOM, CM
C      TEMPERATURE AT TANK BOTTOM MUST BE EQUAL FOR BOTH TWALL DISTRIB.
C      C1,C2 = CURVE FIT COEFFICIENTS ON LIQUID DENSITY AS A FUNCTION OF
C               OF TEMP. RHOFILM(LB/FT3)=C1+C2(T), T(F)
C      DELTA,EPSILON,PHI = CURVE FIT COEFFICIENTS FOR KINEMATIC VISCOSITY
C               OF AIR(FT2/SEC) AS A FUNCTION OF TEMP(F) AT ATMOS. PRESS.
C               NU = DELTA +EPSILON(T)+PHI(T2)
C      TMAX = MAXIMUM TIME FOR DILUTION VENTILATION,MIN
C      DTIME =TIME INCREMENT BETWEEN SUCCESSIVE CONCENTRATION CALCS,MIN
C      STEP = NUMBER OF SUBDIVISIONS OF H, DY=H/STEP
C      NSTEP = INTEGER VALUE OF STEP
C      TGAS = GAS DISCHARGE TEMPERATURE(K)
C                       INTERNAL COMMENTS
C      MDOTXY(I) = LOCAL MASS FLUX ON SURFACES PARALLEL TO X-Y
C                  PLANE, GM/CM2-SEC
C      MDOTZY(I) = LOCAL MASS FLUX ON SURFACES PARALLEL TO Y-Z
C                  PLANE, GM/CM2-SEC
C      MDOTXZ = TOTAL MASS FLUX ON TANK BOTTOM, GM/CM2-SEC
C      TAUXY(I)= LOCAL TIME TO EVAPORATE TFILM ON SURFACES PARALLEL
C               TO X-Y PLANE,SEC
C      TAUZY(I) = LOCAL TIME TO EVAPORATE TFILM ON SURFACES PARALLEL
C               TO Y-Z PLANE,SEC
C      TAUB = TIME TO EVAPORATE TPOOL ON TANK BOTTOM,SEC
C
      READ(10,1010)L,W,H,M,P,TB,G,R,DTIME,STEP,A,B,C1,C2
      READ(10,1010)DELTA,EPSILON,PHI
      READ(10,1005)NSTEP
   10 READ(10,1000)
      IF(EOF(10))2000,20
   20 READ(10,1010)CO,Q,U,TFILM,TPOOL,TMAX,TGAS
      READ(10,1010)ALPHA,BETA,GAMMA
      READ(10,1010)ZETA,ETA,THETA
C
      V=L*W*H
      CO=CO*M/24.5
      WRITE(6,1000)
      WRITE(6,1015)L,W,H,V,CO,Q,P,TB,G,U,M,TFILM,TPOOL
C      CALCULATION OF MDOTXZ AND TAUB
```

D-26

```
           TO=ALPHA+BETA*H+GAMMA*(H**2)
           T=1.8*TO-460.0
           X=A+B*T
           PV=EXP(X)
           PV=PV*760./14.7
           D=0.425/P*SQRT(TGAS**3/(M*TB/G))
           NU=DELTA+EPSILON*T+PHI*(T**2)
           NU=NU*(2.54*12.)**2
           SC=NU/D
           POWER=0.625*(SC**0.3)
           FREC=0.217*(SC**(-0.9))*(SC*U)**POWER
           MDOTXZ=M*D*PV*FREC/(R*TGAS)
           RHOF=(C1+C2*T)*454.0/((12.*2.54)**3)
           TAUB=TPOOL*RHOF/MDOTXZ
           WRITE(6,1020)TO,PV,D,NU,SC,RHOF,MDOTXZ,TAUB,FREC
     C     CALCULATION OF MDOTXY(I),MDOTZY(I),TAUXY(I) AND TAUZY(I) VECTORS
           DY=H/STEP
           I=1
           Y=0.0
           WRITE(6,1022)
           WRITE(6,1024)
     100   TXY=ALPHA+BETA*Y+GAMMA*(Y**2)
           T=1.8*TXY-460.
           X=A+B*T
           PV=EXP(X)
           PV=PV*760./14.7
           D=0.425/P*SQRT(TGAS**3/(M*TB/G))
           NU=DELTA+EPSILON*T+PHI*(T**2)
           NU=NU*(12.*2.54)**2
           SC=NU/D
           POWER=0.625*(SC**0.3)
           FREC=0.217*(SC**(-0.9))*(SC*U)**POWER
           MDOTXY(I)=D*M*PV*FREC/(R*TGAS)
           RHOF=(C1+C2*T)*454./((12.*2.54)**3)
           TAUXY(I)=TFILM*RHOF/MDOTXY(I)
           WRITE(6,1026)Y,TXY,MDOTXY(I),TAUXY(I),D,NU,PV,SC,FREC
           I=I+1
           Y=Y+DY
           IF(Y-H)100,100,105
     C
     105   J=1
           Y=0.0
           WRITE(6,1028)
           WRITE(6,1030)
     110   TZY=ZETA+ETA*Y+THETA*(Y**2)
           T=1.8*TZY-460.
           X=A+B*T
           PV=EXP(X)
           PV=PV*760./14.7
           D=0.425/P*SQRT(TGAS**3/(M*TB/G))
           NU=DELTA+EPSILON*T+PHI*(T**2)
           NU=NU*(12.*2.54)**2
           SC=NU/D
           POWER=0.625*(SC**0.3)
           FREC=0.217*(SC**(-0.9))*(SC*U)**POWER
           MDOTZY(J)=D*M*PV*FREC/(R*TGAS)
           RHOF=(C1+C2*T)*454./((12.*2.54)**3)
           TAUZY(J)=TFILM*RHOF/MDOTZY(J)
           WRITE(6,1026)Y,TZY,MDOTZY(J),TAUZY(J),D,NU,PV,SC,FREC
           J=J+1
           Y=Y+DY
           IF(Y-H)110,110,115
```

```
      115 WRITE(6,1060)
      117 K=1
          TIME(K)=0.0
          NPOINT=NSTEP+1
      120 DO 125 I=1,NPOINT
          IF(TIME(K)*60.0.GT.TAUXY(I))MDOTXY(I)=0.0
          IF(TIME(K)*60.0.GT.TAUZY(I))MDOTZY(I)=0.0
      125 CONTINUE
          IF(TIME(K)*60.0.GT.TAUB)MDOTXZ=0.0
          MDOTB(K)=MDOTXZ*L*W*1.E04
          AREA=0.0
          DO 130 I=1,NSTEP
          AREA=AREA+DY*(MDOTXY(I)+MDOTXY(I+1))/2.0
      130 CONTINUE
          MDOTHL(K)=AREA*L*1.E04
          AREA=0.0
          DO 140 I=1,NSTEP
          AREA=AREA+DY*(MDOTZY(I)+MDOTZY(I+1))/2.0
      140 CONTINUE
          MDOTHW(K)=AREA*W*1.E04
          MDOTG(K)=MDOTB(K)+2.*(MDOTHL(K)+MDOTHW(K))
          K=K+1
          TIME(K)=TIME(K-1)+DTIME
          IF(TIME(K)-TMAX)120,120,150
C         RUNGE-KUTTA INTEGRATION OF CONCENTRATION DE
      150 K=1
          LPRINT=2
          JCOUNT=1
          C(K)=CO
      155 Y=C(K)
          DOTMG=MDOTG(K)
          F=(60000.*DOTMG/V)-Q*Y/V
          X=TIME(K)
          NT=0
      160 CONTINUE
          STUFF=RKLDE0(1,Y,F,X,DTIME,NT)
          CONC=Y
          DOTMG=MDOTG(K)-((TIME(K)-X)/(TIME(K)-TIME(K+1)))*(MDOTG(K)-MDOTG(K
         *+1))
          F=(60000.*DOTMG/V)-Q*CONC/V
          IF(STUFF.NE.2.0)GO TO 160
          K=K+1
          C(K)=CONC
          CRATIO=C(K)/CO
          CONC=CONC*24.5/M
          COR=Q*TIME(K)/V
          IF(JCOUNT-LPRINT)170,165,165
      165 WRITE(6,1070)TIME(K),CONC,CRATIO,COR,MDOTG(K),MDOTHL(K),MDOTHW(K),
         *MDOTB(K)
          JCOUNT=1
          GO TO 175
      170 JCOUNT=2
      175 IF(TIME(K)-TMAX)155,10,10
     1000 FORMAT(80H1         .
         1                              )
     1005 FORMAT(I4)
     1010 FORMAT(6E12.6)
     1015 FORMAT(1H0,9X,22HCOMMON TANK PARAMETERS/
         $         1H0,2X,14HTANK LENGTH(M),27X,F6.1/
         $              3X,13HTANK WIDTH(M),28X,F6.1/
         $              3X,14HTANK HEIGHT(M),27X,F6.1/
         $              3X,15HTANK VOLUME(M3),24X,F8.1/
```

```
     $           3X,28HINITIAL CONCENTRATION(MG/M3),10X,F9.1/
     $           3X,24HVENTILATION RATE(M3/MIN),17X,F6.1/
     $           3X,20HTANK PRESSURE(MM HG),21X,F6.1/
     $           3X,23HLIQUID BOILING POINT(K),18X,F6.1/
     $           3X,32HLIQUID SURFACE TENSION(DYNES/CM),9X,F6.1/
     $           3X,25HWALL AIR VELOCITY(CM/SEC),16X,F6.1/
     $           3X,23HLIQUID MOLECULAR WEIGHT,17X,F7.2/
     $           3X,9HTFILM(CM),32X,F6.2/
     $        .  3X,9HTPOOL(CM),32X,F6.2)
1020 FORMAT(1H0,9X,22HSUMMARY OF TANK BOTTOM/
     $        1H0,2X,20HFLOOR TEMPERATURE(K),21X,F6.1/
     $           3X,21HVAPOR PRESSURE(MM HG),20X,F6.1/
     $           3X,30HDIFFUSION COEFFICIENT(CM2/SEC),10X,F7.4/
     $           3X,35HKINEMATIC VISCOSITY OF AIR(CM2/SEC),2X,E10.4/
     $           3X,14HSCHMIDT NUMBER,23X,F10.4/
     $           3X,12HRHOF(GM/CM3),29X,F6.3/
     $           3X,18HMDOTXZ(GM/CM2-SEC),19X,E10.4/
     $           3X,9HTAUB(SEC),30X,F8.1/
     $           3X,11H1/F(CM**-1),30X,F6.3)
1022 FORMAT(1H1,57X,19HSUMMARY OF X-Y WALL)
1024 FORMAT(1H0,4X,4HY(M),10X,7HTEMP(K),5X,14HMDOTXY(G/C2-S),3X,11H TAU
     $XY(SEC),4X,10HD(CM2/SEC),5X,11HNU(CM2/SEC),5X,9HPV(MM HG),9X,2HSC,
     $9X,11H1/F(CM**-1))
1026 FORMAT(4X,F6.2,9X,F6.1,7X,E11.4,6X,F8.1,5X,F8.5,7X,F7.4,8X,F8.3,8X
     $,F6.3,9X,F8.4)
1028 FORMAT(1H1,57X,19HSUMMARY OF Y-Z WALL)
1030 FORMAT(1H0,4X,4HY(M),10X,7HTEMP(K),5X,14HMDOTZY(G/C2-S),3X,11H TAU
     $ZY(SEC),4X,10HD(CM2/SEC),5X,11HNU(CM2/SEC),5X,9HPV(MM HG),9X,2HSC,
     $9X,11H1/F(CM**-1))
1060 FORMAT(1H1,36X,47HTANK CONCENTRATION AND EVAPORATION RATE HISTORY/
     $         1H0,2X,9HTIME(MIN),5X,12HCONCENT(PPM),7X,4HC/CO,11X,4HQT/V,
     $         6X,13HMDOTG(GM/SEC),4X,14HMDOTHL(GM/SEC),4X,14HMDOTHW(GM/SE
     $C),4X,13HMDOTB(GM/SEC))
1070 FORMAT(4X,F6.2,9X,F8.0,7X,F6.3,10X,F6.2,7X,F9.3,8X,F9.3,9X,F9.3,9X
     $,F9.3)
2000 STOP
     END
```

```
      FUNCTION RKLDEQ(N,Y,F,X,H,NT)
C D2 UCSD RKLDEQ RUNGE-KUTTA-GILL LINEAR DIFFERENTIAL EQUATION SOLVER
C     D2 UCSD RKLDEQ
C     MODIFIED MAY 1963 (Q REMOVED FROM CALLING SEQUENCE)
C     TEST OF ALGOL ALGORITHM
      DIMENSION Y(1),F(1),Q(1)
C     REAL X,H--INTEGER N,NT--COMMENT--BEGIN INTEGER I,J,L-REAL A
      NT=NT+1
      GO TO (1,2,3,4),NT
C     GO TO S(NT)
  1   DO 11 J=1,N
  11  Q(J)=0.
      A=.5
      X=X+H/2.
      GO TO 5
  2   A=.29289321881
      GO TO 5
  3   A=1.7071067812
      X=X+H/2.
      GO TO 5
  4   DO 41 I=1,N
  41  Y(I)=Y(I)+H*F(I)/6.-Q(I)/3.
      NT=0
      RKLDEQ=2.
      GO TO 6
  5   DO 51 L=1,N
      Y(L)=Y(L)+A*(H*F(L)-Q(L))
  51  Q(L)=2.*A*H*F(L)+(1.-3.*A)*Q(L)
      RKLDEQ=1.
  6   CONTINUE
      RETURN
      END
```

SAMPLE OUTPUT FOR

TANK3

COMPUTER CODE

CHECKOUT RUN TANK3,TIME-DEPENDENT MDOT

COMMON TANK PARAMETERS

TANK LENGTH(M)	10.0
TANK WIDTH(M)	10.0
TANK HEIGHT(M)	10.0
TANK VOLUME(M3)	1000.0
INITIAL CONCENTRATION(MG/M3)	118530.6
VENTILATION RATE(M3/MIN)	151.5
TANK PRESSURE(MM HG)	760.0
LIQUID BOILING POINT(K)	329.4
LIQUID SURFACE TENSION(DYNES/CM)	23.7
WALL AIR VELOCITY(CM/SEC)	50.0
LIQUID MOLECULAR WEIGHT	58.08
TFILM(CM)	.20
TPOOL(CM)	.20

SUMMARY OF TANK BOTTOM

FLOOR TEMPERATURE(K)	294.4
VAPOR PRESSURE(MM HG)	195.0
DIFFUSION COEFFICIENT(CM2/SEC)	.0999
KINEMATIC VISCOSITY OF AIR(CM2/SEC)	.1511E+00
SCHMIDT NUMBER	1.5200
RHOF(GM/CM3)	.7910
MDOTXZ(GM/CM2-SEC)	.1964E-03
TAUA(SEC)	803.9
1/F(CM**-1)	3.204

D-33

CHECKOUT RUN TANK3,TIME-DEPENDENT MDOT

    COMMON TANK PARAMETERS

    TANK LENGTH(M)   10.0
    TANK WIDTH(M)   10.0
    TANK HEIGHT(M)   10.0
    TANK VOLUME(M3)   1000.0
    INITIAL CONCENTRATION(MG/M3)   118530.6
    VENTILATION RATE(M3/MIN)   151.5
    TANK PRESSURE(MM HG)   760.0
    LIQUID BOILING POINT(K)   329.4
    LIQUID SURFACE TENSION(DYNES/CM)   23.7
    WALL AIR VELOCITY(CM/SEC)   50.0
    LIQUID MOLECULAR WEIGHT   58.08
    TFILM(CM)   .20
    TPOOL(CM)   .20

        SUMMARY OF TANK BOTTOM

    FLOOR TEMPERATURE(K)   294.4
    VAPOR PRESSURE(MM HG)   195.0
    DIFFUSION COEFFICIENT(CM2/SEC)   .0994
    KINEMATIC VISCOSITY OF AIR(CM2/SEC)   .1511E+00
    SCHMIDT NUMBER   1.5200
    RHOF(GM/CM3)   .7911
    MDOTXZ(GM/CM2-SEC)   .1964E-03
    TAUR(SEC)   803.9
    L/F(CM**-1)   3.204

SUMMARY OF X-Y WALL

Y(M)	TEMP(K)	MDOTXY(G/C2-S)	TAUXY(SEC)	D(CM2/SEC)	NU(CM2/SEC)	PV(MM HG)	SC	1/F(CM**-1)
0.00	311.1	.9135E-03	373.2	.10800	.1695	389.852	1.569	3.2800
1.00	309.9	.3839E-03	402.9	.10713	.1676	363.750	1.565	3.2731
2.00	307.8	.3565E-03	434.9	.10627	.1658	339.346	1.560	3.2660
3.00	306.1	.3310E-03	464.5	.10540	.1640	316.673	1.556	3.2588
4.00	304.9	.3073E-03	506.9	.10454	.1621	295.471	1.551	3.2514
5.00	302.8	.2853E-03	547.3	.10368	.1603	275.688	1.546	3.2439
6.00	301.1	.2648E-03	591.0	.10282	.1585	257.230	1.541	3.2361
7.00	299.9	.2458E-03	634.2	.10197	.1566	240.008	1.536	3.2283
8.00	297.7	.2281E-03	689.2	.10112	.1548	223.934	1.531	3.2202
9.00	296.1	.2117E-03	749.3	.10027	.1530	208.946	1.525	3.2120
10.00	294.9	.1964E-03	803.9	.09942	.1511	194.956	1.520	3.2036

SUMMARY OF Y-Z WALL

Y(M)	TEMP(K)	MDOTZY(G/C2-S)	TAUZY(SEC)	D(CM2/SEC)	NU(CM2/SEC)	PV(MM HG)	SC	1/F(CM**-1)
0.00	311.1	.9135E-03	373.2	.10800	.1695	389.852	1.569	3.2800
1.00	309.9	.3839E-03	402.9	.10713	.1676	363.750	1.565	3.2731
2.00	307.8	.3565E-03	434.9	.10627	.1658	339.346	1.560	3.2660
3.00	306.1	.3310E-03	464.5	.10540	.1640	316.673	1.556	3.2588
4.00	304.9	.3073E-03	506.9	.10454	.1621	295.471	1.551	3.2514
5.00	302.8	.2853E-03	547.3	.10368	.1603	275.688	1.546	3.2439
6.00	301.1	.2648E-03	591.0	.10282	.1585	257.230	1.541	3.2361
7.00	299.9	.2458E-03	634.2	.10197	.1566	240.008	1.536	3.2283
8.00	297.7	.2281E-03	689.2	.10112	.1548	223.934	1.531	3.2202
9.00	296.1	.2117E-03	749.3	.10027	.1530	208.946	1.525	3.2120
10.00	294.9	.1964E-03	803.9	.09942	.1511	194.956	1.520	3.2036

TANK CONCENTRATION AND EVAPORATION RATE HISTORY

TIME(MIN)	CONCERAT(PPM)	C/CO	MDDTG(CM/SEC)	QT/V	MDDTHL(GM/SEC)	MDDTHH(GM/SEC)	MDDTAT(GM/SEC)
1.00	75000.	1.500	1368.153	.15	291.926	291.926	0.000
2.00	96503.	1.930	1368.153	.30	291.926	291.926	0.000
3.00	114472.	2.244	1368.153	.45	291.926	291.926	0.000
4.00	130449.	2.617	1368.153	.61	291.926	291.926	0.000
5.00	144493.	2.840	1368.153	.76	291.926	291.926	0.000
6.00	156218.	3.124	1368.153	.91	291.926	291.926	0.000
7.00	163650.	3.273	1127.887	1.06	232.859	232.859	0.000
8.00	163651.	3.273	852.900	1.21	169.113	169.113	0.000
9.00	159196.	3.184	729.988	1.36	133.385	133.385	0.000
10.00	151311.	3.026	504.971	1.52	78.380	78.380	0.000
11.00	140833.	2.817	411.661	1.67	53.803	53.803	0.000
12.00	129404.	2.542	320.417	1.82	30.992	30.992	0.000
13.00	117294.	2.358	235.739	1.97	9.822	9.822	0.000
14.00	104015.	2.080	0.000	2.12	0.000	0.000	0.000
15.00	89392.	1.788	0.000	2.27	0.000	0.000	0.000
16.00	76825.	1.537	0.000	2.42	0.000	0.000	0.000
17.00	66025.	1.321	0.000	2.54	0.000	0.000	0.000
18.00	56293.	1.135	0.000	2.73	0.000	0.000	0.000
19.00	47826.	.975	0.000	2.88	0.000	0.000	0.000
20.00	40911.	.838	0.000	3.03	0.000	0.000	0.000
21.00	34019.	.720	0.000	3.18	0.000	0.000	0.000
22.00	30855.	.619	0.000	3.33	0.000	0.000	0.000
23.00	26603.	.532	0.000	3.48	0.000	0.000	0.000
24.00	22864.	.457	0.000	3.64	0.000	0.000	0.000
25.00	19644.	.393	0.000	3.79	0.000	0.000	0.000
26.00	16447.	.338	0.000	3.94	0.000	0.000	0.000
27.00	15513.	.290	0.000	4.09	0.000	0.000	0.000
28.00	12273.	.249	0.000	4.24	0.000	0.000	0.000
29.00	10719.	.219	0.000	4.39	0.000	0.000	0.000
30.00	9212.	.184	0.000	4.55	0.000	0.000	0.000
31.00	7917.	.158	0.000	4.70	0.000	0.000	0.000
32.00	6804.	.136	0.000	4.85	0.000	0.000	0.000
33.00	5844.	.117	0.000	5.00	0.000	0.000	0.000
34.00	5026.	.101	0.000	5.15	0.000	0.000	0.000
35.00	4319.	.086	0.000	5.30	0.000	0.000	0.000
36.00	3712.	.072	0.000	5.45	0.000	0.000	0.000
37.00	3190.	.064	0.000	5.61	0.000	0.000	0.000
38.00	2742.	.055	0.000	5.76	0.000	0.000	0.000
39.00	2354.	.047	0.000	5.91	0.000	0.000	0.000
40.00	2025.	.040	0.000	6.06	0.000	0.000	0.000
41.00	1740.	.035	0.000	6.21	0.000	0.000	0.000
42.00	1496.	.030	0.000	6.36	0.000	0.000	0.000
43.00	1285.	.026	0.000	6.51	0.000	0.000	0.000
44.00	1105.	.022	0.000	6.67	0.000	0.000	0.000
45.00	949.	.019	0.000	6.82	0.000	0.000	0.000
46.00	816.	.016	0.000	6.97	0.000	0.000	0.000
47.00	701.	.014	0.000	7.12	0.000	0.000	0.000
48.00	603.	.012	0.000	7.27	0.000	0.000	0.000
49.00	518.	.010	0.000	7.42	0.000	0.000	0.000
50.00	445.	.009	0.000	7.57	0.000	0.000	0.000
51.00	383.	.008	0.000	7.73	0.000	0.000	0.000
52.00	329.	.007	0.000	7.88	0.000	0.000	0.000
53.00	284.	.006	0.000	8.03	0.000	0.000	0.000
54.00	243.	.005	0.000	8.18	0.000	0.000	0.000
56.00	209.	.004	0.000	8.48	0.000	0.000	0.000
57.00	179.	.004	0.000	8.48	0.000	0.000	0.000
58.00	154.	.003	0.000	8.48	0.000	0.000	0.000
59.00	132.	.003	0.000	8.48	0.000	0.000	0.000
	114.	.003	0.000		0.000	0.000	0.000

LISTING OF

DSPOT

COMPUTER CODE

Physical Variable	Code Name	Dimensions
Temperature, T	T	°K
Atmospheric pressure, P	P	mm Hg
Chemical moleculer weight, M	AM	gm/mole
Liquid boiling point, T_b	TB	°K
Liquid surface tension, G	G	dynes/cm
Initial vapor concentration, C_o	CO	mg/m^3
Ventilation flow rate, Q	Q	m^3/min
Tank volume, V	V	m^3
Unused	Z	--
Deadspot inner radius, R_1	R1	cm
Deadspot outer radius, R_o	RO	cm
Mucking evaporation rate, m	DOTM	mg/sec
Output print frequency	PFREQ	--
Coefficients A,B and C describe initial radial concentration profile: $C = C_o (a+br+cr^2)$	A B C	-- 1/cm 1/cm^2
Number of radial integration steps	RNINC	dimensionless
Maximum simulation time	TMAX	sec
Integration stability criterion, $\Delta t / \Delta r^2$	RATIO	sec/cm^2

```
       PROGRAM DSPOT(INPUT,OUTPUT,TAPE1=INPUT,TAPE2=OUTPUT)
       DIMENSION CD(3000,3)
       PI = ACOS(-1.0)
10     CONTINUE
       TIME =0.0
       ITIME= 0
       READ 1000,T,P,AM,TB,G
       IF(EOF(1))9999,15
15     CONTINUE
       D = (0.425*T**1.5) / (P*(AM*TB/G)**0.5)
       READ 1000,CO,Q,V,Z,R1,RO,DOTM,PFREQ
1000   FORMAT(8E10.0)
       READ 1000,A,B,C,RNINC,TMAX,RATIO
       DR = (RO - R1)/RNINC
       DT = DR*DR*RATIO
       NT = TMAX/DT +1.1
C      SET UP INITIAL CONDITIONS AT T = 0.0
       NUMR = RNINC + 1.1
       R=RO + DR
       DO  20   I=1,NUMR
       R=R-DR
       J=NUMR + 1-I
2000   FORMAT(1H112X,*CO=*E12.5,2X,*Q=*E12.5,2X,*V=*E12.5,2X,*D=*E12.5,/
      13X,*R1=*E12.5,2X,*RO=*E12.5,2X,*A=*E12.5,2X,*B=*E12.5,/
      23X,*C=*E12.5,2X,*DOTM=*E12.5,2X,*PFREQ=*E12.5,2X,*RNINC=*E12.5,/
      +3X,*TMAX=*E12.5,2X,*RATIO=*E12.5//)
2010   FORMAT(3X,*INITIAL CONCENTRATIONS AT T=0 */
      13X,*CONCENTRATIONS RANGE FROM R=R1 TO R=RO*/
      2(3X,10E12.5/))
2020   FORMAT(1H03X,*CONCENTRATIONS AT TIME = *E12.5,* SECONDS *
      1*R=R1 TO R=RO*/
      2(3X,10E12.5/))
       CD(J,2) =   CO*(A+B*R+C*R*R)
       CD(J,1) = CD(J,2)
20     CONTINUE
C      R = R1
       FAC = -2.0*DOTM/(PI*(1.0E-6)*R1*R1*D)
       IPRNT = PFREQ + 0.1
       PRINT 2000,CO,Q,V,D,R1,RO,A,B,C,DOTM,PFREQ,RNINC,TMAX,RATIO
       PRINT 2010,(CD(I,1),I=1,NUMR)
22     CONTINUE
       ITIME = ITIME + 1
C      CALCULATE RADIAL CONCENTRATIONS , ITERATE ON TIME
       TIME = TIME + DT
       R = RO
       DO  30   I=1,NUMR
       J=NUMR + 1 - I
       IF(I.GT.1)GO TO 24
       CD(J,3) = CO*EXP(-Q*TIME/(60.0*V))
       GO TO 28
24     CONTINUE
       IF(I.EQ.NUMR)GO TO 26
       CD(J,3)=CD(J-1,1)+2.0*DT*D*(CD(J+1,2)-CD(J-1,2)) /
      1  (R*DR) + 2.0*DT*D*(CD(J+1,2)-2.0*CD(J,2)+CD(J-1,2))/DR**2
       GO TO 28
26     CONTINUE
       CD(J,3)=(-2.0*DR*FAC+4.0*CD(J+1,3)-CD(J+2,3))/3.0
28     CONTINUE
       R=R-DR
30     CONTINUE
       IF(ITIME.EQ.1)GO TO 33
       IF(ITIME.EQ.NT)GO TO 33
```

```fortran
       IF(MOD(ITIME,IPRNT).NE.0)GO TO 35
33     CONTINUE
       PRINT 2020,TIME,(CD(J,3),J=1,NUMR)
35     CONTINUE
C      UPDATE
       DO 40 I=1,NUMR
       DO 40 J=1,2
40     CD(I,J)=CD(I,J+1)
       IF(TIME.LT.TMAX)GO TO 22
       GO TO 10
9999   CONTINUE
       STOP
       END
```

APPENDIX E

METHODOLOGY, INSTRUMENTATION AND
PROCEDURES FOR

- o   SOURCE SAMPLING
- o   AREA SAMPLING
- o   MATRIX SAMPLING
- o   PERSONAL SAMPLING
- o   METEOROLOGICAL MEASUREMENTS

E.1   Source Sampling

Source vapor concentrations were obtained using the instrumentation that was shown in Figure VI.1. The sampling and analysis instrument was a Century Systems Corporation Organic Vapor Analyzer (OVA Model No. 108 with linear readout or OVA Model No. 128 with logarithmic readout). These units and their accompanying strip chart recorders are certified by Factory Mutual Research Corporation as intrinsically safe for use in Class I, Division 1, Groups A, B, C, and D hazardous locations. There are two modes of sample analysis, both of which employ a hydrogen flame ionization detector (FID). In the first mode, the unit functions as a total hydrocarbon (TH) analyzer with concentrations expressed in ppm (parts per million) as methane. The unit can also operate in an optional gas chromatographic (GC) mode with vapor separation in an isothermal column. Instrument sensitivity to methane is 0.5 ppm and 0.2 ppm for Model Numbers 108 and 128, respectively. Response time in TH mode is two seconds to 90% for both instruments. The TH mode was utilized for source sampling because the GC analysis and backflush times were not appropriate for continuous vapor monitoring especially near tank top-off. Operation in the TH mode was acceptable because the vapors discharged from a tank contained a single constituent (no mixtures).

The probe/readout assembly is attached to the analyzer pack via an umbilical cord. A constant flow rate pump in the analyzer pack transports vapor/air mixtures from the point of sample pickup, through the probe/readout assembly and an inert line in the umbilical to the FID. A detector electrical output signal proportional to concentration is displayed on the probe/readout dial.

The sample pickup point was located in the plane of vapor discharge from an open vent immediately above the flame screen. Data was recorded continuously on a permanent strip chart; probe readout level was also recorded periodically. An example of the source sampling data acquisition log is shown in Table E-1. Tank ullage readings were obtained from either the ship's tape gauging system or a hand-held Lufkin tape. A mercury thermometer indicated vapor discharge temperature. During the latter stages of loading when vapor concentration approaches a saturation level, it was necessary to install a diluter on the probe inlet. This device extends the operating range of the OVA by diluting the sampled vapor with fresh uncontaminated makeup air while maintaining a constant total flow rate to the analyzer. The makeup air is prefiltered through a carbon bed to remove background hydrocarbon levels. All diluters were precalibrated in the laboratory as follows. First, the probe readout level was noted when a constant vapor or gas concentration was presented to the OVA without the diluter in place. The diluter was then installed and, in the presence of the same constant concentration, a stream splitter needle valve was adjusted until the desired dilution ratio or attenuation factor was obtained. Diluters were calibrated to either a 10:1 or 50:1 nominal attenuation factor.

Conversion of total hydrocarbon concentration expressed as methane to actual concentration of a single chemical vapor was accomplished through a response factor, R_f. The response factor is defined as the ratio of a known chemical vapor concentration to the concentration "as methane" indicated on the OVA. Thus, the response factors are unique to given chemicals,

E-1

TABLE E-1

SOURCE SAMPLING

OVA I.D. NO. _____ _____

RECORDER I.D. NO. _____

DATE _____

VESSEL _____

TECHNICIAN _____

NOTES:

Dilutor ID	Dilution Ratio
S-1-10	
S-1-50	
S-2-10	
S-2-50	

Order of Sampling

Tank No.	Color Code	Contents	Response Factor R_f

DATA

Tank No.	Ullage (ft)	Time	Temp(°F)	Diluter ID	Range	Probe Readout	Conc.

and they were determined by post-test calibration. During each test, product samples were collected for each chemical of interest. The calibration procedure consisted of preparing known vapor concentrations from each individual liquid sample. These calibration atmospheres were prepared by evaporating a known weight of liquid in a sealed container. Vapor concentration in the container was calculated from the following equation:

$$C = \frac{(W/M) \times 10^6}{(V/\overline{V})}$$

where W = weight of volatile chemical introduced into the container, gm

M = molecular weight of the liquid, gm per mole

V = container volume, liter

$\overline{V}$ = molecular volume of the vapor/air mixture at calibration conditions, liter.

The molecular volume, $\overline{V}$, is a function of pressure and temperature.

$$\overline{V} = 24.45 \left(\frac{760}{P}\right)\left(\frac{T + 273.2}{298.2}\right)$$

where P = atmospheric pressure, mm Hg,

T = ambient temperature, °C.

The contents of the container were then sampled with the OVA, and the indicated concentration was noted. This procedure was repeated for a wide range of vapor concentrations. The data was plotted, and the response factors were then calculated. The true chemical vapor concentration could then be obtained from the field test data.

$$C_T = C_{TH} R_f$$

where C_T = true concentration, ppm

C_{TH} = indicated total hydrocarbon concentration from the source sampling data, ppm

R_f = response factor for the chemical interest.

E.2   Area Sampling

Area sampling consisted of collecting vapor laden air in inert bags at five on-deck sampling stations. Each sampling station was composed of the apparatus that was shown in Figure VI.2. An MSA Model C-200 personal sampling pump was fastened to a weighted vertical boom. Pump inlet was fixed at 5.5 ft (1.68m) above the deck, which closely approximates man's breathing level height. Inert tubing was used to connect the pump outlet to the inlet valve on the inert collection bag. All pumps were calibrated to a nominal flow rate of 0.1 ℓ/min. A description of the pumps and the details of pump calibration are presented in the discussion of personal sampling. Maximum volume of the sample bags was 4.7 liters.

The five sampling stations were typically located downwind of the vapor source. An indication of the deck-level wind direction was obtained with the aid of a specially fabricated wind vane that incorporated a compass rose. The wind direction relative to ship's longitudinal axis was obtained by aligning the zero degree heading with the bow. Two factors influenced selection of the exact station locations:

o   The perceived path of the centerline of the plume as given by the on-deck wind direction indicator, and

o   the downwind and crosswind dispersion of heavier-than-air vapor plumes as predicted by prior application of analytical models.

The locations of the sampling stations were recorded on a scale drawing of the ship deck. Consecutive 30-minute samples were collected at each station location. Collection bags were labeled according to the following scheme:

$$Bag\ ID = AX-Y$$

where   X = 1,2,3,4 or 5 according to the station location,

         Y = sequence number 1,2,....., N

The bag identification was correlated with time using an area sampling data acquisition log at each station. An example of this log is shown in Table E-2. The count columns refer to the stroke count indicator on the pump. Volume of air processed by the pump can be correlated either with the count differential and the pump volume/stroke, or the calibration flow rate and the operating time differential. Following the 30-minute filling period, the inlet valve was closed, and the bag was removed. A new bag for the next filling period was then installed.

Nearly all of the bags were analyzed on-site using an OVA in GC mode in conjunction with a strip chart recorder. Identification of vapor components and concentration levels was accomplished through a post-test calibration of the GC using test atmospheres that were prepared from the liquid chemicals of interest.

E.3   Matrix Sampling

Following identification of the tanks to be monitored, a matrix of sampling points was marked on the ship's deck. This matrix extended downwind and crosswind of the vapor source. Each matrix point was labeled, and its coordinates were referenced to the appropriate open ullage port. The purpose of this grid layout was to define points on the deck where an OVA apparatus could be sequentially positioned to record total hydrocarbon concentrations. To this end, two mobile OVA units of the type that were shown in Figure VI.1 traversed the matrix of points in a prescribed sequence with a 3-minute sampling duration at each grid point. The sample inlet on the probe/readout assembly was again positioned at a breathing level height of 5.5 ft (1.68m) above deck level. A 3-minute sampling duration was selected based on the results of the scale model wind tunnel vapor dispersion tests discussed in Section IV. This duration was judged to be

E-4

TABLE E-2

AREA SAMPLING

PUMP I.D. NO. _____

SAMPLING STATION I.D. NO. _____
(I.D. Nos. A1 to A5 assigned from master plan)

DATE _____

VESSEL _____

TECHNICIAN _____

HEIGHT OF PUMP INLET ABOVE DECK _____

DATA

Bag No.	Sample Point	Time On	Counts On	Time Off	Counts Off	Temp °F	Comments

of sufficient length to permit calculation of a time-averaged concentration for a given point, thus integrating or smoothing the short time, turbulence-induced fluctuations in vapor concentration. During each 3-minute sampling period, the output of the OVA detector was premanently recorded on strip chart paper. With the location of the sample point identified on the strip chart paper, correlation with time during loading was accomplished with the aid of the data log in Table E-3.

The strip chart recorder is a discrete point device that records level at fixed intervals of time (4 points/sec). To reduce the data, a frequency histogram was constructed for each 3-minute period. The number of points within a given concentration interval was tabulated. For example,

Concentration Interval (ppm)	Number of Points in Interval (f_i)
90 – 100	o
80 – 90	o
70 – 80	o
o	o
o	o
o	o

The mean concentration was then calculated as follows:

$$\bar{c} = \sum_{i=1}^{N} S_i f_i \Big/ \sum_{i=1}^{N} f_i$$

where S_i is the concentration at the midpoint of the interval over which f_i was counted.

E.4   Personal Sampling

Selected crew members wore the sampling apparatus that was shown in Figure VI.3. Project personnel also wore the sampling equipment when they accompanied a ship's officer into an empty tank. The individual to be monitored wore a belt-mounted MSA Model C-200 portable pump and lapel-mounted tube holder that housed an SKC Corporation charcoal sampling tube. These pumps are certified by Factory Mutual Research Corporation as in-trinsically safe for use in Class I, Division 1, Groups C and D hazardous locations and non-incendive for use in Class I, Division 2, Groups A, B, C, and D hazardous locations as defined by the National Electrical Code. The outlet of the tube holder was connected to the pump inlet with a section of flexible tubing. Large charcoal tubes were used for all personal monitoring in order to minimize the potential for vapor break-through in high concentration environments. The primary collection section of these tubes contained 400 mg of activated carbon while the backup section contained 200 mg. All tubes were taken from the same lot number. Prior to each test, the pumps were calibrated with a bubble meter to a nominal flow rate of 1.0 ℓ/min. Immediately following the test, the pump

TABLE E-3

MATRIX SAMPLING

OVA I.D. NO._____   TANK NO. _____

RECORDER I.D. NO._____

DATE_____

VESSEL_____

TECHNICIAN_____

NOMINAL SAMPLING TIME/POINT_____

SEQUENCE OF SAMPLING POINTS_____

DATA

Sample Point	Time Start	Time Stop	OVA Range	Diluter I.D. No.	Remarks

flow rates were again determined before the battery pack was recharged. The average of the pre- and post-test calibration flow rates was used in calculating volumetric concentration. An example of the pump calibration form is shown in Table E-4. All pump flow rates were obtained under load, i.e., tube, with glass tips open, tube holder and flexible line in place.

Sampling and analysis was conducted in accordance with recommended NIOSH procedures.[*],[**] The sampling procedure is best described with the aid of the industrial hygiene survey form that is shown in Table E-5. The information on this form is self-explanatory. To initiate sampling, the ends of the glass charcoal tubes were broken with a plier. After the tube was inserted into the holder, the pump was turned on and the appropriate time recorded. At the conclusion of a sample period, the tubes were immediately capped with the supplied plastic caps, wrapped in a fiber towel to prevent damage, and placed in a cooler for transport to the laboratory for analysis. Packaged "Blue-Ice" was used as the cooling medium rather than conventional ice. Per recommended procedures, one tube —a blank—was broken, capped, and transported in the same fashion as the test tubes. A blank was generated for each distinctly different work task that was monitored. Laboratory analysis consisted of desorbing the sampled vapors with carbon disulfide, a gas chromatographic analysis for the vapors of interest, a desorption efficiency study and generation of standards for calibration. The desorption study and calibration standards were based on samples of the liquid chemicals that were loaded. Chemical volumetric concentrations were then calculated as follows:

$$C = \frac{W}{\eta V} \left(\frac{760}{P}\right) \left(\frac{T+273.2}{298.2}\right) \left(\frac{24.45}{M}\right)$$

where W = weight in μg of a particular chemical that was desorbed from the charcoal

η = chemical specific desorption efficiency

P = atmospheric pressure, mm Hg

T = atmospheric temperature, °C

V = volume of air in liters that was processed by the pump during the sampling duration

$$V = Q_c(t_f - t_i)$$

M = molecular weight of a specific chemical.

The analysis procedure also included a GC check of the backup section in the tube to determine if breakthrough had occurred. The value of W reflects any background or contamination levels that were present on the blank.

---

[*] NIOSH Manual of Sampling Data Sheets, National Institute for Occupational Safety and Health, Publication No. 77-159, March 1977.

[**] NIOSH Manual of Analytical Methods, National Institute for Occupational Safety and Health, Second Edition, Volumes 1, 2, and 3, Publication No. 77-157-A, April 1977.

E-8

TABLE E-4

PUMP CALIBRATION

PUMP NO. _____

TECHNICIAN _____

CALIBRATION LOAD--TUBE--BAG   (Circle One)

PRETEST CALIBRATION

DATE_____   TIME_____

Trial No.	V_c (cc)	t_c (sec)	Q_c (ℓ/min) $= V_c/t_c \times \frac{60}{1000}$
1			
2			
3			
4			
5			
			Q_{ci}(ave) = ℓ/min

POST TEST CALIBRATION

DATE_____   TIME_____

Trial No.	V_c (cc)	t_c (sec)	Q_c (ℓ/min) $= V_c/t_c \times \frac{60}{1000}$
1			
2			
3			
4			
5			
			Q_{cf}(ave) = ℓ/min

$$Q_c = \frac{Q_{ci} + Q_{cf}}{2} = \text{_____} \ \ell/min$$

E-9

TABLE E-5
INDUSTRIAL HYGIENE SURVEY

Date _____

Marine Terminal Operator _____

Vessel Operator _____

Vessel Name _____

Name of Participant _____

Title _____

Deck Watch Working Hours _____

Deck Watch Duties/Work Area _____

Vapors to be Analyzed _____

Pump/Trap Data

    Pump No. _____   cc/count _____

    Sample No. _____

    Collection Medium (Circle one): Charcoal   Silica Gel   Other (Specify)

    Lot. No._____ ; Manufacturer_____

    Size of Collection Medium_____

Sample Start

    Time (t_i) _____

    Pump Counts (PC_i) _____

    Temperature (DB) _____ °F

    Temperature (WB) _____ °F   }   Relative Humidity _____ %

    Barometric Pressure (mm Hg) _____

    Sample I.D. Labeled: Yes ____   (Check Complete)

Sample Stop

    Time (t_f) _____

    Pump Counts (PC_f) _____

    Temperature (DB) _____ °F

    Temperature (WB) _____ °F   }   Relative Humidity _____ %

    Barometric Pressure (mm Hg) _____

    Sample of Liquid Obtained & Labeled: Yes ____   (Check Complete)

E.5   <u>Meteorological Measurements</u>

The meteorological parameters of wind speed, wind direction and atmospheric temperature were recorded during each experiment. The instrumentation is described below and was shown in Figures VI.4 and VI.5.

Prior to ship arrival, a shore-based meteorological tower was erected. The location of the tower was selected so as to minimize blockage or interference effects due to buildings, dock piping and above-ground storage tanks. Total tower height was 10.7m. Atop the tower was mounted a 4-blade Gill Propeller Vane (Model 35001, R. M. Young Co.) to provide continuous monitoring of wind speed and direction. Wind velocity is provided by a DC tachometer generator, and wind direction is obtained from a precision potentiometer. The generator and potentiometer electrical outputs were hard wired into a ground-based power supply translator. Translator output was linked to a dual channel recorder, as well as visual display indicators. This system was calibrated in the laboratory before each test, and the calibration was verified in the field after the tower was erected. A proximity device and a certified oscilloscope were used for velocity calibration, and a compass was used for azimuth calibration.

Air temperature was measured at 1m and 10m above ground level using a single sensor that was mounted on a pulley system that was attached to the tower. The measurement system was manufactured and certified by Omega Engineering, Inc. The movable sensor consisted of a Series 700 thermistor housed in a Model 0-90 temperature detector probe. A 50-foot cable connected the sensor housing to a ground-based Model 400A digital temperature indicator and power supply. Approximately once each hour the temperatures were measured and recorded at both elevations. The response time of the system was experimentally determined to be of the order of one minute or less. Therefore, after the movable sensor was repositioned at a different elevation, the system was allowed to stabilize for approximately one minute before temperature was manually recorded.

METRIC CONVERSION FACTORS